

# “MINE VENTILATION CIRCUITS IN AN UNDERGROUND MINE OF NORTHERN ITALY”

## THESIS

Submitted in partial fulfillment of the  
requirements  
for the degree of Master of science in mining  
engineering in the Department of Environmental,  
Land and Infrastructure Engineering of the  
Politecnico di Torino

## BY

Amir Nematollahi Sarvestani

## SUPERVISOR

Professor Pierpaolo Oreste

## COMPANY TUTOR

Engineer Sandro Gennaro

January 2021

Turin, Italy



## **Abstract**

This dissertation is conducted to find an optimized and comprehensive ventilation system solution for Murisengo Chalk Mine in north of Italy. First, we discussed about history of ventilation and different methods have used for this purpose passing times and fundamentals of ventilation have been discussed. Then it's deliberated why we need ventilation and what are the advantages and benefits of a practical ventilation system.

In the third chapter the common ventilation circuits that are employed currently worldwide are discussed and different designs and schemes related with the specifications of various projects are debated in this section. In the consecutive chapter, different devices used for ventilation purposes have been argued such as different types of fans, air doors, airlocks, regulators, ... Then the geological and hydrogeological features of the Murisengo mine have been analyzed. After that other characteristics and properties of Murisengo mine and machines that are present in the mine have been debated.

Subsequently, the calculations and methods that we used are written and discussed.

Finally, two optimized solutions for ventilation system of Murisengo mine have been designed in order to reach the best ventilation with the lowest cost to reach the best economical and practical design as efficient as possible. This model has been planned with Ventsim design software. Moreover, we have discussed about an event of fire in different locations of the mine in order to see what are the conditions in different airways of the mine in a case of fire.

At the end, some important ideas and suggestions have been argued for further improvement in the future.



## **Declaration by author**

This dissertation is created of my original work, and contains no material earlier published or written by another person except where due reference has been made in the text.

I have clearly stated the contribution of others to my dissertation as a whole, including statistical assistance, survey design, data analysis, significant technical procedures, professional editorial advice, and any other original research work used or reported in my dissertation.

I acknowledge that an electronic copy of my dissertation must be lodged with the University Library and, subject to the policy and procedures of Politecnico di Torino.

I acknowledge that copyright of all material contained in my dissertation resides with the copyright holder(s) of that material. Where appropriate I have obtained copyright permission from the copyright holder to reproduce material in this dissertation.



## **Acknowledgment**

I would like to thank the following people, without whom I would not have been able to complete this research, and without whom I would not have made it through my master's degree!

especially to my supervisor Professor Pierpaolo Oreste whose insight and knowledge into the subject matter steered me through this research. His support, guidance and overall insights in this field have made this an inspiring experience for me.

Engineer Gennaro from the Murisengo mine for helping me to know better the mine's map and details.

Mr. Craig Christensen the Product Development Engineer of Ventsim software from the Howden company who helped me a lot for the technical issues of the Ventsim software.

## **Keywords**

Ventilation, Airway, Ventsim, Mine simulation, Fan, Mine ventilation, Airflow, Ventilation circuits, Mine health and safety, Firesim, Fire in mine, Fire in tunnel, Mine planning, Mine design, Miners health, Contaminants in mine.

## **Contributions by others to the thesis**

No contributions by others.



## **TABLE OF CONTENTS**

<b>Chapter 1: Introduction.....</b>	<b>1</b>
1.1 Primary fans for mine ventilation.....	1
1.2 Theory of mine ventilation.....	4
1.3 Mine airway resistance (Atkinson's Law) .....	5
1.4 Shock Losses.....	9
1.5 Ventilation systems.....	10
1.5.1 Mine systems.....	11
<b>Chapter 2: Reasons to have the ventilation plant.....</b>	<b>13</b>
2.1 Balancing air flow to meet safety needs.....	14
2.2 Coal mine methane (CMM) emissions.....	16
2.3 Healthy environment for workers.....	18
2.4 Intensity of dust emissions.....	18
2.5 Permissible exposure limits.....	19
2.6 Explosions.....	20
2.7 Mine gases.....	20
2.8 Heat sources and effects in mines.....	20
<b>Chapter 3: Typical mine ventilation circuits.....</b>	<b>21</b>
3.1 Ventilation design criteria for making gassy mines safe.....	21
3.2 Face ventilation.....	21
3.3 Air flow must be controlled to minimize dust transport.....	22
3.3.1 Regulations related to dust concentration in air.....	22
3.4 For stratified deposits.....	24
3.4.1 Longwall systems.....	25



3.4.2	Room and pillar systems.....	25
3.4.3	Mine with large size entries.....	26
3.4.4	Recirculation of air underground.....	28
3.5	Orebody deposits.....	31
3.6	Airstream direction.....	33
3.7	Ventilation planning/designing.....	33
3.7.1	To minimize friction losses.....	34
3.7.2	To minimize shock losses.....	34
<b>Chapter 4: Methods of dimensioning fans and other devices.....</b>		<b>35</b>
4.1	Active devices.....	35
4.1.1	Main fans.....	35
4.1.2	What is a fan.....	38
4.1.3	Air stream.....	40
4.1.4	Blowing fan.....	40
4.1.5	Exhausting fan.....	40
4.1.6	Augment ventilation with gas drainage.....	41
4.1.7	Booster fans.....	42
4.2	Passive devices.....	43
4.2.1	Air doors and airlocks.....	43
4.2.2	Man-doors.....	44
4.2.3	Airlocks.....	44
4.2.4	Regulators.....	44
4.2.5	Air crossings.....	45
4.2.6	Prefabricated air crossings.....	45
4.2.7	Stoppings and seals.....	46
4.2.7.1	Stoppings (temporary or permanent) .....	46
4.2.8	District systems.....	48
4.2.9	Auxiliary systems.....	48
4.2.10	Line brattice or vent tubing.....	49
4.2.10.1	Line brattices.....	49



4.2.11 Fan and duct systems.....	50
4.2.12 Air movers and jet fans.....	52
4.2.13 Over cast or under cast.....	53
4.2.14 Machine-mounted water sprays and scrubbers.....	54
4.3 Ventilation surveys.....	55
4.3.1 Air quantity surveys.....	56
4.3.2 Pressure surveys.....	58
4.4 Mine ventilation network analysis.....	58
4.4.1 Fundamentals of the ventilation network analysis.....	59
4.5 Deviations from the Square Law.....	61
4.6 Methods of solving ventilation networks.....	62
4.6.1 Analytical methods.....	62
4.6.2 Equivalent resistances.....	62
4.6.3 Numerical methods.....	62
4.7 Ventilation network simulation programs.....	63
4.8 Mine ventilation planning.....	63
4.9 Coal and metalliferous ventilation.....	67
4.10 Stratified deposits.....	67
4.10.1 Longwall systems.....	67
4.10.2 Room and pillar systems.....	68
4.11 Ore body deposits.....	69
4.12 Air exhaust ducts.....	71
4.13 Aerodynamics of dust airflows in the spectra of air exhaust ducts.....	71
<b>Chapter 5: Description of the Murisengo mine.....</b>	<b>74</b>
5.1 Geographical framework and description of the quarry.....	74
5.2 Geological framework.....	75
5.3 Hydrogeological framework.....	76
5.4 Description of the field.....	76
5.4.1 The plaster.....	77
5.4.2 Characterization of the Murisengo plaster.....	77



5.4.3 Analysis of the physical-mechanical properties of gypsum.....	78
5.5 Cultivation operations.....	80
5.5.1 Cultivation method: (chambers and pillars).....	80
5.5.2 Explosive abatement.....	82
5.5.3 Analysis of the muzzle.....	83
5.6 Bolting.....	85
5.6.1 Case of the Murisengo quarry.....	85
5.6.2 Pull-out resistance tests.....	88
5.7 Applications in the quarry.....	90
5.7.1 Museum area security.....	90
5.7.2 Stabilization of a rock block.....	90
5.7.3 Stabilization with safety net.....	90
5.8 Conclusions.....	90
5.9 Introduction to Ventilation of The Mine.....	91
5.10 Ventilation System of the Murisengo Mine.....	92
5.10.1 Minimum Capacity for Correct Sizing of the Ventilation System.....	93
5.10.2 Ventilation System.....	96
5.11 Performance Verification.....	98
5.12 Computation Theory.....	98
5.12.1 Straight Sections.....	99
5.12.2 Wells.....	100
5.12.3 Elbows.....	100
5.12.4 Changes of Section.....	101
5.12.5 Chokes.....	101
5.12.6 Total Pressure Losses and Power.....	101
5.13 Calculation of Head Losses.....	102
5.13.1 Calculation of the Power.....	103
5.13.2 Calculation of the Power to be Installed in Ventilation Arrangement Using an Air Pipe.....	104
5.14 Secondary Ventilation.....	106
5.15 Measurement Ratio of Airborne Pollutants.....	108
5.16 General Farm Data.....	108



5.17 Job description.....	108
5.18 Sampling mode.....	110
5.19 Sampling Plan.....	110
5.20 Comparison Parameters.....	111
5.21 Results.....	113
5.21.1 Presentation of results.....	113
5.22 Evaluation of results.....	118
<b>Chapter 6: The calculation method used (characteristics and ability).....</b>	<b>122</b>
6.1 Head Losses in Fluid Flow.....	123
6.2 Overall or Mine Heads.....	124
6.3 Head gradients.....	124
6.4 Blower Systems.....	125
6.5 Exhaust Systems.....	126
6.6 Booster Systems.....	127
6.7 State of airflow in mine openings.....	128
6.8 Effect of State of Flow on Velocity Distribution.....	128
6.9 Calculations of head losses.....	130
6.9.1 Velocity Head.....	130
6.9.2 Friction Loss.....	131
6.9.2.1 Atkinson Equation for Friction Loss.....	131
6.9.2.2 Determination of Airway Friction Factor.....	133
6.9.2.3 Determination of Friction Factor for Vent Pipe.....	136
6.9.2.4 Estimation of Friction Loss by Graph.....	136
6.9.2.5 Calculation of Friction Loss by Formula.....	137
6.9.3 Shock Loss.....	137
6.9.3.1 Calculation of Shock Loss by Increase in Friction Factor.....	137
6.9.3.2 Calculation of Shock Loss by Equivalent Length Method.....	137
6.10 Combined Head Losses and Mine Heads.....	139
6.11 Air power.....	139
6.12 Thermodynamic approach to mine ventilation.....	140
6.13 Air specific-weight determinations.....	143



6.14 Humidity Calculations.....	144
<b>Chapter 7: The developed model and obtained results.....</b>	<b>145</b>
7.1 Automatic 3D underground mine mapping.....	145
7.1.1 Data collection.....	145
7.2 Introduction to Ventsim.....	145
7.3 Map of the levels of the mine.....	145
7.4 First problem of the ventilation system in the Murisengo mine.....	148
7.5 Contaminations in Murisengo mine.....	155
7.6 Second problem of the ventilation system in the Murisengo mine.....	164
<b>Chapter 8: Proposals in order to improve the ventilation system in the mine.....</b>	<b>170</b>
8.1 First solution.....	170
8.2 Second solution.....	178
8.3 Future works.....	182
8.4 Final improvement of the ventilation system.....	185
<b>Chapter 9: Conclusions.....</b>	<b>189</b>
<b>REFERENCES.....</b>	<b>192</b>



## List of Figures

Figure 1.1: Guibal's successful centrifugal fan.

Figure 1.2: Factors contributing to hazards and methods of control in mine ventilation [23].

Figure 1.3: Mine airpath resistance.

Figure 1.4: Simple mine ventilation system [23].

Figure 2.1: Primary underground ventilation system where D is a ventilation door or airlock, R is a mine regulator, and 1, 2, 3 are operational areas with a surface exhaust fan.

Figure 2.2: Global anthropogenic greenhouse gas emissions.

Figure 2.3: the allocation of global anthropogenic methane emissions Sources.

Figure 2.4: US Coal Mine Methane emissions since 1990.

Figure 3.1: Different types of ventilation systems.

Figure 3.2: Airflows required per production mass at the face.

Figure 3.3: Airflows required for diluting longwall methane emissions to 2%.

Figure 3.4: Example of power requirements for ventilation air.

Figure 3.5: Elementary ventilation systems (a) U-tube and (b) through-flow (McPherson, 1993).

Figure 3.6: Arrangements of longwall ventilation systems: (a) single-entry advancing; (b) Single-entry retreating; (c) single-entry retreating with back bleeder; (d) double-entry retreating with back bleeder (McPherson, 1993).

Figure 3.7: Groupings of longwall ventilation systems: (e) Y system; (f) double Z system; (g) W system. (McPherson, 1993).

Figure 3.8: Room and pillar development with line brattices to control airstream in conveyor belt entry: (a) bi-directional system; (b) uni-directional system.

Figure 3.9: Continuous brattice curtains line will diminish leakage around peripherals.

Figure 3.10: A theoretical underground mine of limestone where a module system is used instead of stoppings to direct air to working areas.

Figure 3.11: Fan duct is used to deflect exhaust air and to recover lost velocity pressure.

Figure 3.12: Fan duct is used to deflect exhaust air and to recover lost velocity pressure.



Figure 3.13: Changes in mine air specific humidity as a function of air residence time.

Figure 3.14: Changes in mine air temperature as a function of air residence time.

Figure 3.15: Section showing the ventilation system for a metal mine.

Figure 3.16: An example of a simple ventilation system for shrinkage or cut-and-fill stopes.

Figure 3.17: Diagram showing a positive pressure of mine for blowing system and a negative pressure of mine for the exhausting approach.

Figure 3.18: Factors considered in planning a new mine (Viljoen, 1990).

Figure 4.1: Mine primary centrifugal air fans (AIRENG Pty Ltd).

Figure 4.2: Possible locations for main fans [23].

Figure 4.3: Forcing Overlap System (Zhang et al., 2011).

Figure 4.4: The airflow distribution in the push-pull ventilation system (Based on Niu et al., 2006; Wang, 2008).

Figure 4.5: Mine auxiliary fan "Hurricane" (AIRENG Pty Ltd).

Figure 4.6: The five main generic fan types.

Figure 4.7: Forcing the duct fan ventilation system (Thorp, 1982)

Figure 4.8: Exhaust Overlap System (Zhang et al., 2011)

Figure 4.9: (A) Fan pressure-quantity characteristic curve, and (B) superimposed mine resistance characteristic and fan operating point.

Figure 4.10: Booster fan installation (Courtesy of De Souza et al. 2003.)

Figure 4.11: Airlock (American mine door)

Figure 4.12: Automatic Regulator [24].

Figure 4.13: USBM method of measuring single stopping resistance.

Figure 4.14: Explosion-proof seal. (Chalmers, 2008.)

Figure 4.15: Line brattices used in auxiliary ventilation [23].

Figure 4.16: line brattice (ABC Industries, inc. [25])

Figure 4.17: Auxiliary fan and duct systems [23].

Figure 4.18: Jet fans [26].

Figure 4.19: Overcast (MSHA 2203, 1981).

Figure 4.20: Rotating bed scrubber [27].

Figure 4.21: Venturi spray [27].

Figure 4.22: Path of an anemometer traverse [23].



Figure 4.23: Generic mine ventilation planning.

Figure 4.24: U-tube ventilation [23].

Figure 4.25: through-flow ventilation [23].

Figure 4.26: Longwall district ventilation systems [23].

Figure 4.27: Room-and-pillar development with line brattices (high face resistance) [23].

Figure 4.28: Room-and-pillar development with auxiliary fans (zero face resistance) [23]

Figure 4.29: Principle of through-flow ventilation applied to the levels of a metal mine [23].

Figure 5.1: Geographical framework of the quarry.

Figure 5.2: Quarry level diagram.

Figure 5.3: Stratification of the area under analysis.

Figure 5.4: gypsum crystals

Figure 5.5: Murisengo crystal

Figure 5.6: Phase A of progress.

Figure 5.7: Phase B of progress.

Figure 5.8: Phase C of progress

Figure 5.9: Scheme of the "chambers and pillars" cultivation method, plan.

Figure 5.10: Drill & blast cultivation technique.

Figure 5.11: View of the muzzle diagram.

Figure 5.12: Section of the muzzle diagram.

Figure 5.13: Principle of the adhesion mechanism on the left and the friction mechanism on the right.

Figure 5.14: Swellex type bolts.

Figure 5.15: Pipe expansion.

Figure 5.16: Normal distribution of available data.

Figure 5.17: A view of the inside of the Murisengo mine.

Figure 6.1: Fluid-flow system showing energy relations [22].

Figure 6.2: Arrangement of a duct (a) horizontally and (b) vertically to demonstrate the effect of elevation.

Figure 6.3: Head gradients for a basic fluid-flow system.

Figure 6.4: Head gradients for an exhaust system in mine ventilation.



Figure 6.5: Head gradients for a booster system in mine ventilation.

Figure 6.6: Velocity distributions in circular conduits, average velocity constant. (After Rouse, 1937. Reprinted from Trans. Amer. Soc. Civil Engr., Vol. 102, p. 163 with permission of the ASCE.)

Figure 6.7: Relation of velocity ratio  $V/V_{\max}$  and Reynolds number. (After Vennard, 1940. Reprinted by permission of John Wiley & Sons, Inc.)

Figure 6.8: Effect of spacing of timber sets on friction factor K. (After McElroy, 1935)

Figure 6.9: Indicator diagram for the system in Figure 6.1.

Fig 7.1: Level A of Murisengo Mine.

Fig 7.2: Level B of Murisengo Mine.

Fig 7.3: Level C of Murisengo Mine.

Fig 7.4: Level D of Murisengo Mine.

Fig 7.5: Level E of Murisengo Mine.

Fig 7.6: Level F of Murisengo Mine.

Figure 7.7: simulation of E, D, and F floors of the Murisengo Mine.

Figure 7.8: Front view 1st angle simulation of A, B, C, E, D, and F floors of the Murisengo Mine.

Figure 7.9: Front view 2nd angle simulation of A, B, C, E, D, and F floors of the Murisengo Mine.

Figure 7.10: Front view 3rd angle simulation of A, B, C, E, D, and F floors of the Murisengo Mine.

Figure 7.11: Front view 4th angle simulation of A, B, C, E, D, and F floors of the Murisengo Mine.

Figure 7.12: Top view simulation of levels A, B, C, E, D, and F of the Murisengo Mine.

Figure 7.13: Top view simulation of A, B, C, E, D, and F floors of the Murisengo Mine.

Figure 7.14: Bottom view simulation of A, B, C, D, E, and F floors of the Murisengo Mine

Figure 7.15: Airflow simulation of every airways of the Murisengo Mine. The highest airflow: pink color. The lowest airflow: blue color. The colors from highest airflow to lowest airflow: Pink, Red, Yellow, Green, Blue.

Figure 7.16: The distribution of CO (ppm) after 15 minutes of starting of machines.

Figure 7.17: The distribution of  $CO_2$  (%) after 15 minutes of starting of machines.

Figure 7.18: The distribution of CO (ppm) after 30 minutes of starting of machines.

Figure 7.19: The distribution of  $CO_2$  (%) after 30 minutes of starting of machines.



Figure 7.20: The distribution of CO (ppm) after 8 hours (1 shift) of starting of machines.

Figure 7.21: The distribution of  $CO_2$  (%) after 8 hours (1 shift) of starting of machines.

Figure 7.22: Airflow simulation of every airways of the Murisengo Mine without Natural ventilation. The highest airflow: pink color. The lowest airflow: blue color. The colors from highest airflow to lowest airflow: Pink, Red, Yellow, Green, Blue.

Figure 7.23: The amount of temperatures inside the rock for each level of the mine in the current condition.

Figure 7.24: Recirculation of air inside some airways of the level A in the current situation of the mine.

Figure 7.25: Recirculation of the air inside a small portion of the level B in the current situation of the mine.

Figure 7.26: Recirculation of the air inside several airways of the level C in the current situation of the mine.

Figure 7.27: The most important recirculation of the air inside a large portion of the level D, E, and F in the current situation of the mine.

Figure 7.28: The dispersion of CO throughout the mine after 15 minutes of fire of a loader in level F and 5 machines produce contaminations are also present. It is also interesting to note that in this situation the direction of the flow in San Pietro ramp will change. It means that after we have a fire in the level F, most of the air will flow out of the mine through San Pietro.

Figure 7.29: The dispersion of CO throughout the mine after 15 minutes of fire of a truck in the San Pietro ramp between levels D-E and 5 machines produce contaminations are also present. It is also interesting to note that in this situation the direction of the flow in San Pietro ramp and Prato Nuovo ramp will change.

Figure 8.1: Front view 1st angle simulation of A, B, C, E, D, and F floors of the first solution for Murisengo Mine.

Figure 8.2: Front view 2nd angle simulation of A, B, C, E, D, and F floors of the first solution for Murisengo Mine.

Figure 8.3: Front view 3rd angle simulation of A, B, C, E, D, and F floors of the first solution for Murisengo Mine.

Figure 8.4: Front view 4th angle simulation of A, B, C, E, D, and F floors of the first solution for Murisengo Mine.

Figure 8.5: Top view simulation of A, B, C, E, D, and F floors of the first solution Murisengo Mine.

Figure 8.6: Top view simulation of A, B, C, E, D, and F floors of the first solution for Murisengo Mine.

Figure 8.7: Bottom view simulation of A, B, C, D, E, and F floors of the first solution for Murisengo Mine.



Figure 8.8: There is a recirculation of airflow in the entrance of Prato Nuovo ramp between levels D-E.

Figure 8.9: The block (door) at the entrance of Prato Nuovo ramp between levels D-E.

Figure 8.10: Airflow simulation of every airways of the Murisengo Mine. The highest airflow: pink color. The lowest airflow: blue color. The colors from highest airflow to lowest airflow: Pink, Red, Yellow, Green, Blue.

Figure 8.11: The distribution of CO (ppm) after 15 minutes of starting of machines.

Figure 8.12: The distribution of CO<sub>2</sub> (%) after 15 minutes of starting of machines.

Figure 8.13: The distribution of CO (ppm) after 30 minutes of starting of machines.

Figure 8.14: The distribution of CO<sub>2</sub> (%) after 30 minutes of starting of machines.

8.15: The amounts of pressures inside different levels of the mine in the simple solution.

8.16: The amounts of temperatures inside the rocks of each level of the Murisengo mine after putting blocks.

8.17: There is no recirculation of the air inside the airways in the simple solution of the ventilation system for Murisengo mine.

Figure 8.18: The dispersion of CO throughout the mine after 15 minutes of fire of a loader in level F and 5 machines produce contaminations are also present. It is also interesting to note that in this situation the direction of the flow in San Pietro ramp will change. It means that after we have a fire in the level F, most of the air will flow out of the mine through San Pietro.

Figure 8.19: The dispersion of CO throughout the mine after 15 minutes of fire of a truck in the San Pietro ramp between levels D-E and 5 machines produce contaminations are also present. It is also interesting to note that in this situation the direction of the flow in San Pietro ramp and Prato Nuovo ramp will change. It means that after we have a fire in the end of San Pietro ramp, the air will enter the mine from Prato Nuovo ramp and will flow out through San Pietro ramp.

Figure 8.17: The blocks in the middle of level B, C, and D.

Figure 8.18: The amount of airflows inside different airways in the second solution.

Figure 8.19: The dispersion of contaminations (co (ppm)) after 15 minutes from the start of 5 machines in the second solution. The red area is with highest contamination (CO), then the yellow area, and green and blue areas are with lowest amounts of contaminations.

Figure 8.20: The dispersion of CO in the second solution of the mine after 15 minutes from the start of fire of a truck in the inclined ramp between level D-E. The red area is with highest contamination (CO), then the yellow area, and green and blue areas are with lowest amounts of contaminations.

Figure 8.21: The dispersion of CO in the second solution of the mine after 15 minutes from the start of fire of a loader in level F. The red area is with highest contamination



(CO), then the yellow area, and green and blue areas are with lowest amounts of contaminations.

Figure 8.22: The small recirculation of airflow in the entrance of the Prato Nuovo ramp between level D-E in the second solution. It's lower than the recirculation of airflow in this segment in the current situation but by adding a door in the entrance of the Prato Nuovo ramp between level D-E I reduced it to zero.

Figure 8.23: The recirculation of airflow inside the entrance of the Prato Nuovo ramp between level D-E in the second solution becomes zero.

Figure 8.24: The recirculation inside second solution of the ventilation system.

Figure 8.25: New ramp at the left side of Level F.

Figure 8.26: The spread of contaminations (CO) after 15 minutes from the starting of the machines' working.

Figure 8.27: The spread of contaminations ( $CO_2$  (%)) after 15 minutes from the starting of the machines' working.

Figure 8.28: The dispersion of CO (ppm) in the second solution of the mine after 15 minutes from the start of fire of a truck in the inclined ramp between level D-E. The red area is with highest contamination (CO), then the yellow area, and green and blue areas are with lowest amounts of contaminations.

Figure 8.29: The dispersion of CO (ppm) in the second solution of the mine after 15 minutes from the start of fire of a loader in the entrance of the current ramp in level F. The red area is with highest contamination (CO), then the yellow area, and green and blue areas are with lowest amounts of contaminations.

Figure 8.30: The dispersion of CO (ppm) in the second solution of the mine after 15 minutes from the start of fire of a loader in the entrance of the future ramp in level F. The red area is with highest contamination (CO), then the yellow area, and green and blue areas are with lowest amounts of contaminations.

Figure 8.31: The amount of airflows inside different airways in the final solution.

Figure 8.32: The spread of contaminations (CO (ppm)) after 15 minutes from the starting of the machines' working.

Figure 8.33: The spread of contaminations ( $CO_2$  (%)) after 15 minutes from the starting of the machines' working.

Figure 8.34: The dispersion of CO (ppm) in the final solution of the mine after 15 minutes from the start of fire of a loader in the entrance of the future ramp in level F. The red area is with highest contamination (CO), then the yellow area, and green and blue areas are with lowest amounts of contaminations.

Figure 8.35: The dispersion of CO (ppm) in the final solution of the mine after 15 minutes from the start of fire of a truck in the inclined ramp between level D-E. The red area is with highest contamination (CO), then the yellow area, and green and blue areas are with lowest amounts of contaminations.



Figure 8.36: The dispersion of heat of temperature dry bulb (°C) in the final solution of the mine after 15 minutes from the start of fire of a truck in the inclined ramp between level D-E. The red area is with highest temperature (°C), then the yellow area, and green and blue areas are with lowest amounts of contaminations.

### **List of Tables:**

Table 1.1: Friction factors (for  $1.2 \text{ kg/m}^3$  air density) for a variety of mining situations [23].

Table 1.2: Summary of the German mine regulations for climatic conditions in non-salt mines.

Table 4.1: Recommended maximum air velocities.

Table 5.1: Physical-mechanical properties of the lithotypes involved.

Table 5.2: Physical-mechanical characteristics of the substrate.

Table 5.3: Characteristics of the nails.

Table 5.4: Nail pull-out resistances.

Table 5.5: Minimum air quantities in different sites.

Table 5.6: Personal Sampling.

TABLE 5.7: Exposure Threshold Values and DPR References 128/59.

Table 6.1: Friction factor K for noncoal mine airways and openings.

Table 6.2: Friction factor K for coal mine airways and openings.

Table 6.3: Equivalent Lengths for Various Sources of Shock Loss.

# Chapter1

## Introduction on mine ventilation problems in mining

Ventilation can be defined as airflow control, direction, and quantity. Even though ventilation does not influence the production section of the activity directly, often lower staff work rate and reduced efficiency of mine, increased situations of potential hazards, and little worker motivation and enthusiasm are the consequences of the improper ventilation. Air is necessary for breathing, moreover, for the dissemination of chemical and physical pollutants such as gases, dust, heat, and humidity.

It is vital to ventilate the underground mines for ensuring mineral production safely. Any ventilation system has clear and straightforward fundamentals: providing adequate oxygen as a result of delivering enough quantity and quality of airflows, and for achieving safe concentrations of contaminants and eliminate them from the mine. These fundamental elements are legislated in the law of all countries; however, the quantity and quality requirements can alter significantly in different countries depending on several factors as well as the situation being ventilated: metalliferous, industrial minerals, coal, or gassy/no gassy.

The overall necessity is that miners must be able to work, live, and move in a safe and healthy environment and have satisfactory comfort. Ventilation can also be employed in situations where human intervention is not required or possible. Still, proper and sufficient oxygen supply is necessary to operate and cold machinery or to provide oxygen to combustion processes.

### 1.1 primary fans for mine ventilation:

The first use of fans was in several metal mines of Germany, illustrated by Agricola, utilization of those fans decreased for almost 250 years. In 1827 in a colliery near Paisley, Scotland, a fan for ventilation of a mine was launched. Several blades were installed on that fan that was inclined and attached to a vertical shaft that was rotated in a circular casing. The fan was installed on the upcast shaft, and the air was running into it and pushed out to the surface. This fan was the primary axial flow fan. Numerous mines in France and Germany conduct a number of experiments with fans employed on the Archimedean screw basis at the same time; however, those were unsuccessful, not only from the absence of knowledge of the aerodynamic concept but as well due to the metallurgy of the time did not allow those fans to rotate at the velocities essential for adequate flow rate and pressure. Hence, a curiosity turned again to the centrifugal fan. The impeller of this was fundamentally more potent while the created pressure was increased by the centrifugal energy applied to the air, added to the blade action. Lesser rotating velocities, within the size of a primary steam engine, empowered obligations to be performed effectively. In 1849 an open running 6 m diameter radial-bladed centrifugal fan with a vertical shaft was established at Gelly Gaer Colliery in South Wales. William Brunton (1777-1851) created its design which was tutored under Boulton and James Watt at the Soho Foundry, Birmingham. A prototype was presented at the Great Exhibition of 1851, held in Hyde Park, London.

In 1851, James Nasmyth (1808-1890), the creator of the steam hammer, delivered a paper to the British Association at its meeting in Ipswich. James Nasmyth delineated a double-inlet radial-bladed centrifugal fan another time straightly operated by a steam engine. His model was built in 1854 at Abercarn Colliery, South Wales, with an impeller diameter of 4.12m and rotated at 60 revs/min for an air quantity of 21.25 m<sup>3</sup>/s against 125 Pa. A giant fan (Thereupon) of 4.57 m diameter turning at 80 rev/min was positioned at Skiar Spring Colliery, Elsecar, Yorkshire, UK. The most victorious centrifugal fan of the mid-19<sup>th</sup> century was created by Theophile Guibal [34] (1814-1888) (Figure 1.1). That fan, mounted on the Jean Bart Colliery, firstly was shown in L'histoire general des Techniques aux R U.F., in 1859. Guibal was a Professor of the mine exploitation at the University of Mons, Belgium at the time of his creation [9].

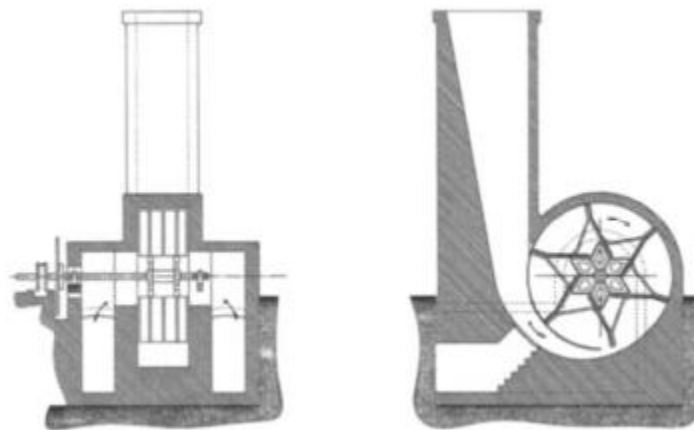
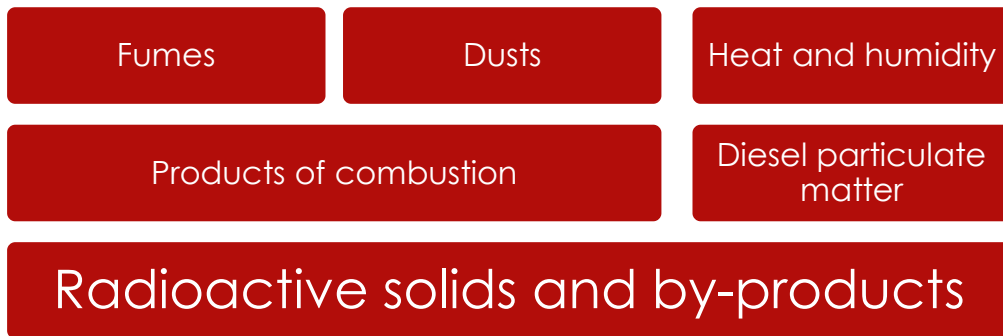
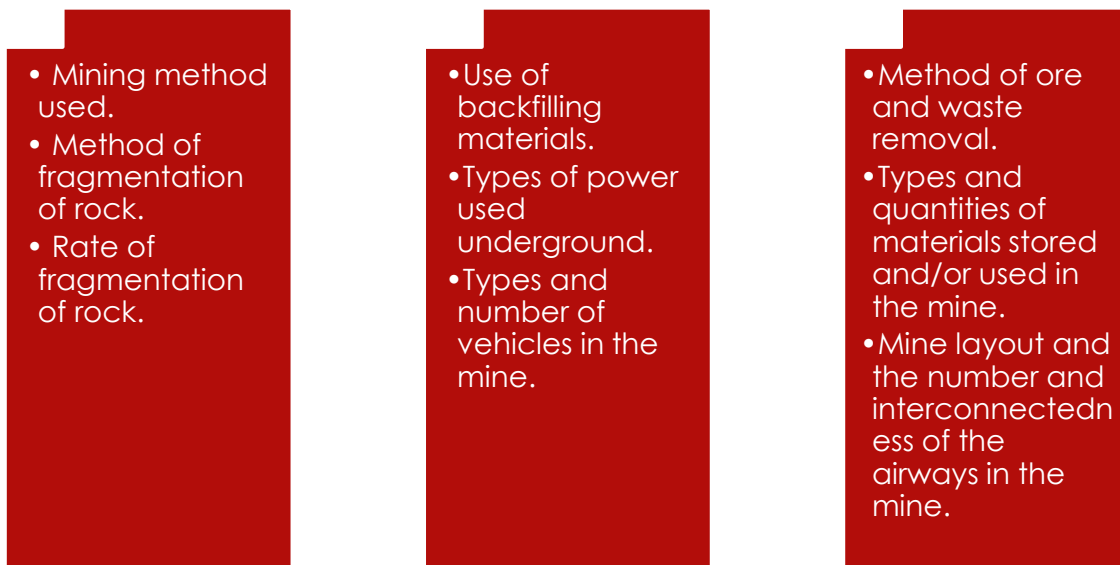


Figure 1.1: Guibal's successful centrifugal fan [9].

The critical purpose of ventilation is to keep an atmosphere that promotes safe and productive working surroundings around the mine. This includes management of oxygen content by volume for different reasons, which will be discussed later, and pollutant levels (comprising ignition products, contaminated fumes, and dust, plus sustaining temperature surroundings of the mine site at levels where miners able to achieve maximum workability and not to reach harmful reactions ignition point in some mines such as coal mines). Legal limits relating to precise standards for the work environment vary depending on the aim of ventilation as well as from country to country and state to state within some countries. Other than where advised by a legitimate superior level, a practical minimum oxygen concentration to put into the design of any ventilation system is a 19% volume fraction of oxygen [35]. Contaminants enter the current of the air of ventilation from different kind of origins. The goal of any ventilation system is to dilute any pollutants to a harmless level and eliminate them. The range of contaminants that can be released into a ventilation system depends on the situation under consideration. Some of the more usual kind of contaminants encountered include:



The elements that play a part in hazards faced in mine ventilation and the handling techniques have shown in the following figure. The constituents are split into those established by natural conditions and those affected by the decisions of designers and engineers regarding how to develop the mine and ore producing. The natural components comprise surface climate, gases, geology, depth involved in the groundwater and other fluids, rock mass, the features of the rock (both physical and chemical), and the workings age. The engineering design of a mine influence the hazards through the:



Every mine could have different standards and features, so the contaminants and their influences differ between mines, locations, and the cycle of workings within a mine. For instance, a bottomless pit in Canada may have problems with cold surroundings in the shallower sections of the mine, demanding mine heating during the winter months, while air at the deeper levels should be refrigerated. Furthermore, other hazards

associated with the ventilation system are fires and explosions in underground mines. Airflow is the primary technique of controlling the atmospheric conditions in an underground. Generally, fans produce the airflow in mines, although air density changes of natural ventilation could supply some airflow in modern quarries. Main fans operate the whole mine flow of air (singly or in combination) and are frequently located on the surface; however, at several mines, they are positioned underground. Law and legislation in some areas may require that main mine fans could only be placed on the surface and, in several cases, may have to be reversible. While the main fans generally operate all the airflow in a mine, we can use other fans in mines to increase the energy of the airflow to circulate the air more magnificent spaces. These are called booster fans, and they generally handle specific areas of the mine. In mine development headings, a through-flow of ventilation may not be possible due to the single entry. An intake and return route for the air has to be developed for these cases. In modern mining, this is generally undertaken by using auxiliary fans to push air to flow through ducts for ventilating the blind entries. Alternatives comprise the use of brattice cloth, and in some cases, jet fans, regulators, stoppings, Air doors, seals, and air crossings control airflow dissemination further. While airflow is the crucial technique to attain the aims of mine ventilation, in some cases, the airflow demanded would become too costly for economical mining. In such cases, other technologies of control can be hired to decrease the load on the ventilation system so that the ventilation costs could be reduced [36]. These techniques involve drainage of methane, heating and cooling systems, suppression systems for dust, and different other controlling and monitoring systems [2].

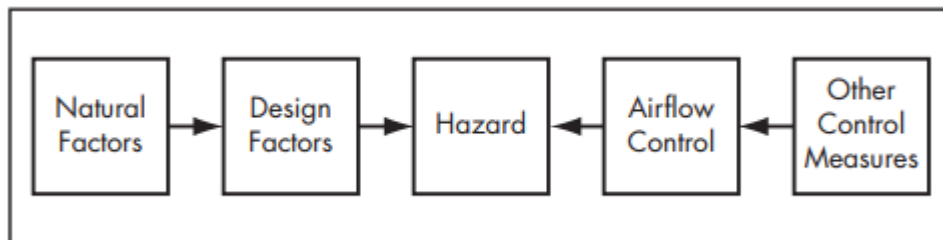


Figure 1.2: Factors contributing to hazards and methods of control in mine ventilation [23].

### 1.2 Theory of mine ventilation:

Fluid mechanics and thermodynamics are two fundamentals of the theory of mine ventilation, particularly the Bernoulli equation, the Chezy–Darcy law for pipe frictional pressure drop, and the steady flow energy equation. Basis of the theory of mine ventilation developed by Atkinson (1854) that still is in use today. By using the base of fluid mechanics and considering several simplifying premises, he derived several relations that currently is the basis of the theory of ventilation and ventilation designing software in modern mines. As discussed, this approach is based on the incompressibility assumption; however, in Ventsim design that we use, we can also have compressible fluid beliefs. As recent mines forward movement to deeper and deeper, this premise commonly comes to be invalid because of the changes in the density of air. Where changes in a density greater than 5% due to the variations in elevation and temperature, the incompressibility assumption becomes weakened and should be

considered [2]. It is necessary to have cautious advance ventilation designing to maintain adequate ventilation through the life of the mine. Advance ventilation includes the consideration of two fundamental parameters: the mine fan(s) pressure, and the total volume flow rate of air, and its adequate and economic spreading [3].

### 1.3 Mine airway resistance (Atkinson's Law):

The French hydraulic engineers' (Chezy and Darcy) works is the fundamental of the Atkinson equation. The Chezy–Darcy studies express the subsequent equation for a pipe [37]:

$$P = fL \frac{per}{A} \rho \frac{u^2}{2} \quad (1.1)$$

Where:

- P = pressure drop of the pipe (Pa),
- f = friction coefficient of the pipe surroundings,
- L = length of the pipe (m),
- per = perimeter of the pipe (m),
- A = cross-sectional area of the pipe ( $m^2$ ),
- $\rho$  = density of the fluid ( $kg/m^3$ ),
- u = velocity of the fluid (m/s),

For completely advanced turbulent flow, Atkinson supposed constant friction coefficient. Also, the density of the air was a regular as another assumption, the Atkinson friction factor,  $k$  ( $kg/m^3$ ) is the combination of the constants into one consideration,

$$K = \frac{f\rho}{2} \quad (1.2)$$

Giving

$$P = KL \frac{per}{A} u^2 \quad (1.3)$$

This equation is recognized as Atkinson's equation and could be written down in terms of airflow rate volume  $Q$  ( $m^3/s$ ), where  $Q = U.A$ , giving

$$P = KL \frac{per}{A^3} Q^2 \quad (1.4)$$

For any air path, the perimeter, per, length, L, and cross-sectional area, A, are known., the friction factor varies only with the roughness of the airway lining for fully developed turbulent flow if we ignore the dependency on density, so to achieve a single variable or characteristic number, R, all these factors could be collected for that airway, where R is known as the airway resistance.

$$R = KL \frac{per}{A^3} \quad (1.5)$$

Then we can obtain the mine ventilation's square law:

$$P=RQ^2 \tag{1.6}$$

where

p = pressure across airpath (Pa)

R = Atkinson resistance ( $Ns^2/m^8$ )

Q = air quantity or flow rate ( $m^3/s$ )

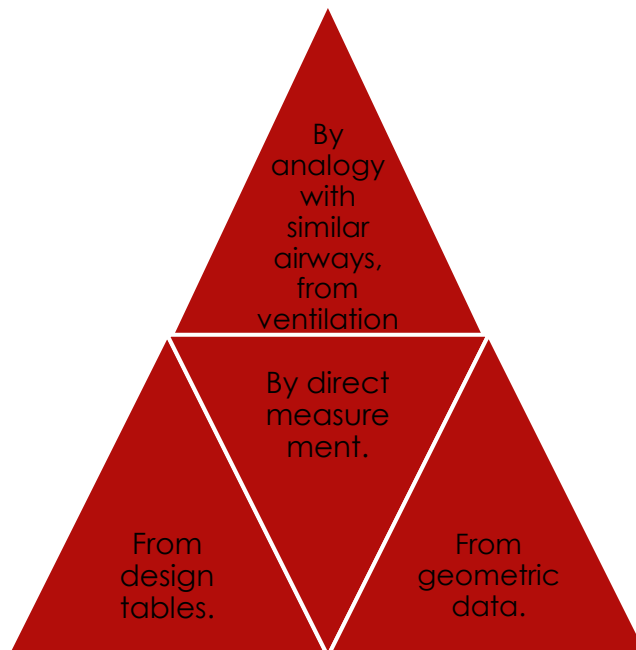
this equation supposes that density is constant as discussed before; regularly, the standard air density is assumed  $1.2 (kg/m^3)$ . Values of R mentioned in tables typically refer to this value. For other air densities,  $\rho$ , the following equation could be used to achieve the frictional pressure drop and resistance:

$$P=k_s L \frac{per}{A^3} Q^2 \frac{\rho}{1.2} \tag{1.7}$$

$$R=k_s L \frac{per}{A^3} \frac{\rho}{1.2} \tag{1.8}$$

where  $k_s$  is the friction factor that is obtained at an air density of  $1.2 kg/m^3$ .

From these calculations, it is evident that the underground opening roughness degree (k) has an essential effect on the Atkinson resistance and the cost of flowing air through that opening. It also directly affects the heat transfer rate between the airflow and the rock. The k (friction factor) can be determined in several ways, details of which can be found in McPherson (1993):



One of the crucial concepts in ventilation engineering is airpath resistance  $I$ . The mine ventilation's square law states:

$$P=RQ^2 \tag{1.9}$$

The above equation illustrates the resistance to be a proportionality constant between the frictional pressure drop ( $p$ ) and the square of the airflow rate ( $Q$ ) at a given air density. The parabolic form of the plot on a  $p, Q$  graph that could be observed in Figure 1.3 is identified as the curve of the airpath resistance.

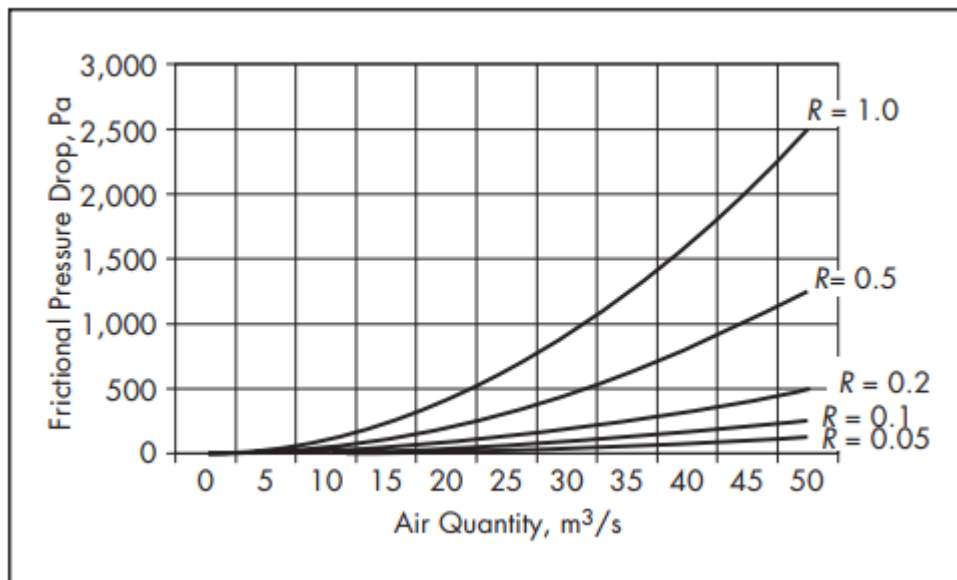


Figure 1.3: Mine airpath resistance [23].

The cost of passing any stream of the air through an airpath differs directly with airpath resistance. The price could be evaluated by the airpower used up in an airpath utilizing air power= $P.Q$  or considering  $p=RQ^2$ , leading to air power= $RQ^3$ .

Assuming electricity has a fixed cost per kilowatt-hour, then we can obtain simply the price to ventilate an airpath. Moreover, this equation represents that doubling the airstream in a specific route has the outcome of multiplying the airpower; hence, the ventilation cost by a factor of 8 [2].

Table 1.1: Friction factors (for  $1.2 \text{ kg/m}^3$  air density) for a variety of mining situations [23].

Type of Airway/Ducting	Friction Factor k, <i>kg/m<sup>3</sup></i>
Rectangular airways	
Smooth concrete lined	0.004
Shotcrete	0.0055
Unlined with minor irregularities only	0.009
Girders on masonry or concrete walls	0.0095
Unlined, typical conditions, no significant irregularities	0.012
Unlined, irregular sides	0.014
Unlined, rough or irregular conditions	0.016
Girders on side props	0.019
Drift with rough sides, stepped floor, handrails	0.04
Steel arched airways	
Smooth concrete all round	0.004
Bricked between arches all round	0.006
Concrete slabs or timber lagging between flanges all round	0.0075
Slabs or timber lagging between flanges to spring	0.009
Lagged behind arches	0.012
Arches poorly aligned, rough conditions	0.016
Shafts	
Smooth lined, unobstructed	0.003
Brick lined, unobstructed	0.004

Concrete lined, rope guides, pipe fittings	0.0065
Brick lined, rope guides, pipe fittings	0.0075
Unlined, well-trimmed surface	0.01
Unlined, major irregularities removed	0.012
Unlined, mesh bolted	0.014
Tubbing lined, no fittings	0.007–0.014
Brick lined, two side buntons	0.018
Two side buntons each with a tie girder	0.022
Longwall face with steel conveyor and powered supports	
Good conditions, smooth wall	0.035
Typical conditions, coal on conveyor	0.05
Rough conditions, uneven faceline	0.065
Ventilation ducting	
Collapsible fabric ducting (forcing systems only)	0.0037
Flexible ducting with fully stretched spiral reinforcement	0.011
Fiberglass	0.0024
Spiral-wound galvanized steel	0.0021

#### 1.4 shock losses:

The theory discussed above represents how the frictional pressure drop could be calculated for an airpath. Furthermore, other losses of energy, termed shock losses, could be incurred. New turbulent vortices are set up whenever airstream is needed to have a different direction. These utilize power as they disseminate, and the airpath resistance can grow significantly. The losses take place at junctions, bends, and changes of cross-sections due to obstructions and regulators, and at points of entry/exit from the mine [2].

The shock losses' influences are the most indeterminate of all the factors influencing resistance. Assessment of the additional resistance due to shock losses could be

assessed by two techniques. The pressure loss due to a shock loss could be represented as a shock pressure loss or  $P_{shock}$ :

$$P_{shock} = X\rho(u^2/2) \quad (1.10)$$

where

X = shock loss factor,

$\rho$  = air density (typically  $1.2 \text{ kg/m}^3$ ), and

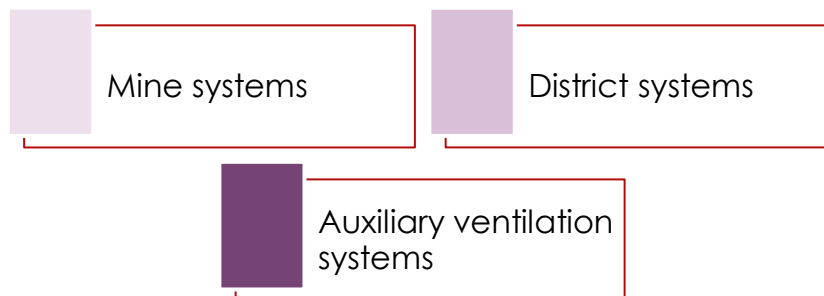
u = velocity of the air (m/s).

This could be turned into a shock loss resistance,  $R_{shock}$ , by the square law:

$$R_{shock} = R_S = (X\rho/2A^2) \quad (1.11)$$

### 1.5 Ventilation systems:

in terms of its geology, geometry/layout, extent/size, and pollutants of every underground mine are unique. As such, the pattern of airflows and pressure drop through the air paths that make up the mine workings are also highly changeable. However, specific characteristics of all ventilation systems have some commonality, and ventilation systems and subsystems classifications could be recognized. The purpose of the current and further section is to debate the necessary criteria of underground ventilation systems, delineate the critical components of ventilation infrastructure, moreover, present some of the ventilation engineers' technical terms. A well-made ventilation system has to be adaptable, economical, adequate, and flexible [3]. Ventilation systems can be generally put in sets as follows:



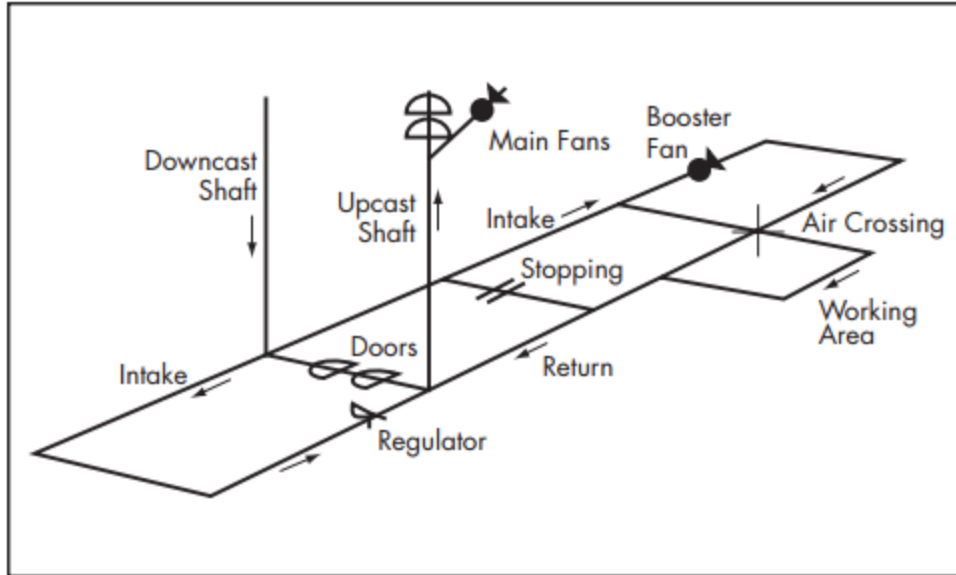
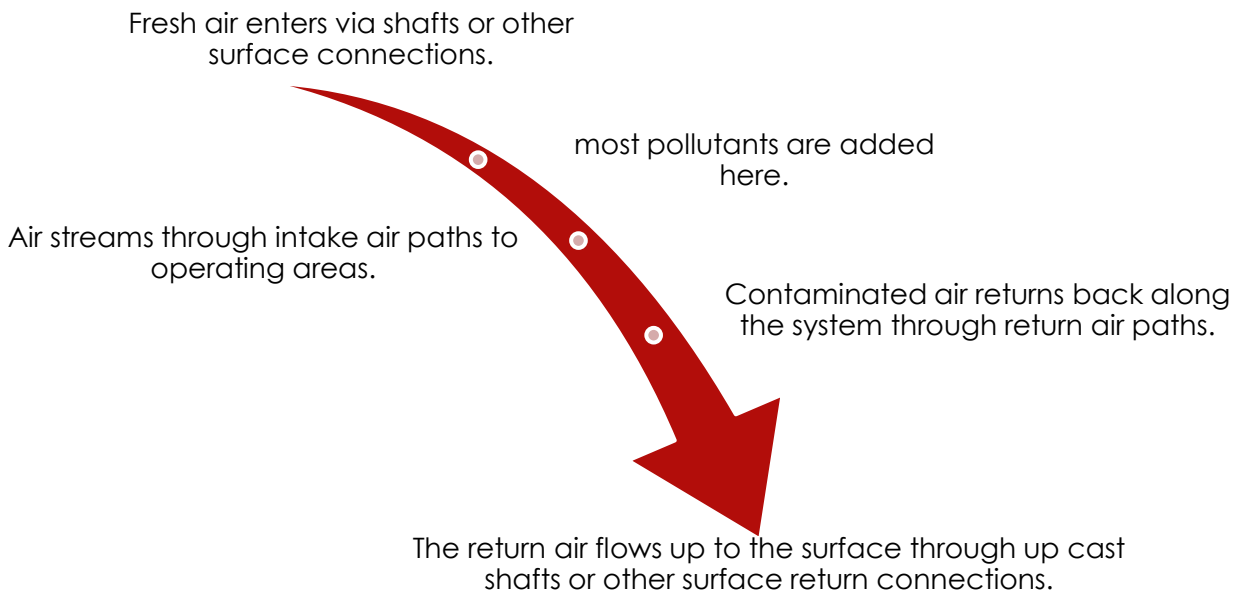


Figure 1.4: Simple mine ventilation system [23].

### 1.5.1 Mine systems:

The figure above elucidates an illustrative mine ventilation system showing a primary and straightforward system layout and some of the ventilation control devices that can be used. The figure above illustrates the following:



However, ventilation is more convoluted than this schematic description. Air, like most fluids, will try to follow the route with lower resistance from one point to another, and the route to the areas demanding ventilation often recline along a high resistance route. To

get the air to the places where it is required, airstream control devices are needed. These could be classified into two main categories: active devices that add energy to the air to direct it to where it is required, or passive devices that add resistance to flow paths to persuade the air to pass through other routes. Instances of active devices include main fans and booster fans. Examples of passive devices comprise air crossings, stoppings, air doors, regulators, and seals, which by adding resistance, enlarge pressure drop. Both types are debated in the subsequent sections [2].

According to the conditioning of the air in Mines Regulation (Klimabergverordnung) of the German coal mining industry, there is not any constraint at effective temperatures of up to 25 °C for on-site operational hours for the underground operations. Operating hours are reduced from the average level of eight hours per shift to six or five hours per shift at higher effective temperatures. Above a sufficient temperature of 30 °C, work underground is permitted under exceptional situations only. Moreover, it is entirely banned at effective temperatures above 32 °C. A survey of the 'Klimabergverordnung' is given in Table 1.2 . Several European countries have taken over at least sections of this act for tunneling workings [8].

Table 1.2: Summary of the German mine regulations for climatic conditions in non-salt mines [8].

Temperature		Duration of shift (h)	Duration of Working time (h)	Additional work break (min)
$t_d$	$t_{eff}$			
$\leq 28^\circ\text{C}$	$\leq 25^\circ\text{C}$	8	No restriction	-
$> 28^\circ\text{C}$	$> 25^\circ\text{C}$	8	6	-
	$> 29^\circ\text{C}$	8	5	10
		Working only under exception		
	$> 30^\circ\text{C}$	8	5	20
	$> 32^\circ\text{C}$	No working		

## Chapter 2

### Reasons to have the ventilation plant in an underground mine

# There are three main reasons to ventilate a construction:

Firstly, ventilation is needed to provide adequate air for respiration purposes. Unless a building is made particularly airtight, the provision of air for this purpose is not likely to pose any problem. At present, such buildings do not exist, although some extremely high levels of airtightness are being claimed for some of the new modular type constructions (which is more detailed in Chapter 8) which might give rise to concerns if the purpose provided by means of ventilation is not functioning correctly.

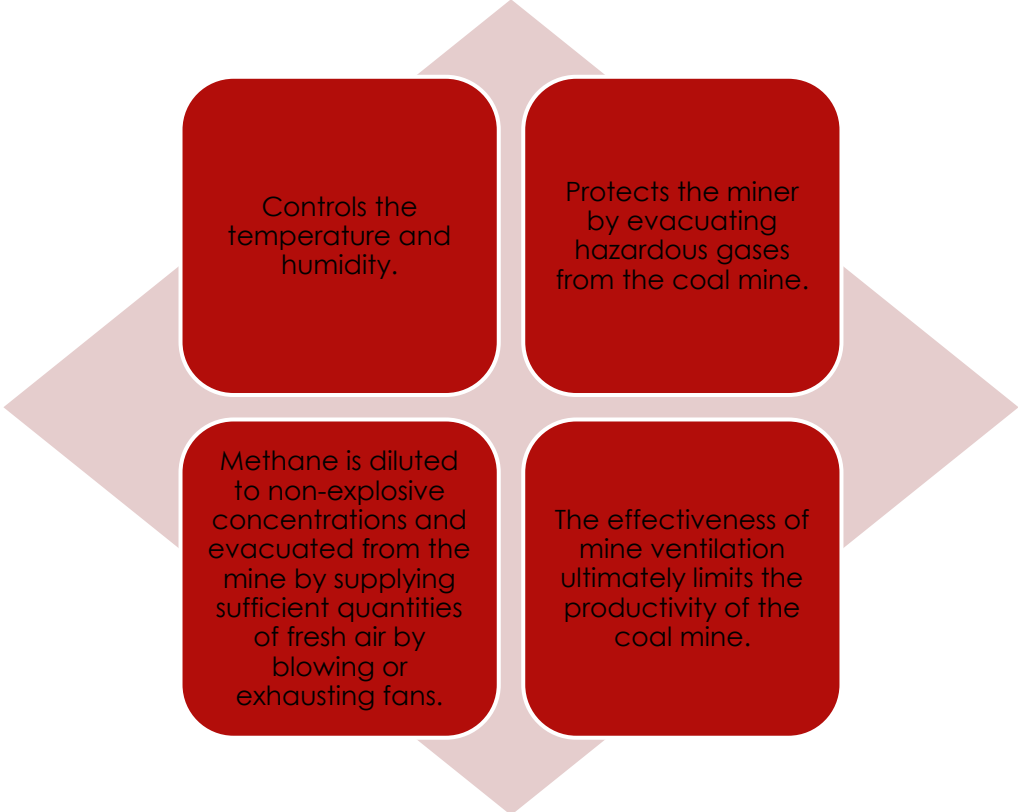
Secondly, ventilation is required in order to provide cooling effect in the summer. Given the occupancy patterns typically encountered in dwellings, not much attention is paid to the cooling of dwellings in comparison to commercial buildings such as offices. Window opening, in offices, is generally deemed to be adequate, and within the UK at any rate there seems to be, but a limited scientific rationale, behind the provision made. Air conditioning or comfort cooling is provided only on the rarest of occasions, presumably on the grounds of cost, although its use is quite common in the US and particularly in apartment blocks.

Finally, the most important reason for the provision of ventilation within dwellings is for the removal and dilution of airborne contaminants. Of these, the most important one is water vapor, although there are others that are worthy of consideration [10].

Mine ventilation is the implementation of the concept and fundamentals of thermodynamics and fluid mechanics for the flowing of air through mine openings and

voids. Air will be brought to the mine site from the atmosphere, it will pass through the mine, and it is discharged back into the atmosphere by the creation of differential pressure between the in and out openings of the tunnel. To accomplish this purpose, the mine ventilation system includes interconnected rooms, airways, and working zones within the mine, connections to the surface such as shafts, other fans to produce airflow, and control devices to ensure that the air courses around the mine as needed. Controlling a ventilation system requires quality as well as air quantity control, and ventilation planning techniques are employed to reach this.

Ventilation systems are established to deliver breathable fresh air:



**2.1 Balancing airflow to meet safety needs:**

- Lower velocities of the air could result in low mixing between air and methane.
- low mixing results in fluctuations in the concentration of the methane that leads to ignition more likely.
- Higher velocities of the air are better for mixing, but if it is too high, more dust is entrained creating safety and health hazards [1].

To guarantee necessary mine ventilation, the arrangement is completed for apposite routes (air paths) for the air to stream down the mine to the operational areas and appropriate ways out of the mine when it has become inapposite for additional use. Mine fans could be mounted on return airshafts, intake airshafts, or both, either on the surface area or underground (Figure 2.1) [3].

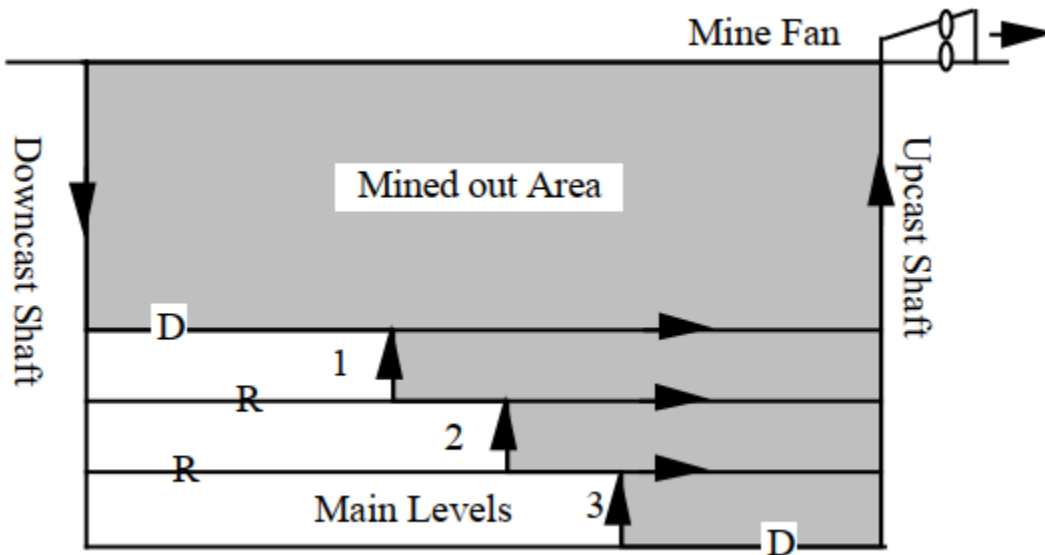


Figure 2.1: Primary underground ventilation system where D is a ventilation door or airlock, R is a mine regulator, and 1, 2, 3 are operational areas with a surface exhaust fan [3].

A well planned and appropriately executed ventilation system will make available favorable side effects (physiological and psychological) that increase workers' protection, comfort, healthiness, morale, and generally their enthusiasm to work more efficiently. In the ventilation system design, the quantity of the air that is required to flow to meet all standards of the health and safety has to be determined in the beginning. Once the amount needed has been calculated, the precise dimensions of shafts, the number of air paths and their design, and fans could be ascertained. Fresh air passes through intake air paths to the operational areas where the more considerable portions of contaminants are mixed with the air. The polluted airflow passes through returns airways. The pollutants' concentrations are not permitted to surpass obligatory threshold limits enacted by rules and law [3].

## 2.2 Coal mine methane (CMM) emissions:

The emissions of coal mine methane (CMM) are a dominant origin of greenhouse gas outpourings globally and stand for a remarkable chance for flourishing economically viable resources of energy [4].

Methane is one of the crucial constituents of natural gas and is a primary source of clean energy. It is also a powerful greenhouse gas (GHG), second in significance only to carbon dioxide, that reckons for 16% of all worldwide GHG emissions due to human activities (Figure 2.2) [4].

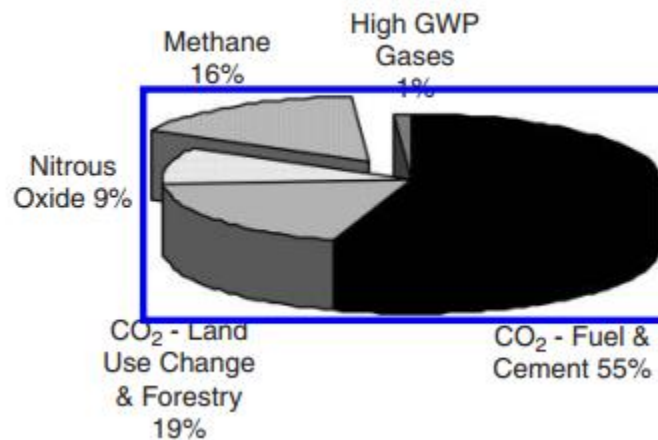


Figure 2.2: Global anthropogenic greenhouse gas emissions [4].

Widespread sustain for and allure in methane continues for several main reasons [4].

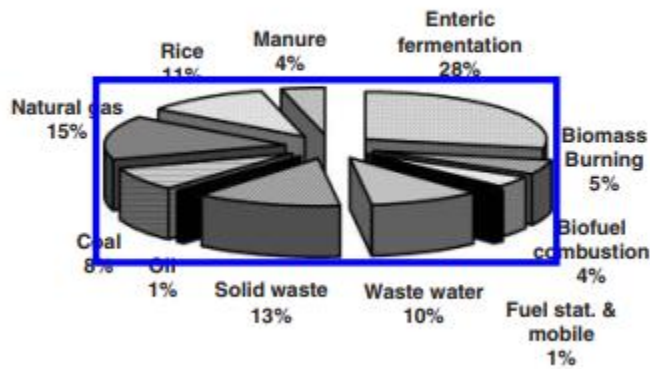


Figure 2.3: the allocation of global anthropogenic methane emissions Sources [4].

The sources of methane emission change, notably among different countries. For instance, coal mining and the production of rice are the two primary sources of methane emissions in China. In contrast, landfills are the most exceptional origin of emissions of methane in the United States.

The Coal Mine Methane Subcommittee identified four main types of obstacles that impede CMM project advancement in the first year of the Partnership:

1. need of proper information about project opportunities.

2. need of suitable technical knowledge and technology.

3. need of demonstration of the technical or economic feasibility.

4. need of financing or [4].

Some of these alternatives comprise natural gas pipeline injection, power production, co-firing in boilers, district heating, coal drying, and vehicle fuel. There are several interests and profits for recovering and using coal mine or other types of mine methane:

enhancing mine safety, decreasing greenhouse gas emissions, alleviating local air quality, supplying local energy resources, and improving mine productivity.

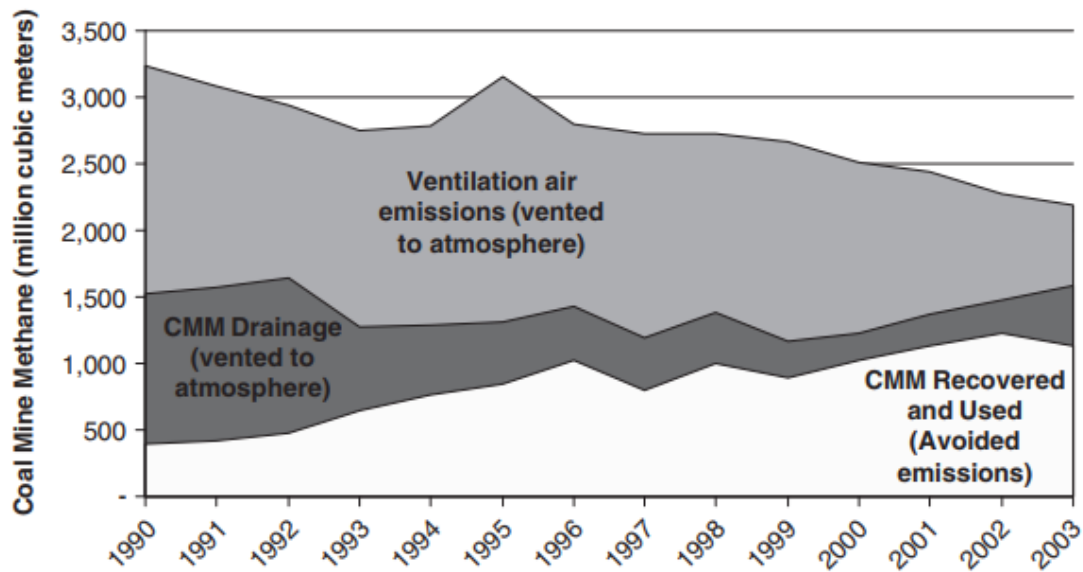


Figure 2.4: US Coal Mine Methane emissions since 1990 [4].

Although realistically, all CMM enterprises worldwide have used drained gas, the most significant origin of CMM emissions is from ventilation shafts. Although ventilation air methane (VAM) encompasses deficient concentrations of methane (usually below 1 percent), the sheer volume of ventilation air makes this the single most significant origin of coal mine methane [4].

### 2.3 Healthy environment for workers:

Deaths tend to happen after a long development, leading to one year of life expectancy is lost on average for these cases [18], [19]. One of the main origins of occupational illnesses in miners is emissions of dust, contaminants, heat, and water vapor that are inherent to production processes in the mining industries [15].

### 2.4 Intensity of dust emissions:

In terms of atmospheric contamination, groups of the dust are traditionally split into internal and external kinds. The emissions of external groups of dust contaminate the ground level air of mine sites, which will be debated later. Internal groups are positioned in working areas.

The dust emissions strength relies on the process operations' kind and the features of the reprocessed material (both physical and mechanical), as well as the dust control arrangements' availability.

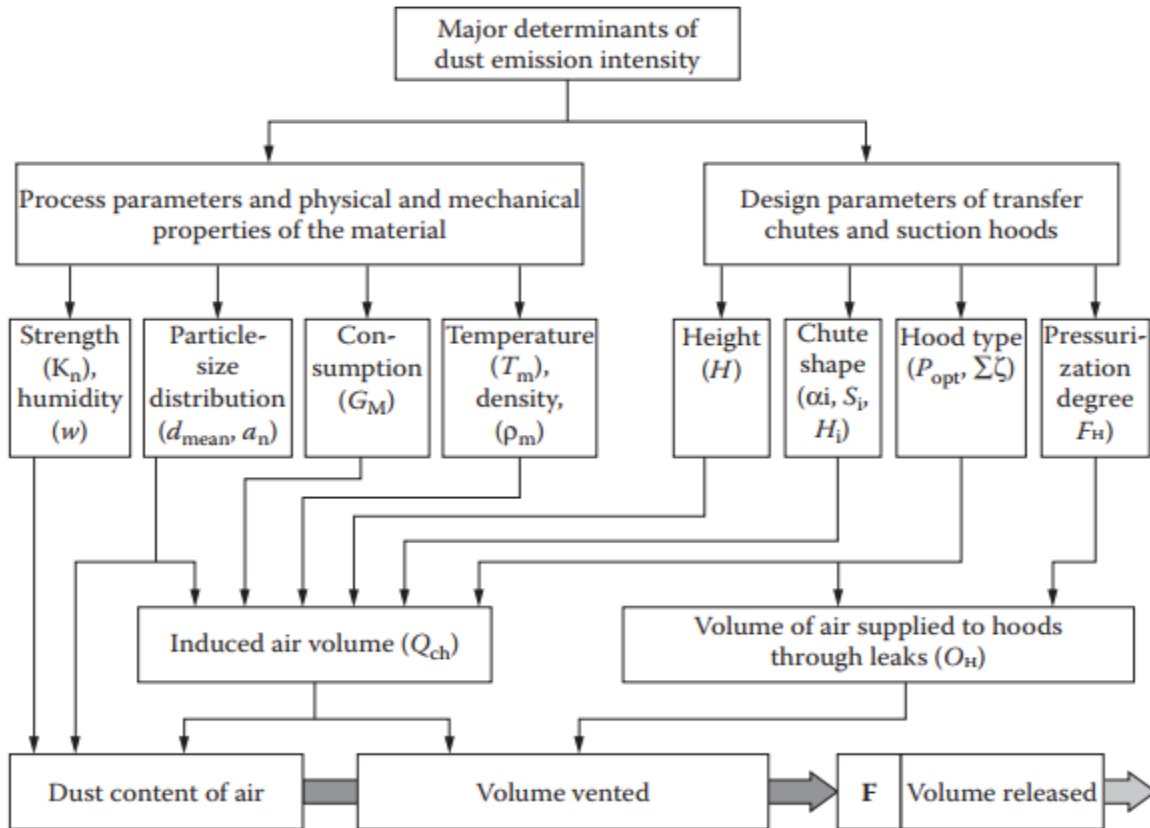


Figure 2.5: Gross dust emissions' significant determinants in the bulk materials' transfer [13].

The best universal and usual dedusting technique are aspiration utilized for managing loose substances at pretreatment plants of the ore. This makes certain free dust containment by the use of aspirated cowls with successive dust separation from air evacuated by suction [13].

### 2.5 Permissible exposure limits:

In coal mines, both operators of the coal mine and MSHA (the Mine Safety and Health Administration) collect dust samples using a size-selective sampling device (cyclone) that separates dust in a way that reflects the efficiency of deposition in the gas-exchange region of the lungs. This so-called "respirable size fraction" has a lung deposition efficiency of 100% at one  $\mu\text{m}$  or below, 50% at 5  $\mu\text{m}$ , and zero efficiencies for particles of 7  $\mu\text{m}$  and upward (NIOSH 1995).

The PEL (permissible exposure limit) is two  $\text{mg}/\text{m}^3$  for respirable dust of the coal mine, which is measured gravimetrically as an 8-hour TWA (time-weighted average) concentration. When the respirable silica (quartz) content surpasses 5%, this limit is reduced [21].

A respirable dust PEL has not been established for noncoal mines, but a nuisance dust standard of  $10\text{mg}/\text{m}^3$  is regulated. The nuisance dust sample is comprised of "total dust," which represents airborne particles that are not selectively collected concerning their size. However, respirable dust sampling is conducted in non-coal mines if potential

exposure to silica dust is suspected. If the silica content of the respirable dust sample exceeds 1%, the formula used to establish the dust PEL is 10 divided by (the percentage of silica + 2). Thus, a representative with eight pct silica would have a dust PEL of 1  $mg/m^3$  [21].

## **2.6 Explosions:**

Explosions may or may not be associated with a mine fire. In other words, an explosion may simply be an event in the mine, or it may occur as a result of an ongoing fire, or it may even lead to the development of a fire. A distinguishing characteristic of the explosion is the very rapid conversion of chemical energy to heat and mechanical work. Even a relatively small blast can blow out stoppings, bulkheads, and structural steel, and to displace heavy machinery.

In a typical description of an explosion, a shock wave expands out from the source of ignition. A methane, coal dust, and air mixture can produce a shock wave that travels as much as six times the speed of sound through the mine workings. Confinement is a physical factor to consider in explosion development. This shock wave begins to occur as the expanding gases accelerate into the ambient air. This can be exacerbated in the mining environment because the paths of release are limited (i.e., the mine opening dimensions are restricted) [21].

## **2.7 Mine gases:**

The engineer of the mine ventilation has to be noticed not only with the quantity of air the mine ventilation system can deliver but also with the chemical composition of the air. That part of total air conditioning dealing with the purity of air is termed quality control.

The control of air quality is often one of the more critical problems while planning or dealing with a mine ventilation system [22].

## **2.8 Heat sources and effects in mines (Need for air conditioning in mines):**

Temperature-humidity control, one of the three functions of total mine air conditioning, is essentially heat control. It consists of those processes that are designed to regulate the sensible- and latent-heat content of the air: heating, cooling, humidification, and dehumidification. Temperature-humidity control is akin to quality control, in that it pertains to the physical quality of the air. In contrast, quality control relates to the chemical quality of the air. The usual reason for employing air conditioning in mines is for comfort rather than product or operation purposes. The heat content of the air of the mine is sustained within restrictions set for the comfort, safety, and operational effectiveness of human beings. Occasionally, product air conditioning is employed, as in coal mines where slaking of the roof in the warm, moist, summer air, or in salt mines where excessive absorption of moisture by the mineral product may constitute environmental problems.

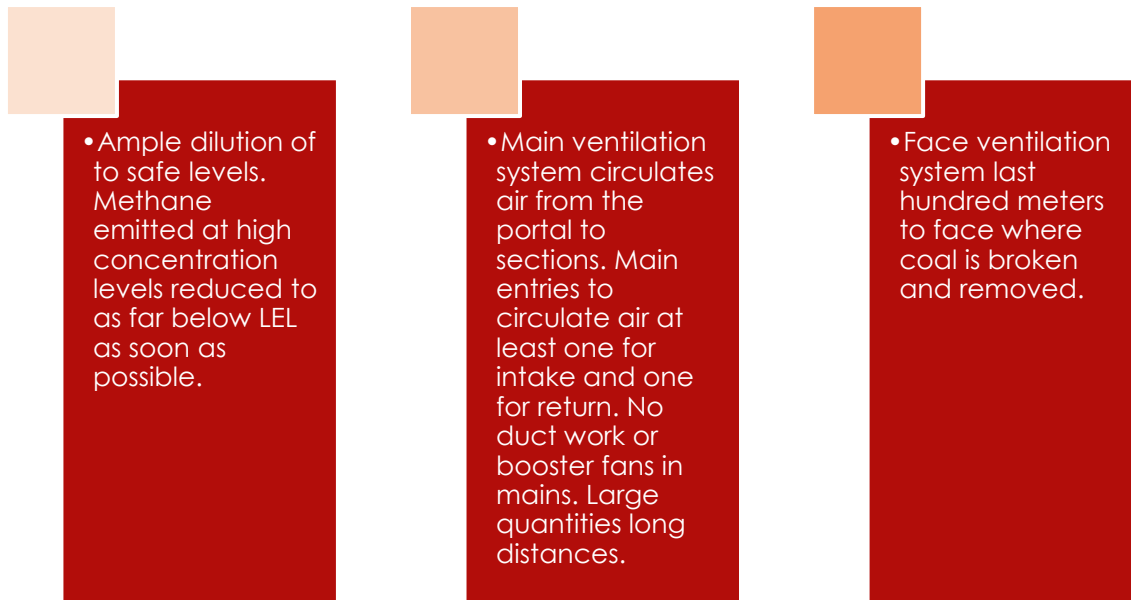
When ventilation alone is insufficient to sustain atmospheric-heat standards at acceptable levels, air conditioning of the mine for temperature-humidity control becomes essential. The number of mines and mining districts finding it necessary to condition the air, although still small, has risen sharply in the last few decades. Air conditioning can be expected to play an increasingly important role in mining under the increasingly hostile environmental conditions now being encountered underground [22].

# Chapter 3

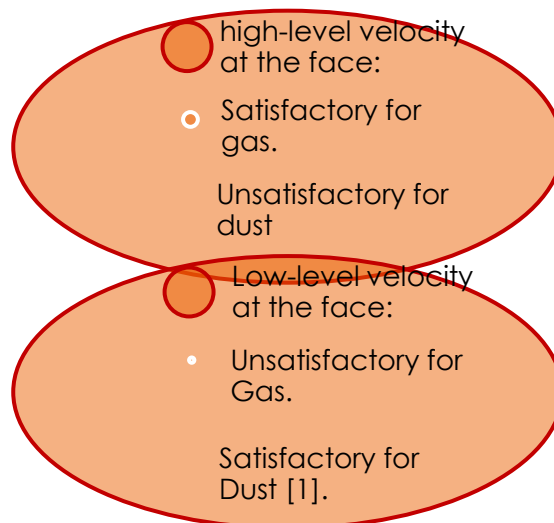
## Typical mine ventilation circuits in underground mining

### 3.1 Ventilation design criteria for making gassy mines safe [39]:

Appropriate if:



### 3.2 Face ventilation:



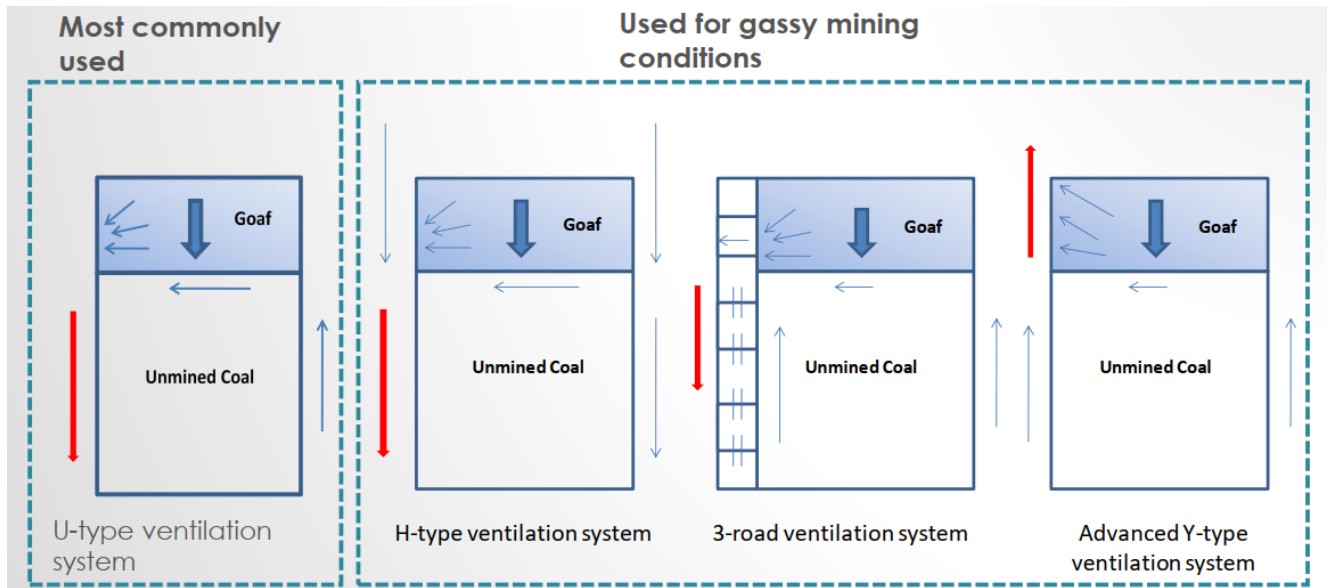


Figure 3.1: Different types of ventilation systems [39].

### 3.3 Airflow must be controlled to minimize dust transport:

#### 3.3.1 Regulations related to dust concentration in air:

- Was  $1 \text{ mg/m}^3$ .
- Became  $0.5 \text{ mg/m}^3$  in 2016 [2].

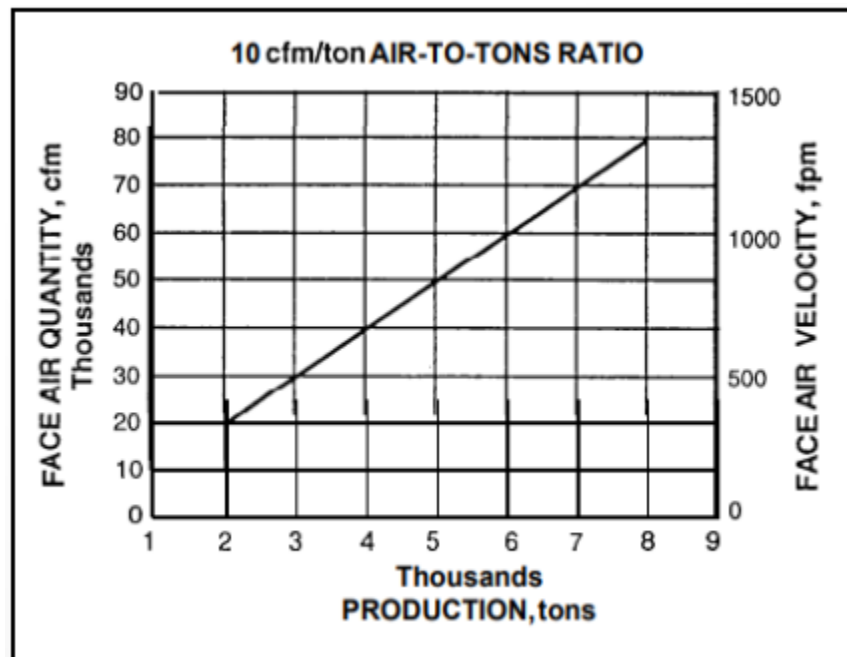


Figure 3.2: Airflows required per production mass at the face [39].

Calculate airflow:

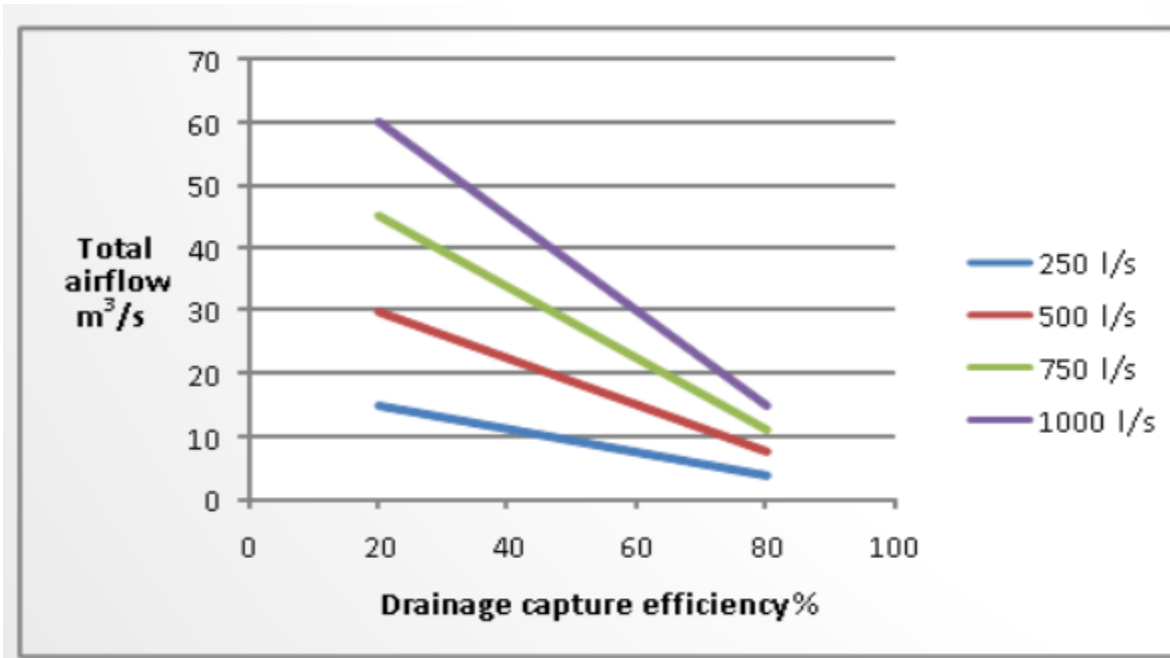


Figure 3.3: Airflows required for diluting longwall methane emissions to 2% [2].

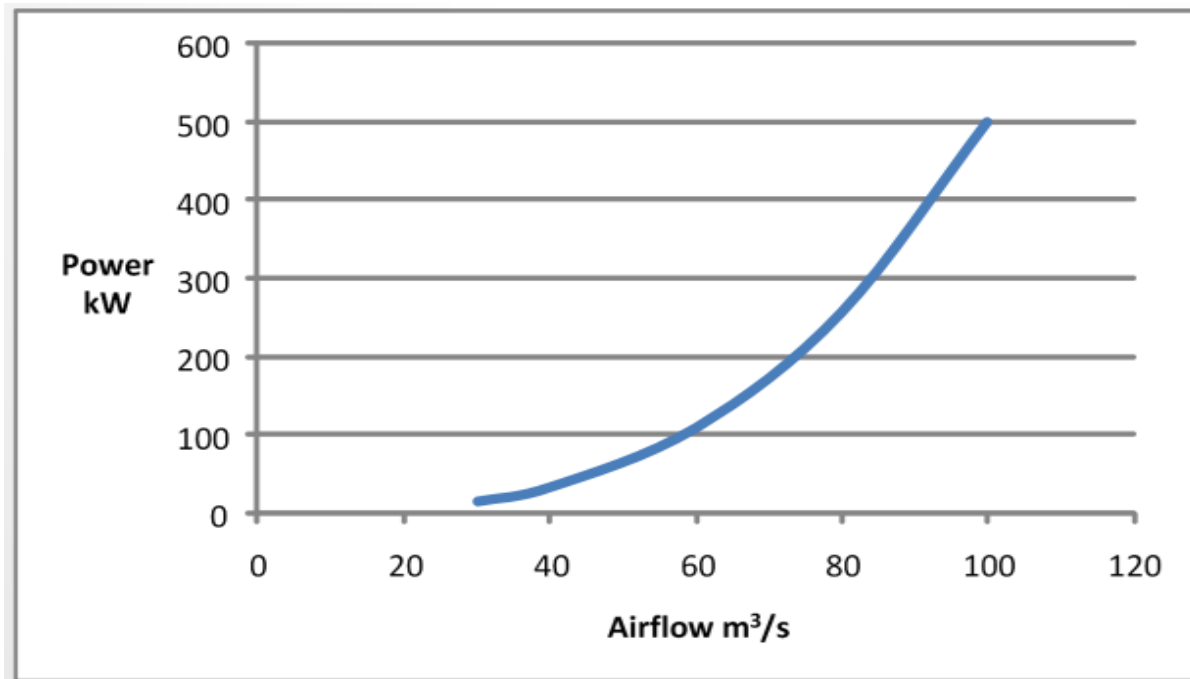


Figure 3.4: Example of power requirements for ventilation air [2].

Air always passes through the route of least resistance; however, it might not be where that is needed for usage. To conduct the air where is required, devices for ventilation are essential; the necessary means of providing and managing the airstream for the

whole structure are fans. Moreover, several other controls plan also are requisite for successful air dispersal in underground, which will be discussed later.

Any ventilation system's purpose is two-fold. On the one hand, the primary ventilation has to direct the air via the central air paths to the operational area out by the working faces, hence, providing fresh air for ventilation of the face, then return the polluted air via return air paths to the atmosphere. On the other hand, the ventilation system of the face has to be sketched to efficaciously use the air that is available in the immediate operational zone to clean the working face, to catch and eliminate dust, and to attenuate and carry away gas, if any, released during mining operations. Leaning on the kind of mine and local geology nature, layouts of the ventilation could be split into two broad groupings; 1. a U-tube arrangement or 2. a through-flow system (Figure 3.5, McPherson, 1993). Figure 3.5a represents a primary U-tube arrangement where air passes via the operational area, then comes back through adjoining air paths. Usually, long pillars and stoppings go between them to separate them from intakes. Stoppings' access doors make traffic between consumption and return air paths easier. This disposition's variation would be longwall and room and pillar type mining methods. The other arrangement is observed in Figure 3.5b, where intakes and returns often are geographically partitioned from adjoining air paths, which are either all intakes or returns. Although fewer airways and stoppings are required due to the geographical separation, which usually leads to fewer boosters, current air regulations and air leakage might be necessary for airstream management in operational zones (McPherson, 1993) [3].

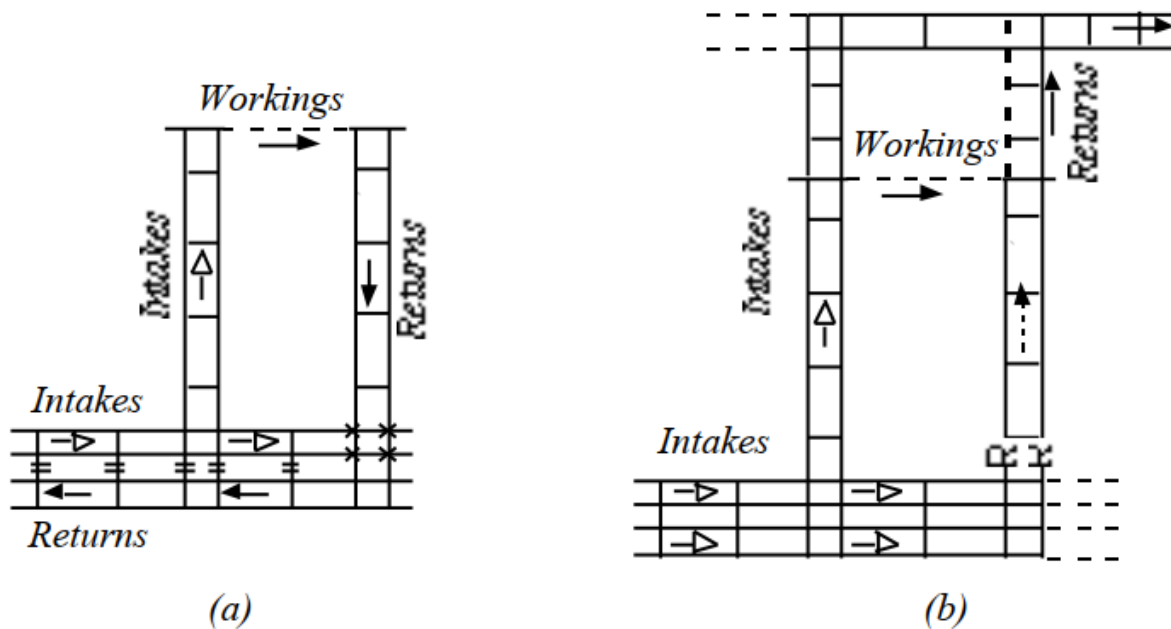


Figure 3.5: Elementary ventilation systems (a) U-tube and (b) through-flow (McPherson, 1993) [3].

Actual layouts underground can be variants of any one system or an amalgamation of the two systems.

### 3.4 For stratified deposits:

Most of the underground mines mining tabular forms of orebodies (coal, potash, limestone, salt, etc.) commonly utilize one of two techniques, room and pillar or longwall mining. While original layouts could differ meaningfully from mine to mine and zone to zone based on circumstances of the local geology, the original sketch for these techniques remains the same. The subsequent sectors delineate the airstream dispersal system commonly used.

### 3.4.1 Longwall systems:

Figure 3.6 illustrates some of the frequently utilized layouts of the ventilation used on longwall segments [3].

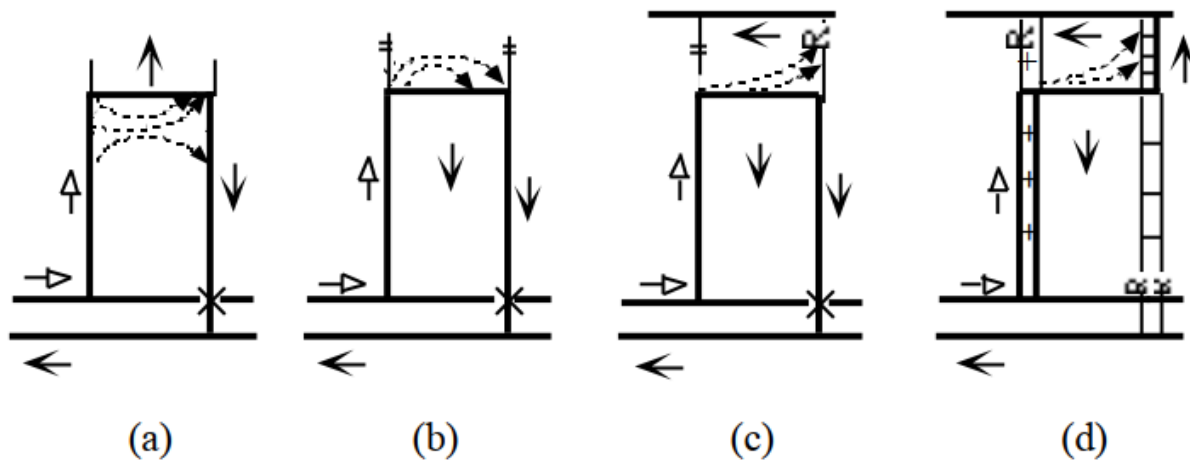


Figure 3.6: Arrangements of longwall ventilation systems: (a) single-entry advancing; (b) Single-entry retreating; (c) single-entry retreating with back bleeder; (d) double-entry retreating with back bleeder (McPherson, 1993) [3].

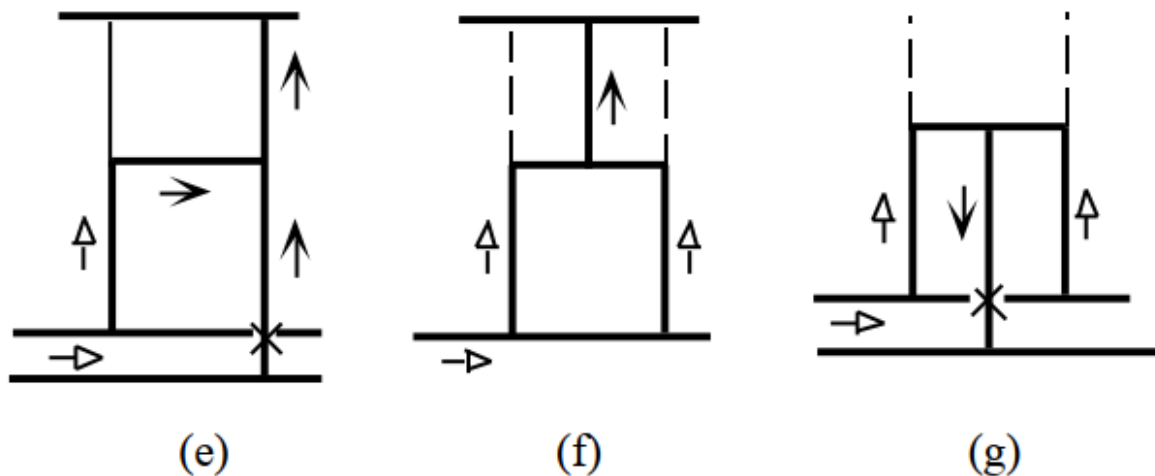


Figure 3.7: Groupings of longwall ventilation systems: (e) Y system; (f) double Z system; (g) W system. (McPherson, 1993) [3].

### 3.4.2 Room and pillar systems:

Figure 3.8 represents two techniques to ventilate a room and pillar advancement panel in a coal mine where several entrances are operated. Figure 3.6 is the directional, or W-system, in which intake air routes are air paths in the panel's central slice, with return air paths on both sides, usually directed as the fish-tail technique. The technique in figure 3.8b is the unidirectional system in which intake and return are positioned on both sides of the neutral airpath.

In U.S. coal mines, the air in these entrances is not considered to be utilized for ventilation of operational areas; hence, they are directed to the return air path via a regulator. An evident weakness is that we need double stoppings compared with the uni-directional system. Also, we can observe twice air leakage compared with the extra stoppings (McPherson, 1993).

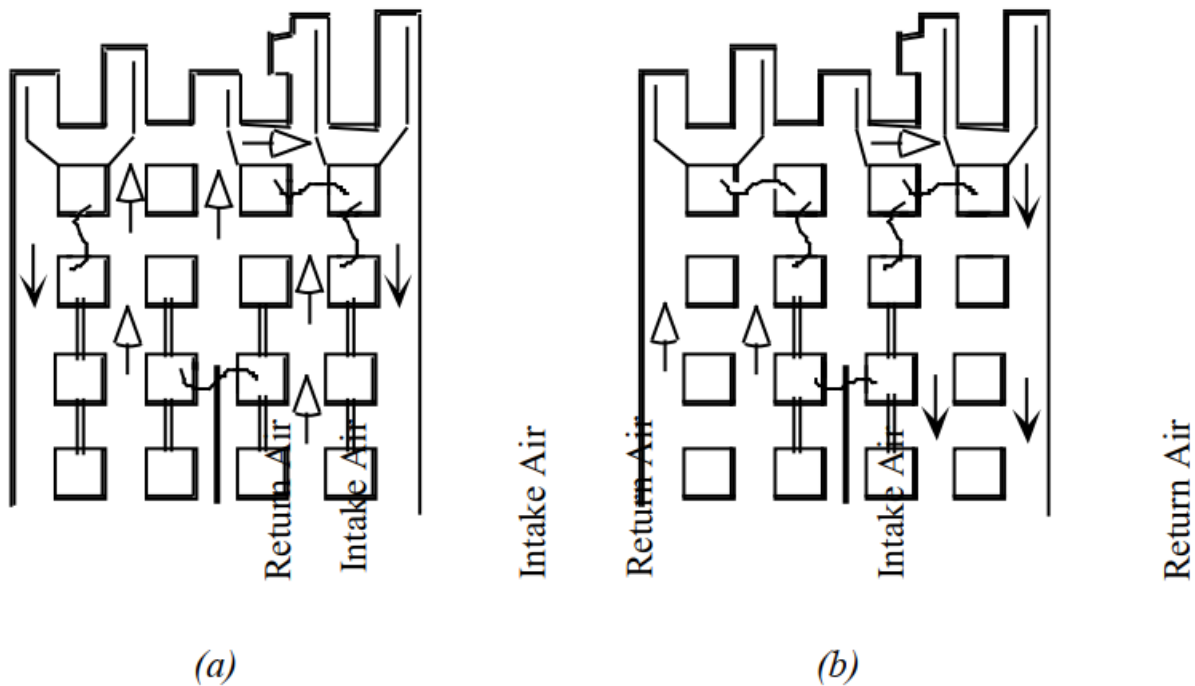


Figure 3.8: Room and pillar development with line brattices to control airstream in conveyor belt entry: (a) bi-directional system; (b) uni-directional system [3].

### 3.4.3 Mine with large size entries:

Naturally, mines with huge dimensions entrances demand vast ventilating air volume rate to ventilate underground operations appropriately. In trying to encounter this necessity, two significant issues often come across: local air recirculation and air leakage through stoppings, both of which are due to inappropriately built (and maintained) stoppings, or in many cases, the absence of the adequate number of stoppings, and both could adversely influence the underground operational area. Frequently, management of the mine is reluctant to lack of stoppings, either due to technical issues or the related costs. Every logical measure must be taken into consideration to guarantee that fresh air is efficaciously transferred to operational areas where the air is required. The consequence of not maintaining proper ventilation is a low functional area that is not only in federal and state law violations but could unfavorably influence employee efficiency and productivity. To direct fresh air to

operational areas over large spaces, control devices are needed. The accurate and exact expense of building conventional metal-frame stoppings in a 35 ft wide by 20 ft high entrance is hard to acquire due to the several parameters included. In many instances, curtains of brattice are the only solid substances for underground use; the cost of these brattice curtains varies from \$1,500 to \$3,000 per stopping (1997 dollars). The price involves the expense of workers and substances. However, these stoppings are exposed to more significant leakage among the strips of brattice and around the peripherals. Leakage differs relying on several parameters, such as workmanship, maintenance, mining practices (stoppings too close to the operational environment will suffer common blasting damage), and, to a lesser extent, features of the geology (roof sagging and bottom heaving could damage stoppings) which will be discussed later (Figure 3.9).

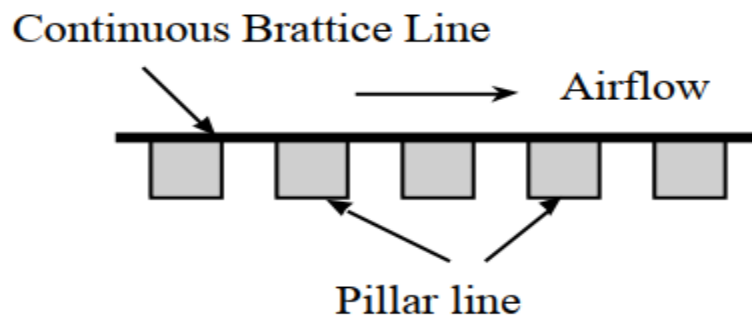


Figure 3.9: Continuous brattice curtains line will diminish leakage around peripherals [3].

Even though the undeniable influence on the cost of the power caused by leakage is hard to implement, it is recognized to be notable. Since any leakage via a stopping must be reimbursed by "pumping" additional air underground to satisfy safety needs, it will intensely enhance demands for the energy at the fan due to the fact that the power of the fan and quantity of the air has a cubic relationship. For example, a 26% rise in the air stream doubles the cost of the airpower. Other kinds of expenses of the stoppings also could be evaluated approximately using published information (Adam et al., 1987; Thimons et al., 1988). A modular arrangement gives an alternative. In this layout, it deliberately leaves massive barrier pillars at four sides of a preplanned block of mining; thus, air could be effectually directed over larger spaces. The next drawing (Figure 3.10) presents a theoretical mine operation with a modular arrangement [3].

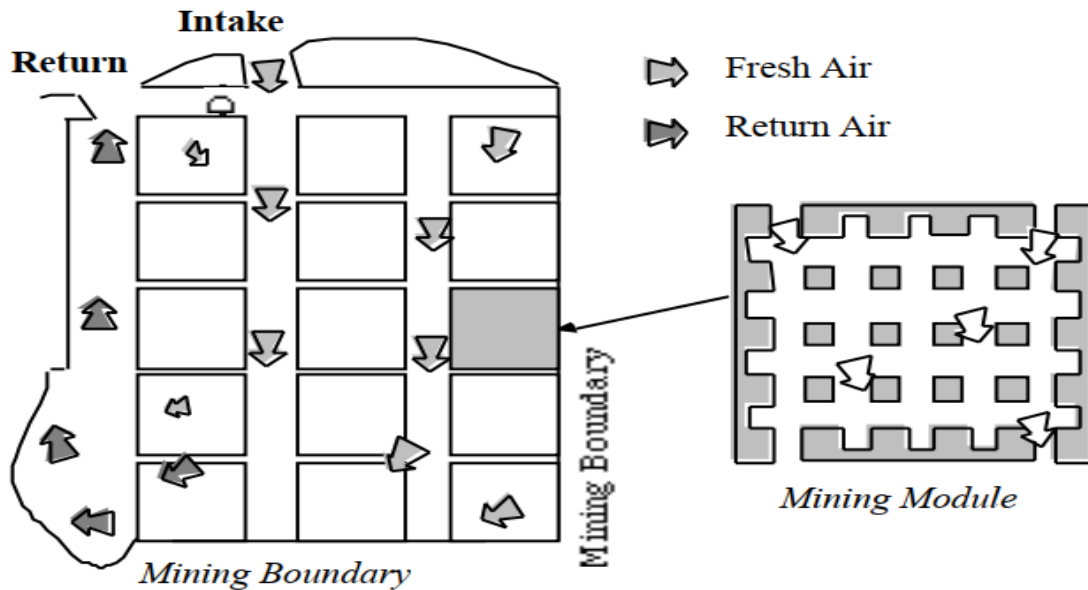


Figure 3.10: A theoretical underground mine of limestone where a module system is used instead of stoppings to direct air to working areas [3].

#### 3.4.4 Recirculation of air underground:

In addition to inappropriately constructed and inadequately maintained stoppings, another considerable origin of recirculation of the air in the underground is inappropriate mine organization [38]. One of the frequently experienced designing errors in underground limestone workings is that the central intake and return air paths are sited beside each other, generating recirculation of the exhaust air back into the intake airpath(s). This condition is worsened when a box cut, usually utilized in limestone and coal mines where ore crops out, is being used for entering the tunnel. The air cannot be expelled from the intake environment. At the early phase of the mine development, the central intake and return air paths have to be positioned close by each other, and it will be at least some years before an air shaft could be drilled some distance from the portal and the whole ventilation circuit could be accomplished. It is approved that intake and returns in the portal environments be physically separated in the startup of the mine to prevent air recirculation (Figure 3.11) [3].

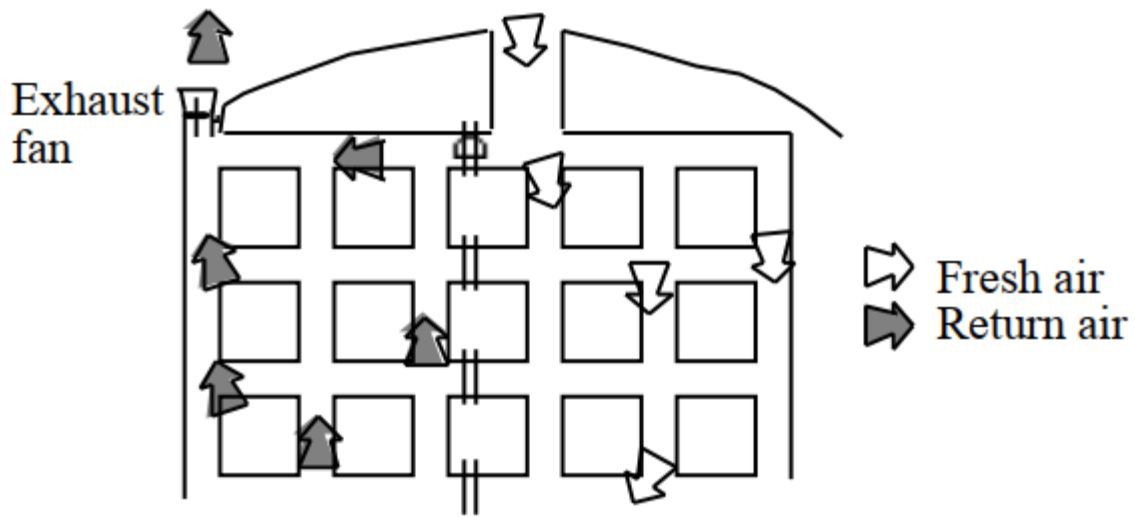


Figure 3.11: Fan duct is used to deflect exhaust air and to recover lost velocity pressure [3].

If this is not feasible, and both intake and return must be placed adjacent to each other at the bottom of the box cut, Figure 3.12 depicts a surrogate technique of segregating intake air and return air by the operation of a vertical fan duct at the discharge end of the exhaust fan.

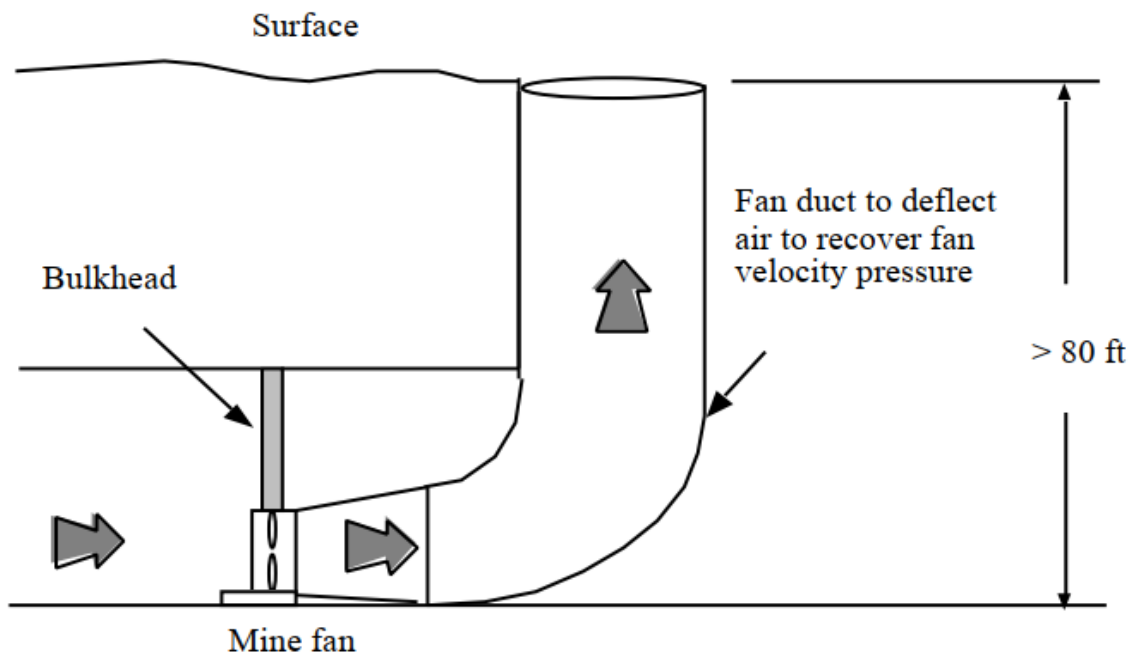


Figure 3.12: Fan duct is used to deflect exhaust air and to recover lost velocity pressure [3].

Figure 3.12 delineates a recommended layout where exhaust air is deviated upward, utilizing a vertical duct (evase) at least 80 feet in length. The evase also serves a

further profitable aim: it could improve fan velocity pressure, which otherwise would be lost. To prevent additional shock losses, the connecting bend has to be round and smooth.

Figures 3.13 and 3.14 depict the seasonal influences for a prior study in a coal mine where the roof was a shale.

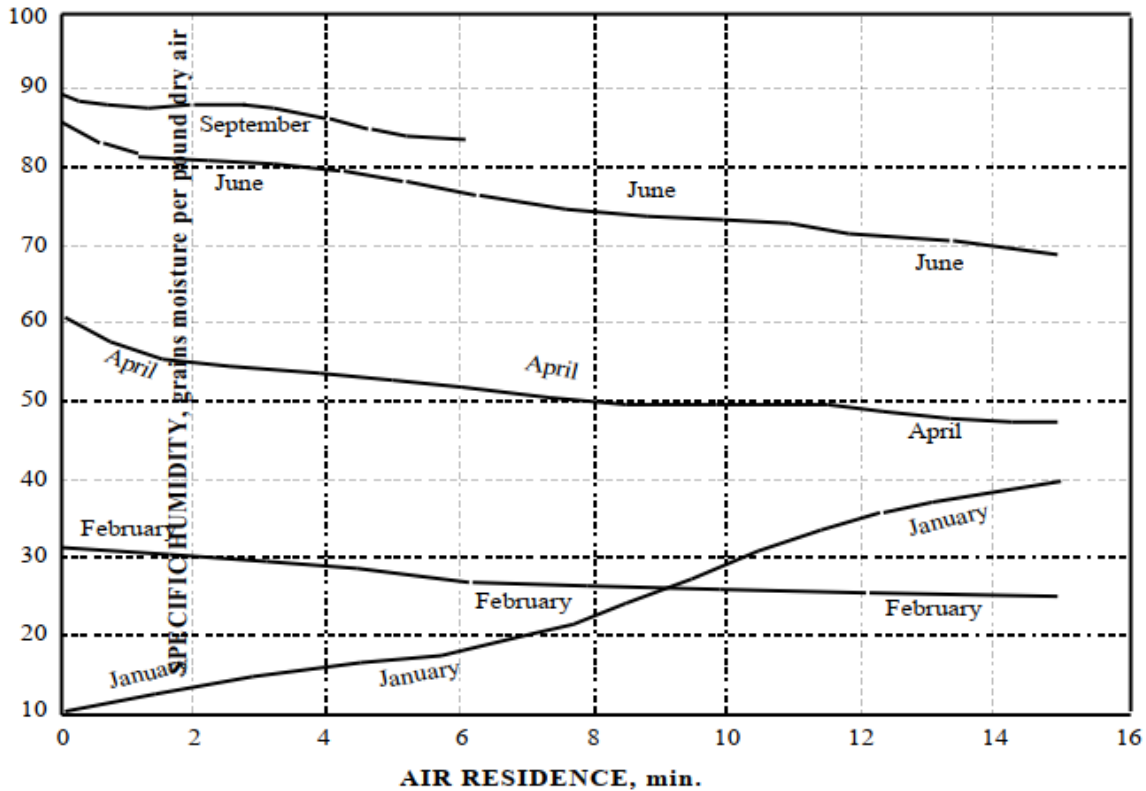


Figure 3.13: Changes in mine air specific humidity as a function of air residence time [3].

The exchanges of moisture between incoming air and surrounding rocks are particular for each site. Although the precise moisture soaking features of the foundation are not well defined, studies on shale in other mines could be utilized as a benchmark to logically evaluate their interactions (Cummings et al., 1983) [3].

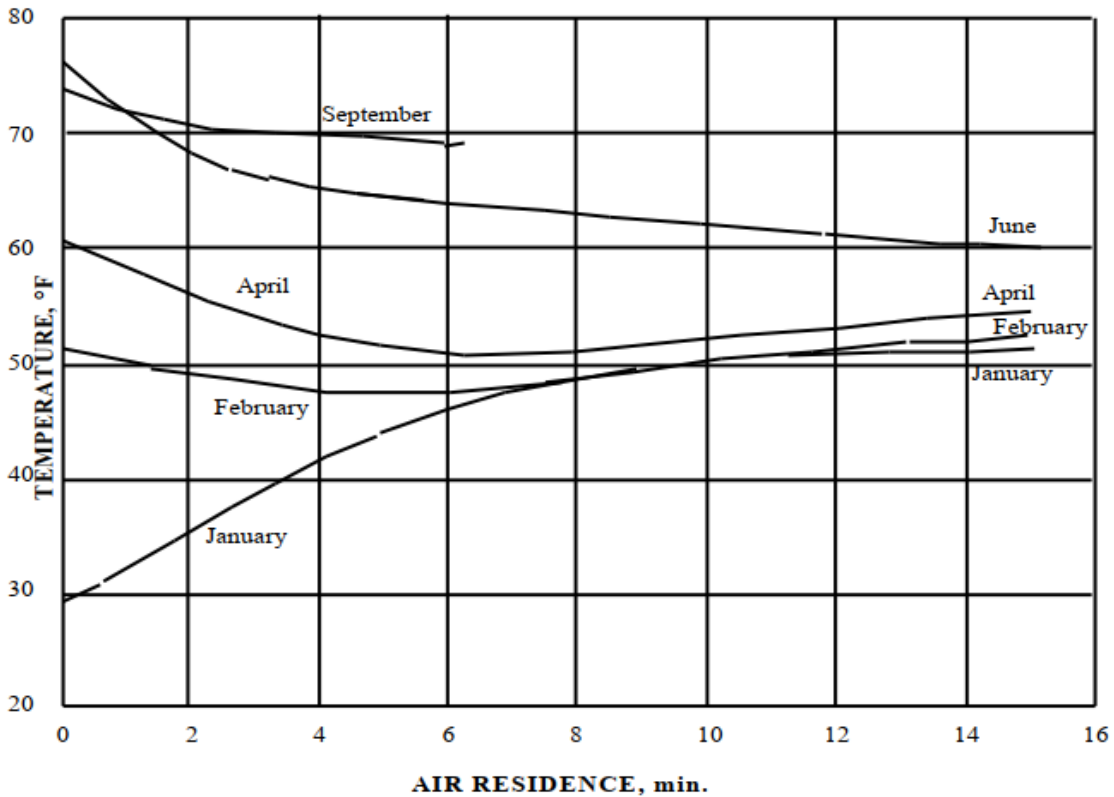


Figure 3.14: Changes in mine air temperature as a function of air residence time [3].

### 3.5 Orebody deposits:

The grade disparity in metal mines and the fluctuating market of metals entails that more stopes or working areas be developed than would give the impression of being ineluctable, while with perhaps only a fraction of them operating on any one shift (McPherson, 1993).

Networks of ventilation for metal mines have a tendency to be more complicated than for stratified deposits and often are also three dimensional. Figure 3.15 elucidates the ventilation design of many metal mines, despite the fact that the real geometry will differ widely [3].

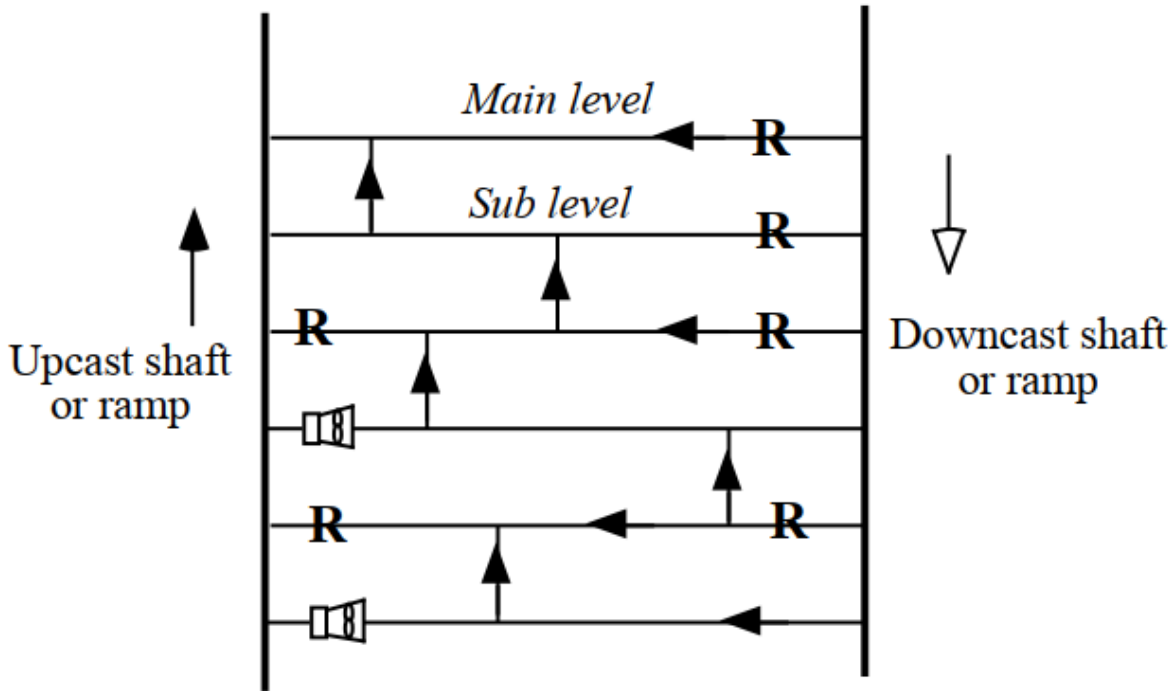


Figure 3.15: Section showing the ventilation system for a metal mine [3].

Airstream dissemination systems for individual stopes also are subject to enormous variability, depending on the dimension, geometry, and grade difference of the orebody. Series ventilation between stopes have to be kept, thus blasting gases could be discharged rapidly and effectively (Figure 3.16).

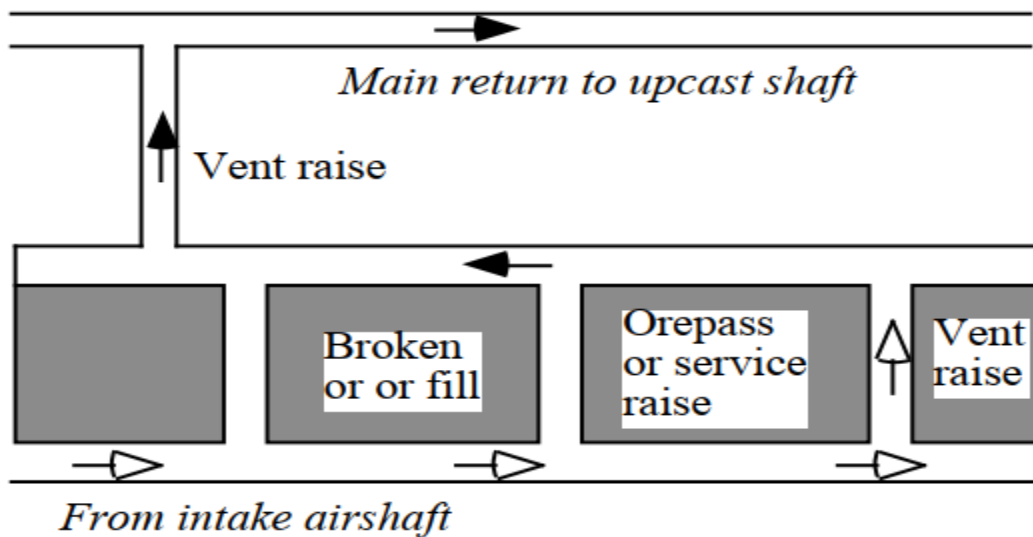


Figure 3.16: An example of a simple ventilation system for shrinkage or cut-and-fill stopes [3].

Concerning fan positions and airstream route, there are three ventilation systems: exhaust (pull) system, where the mine fan is sited on top of the return air shaft; blowing (push) system, with the mine fan placed at the intake air shaft; and combined system (push-pull), with fans on both the intake and return airshafts. This point out the main ventilation systems only; local organizations, for instance, a face ventilation system for an operational environment, could be different from the central system. Depending on the specific plan, the pressure of the mine can be either negative (exhausting system, since the fan generates a suction in the design, putting mine pressure less than the atmospheric datum) or positive (blowing approach). The reason for this is the fact that the mine pressure is assessed against atmospheric pressure, as shown in Figure 3.17:

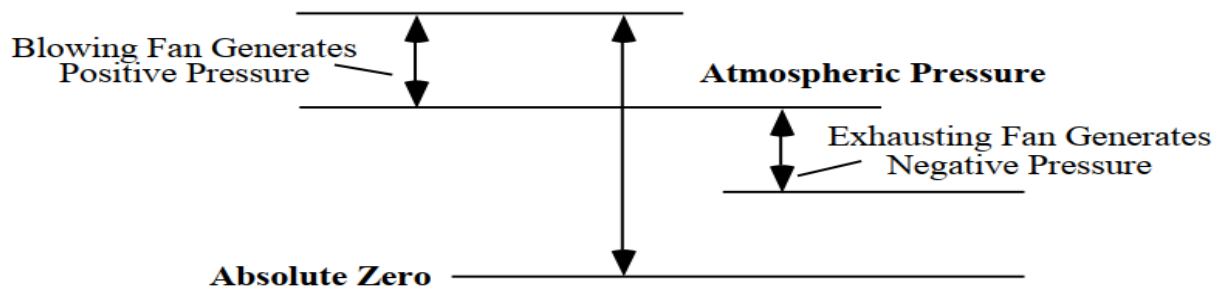


Figure 3.17: Diagram showing a positive pressure of mine for blowing system and a negative pressure of mine for the exhausting approach [3].

### 3.6 Airstream direction:

Airstream direction is influenced by the position of the main fan, which, in turn, will remarkably influence the other sides of working or transportation. On the one hand, the antitropal system is one in which the airstream and transported rock move in reverse directions, hinting that mineral transportation is carried out in intake air paths. This shows a tendency to put limitations on the air velocities in intake air paths so that dust and other fumes will not be too excessive. On the other hand, a homotropal system is one where the airstream and the mined rock are transferred in the same direction, or the haulage is carried out in return air paths. This system will ensure that dust, heat, and other contaminants from the broken rock will be vented directly to the outside. Moreover, this system also is beneficial in case of being met with fire in the haulage way. Another element in the airstream direction is the inclination of the airpath. When the airstream is pushed upwards via inclined workings, it's called ascensional ventilation [3].

### 3.7 Ventilation planning/designing:

The ultimate purpose of ventilation designing is to plan a system that will be able to appropriately ventilate all operational faces, air paths, and underground environments at least expenses. A suitable mine ventilation system always initiates with the first development of the mining design, which still must have alternatives. Figure 3.18 depicts a primary model for designing a new underground mine (Viljoen, 1990). Despite many factors enter into a final ventilation planning scheme, minimizing friction and shock losses are the two most dominant among all the items considered.

### 3.7.1 To minimize friction losses:

From the equation:

$$R = \frac{KPL}{5.2A^3N^2} \quad (3.1)$$

Anything that could reduce K, P, and L and enhance A and N will diminish R, and eventually reduce expenses in terms of having lower total ventilation pressure, perceiving that there will be practical and feasible restrictions.

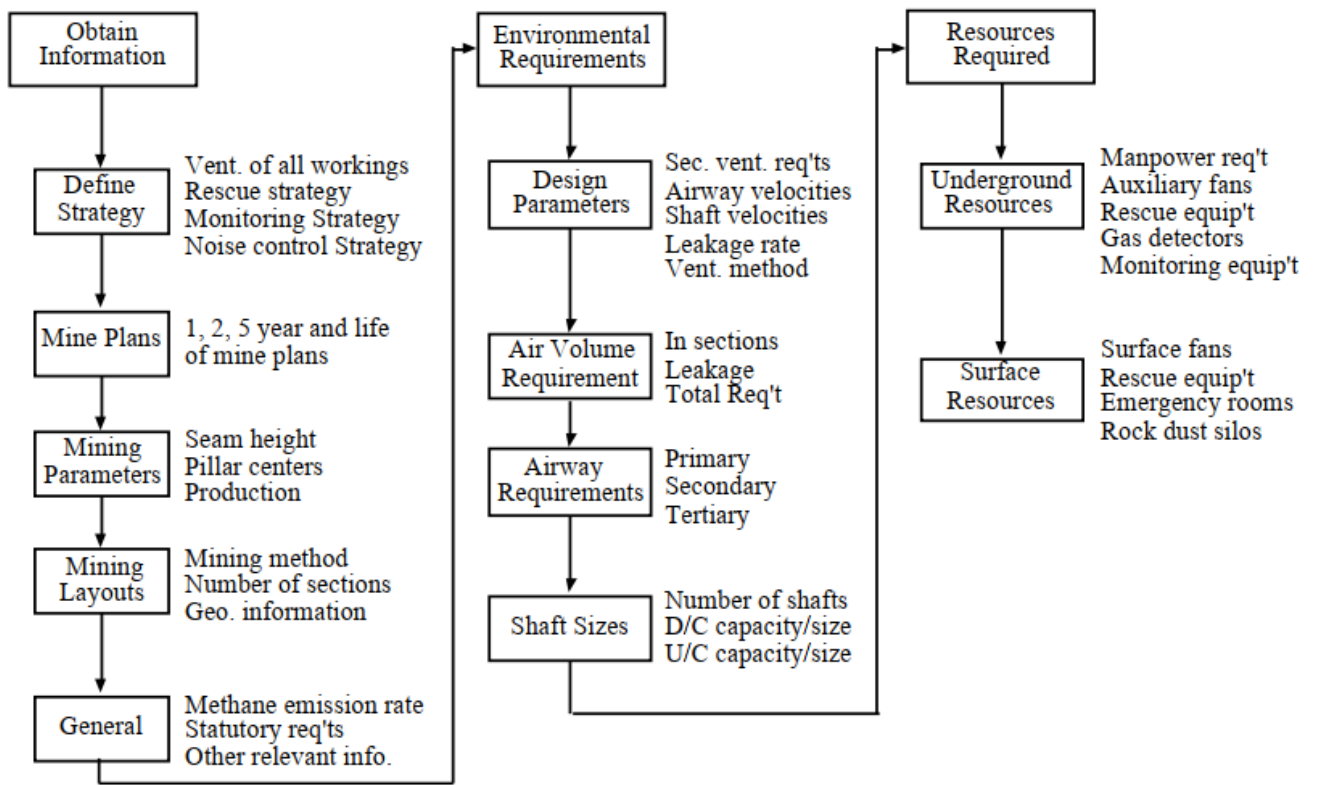


Figure 3.18: Factors considered in planning a new mine (Viljoen, 1990) [3].

### 3.7.2 To minimize shock losses:

Since up to 30% of entire injuries underground originate in shock losses, shock losses must be reduced to diminish expenses. From the equation:

$$H_x = X \cdot H_v \quad (3.2)$$

Achieving this goal, it is clear that to reduce the shock loss factor, X, for given air velocity. This could be accomplished by rounding off corners, keeping away from unexpected air velocity and airstream direction changes, etc. [3].

# Chapter 4

## Methods of dimensioning fans and other devices inside an underground mine

Maybe the remarkable characteristic of more recent tunnels has been the nearly universal utilization of axial flow fans [9].

### 4.1 Active devices:

#### 4.1.1 Main fans:



Figure 4.1: Mine primary centrifugal air fans (AIRENG Pty Ltd).

Fans are the principal means of generating and managing ventilation airstream. Main fans control all the air flowed in the mine and are often positioned at or close to the surface [40].

---

Main fan systems could be:

Forcing

---

Exhausting

---

Push-pull  
(a combination of the two)

---

Surface fans have the following advantages:

• Simpler testing.

• Simpler installation.

• Simpler maintenance.

• Easier access.

• Better protection in an emergency situation.

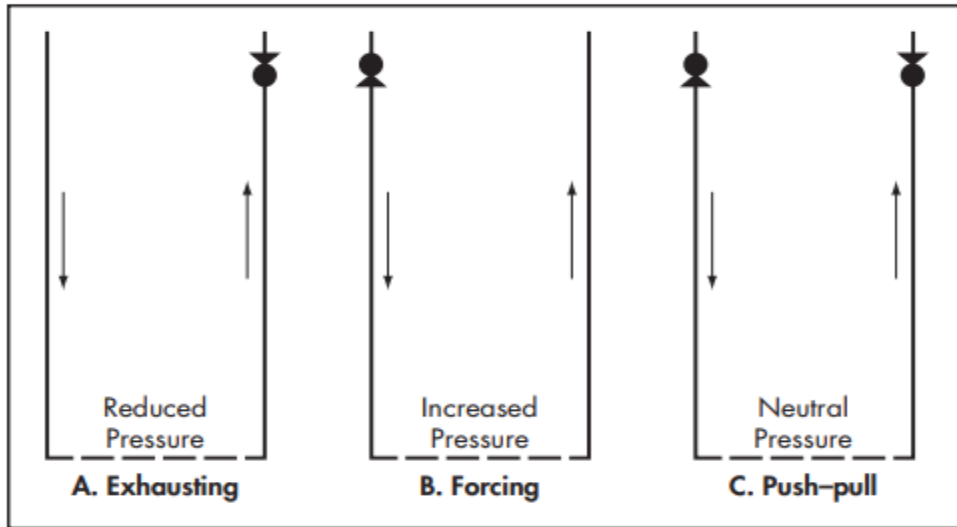


Figure 4.2: Possible locations for main fans [23].

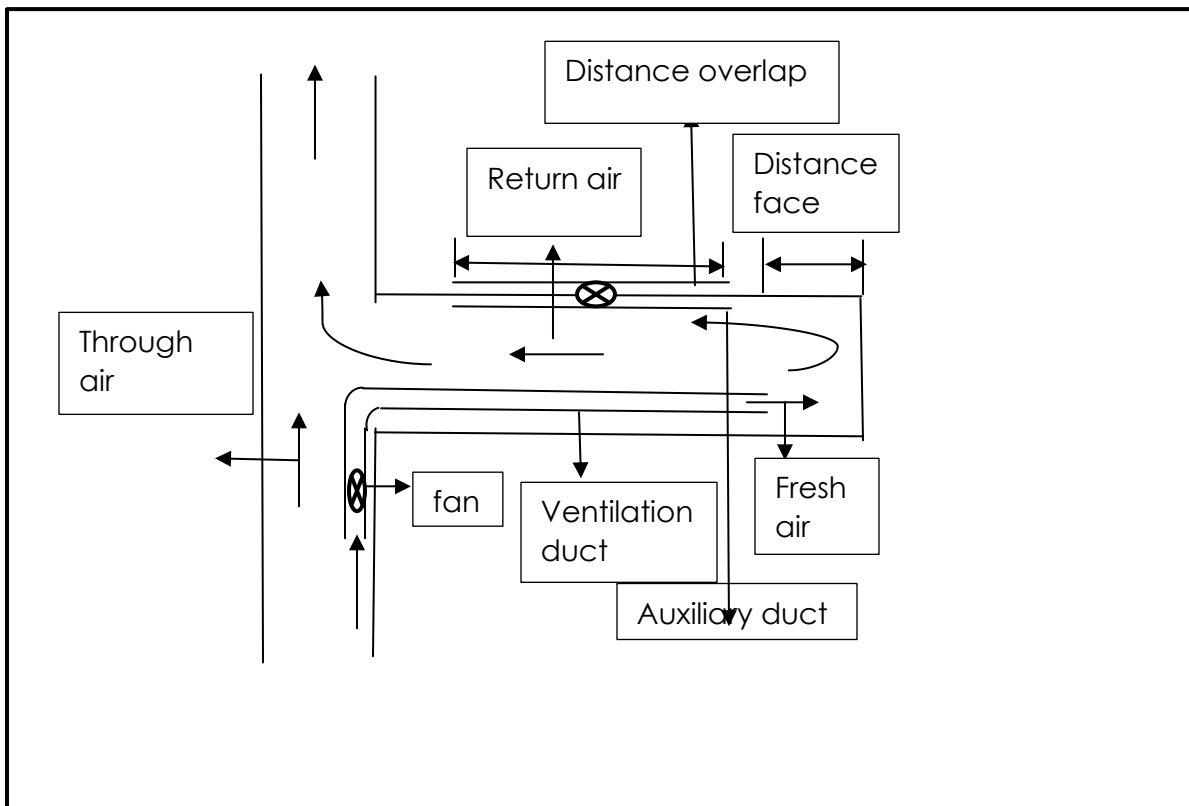


Figure 4.3: Forcing Overlap System (Zhang et al., 2011).

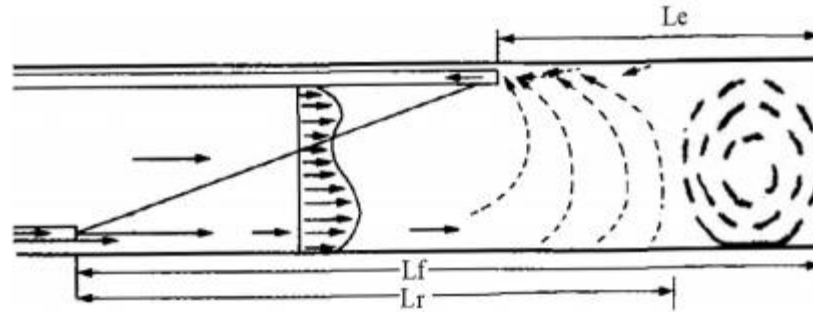


Figure 4.4: The airflow distribution in the push-pull ventilation system (Based on Niu et al., 2006; Wang, 2008).

Main fans could be sited underground when the noise of the fan is supposed to be an issue or if shafts require to be entirely free of airlocks. Underground fans lead to additional issues related to extra doors, airlocks, and leakage routes. The choice of surface main fan place is elucidated in Figure 4.2. In Figure 4.2A, exhaust ventilation connects the central fan to the upcast shafts; in Figure 4.2B, forcing ventilation connects the main fans to the downcast shaft; and in Figure 4.2C, push-pull ventilation connects main fans to both the upcast and downcast shafts. Most mines ventilate utilizing exhaust ventilation (i.e., linking the central fan to the exhaust shaft).



Figure 4.5: Mine auxiliary fan "Hurricane" (AIRENG Pty Ltd).

#### 4.1.2 What is a fan?

Fans are assembled in all shapes and dimensions. They run from the very lowest to high speeds. Their operations are just as disparate. While it might be clear, let us, therefore, have a broader definition, on which hopefully we can all agree, of what we are talking about. That enshrined in Eurovent 1/1 and ISO 13348 is as follows:

"A fan is a rotary-bladed machine that receives mechanical energy and utilizes it employing one or more impellers fitted with blades to maintain a continuous flow of air

or other gas passing through it and whose work per unit mass does not normally exceed 25 kJ/kg."

There is, as has been formerly declared, a diversity of fan designs, but realistically and for the sake of Fans & Ventilation, we might identify five generically different types (Figure 4.6) distinguished by their impellers and the flow through them:

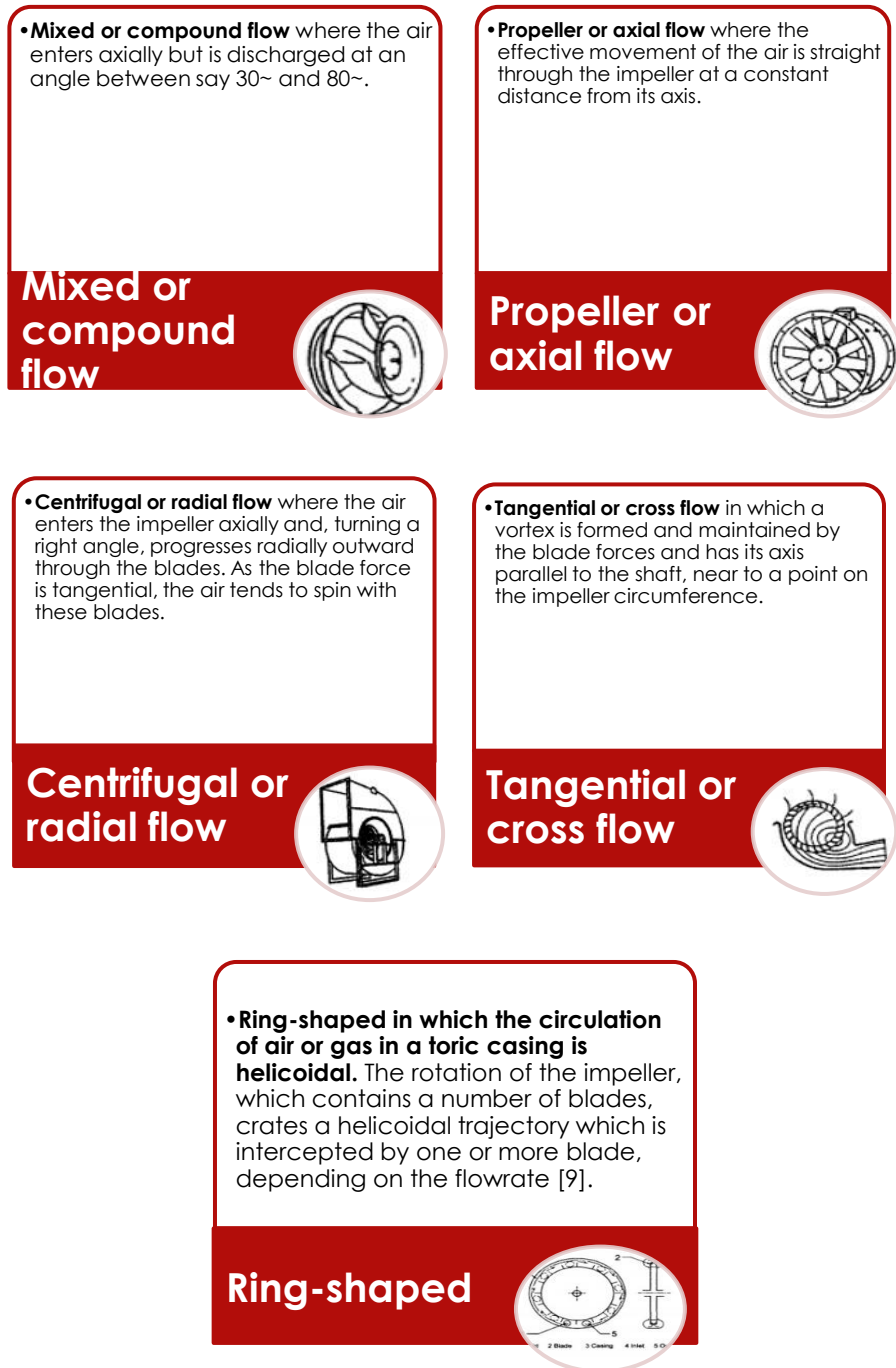


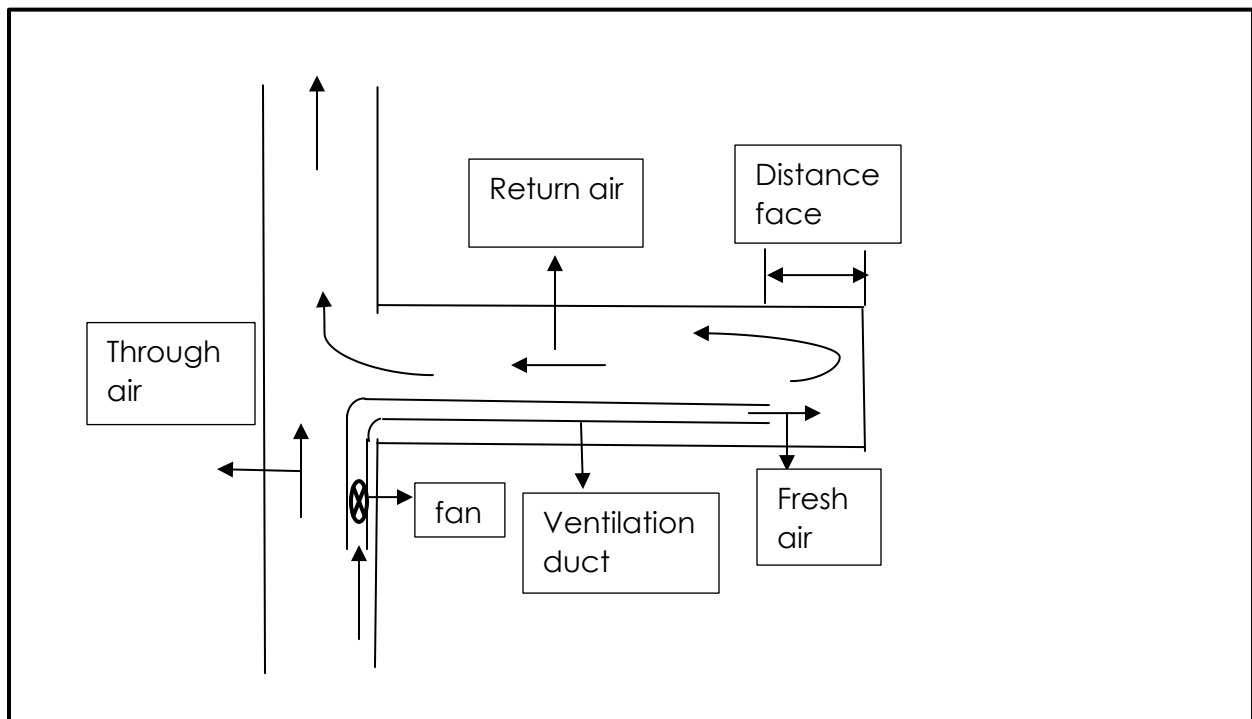
Figure 4.6: The five main generic fan types [29].

#### 4.1.3 Air stream:

- Air always flows from the point of higher pressure to lower pressure.
- Blowing fans generate a high-pressure point instantly in by the fan.
- Exhausting fans generate a low-pressure point instantly in by the fan.

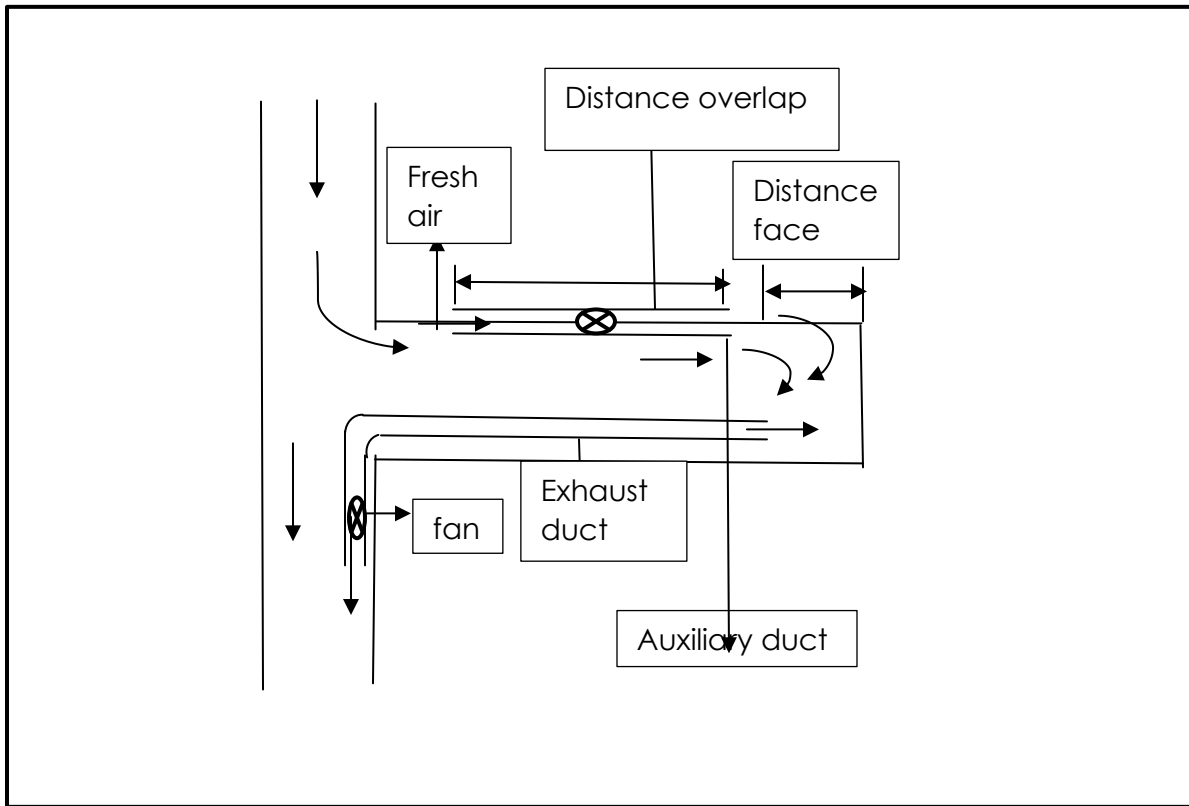
#### 4.1.4 Blowing fan:

- Neutral streams to outside. Smoke will not move to the face area.
- Gob area is “pressurized”. Less influx of pollutants from gobs until fan stops.
- Harder to maintain needed LOC quantities.
- Best for mining close to old workings [29].



#### 4.1.5 Exhausting fan:

- Neutral flows toward the face. Smoke will move toward the face area.
- Gob area is “under suction”. Pollutants flow from gobs until the fan stops.
- Easier to maintain needed LOC quantities.
- Worse for mining close old workings [29].



#### 4.1.6 Augment ventilation with gas drainage:

- Implementing gas drainage could diminish the load on the ventilation system.
- Lowers power consumption and electricity expenses.
- Allows air volume and velocity to be lowered.
- decreases entrained dust.
- Drained gas could be utilized; ventilation air methane is costly to use or abate [1].

The combination or push-pull system of ventilation is commonly installed in metalliferous mining situations, such as where caving methods are recruited and where the zone of fragmentation has enlarged to the surface. This is of the specific issue where the fragmented rock is tending to extemporaneous combustion. Push-pull systems could also be used in multi-shaft mines, where many main fans are used. In this case, it provides the potential to accomplish better dissemination of airstream, more acceptable management overpressure and leakages, more extensive flexibility, and less operating expenses. However, multi fan systems need skilled adaptation, designing, and balancing. Fans produce airstream by converting rotational mechanical energy into hydraulic energy [41].

Several kinds of fans are available; the two most frequently installed fans in mine ventilation are centrifugal fans and axial fans, although, in some situations, mixed-flow fans are used. Every fan has its features of performance or characteristic curves in terms of pressure-quantity, power-quantity, and efficiency-quantity curves. Figure 4.9A elucidates a normal pressure-quantity curve of a fan, while Figure 4.9B depicts a

resistance curve of a mining system that superimposed on the fan curve. The point at which the two curves intersect is termed the operating point for the fan representing the fan pressure and associated flow [2].

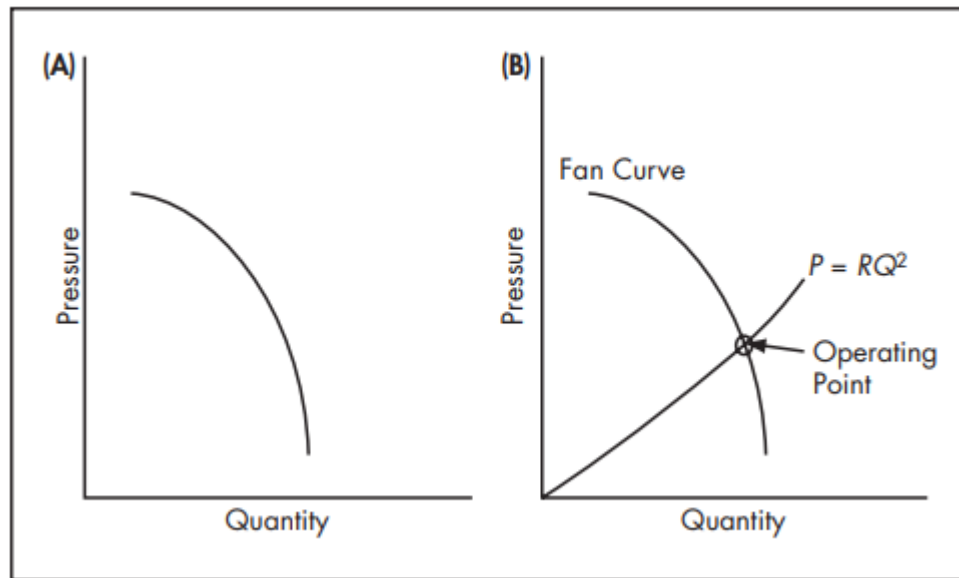


Figure 4.9: (A) Fan pressure-quantity characteristic curve, and (B) superimposed mine resistance characteristic and fan operating point [2].

#### 4.1.7 Booster fans:

As the air streams via a ventilation network, its energy will be reduced. As mines become more profound and more spacious, the mine resistance enhances, and the reliance on a single primary (i.e., its energy input) leads to a depletion in the ventilation volume transferred to the boundaries of the mine. Rather than ameliorating the main fans to tackle this loss in energy, it is recommended to reinforce the airstream energy in sectors of the tunnel by installing supplementary booster fans underground [42]. This has several advantages, including:

- No need to upgrade existing main fan facilities, avoiding capital and operating cost increases

- Only a proportion of the whole mine airflow is boosted, saving operational costs compared to having to boost the whole mine airflow.



Figure 4.10: Booster fan installation (Courtesy of De Souza et al. 2003).

Figure 4.10 depicts a routine booster fan facility. De Souza et al. (2003) offer an adequate example of the design and operation of a booster fan facility and the advantages that could be attained. These comprise enhanced ventilation streams in remote mining sectors, better pressure control, decreased use of energy, and enhanced air velocities lead to the increased power of cooling in hot mines.

## **4.2 Passive devices:**

### **4.2.1 Air doors and airlocks:**

When access is still needed between intake and return, air doors are used to reduce short-circuiting of ventilation stream by enhancing the resistance of a potential short-





Figure 4.12: Automatic Regulator [24].

#### 4.2.5 Air crossings:

Where intake and return airpaths require to intersect over each other, the leakage between the two must be controlled employing an air crossing.

---

#### Air crossings can take the following forms:

- 
- Natural: one of the airways is elevated above the other leaving a beam of strata separating the two airways.
- 
- Intersection: this is the more usual method. Both airways intersect during construction, and the roof of one or the floor of the other is excavated to expand the zone of intersection. The high-pressure side is further sealed by the application of shotcrete or another sealant.
- 

#### 4.2.6 Prefabricated air crossings:

In all cases, the substance from which the crossing is fabricated must be fireproof and able to maintain its integrity in case of a fire. Aluminum and other low-melting-point substances must not be utilized for building an air crossing.

#### 4.2.7 Stoppings and seals:

##### 4.2.7.1 Stoppings (Temporary or permanent):

Stoppings are simply air walls made of prefabricated steel, gob walls, concrete blocks, or any other transferor utilized to channel airflow for efficacious air dissemination.

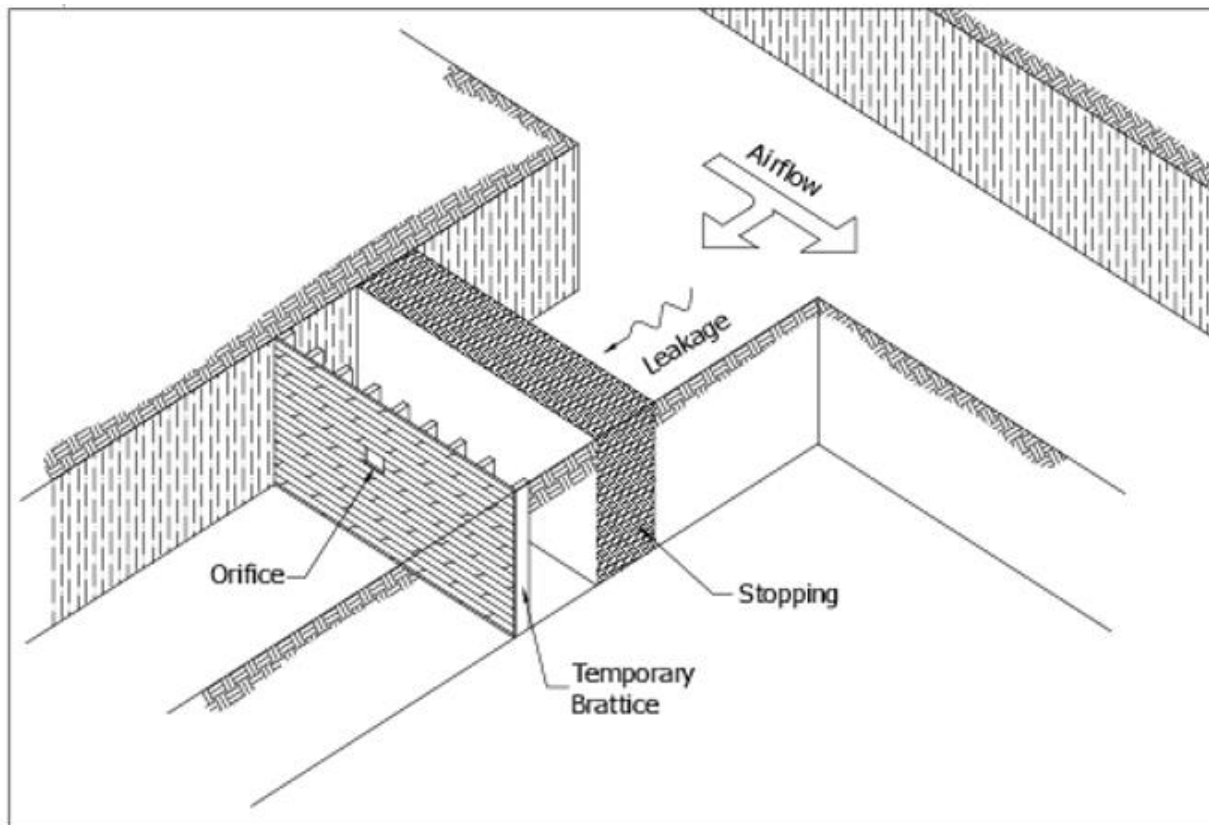
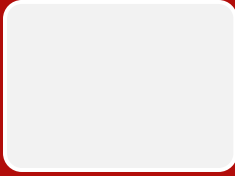


Figure 4.13: USBM method of measuring single stopping resistance [2].

In developing a mine, connections are inevitably made between the intake and return air paths due to providing instant access during mine development and to contribute through ventilation. These must be well constructed, keyed into solid rock, and leakage through have to be minimized (e.g., by being coated with a sealant). As a short-term technique, brattice curtains could be utilized when pressure differentials are low. When needed to isolate abandoned areas of the mine, seals have to be used. Chalmers (2008) details the prerequisites for sealing abandoned coal mining environments, and many of the details argued in his paper also out in application into other forms of mining. Seals are built for several reasons, such as avoiding undesirable air loss from a ventilation system and to preclude oxygen from entering mined-out areas to avoid extemporaneous combustion. Regardless of the reason for the seal, Chalmers propounded several features that an adequate seal must have:



- Strong.
- Ability to cope with strata convergence.
- Nonreactive.



- Highly resistant to airflow.
- Fire resistant.
- Easily and rapidly deployed.



- Insolubility.
- Sampling points installed.
- Stable, not easily blown over.

The accurate construction depends on local characteristics and substances and materials accessible; however, a distinction can be made between seals that are planned to entirely stop air leakage and a seal that is needed to be explosion-proof. Figure 4.14 depicts the prototypical fabrication of an explosion-proof seal. Backfill is becoming more widely utilized, specifically in hard-rock mining. Backfilling worked-out stopes could as well function as a very efficacious seal.

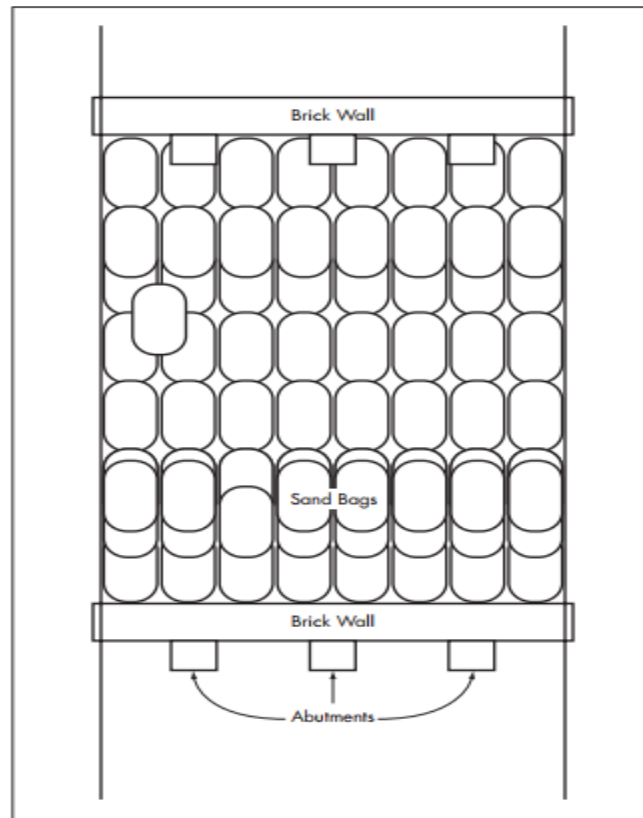


Figure 4.14: Explosion-proof seal. (Chalmers, 2008.)

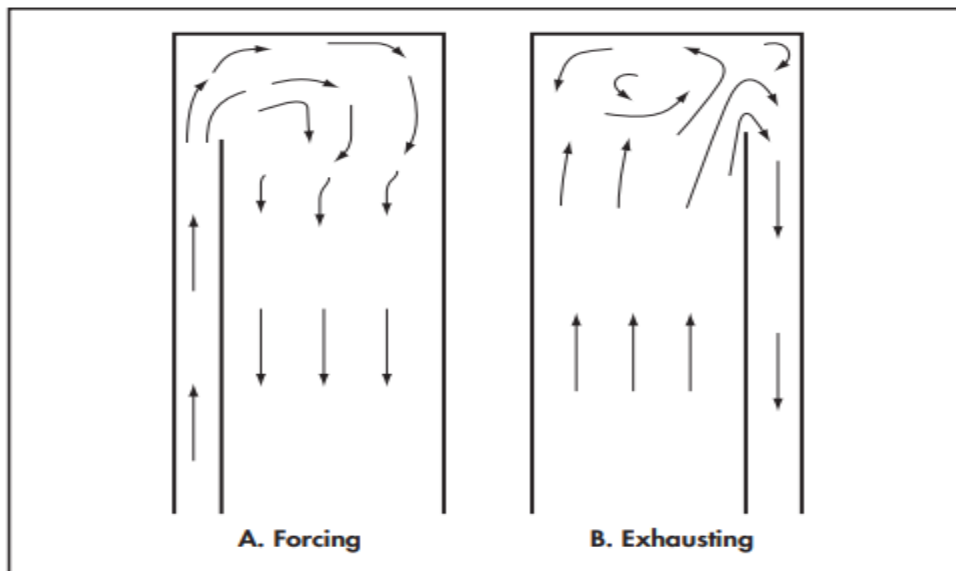


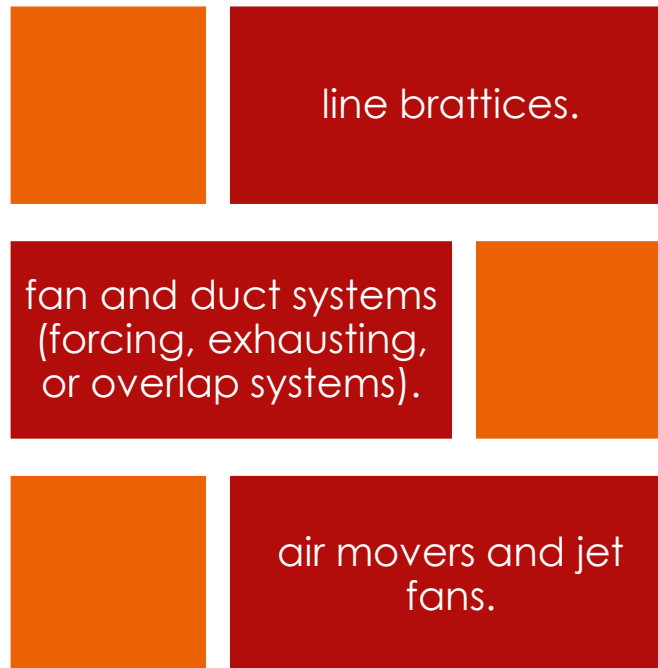
Figure 4.15: Line brattices used in auxiliary ventilation [23].

#### 4.2.8 District systems:

District systems will be discussed later.

#### 4.2.9 Auxiliary systems:

Methods utilized to provide air to the working faces of blind headings, sublevels, and so on include three primary types:



#### **4.2.10 Line brattice or vent tubing:**

Fire-resistant line brattices may be attached to floor, walls, and roof in underground mines. Vent tubing also is usually could be amalgamated with auxiliary fans [44].

##### **4.2.10.1 Line brattices:**

Brattice cloth hung from floor to ceiling, produces an artificial intake or return in a dead-end drive. Also, these systems are very leaky. The benefits are that they are cheap, need no power, and does not generate any noise. Figure 4.15 elucidates the utilization of line brattices.



Figure 4.16: line brattice (ABC Industries, inc. [25])

#### **4.2.11 Fan and duct systems:**

These systems comprise of a duct or a multiplicity of ducts attached to set up a ventilation network with a fan or fans to supply the air movement. As such, fan and duct systems could be complicated or straightforward ventilation networks [45]. The main distinction between these systems and the ventilation systems debated formerly is that they depend on open atmospheric connections in a factory, mine, or another context to achieve the ventilation circuit. Fan and duct systems fundamentally attain in four configurations as exhibited in Figure 4.17:

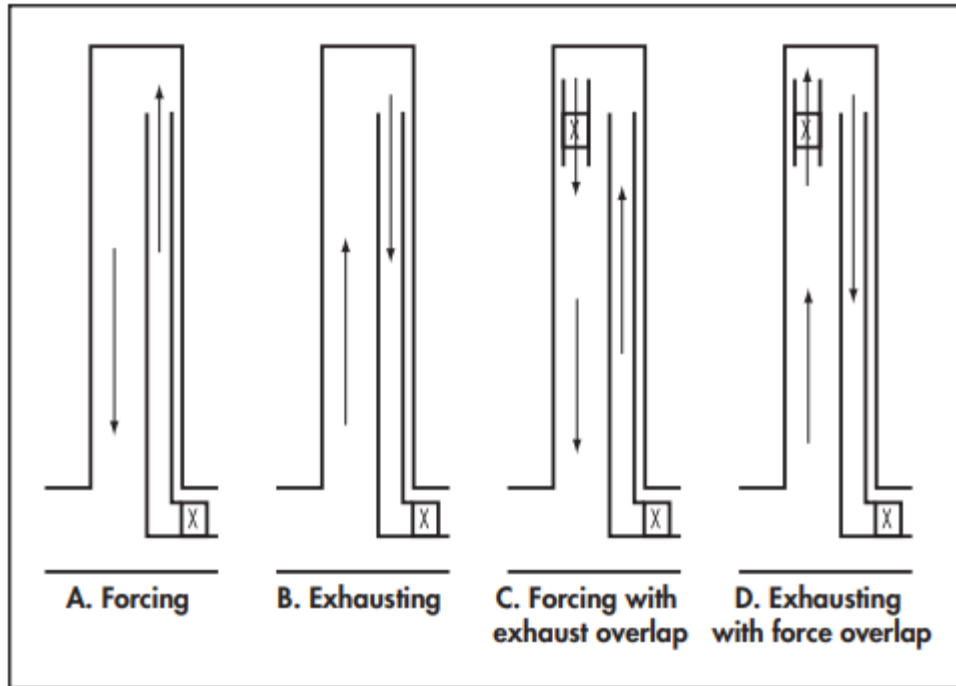


Figure 4.17: Auxiliary fan and duct systems [23].

Within such systems, the accustomed selection of fans is an inline axial fan. In mining situations, if the dead-end heading is more than 30 m in length, such systems are often the only means of felicitous ventilation, which is applicable achievable. The latter of these relies on the contaminants to be eliminated. The resistance of the tube is created in the same way as for other ventilation systems by calculating the frictional losses related to the duct and affixing further losses incurred at bends, changes in the cross-section, and entry and exit losses. The choice of which system to choose relies on the contaminants of significant apprehension. The higher velocity coming out from the exit of a forcing duct creates a scouring reaction, which brushes the area effectively. This is suitable for eliminating gases by creating turbulent mixing. Where heat is the main issue, forcing systems to produce high airstreams and increase air-cooling power. The main weakness of the forcing system is that contaminants attached to the airflow move back through the open atmosphere along with the heading in mines. Hence, tainting the general atmosphere proportionately steady and slow. The critical flaw of the exhausting technique is the lack of effective scouring action as there is no high-velocity jet of air to accomplish this.

Another defect of the exhaust system is that rigid or reinforced ducting requires to be utilized. These are more expensive than the flexible ducting types that could be used in forcing systems. The force/exhaust and exhaust/force overlap systems have been developed to tackle the flaw of the single forcing or exhausting systems. The choice of which of these techniques for using relies on the contaminants under consideration. Where long lengths of ducting are demanded (e.g., in tunneling work), the resistance of the duct might be such that multiple fans connected in series may be required. As ducting leaks, it is not recommended, and appropriate to cluster fans at one end of the ducting system as the pressures developed will increase leakage. The favorable

technique is to space the fans out along the duct to prevent excessive gauge pressures.

Ducting shapes the dispersal network for air-based air conditioning systems. Their operation is comparable to pipes in wet heating systems. This cautious factor has to be made first in the construction planning stage to accommodate and integrate ducting runs into the structure and fabric of the construction. This is particularly so close to the plant room where duct dimensions are at their most substantial amount.

The meticulous design of ducting structures is dominant as the way the ducting carries air to the diffusers severely affects the way air enters the room. The air must flow in a smooth manner as turbulence could change the air dispersion features of the diffusers. The layout of the ducting imposes how much energy is required for the fan to tackle resistance to the airstream. Changes in the ducting such as 90-degree bends, size diminutions, and other components enhance airflow resistance. Hence, ducting runs must be as linear and straightforward as feasible. The fan has to be sized to tackle air resistance in the ductwork, and so duct sketch has significant implications for fan size and energy utilization. Ducts transfer heated or cooled air. Loss of this conditioned air from leaks in the distribution network leads to wasted energy and a lack of control. This also originates from heat transfers via the walls of the ducts. To control this, ducting joins have to be well plugged and sealed, and ducts insulated where the temperature gap between the air in the ducting and ambient conditions command it.

Finally, ducting could be an origin of noise in the rooms being served. The roots are the transfer of noise and vibrations from the plant room and noise because of the airstream in the ducts. Air streaming via ducting and dampers generates noise. There are constraints on maximum air velocities in ducting and dampers to control this and have to be positioned as far away from the room air outlet as feasible [12].

#### **4.2.12 Air movers and jet fans:**

Air movers are utilized to increase and manage air motion within constrained areas. They are freestanding and could be powered by several origins, including electricity, compressed air, and water. Jet fans, otherwise known as a ductless, vortex, or induction fans, are usual and come several forms and sizes. A spray of water could also create airstream.



Figure 4.18: Jet fans [26].

#### 4.2.13 Overcast or undercast:

Overcasts are bridges for air where the intake and return air paths are needed to intersect each other.

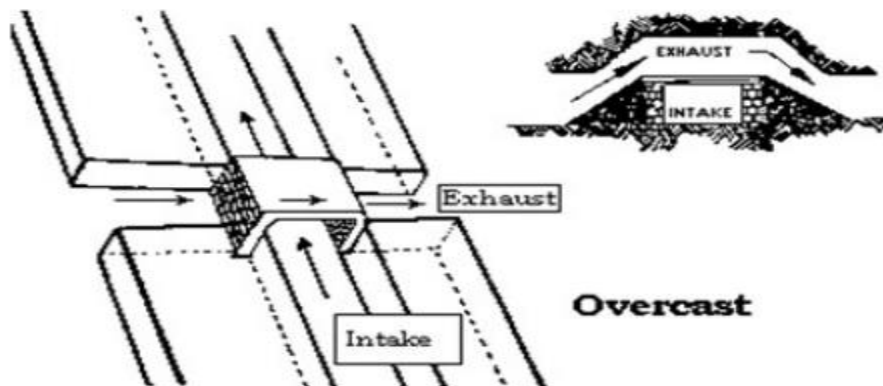


Figure 4.19: Overcast (MSHA 2203, 1981).

#### 4.2.14 Machine-mounted water sprays and scrubbers:

These are tools employed to increase the flow of fresh air in face areas. Scrubbers are "vacuum cleaners" utilized for dust suppression [3].

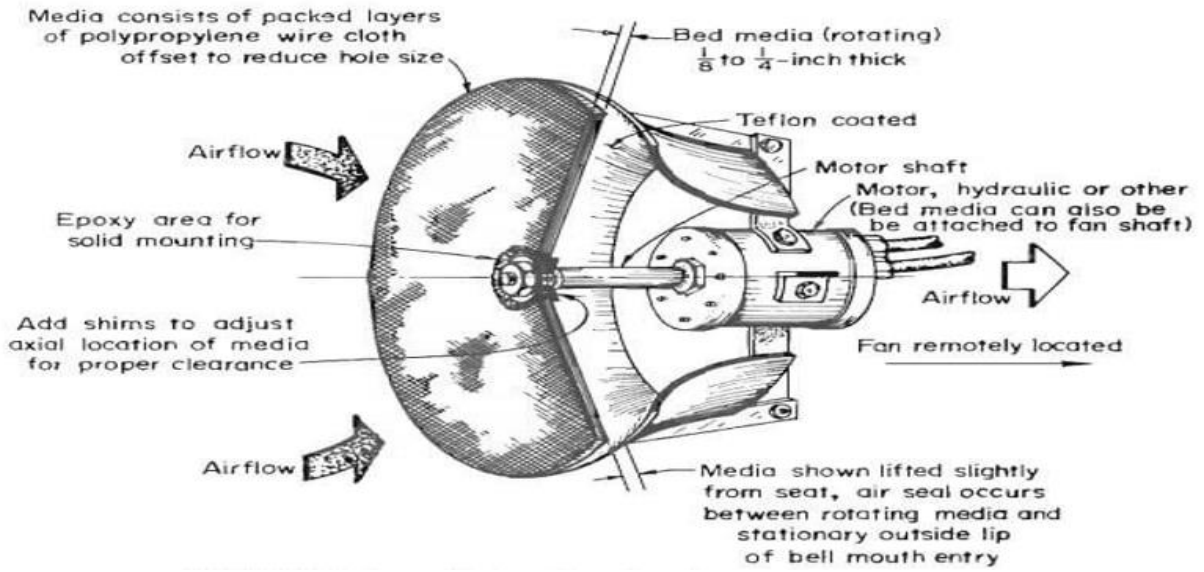


Figure 4.20: Rotating bed scrubber [27]

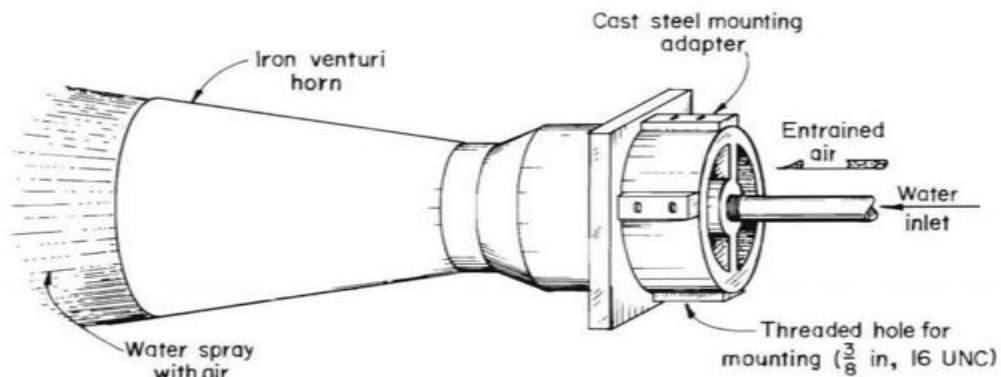
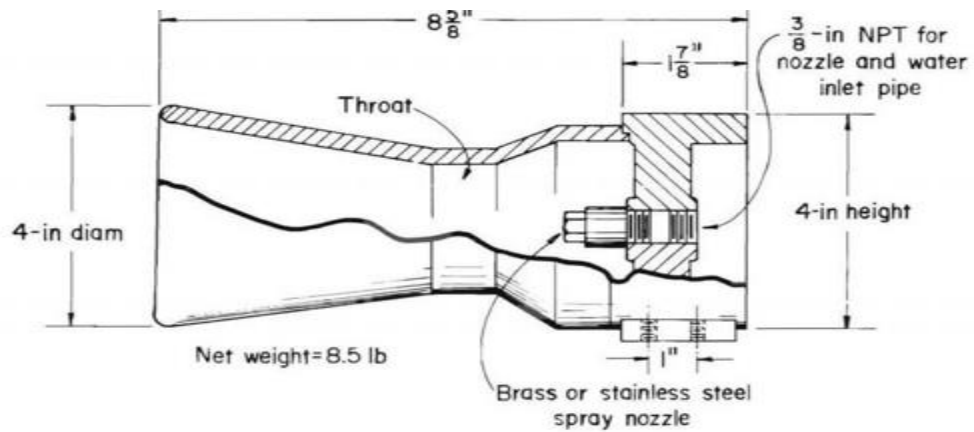
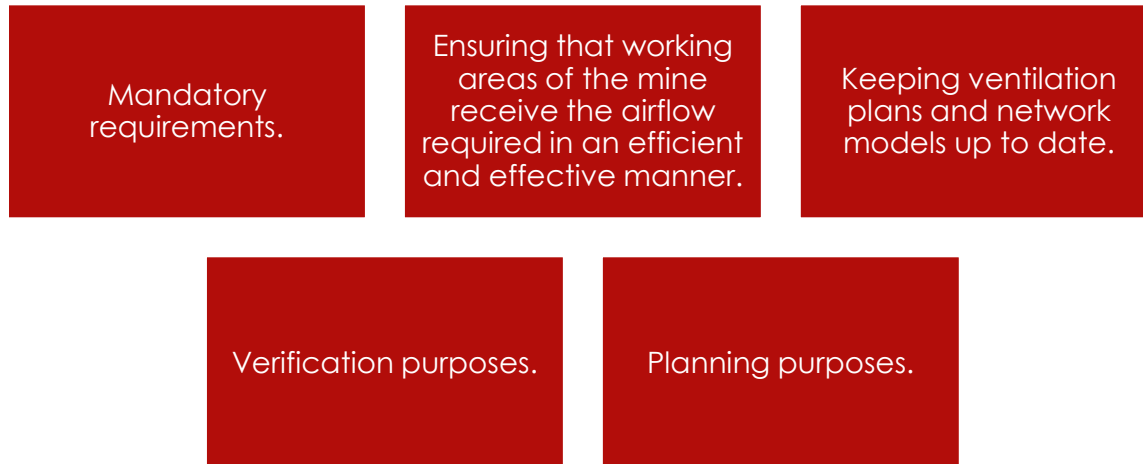


Figure 4.21: Venturi spray [27].

### 4.3 Ventilation surveys:

A ventilation survey is a well-ordered approach to obtain data to ferret out the quantity, pressure, and air quality dissemination within a mine. The precision, correctness, and needed detail of the survey rely on the aim of the survey. Surveys are undertaken for a different reason, inclusive of [46]:



A vital intention of ventilation surveys is to assess and acquire the frictional pressure drop,  $p$ , and corresponding airstream,  $Q$ , for each branch within the ventilation network. From these data, the subsequent parameters might be computed for both designing and ventilation control aims:

- Distribution of airflows, pressure drops, and leakage.
- Branch resistances.

- Volumetric efficiency.
- Air-power losses.

- Natural ventilation effects.
- Friction factors.

Besides, pressure and airstream assessment, other quantifications are taken either as an integral part of the survey or individually. There are two principal sides of a ventilation survey: the assessment of air quantity and pressure drop [2].

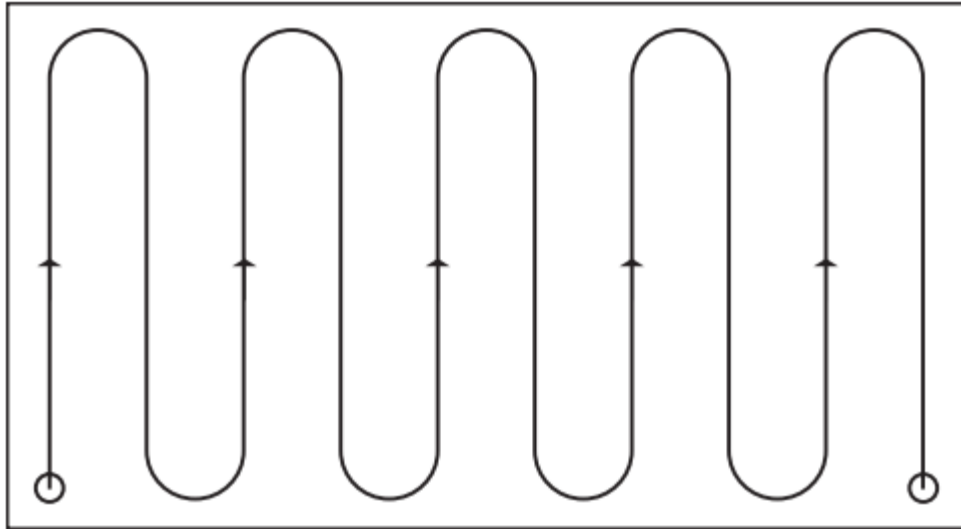


Figure 4.22: Path of an anemometer traverse [23].

### 4.3.1 Air quantity surveys:

The volume of air passing a given point in an air route or duct,  $Q$ , is typically assessed as the product of the cross-sectional area of the airpath or duct,  $A$ , and the mean air velocity,  $u$ :

$$Q = u \times A \quad (4.1)$$

Therefore, most common methods of calculating  $Q$  are amalgamations of the techniques at hand for computing area and mean velocity. Modern techniques of calculating airspeed or velocity can be split into three groups depending on:

<p>1. Mechanical effects.</p>	<p>2. Dynamic pressure.</p>	<p>3. Thermal effects.</p>

Mean velocity at a point could be calculated either by a traversing tool that integrates assessments as the cross-section is traversed or mathematically combining fixed-point assessments to arrive at an average air velocity. Details of the techniques utilized to undertake such assessments are delineated by several authors such as McPherson (1993) and an outline of that comes in the following paragraphs.

Figure 4.22 depicts a usual technique utilized to undertake an anemometer traverse assessment. These are taken with a vane anemometer or the same kind of integrating instrument. Anemometers are proportionately insensitive to yaw; this is a misalignment with the airstream, so long as the angle of yaw does not surpass over  $5^\circ$ .

The spectator faces the airstream and holds the tool at least 1.5 m away from his or her body by attaching the tool to an extendible arm. The device is then started while another spectator starts a stopwatch. The device is then moved as depicted in Figure 4.22, the purpose being to sweep equal areas of the traverse at the same time. The traverse must not take less than 60 seconds. After the whole area is swept, the anemometer is stopped, the total stream through the instrument noted and the time taken, give the average velocity permission to be computed. The process is reiterating until three readings yield a similar average velocity to within  $\pm 5\%$ . The measuring sites have to be selected to prevent potential issues wherever feasible. Booking of outcomes must comprise the following:

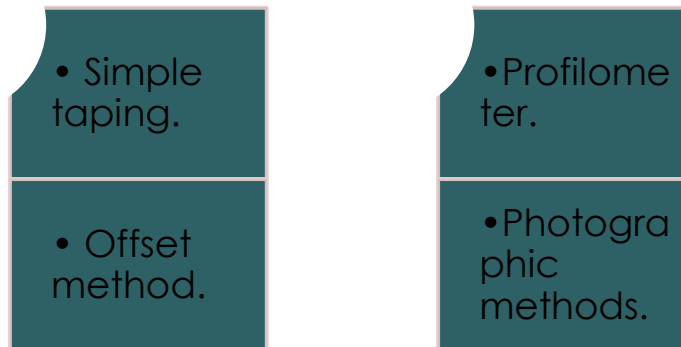
- Location of station, time, and date.
- Anemometer readings and corrections.
- Calculation of air volume flow.

- Air dry and wet bulb temperatures and barometric pressure.
- Dimensioned sketch of the cross section.

- Observers' names.
- Calculation of area.

An anemometer traverse could also be undertaken at the ends of ducts, but not if the duct diameter is less than six times the anemometer diameter. Anemometers could also be utilized for fixed-point assessments with corrections installed to attain the real stream. These modifications are assessed via traverses taken earlier in the same place. When the duct/anemometer ratio of 6 precludes installation of an anemometer survey, pitot tube methods are most frequently used, as delineated in McPherson (1993).

The assessment of a cross-sectional area could be carried out in several ways:



#### 4.3.2 Pressure surveys:

A pressure survey aims to calculate the frictional pressure droplet corresponding to a specific stream in an airpath. Principally, there are two techniques, the more precise being the trailing hose or gauge and tube technique, which is time-consuming but favorable where foot travel is relatively easy. The second technique is the barometer or altimeter technique, utilized where access is tight, such as in multilevel mines and shafts. Details of these techniques could be found in Hemp (1989) and are delineated in the subsequent paragraphs in brief. The concept of the trailing hose technique is not complicated: A hose is laid along the length of the airpath being surveyed, and a manometer or other acceptable differential pressure gauge is linked to one end of the hose. In the case of a horizontal airpath, this gauge will show a differential pressure precisely equal to the pressure loss. When the air path is not horizontal, the differential pressure will differ from the pressure loss; however, techniques are available to compute the pressure loss derived from the airpath equations, which are adjusted versions of the steady-flow energy equation for mining conditions. In its basic form, the barometer technique comprises the simultaneous measurement of barometric pressures and wet and dry bulb temperatures at either end of the airpath. Airstream also requires to be assessed. If the elevations of the two measuring stations are precisely known, the pressure and energy loss can be calculated from the airpath equations [47].

#### 4.4 Mine ventilation network analysis:

A necessary component in the sketch of new mines is the quantified designing of the dissemination of airstreams, regulating the position and duties of fans and other ventilation control devices to attain the purpose of supplying adequate environmental circumstances throughout the ventilation system. In existing mines, it is better to design ahead to make sure that new fans, shafts, and other air paths are accessible promptly for well-planned ventilation of the tunnel and extensions to the mine. Ventilation designing must, therefore, be a continual and routine process. The laws of fluid mechanics handle the behavior of air in air paths, ducts, and pipes. As shown formerly, concerning mining, this includes using Atkinson's equation, the square law, and in some situations, the laws of thermodynamics.

Ventilation network analysis issues can be addressed and formulated quite simply as stated by McPherson (1993):

• If the resistances of the branches of a network and how these branches are interconnected are known, how can the distribution of airflows for given locations and duties of fans be predicted?

• If the airflows in specific branches are known, how are the combination of fans and the structure of the network to provide these airflows determined?

Ventilation network analysis is a generic term for several techniques, a family, which enables such questions to be addressed. Practical determinants will limit the number of satisfactory alternatives. One necessary aspect of any method to be recruited is that it has to be simple to use and be adequately rapid and flexible to permit the investigation of multiple solutions [2].

#### 4.4.1 Fundamentals of the ventilation network analysis:

The key relationships that rule the behavior of electrical current within a network of conductors were first recognized by Gustav R. Kirchhoff (1824–1887). These same fundamental relationships are now known as Kirchhoff's laws and are also apposite to fluid networks. Kirchhoff's first law (hereafter referred to as Kirchhoff 1) expresses that the mass flow entering a junction equals the mass flow leaving that junction (a result of the law of conservation of mass) and could be written as:

$$\sum_j M=0 \quad (4.2)$$

where M is the mass flows, positive and negative, entering junction j. However:

$$M=Q\rho \quad (4.3)$$

where Q is the volume of the flow ( $m^3/s$ ), and  $\rho$  is the air density ( $kg/m^3$ ), hence:

$$\sum_j Q\rho=0 \quad (4.4)$$

If the density variation around the ventilation network is negligible (i.e., the flow could be regarded as incompressible), then:

$$\sum_j Q=0 \quad (4.5)$$

This gives a means of checking the precision of airflow measurements taken around a junction when undertaking a ventilation survey. Kirchhoff's second law (hereafter referred to as Kirchhoff 2) declared in its basic form is that the algebraic sum of all pressure drops around a closed path, or mesh, in the network must be zero, taking into account the effect of fans and/or natural ventilation pressures, an outcome of the law of conservation of energy. The steady-flow energy equation for a single airpath could be written as:

$$\frac{\Delta u^2}{2} + \Delta Z_g + w = \int V dp + F \text{ J/kg} \quad (4.6)$$

Where:

u = air velocity (m/s),  
 Z = height above datum (m),  
 g = acceleration due to gravity ( $m/s^2$ ),  
 W = work input from fan (J/kg),  
 V = specific volume ( $m^3/kg$ ),  
 P = barometric pressure (Pa),  
 F = work done against friction (J/kg).

Considering several branches shaping a closed-loop or mesh within a network, the algebraic aggregate of all  $\Delta Z$  must be zero, and the sum of all the changes in kinetic energy,  $\Delta u^2/2$ , is negligible. Summing the remaining terms around the mesh, m gives:

$$\sum_m \int V dp + \sum_m (F - W) = 0 \quad (4.7)$$

The summation of the V.dP terms is the natural ventilation energy, NVE, which arises from thermal additions to the air, thus:

$$\sum (F - W) - NVE = 0 \quad (4.8)$$

This calculation is in joules per kilogram and could now be converted to pressure units by multiplying by density,  $\rho$ .

$$\sum (F - W) \rho - \rho NVE = 0 \quad (4.9)$$

But if  $\rho_f = p$ , the frictional pressure drop, and  $\rho_p = pf$ , the rise in total pressure across a fan, and  $\rho_{NVE} = NVP$ , the natural ventilation pressure, then Kirchhoff's second law becomes:

$$\Sigma(P - \rho_f) - NVP = 0 \quad (4.10)$$

Kirchhoff's laws could be applied to fluid networks that have either compressible or incompressible flow. In the case of compressible flow, the analysis is undertaken based on mass flow; in the case of incompressible flow, the review is being conducted on the basis of volume flow. From this point forward, the incompressible flow will be assumed. The square law requires to be incorporated within Kirchhoff's laws for incompressible flow.

Kirchhoff 1

$$\Sigma_j Q = 0 \quad (4.11)$$

Kirchhoff 2

$$\Sigma_m (RQ|Q| - P_f) - NVP = 0 \quad (4.12)$$

where

R = resistance ( $Ns^2/m^8$ )

|Q| = the absolute value of airflow

This ensures that the frictional pressure drop always has the same sign as the airflow and removes the complication of squaring or square-rooting negative numbers.

#### 4.5 Deviations from the square law:

The fundamental relationship of mine ventilation is the square law  $p = RQ^2$ . This is developed from the Chezy–Darcy relationship and is valid for fully developed turbulent flow. The resistance, R, is a function of the friction factor, k, which is itself related to the Darcy friction factor, f. If the flow regime falls into the transitional zone or the laminar flow zone, f, and, hence, k becomes a function of the Reynolds number, Re, the value of R varies with airflow. In these cases, the square law is inapplicable.

For the transition zone, the following relationship applies:

$$P = RQ^n \quad (4.13)$$

Values of n have been reported to be in the range of 1.8–2.05. In the case of laminar flow, the following equation can be used:

$$P = R_L Q \quad (4.14)$$

where RL is laminar resistance.

In the following sections, it is assumed that the square law applies.

#### 4.6 Methods of solving ventilation networks:

Basically, there are two methods for solving ventilation networks:

1. Analytical methods formulate governing laws to produce equations that yield exact solutions.
2. Numerical methods iterate until a solution is found to a required degree of accuracy.

##### 4.6.1 Analytical methods:

The following paragraphs describe analytical methods to solve ventilation networks.

##### 4.6.2 Equivalent resistances:

This is the most basic technique of network analysis [48]. When two or more air paths are lined in series or parallels, each of these resistances could be incorporated into a single equivalent resistance in an analogous behavior to electrical circuits. A mine ventilation network is built of several paths and tunnels joined together; these links between branches could be broken down into tunnels linked in series and parallels.

- Series circuits: the usual component is that the air quantity streaming in each branch is similar. The equivalent resistance of n branches linked in series is:

$$R_{total}=R_1+R_2+\dots+R_n \text{ (N.S}^2\text{/m}^8\text{)} \quad (4.15)$$

- Parallel circuits: the usual component is that the pressure drop across every branch is similar. The equivalent resistance if n branches are linked in parallel is:

$$1/\sqrt{R}=\sum_1^n 1/\sqrt{R_n} \text{ (N.S}^2\text{/m}^8\text{)} \quad (4.16)$$

##### 4.6.3 Numerical methods:

Numerous numerical methods exist. The primary differentiation between the methods revolves around mesh selection and numerical solving of the equations. The most robust-though not always the most efficient-plan was devised by Professor Hardy Cross in 1936 at the University of Illinois for water distribution systems. This technique is the most widely used and was modified for use in mine ventilation systems by Professors F.B. Hinsley and D.R. Scott at the University of Nottingham in 1951 [2].

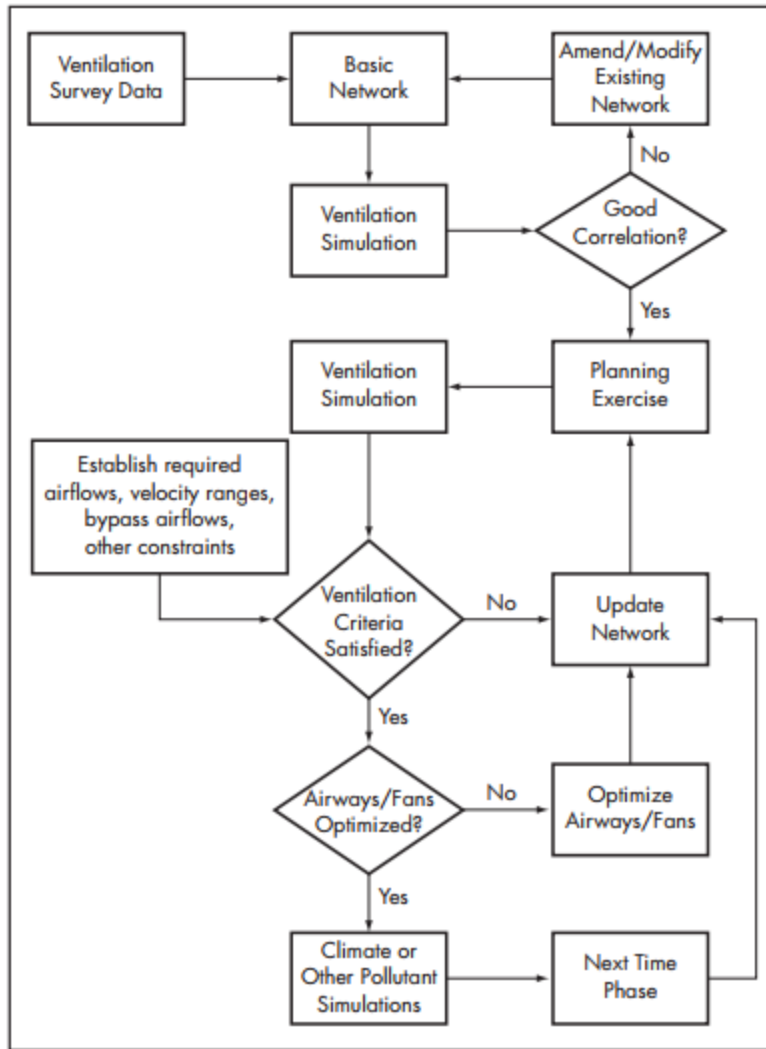


Figure 4.23: Generic mine ventilation planning [2].

#### 4.7 Ventilation network simulation programs:

There are numerous ventilation network simulation packages on the market. These are mathematical models and are designed to simulate real systems. The use of these packages has revolutionized mine ventilation planning (Mine Ventilation Services 2007; Ventsim 2010).

#### 4.8 Mine ventilation planning:

Planning of new mines and extensions to existing mines is a critical part of overall mine planning. Without adequate airflow provided in a timely and efficient manner, likely outcomes include poor environmental conditions for the workforce, with associated health and safety issues, and reduced production. Ventilation planning is also essential in the testing of emergency and evacuation procedures [49]. A generalized approach to mine ventilation planning is shown in Figure 4.23. The figure has been simplified for clarity and indicates that a step-like approach should be taken with constant feedback between stages, similar to other mine design problems. All mines are different in terms of the pollutants to be diluted and removed, so generic rules do not apply to all situations.

Ventilation planning should be an integral part of overall mine planning, as well as production planning. Concerning ventilation planning, the following factors should be considered:

- The method should fit with the remainder of the mining operation.
- The method should be flexible.
- The method should be economical.
- The method must be adaptable for extensions and future mining activities.

Regarding Figure 4.23, the initial stage is to create a simulation model of the mine. For an existing mine, this should be created using the results of ventilation surveys. For a new mine, typical design data such as friction factors should be combined with geometric data and layout data from other mine planning activities. For extensions to existing mines, a combination of survey data and design data will need to be used. After this has been achieved, the next stage is to test the ventilation network for existing mines to ensure that the results of the simulation correlate well with the real ventilation survey data. If a reasonable correlation ( $\pm 5\%$ ) is not achieved, the ventilation network needs to be modified by examining assumptions and data against reality until a suitable relationship is achieved. Possible reasons why correlation is not achieved include compressibility occurring in the network while an incompressible analysis is being undertaken, airways not conforming to actual design specifications, shock losses not being accounted for, and numerous other reasons. For a new mine, after underground workings exist, ventilation surveys should be undertaken and compared against the simulated network to ensure that the simulations match the mining reality. After a suitable network simulation has been developed, the next stage is to ensure that the predicted flows are reaching the production and other areas that require ventilation. To do this, the required airflows, air velocity limits, bypass airflow, requirements to eliminate recirculation, and other requirements such as establishing boundaries for the concentration of pollutants need to be developed.

Table 4.1: Recommended maximum air velocities [49].

Area	Velocity(m/s)
Working faces	4
Conveyor drifts	5
Main haulage routes	6
Smooth-lined airways	8
Hoisting shafts	10
Ventilation shafts	20

In some cases, these limits are dictated by law, in other cases, not. In some countries and states, best practice is mandated by health and safety legislation. In the case of

gases, the required airflow can be simply determined if the release rate of the gas is known, and the concentration of maximum needed is known as detailed by McPherson (1984). For dust and some other requirements such as bypass airflows, air velocity limits such as those shown in Table 4.1 can be applied. Minimum velocity standards can also be fixed; a commonly asked standard is 0.3 m/s (McPherson 1993). For diesel dilution, a common method is to specify airflow per rated kilowatt of diesel power in a location (Brake and Nixon 2008). For heat and humidity, heat stress indices need to be applied to define safe work, to reduce work and stop-work conditions, and to undertake climate simulations in addition to ventilation simulations (Tuck 2008). After the required air velocities, quantities, and other criteria have been set, the results of the ventilation simulation need to be carefully checked against these criteria. If the criteria are not satisfied, amendments need to be made to the network, such as changing the duty of fans, changing airway lining or other inputs, and the simulation rerun until the criteria are realized. The third stage involves an economic overview of the system. Mine ventilation systems can be significant electricity consumers, so trying to optimize the system to minimize the total capital and operating cost is prudent. Following this stage, if ventilation alone is not sufficient to dilute and remove the contaminants, the design requirements for auxiliary systems such as methane drainage, mine cooling, and mine heating can be investigated as required. These considerations give a broad, simple overview of the ventilation design process (McPherson 1993). However, planning of mine ventilation is not simple, and a lack of care and attention at each stage of the process can result in a system that fails to deliver the outcomes required. A good illustration of this is provided by Brake and Nixon (2008), who examined the requirements to estimate the primary airflow requirements in underground metalliferous mines correctly. Brake and Nixon found that airflows were underestimated for failure to:

- Provide for leakage in the auxiliary ventilation ducts,
- Provide for leakage in the workings,
- Supply essential anti-recirculation bypass flows,
- Provide for diesel equipment mobility,
- Provide for ramps and other underground fixed plant and infrastructure travel ways,
- Understand the relationship between airway dimensions and minimum wind speeds,
- Recognize which is the critical airborne contaminant to be diluted,
- Plan for reasonable capacity increases and other contingencies,
- Provide for likely changes in diesel technology,
- Provide for increased mine resistance,
- Understand the impact of both increased mine resistance and leakage on airflow requirements and fan performance,
- Understand that providing extra capacity in a ventilation system at the start of the project while it is an initial additional capital expenditure is less expensive than fixing the ventilation at a later date,
- Properly assess ventilation planning and implementation lead times. An essential part of mine, ventilation planning is that it should be a continual process and that the effects of time need to be carefully assessed. An excellent example of this has been reported by Sedlacek (1999). In this paper, four scenarios were investigated to enable the Kidd Creek mine (Canada) to develop to greater depths with the potential to extend to 2,987 m below the surface. The situation in 1998 involved the use of several fans arranged in a series of parallel arrangements to provide the required airflow. In total,

220 intake and return level exhaust fans were in use. Besides, the airflow within the system was severely constrained by an inadequate return airway system. Sedlacek details four possible solutions to the long-term ventilation needs for Kidd Creek; of these, the preferred option involved the mine being separated into 15 distinct ventilation districts or circuits, each controlled by a single major supply fan. The overall volume of air is controlled by strategically located unique exhaust fans placed at or close to the top of the significant exhaust raises. This system reduced the number of main fans from more than 200 to 18 and enabled considerable savings in operating costs.

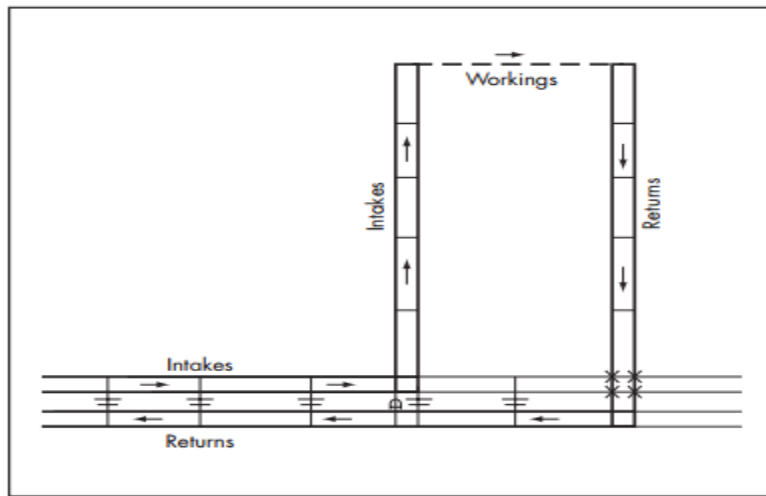


Figure 4.24: U-tube ventilation [23].

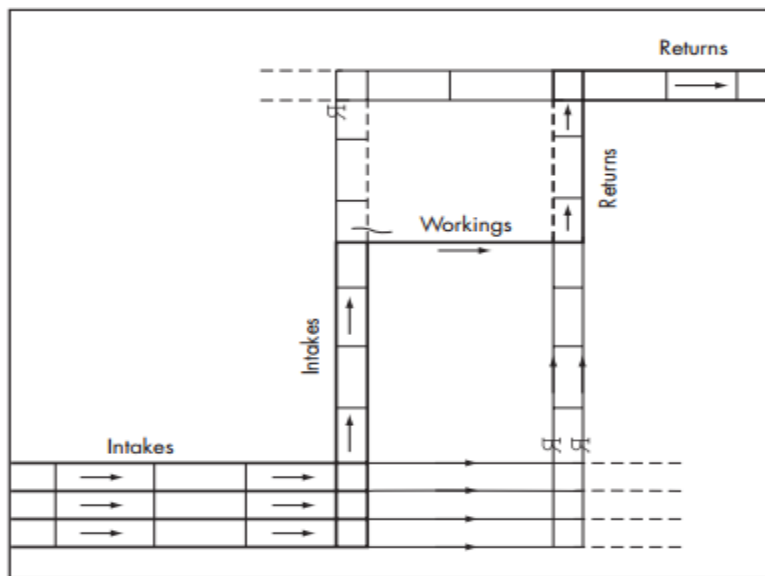


Figure 4.25: through-flow ventilation [23].

A more modern approach to ventilation design is the potential to apply ventilation on-demand to working stopes (Hardcastle et al. 1999). The principle can also be used to mine cooling systems (Gundersen et al. 2005). Production stopes in mining do not require the same amount of air continuously; currently, ventilation design assumes

worst-case conditions for specifying the airflow required—right from a safety perspective, but poor regarding economics. The principle of ventilation on demand is to match the air supply to the requirements of individual stopes depending on the point in the production cycle where they are currently operating. This has the potential to reduce overall mine airflows and to achieve considerable savings in power costs. One main concern is that mine ventilation systems are highly inertial in nature, and the changes induced to provide ventilation on demand for a specific stope could have a reduced impact elsewhere in the system, even if only for a short, transient period of time. This could have serious safety implications.

#### **4.9 Coal and metalliferous mine ventilation:**

Before describing some of the main points of ventilating coal and metalliferous mines, a general overview of the two main forms of ventilation applied in both cases will be made. There are two broad classifications: U-tube systems (Figure 4.24) and through-flow systems (Figure 4.25). Figure 4.24 shows the principle of U-tube ventilation. Figure 4.25 illustrates the through-flow system. In these systems, although leakage occurs, it is generally smaller. It can be used to enhance flows as, for instance, at the return end of the working zone, which is a hot and humid mine is generally one of the main problem areas; the leakage flow increases the air velocity, enhancing the cooling power of the airflow. Division can be made between stratified deposits (longwall or R&P systems) such as coal, gypsum, potash, and trona, and metalliferous ore-body deposits (also known as hard-rock deposits). Stratified deposits usually have a more straightforward two-dimensional system; ore-body deposits tend to be more complicated. This is due to their three-dimensional nature and the need to have more numerous working sections, not all of which are working at a particular time (in other words, air requirements are on a day-to-day basis, and air must be directed to where it is needed).

#### **4.10 Stratified deposits:**

Underground coal, potash, and other tabular forms of mineral deposits use either the longwall method of mining or the R&P mining method. Layouts can vary from country to country; however, the following sections highlight the modes of airflow distribution used. Other differences between these types of mines and hard-rock mines are the dominant pollutants that need to be accounted for. In coal mines, methane gas, dust, and in some cases, diesel emissions are the dominant pollutants. In hard-rock mines, diesel pollutants, dust, and blast fumes are of concern. Because all mines will have different critical pollutants, assessment should be made on a mine-to-mine basis.

##### **4.10.1 Longwall systems:**

Two main features have influenced the design of longwall systems: methane and other gas control from the waste areas, and the high rate of rock breakage. A typical layout is shown in Figure 4.26. Regarding Figure 4.26, single-entry systems are conventional in Europe where the deposits are mined at considerable depth, and geotechnical issues would require enormous pillars to be left if multiple access systems were used. With the advancing system, some leakage occurs through the waste area; control of this is achieved by roadside packing. This leakage air flushes gas out of the waste and can cause problems of high gas concentration at the return end of the face. Leakage of air through the waste can cause gob fires. In the retreating system in Figure 4.26B, the amount of air leaking through the waste is generally reduced, but the same problems

can occur as in the advancing case. The method illustrated in Figure 4.26C is a combination of U-tube and through-flow ventilation. Multiple opening systems such as those illustrated in Figure 4.26D are more common in the United States, South Africa, and Australia, where shallower coal seams are mined. If retreat mining is used, back bleeders can be used to control waste or gob gas. In some states, air from conveyor belt drives cannot be used to ventilate production areas actively; the use of multiple entry systems enables this requirement to be achieved. The types shown in Figures 4.26E through 4.26G are used when the gas is very heavy. An additional fresh air feed helps to maintain gas concentrations to safe levels by feeding fresh air directly to the return end of the face. These systems can also be applied in hot workings.

#### **4.10.2 Room-and-pillar systems:**

In R&P mining, the potential for leakage is high because of the large number of interconnected entries, as shown in Figure 4.27. The figure illustrates two methods of ventilating R&P development: a bidirectional or W-system in which intake air passes through one or more central airways with return airways on both sides, and a unidirectional or U-tube system in which intake and return airways are on opposite sides of the panel. In both cases, the conveyor is sited in the central airway, and line brattices regulate the air through it. The bidirectional system offers the advantage that the air splits at the end of the panel, and each airstream only has to ventilate half the panel. Also, the rib side gas emission is likely to be more substantial in the outer airways. Its disadvantage, however, is that it requires double the number of stoppings, and hence has more leakage paths than the unidirectional system. Thus, the unidirectional system has higher volumetric efficiency. In both cases, the use of brattice cloth to control air distribution at the face end offers high resistance. This problem can be overcome by employing auxiliary fans and ducts at the face end to force or exhaust air from the headings; the resistance of the face end effectively becomes zero. This is illustrated in Figure 4.28. All the methods shown in the previous figures for longwall mining can also be applied to R&P workings. There are different strategies between R&P and longwall mining [2].

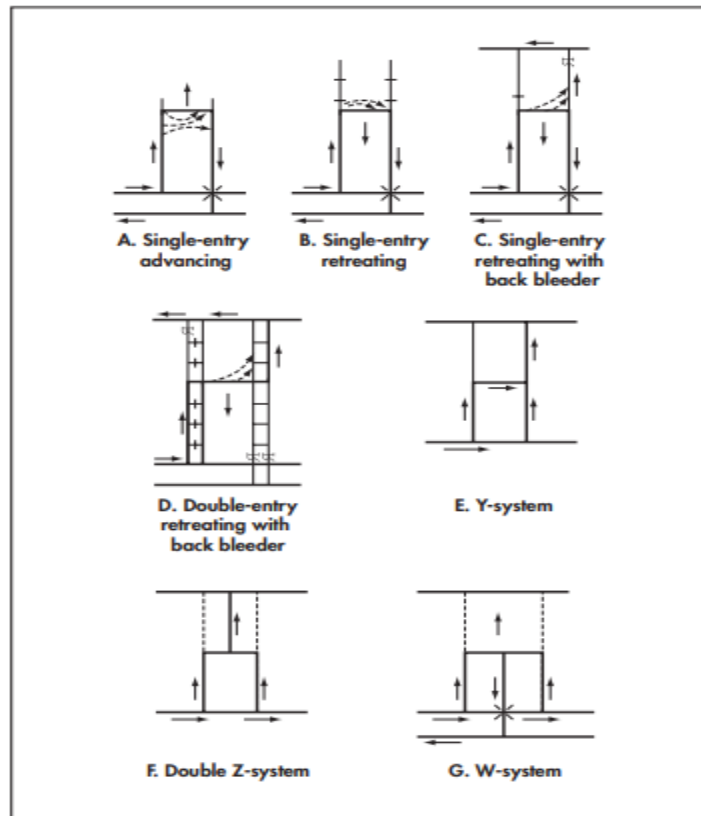


Figure 4.26: Longwall district ventilation systems [23].

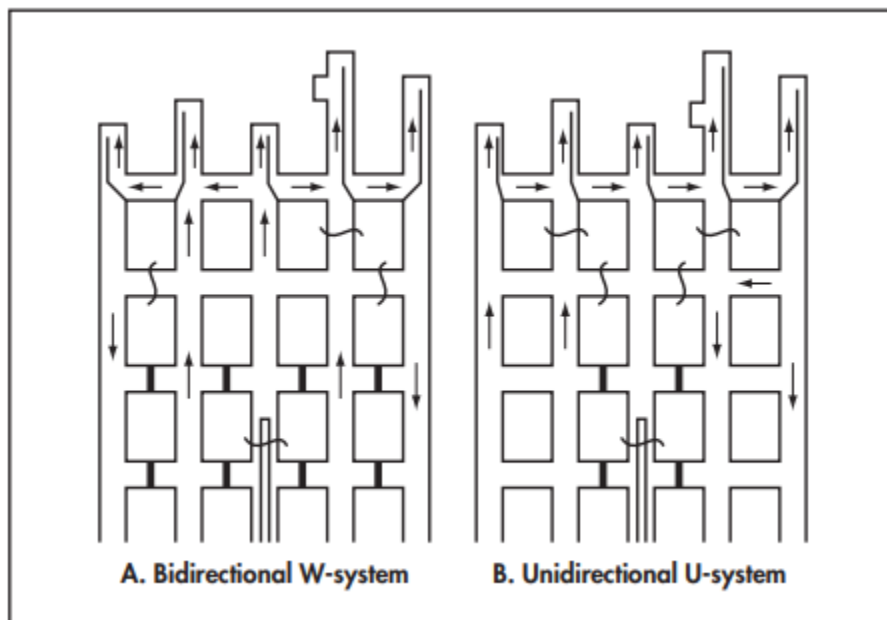


Figure 4.27: Room-and-pillar development with line brattices (high face resistance) [23].

#### 4.11 Ore-body deposits:

The irregular geometry of metalliferous deposits, coupled with grade variation and fluctuating market prices, results in highly complex mine development in metal mining.

Mine development can, in many cases, be related to chasing the grade, dictated by commodity prices at a particular point in time. These factors and the fact that drill-and-blast operations are cyclic in the process also necessitate many more stopes than would be required in a stratified deposit mine, some of which may not be worked on a particular shift. Consequently, metal mines are characterized by a three-dimensional aspect and require much more flexible ventilation arrangements. Ventilation networks in metal mines are more complex than those for stratified deposits. Figure 4.29 illustrates the basic principles of ventilating a metal mine. Airflow distribution in various stoping systems is highly variable. The guiding principles are as follows:

- Use ascensional ventilation.
- through-flow ventilation has to be utilized wherever feasible; however, the use of fan and duct systems is recognized as a requirement in specific systems.
- Series ventilation should be avoided.
- Leakage through ore passes is an issue; attempt to prevent large pressure drops across ore passes to minimize leakages [2].

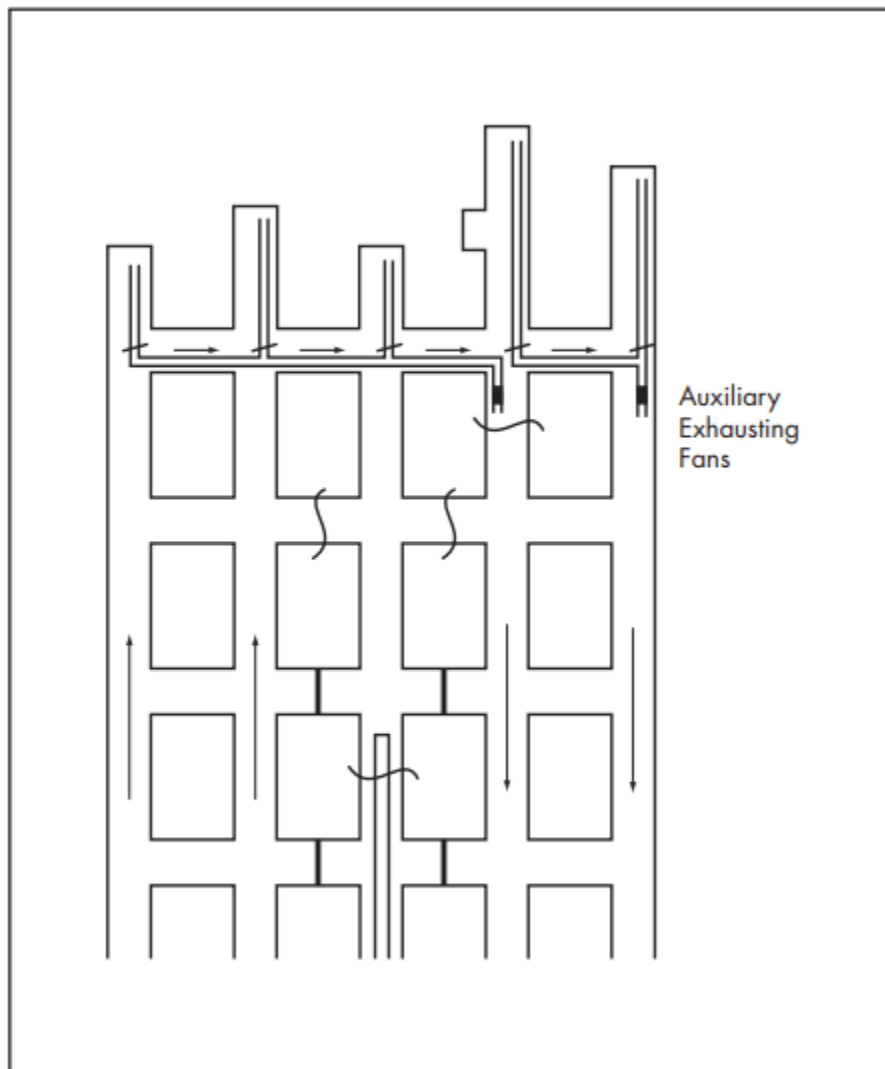


Figure 4.28: Room-and-pillar development with auxiliary fans (zero face resistance) [23].

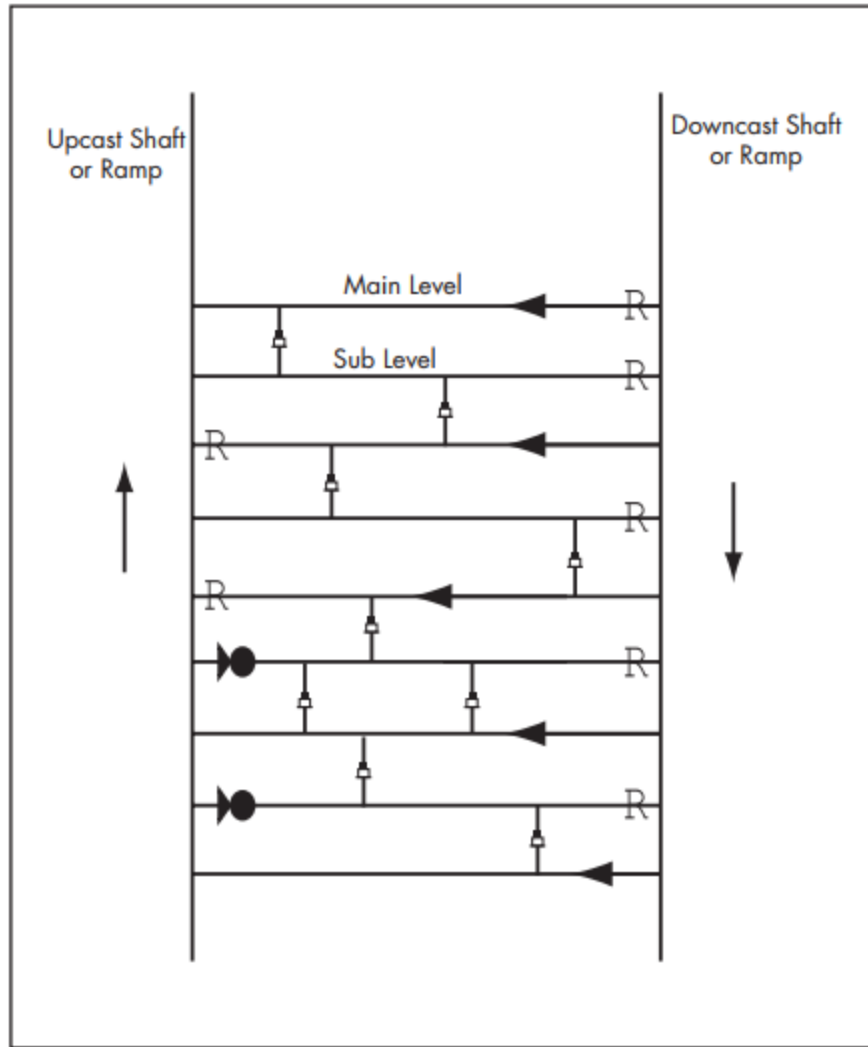


Figure 4.29: Principle of through-flow ventilation applied to the levels of a metal mine [23].

Reduction in airflow resistance characteristics with thin spray-on liners [14].

#### 4.12 Air exhaust ducts:

The right choice of local exhaust design and its location depends not only on production technology but also on the methods used to calculate dust and gas flow near suction inlets. The development of these calculation methods can be classified into three stages:

1. Construction of empirical relationships and absorption spectra
2. Determination of analytical formulas for the simple boundaries of air inflow to a suction unit.
3. Numerical simulation of flows at local suction units [15].

#### 4.13 Aerodynamics of dust airflows in the spectra of air exhaust ducts:

The first stage is associated with the research by V.V. Baturin, A.F. Bromley, A.S. Pruzner, Della Valle, Engels, Koop, Willert, and others .

To calculate the rectangular and circular cross-sections of the suction intake, Della Valle proposed an empirical relationship:

$$Q=(10X^2+A)V_X \quad (4.17)$$

where

Q is the volume flow rate

A is the suction inlet area

$V_X$  is the axial air velocity at a point located at a distance x from the suction port for the same inlets with a flange:

$$Q=0.75(10X^2+A)V_X \quad (4.18)$$

where the hole vs. flange areas ratio may range from 1/2 to 1/2.5.

Koop obtained a relationship for a round suction intake:

$$V_X = V_0 e^{-3.2X/d} \quad (4.19)$$

where

d is the diameter of the suction inlet

$V_0$  is the air suction velocity for a rectangular inlet, the following formula is proposed:

$$V_X = V_0 e^{-3.2 \frac{xU}{4A}} \quad (4.20)$$

Where U is the perimeter. Engels and Willert obtained a combined relationship for round and rectangular inlets [15]:

$$\begin{cases} \frac{V_X}{V_0} = \frac{(X/r_h)^{-1.6}}{1+(X/r_h)^{-1.6}} , & X/r_h \leq 2 \\ \frac{V_X}{V_0} = \frac{(X/r_h)^{-1.6}}{1+(X/r_h)^{-1.6}} , & X/r_h > 2 \end{cases} \quad (4.21)$$

where  $r_h = A/U$  is the hydraulic radius.

For similar junction pipes with a flange:

$$\begin{cases} \frac{V_X}{V_0} = \frac{1.35(X/r_h)^{-1.45}}{1+1.35(X/r_h)^{-1.45}} , & X/r_h \leq 2 \\ \frac{V_X}{V_0} = \frac{2(X/r_h)^{-1.9}}{1+2(X/r_h)^{-1.9}} , & X/r_h > 2 \end{cases} \quad (4.22)$$

For circular inlets:

$$\frac{V_X}{V_0} = \left(\frac{X}{r_h}\right)^{-2}, \quad \frac{X}{r_h} > 2 \quad (4.23)$$

For square inlets:

$$\frac{V_X}{V_0} = \frac{4}{\pi} \left(\frac{X}{r_h}\right)^{-2}, \quad \frac{X}{r_h} > 2 \quad (4.24)$$

# Chapter 5

## Description of the Murisengo Mine

### 5.1 Geographical framework and description of the quarry:

The gypsum quarry object of the analysis is located on a hilly relief in San Pietro in the municipality of Murisengo (AL). It is one of the leading suppliers of the cement industry.

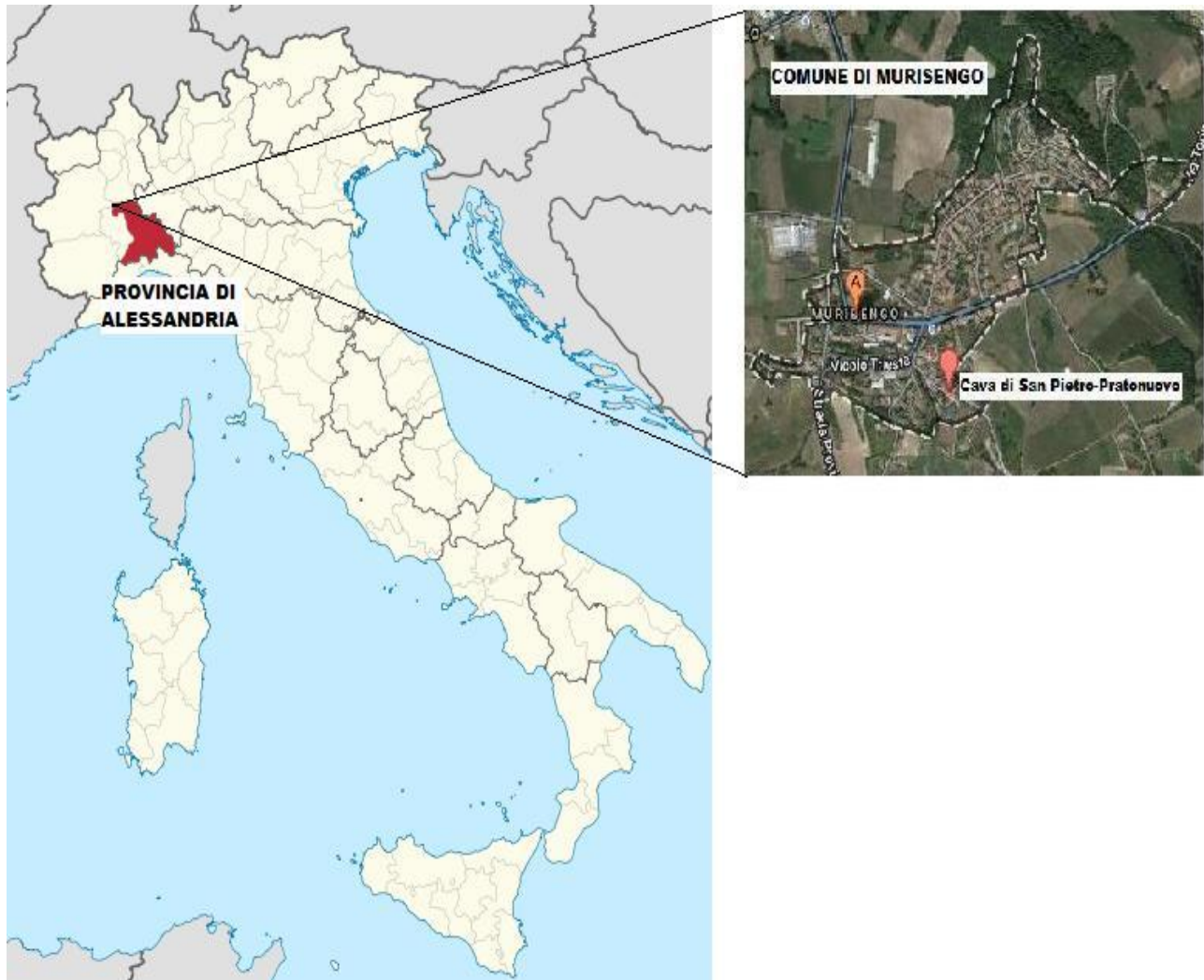


Figure 5.1: Geographical framework of the quarry.

It is located near the Pratenuovo quarry; thanks to the five levels of cultivation of both and the displacement of only 4 m between the stories of the first and those of the second, it was possible to create an underground connection between the two quarries to increase the total supply of raw material.

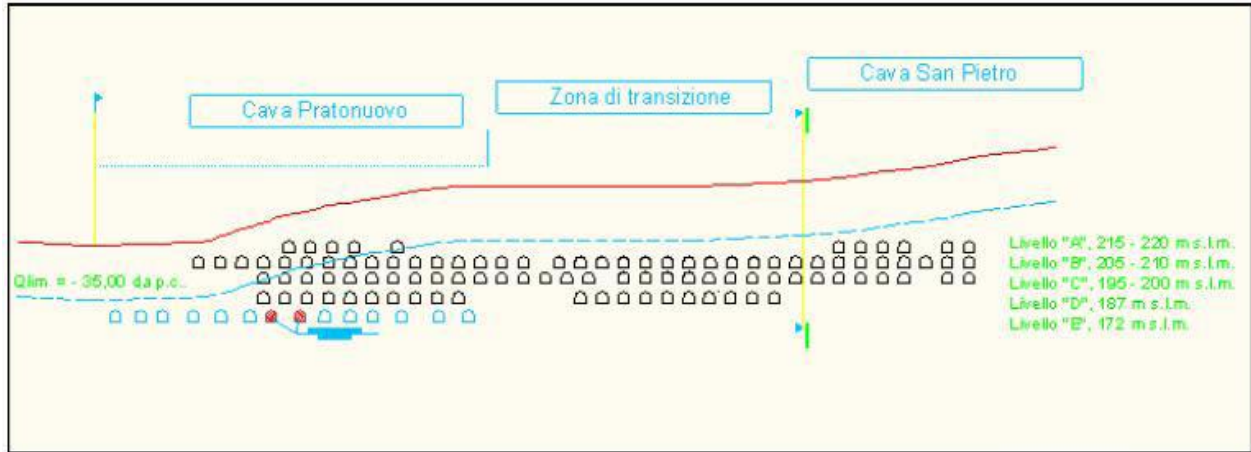


Figure 5.2: Quarry level diagram.

The level analysis provides for level "A" characterized by the oldest and most geomechanically unstable portion. The field has been exhausted and cannot be expanded due to historical artifacts on the surface. Going down, we find level "B" which includes the connecting ramp between the two quarries and is exhausted and unexpandable and level "C" which has better characteristics but is also finished and not expandable. Then there is level "D" consisting of chalky rock of excellent quality that is exhausted but with the possibility of expansion in the area of the oldest quarry and level "E" which is the best quality and still under cultivation.

Following the connection of the two quarries by straight descent (maximum slope of 20%) located in the extreme sectors of the "San Pietro" quarry, it was possible to complete the planimetric cultivation of levels B, C, and D, which is about to reach the maximum extractable cubage, within the limits of ownership and safety. In an axonometric view, the quarry appears as a 4-story structure, interconnected by plaster slabs and supported by systematic squat pillars. Altimetrically, each level can be considered horizontal, except for the central area connecting the two quarries.

As for the roof, it is thought that it can be totally composed of gypsum due to chalky minerals on the surface.

The cultivation method, unique for the two portions of the quarry, is of the type with abandoned chambers and pillars arranged in a regular checkerboard pattern for the area of the San Pietro quarry and random for that of Pratonuovo. The connecting ramp between the two quarries is straight, with a maximum gradient of 20%. In contrast, the connecting ramps between the various levels are helical with a track between 7 and 10 m wide, to allow the passage of two dumpers in Contemporary.

## 5.2 Geological framework:

The creation of the chalky-sulphurous formation dates back to the "Messinian Plan" (5-7 million years ago), which, due to the movement of African crustal clods, saw several phases of complete evaporation of the Mediterranean Sea. The subsequent tectonic upheavals allowed the emergence of all areas of Monferrato and Langhe and created a series of lagoons along the southern coast of the Padano Sea. The seawater,

overflowing in these areas, evaporated, transforming itself into a solution rich in mineral salts, which, in turn, crystallized on the bottom giving rise to evaporitic rocks and, above all, to gypsum.

In the area of interest, the formation is composed of three layers for a total thickness of 100 m. The deeper layer is formed of marly sediments with masses of selenitic gypsum; the intermediate one is when the quarries were created. In contrast, the more superficial one is characterized by clayey sediments interspersed with layers of alluvial sands.



Figure 5.3: Stratification of the area under analysis.

### 5.3 Hydrogeological framework:

The gypsum, clays, and marls that make up the cultivated mass, the bed and the roof of the deposit respectively behave as entirely waterproof materials. The gypsum has a modest water circulation, which becomes unsaturated in the areas of secondary discontinuity. In contrast, in the clays and marls, the circulation is blocked by the cracks tightly closed.

The cultivated chalky mass is, therefore, a single and compact rock body with waterproofing characteristics that increase with depth.

### 5.4 Description of the field:

The cultivated chalky deposit appears as a more or less flattened and relatively lens homogeneous and regular with dimensions of a few hundred meters in plan and an average thickness of 30-40 meters, with a modest elongation in the direction of E-W. The cultivated deposit near the outcrops, extending from the upper part of the hillside (Torre S. Pietro), has a regular shape and a relatively limited surface. The cultivated bank is covered by a thickness of about 20 meters of incoherent eluvial-colluvial soil and rests on layers of marl and calcareous sandstones. Inside the reservoir, there are two stratification surfaces represented by levels of marl whose position is also representative

of that of the gypsum mass having parallel immersion and inclination varying from 45 ° of the first to 55 ° of the second.

#### 5.4.1 The plaster:

The chalky rock is formed by a single mineral and is initially created in the salt flats along the coasts and in estuaries. It is dissolved in seawater, where the intense evaporation of the latter leads to the precipitation of calcium sulfate on the bottom. The crystals can be irregular and fragmented or have the characteristic shape called a spearhead or dovetail.



Figure 5.4: gypsum crystals.

The chemical formula of gypsum is  $\text{CaSO}_4 \cdot 2\text{H}_2\text{O}$  and has as a typical composition:

- 32.6% of CaO;
- 46.5% of SO<sub>3</sub>;
- 20.9% of H<sub>2</sub>O.

Its main features are:

- Solubility: it can therefore be mobilized by dissolution from the original formation due to hydrological variations to precipitate and recrystallize in different sedimentation zones;
- Hardness 1,5 - 2, therefore, a soft mineral;
- Variable color according to impurities;
- Chemically inert if pure but dissolves when hot in acids.

The main application of mineral gypsum is in building materials. It is the basis of a large number of products obtained by mixing semi-hydrated gypsum, insoluble anhydrite, and soluble anhydrite in various proportions, with the addition of any additives and using different grinding and cooking methods.

#### 5.4.2 Characterization of the Murisengo plaster:

Murisengo gypsum is characterized by brown-colored transparent lenticular crystals, and its good characteristics make it a highly appreciated product by the cement industry.



Figure 5.5: Murisengo crystal.

The field under examination shows a slight mineralogical inhomogeneity caused by various crystallizations. You can easily distinguish chalky volumes with coarse-grained crystals from chalky works with a fine-grained crystallization: the contacts are clear and often masked by marly-clayey intercalations, with a too contorted course, a consequence of past geological movements. This inhomogeneity can be recorded at all levels of cultivation.

#### 5.4.3 Analysis of the physical-mechanical properties of gypsum:

From the laboratory tests carried out in the past on samples coming from level A of the quarry, the physical-mechanical characteristics of the lithotypes involved in the mining works were obtained. Coarse-grained gypsum (gypsum g.g.), fine-grained gypsum (gypsum g.f.), and clayey marl constituting the filling of the discontinuities were investigated. The average values obtained are in agreement with the average amounts of the gypsum and marls that Fornaro (1993) summarizes in the following Table 5.1:

Table 5.1: Physical-mechanical properties of the lithotypes involved.

Material	$\gamma_n$ [kN/m <sup>3</sup> ]	Ed [MPa]	Co [MPa]	Et [MPa]	Es [MPa]
gypsum	21,8	22,8	10,0	4000	2600
Marne	21,8	-	-	-	-

Material	To [MPa]	Cp [MPa]	$\varphi_p$ [°]	$\varphi_r$ [°]
gypsum	0,8	4,2	44	35
Marne		1,5	35	30

The covering ground is a material consisting of the product of the alteration of the gypsum mass together with more superficial colluvial type material. Based on experimental data from laboratory tests, the average characteristics are obtained:

Table 5.2: Physical-mechanical characteristics of the substrate.

Material	$\gamma_n$ [kN/m <sup>3</sup> ]	Cp [kPa]	$\varphi_p$ [°]	$\varphi_r$ [°]
Silt and clay	19,0	50	20°-25°	15°-18°

The detailed survey of the underground allowed us to consider the quality of the mass as "good" with a reduced number of discontinuities. From the data relating to old cores, an R.Q.D. Equal to 80%.

From the geomechanical classification of Bieniawski we obtain a value of the R.M.R. of 72, which corresponds to a pile of excellent qualities. In reality, gypsum has perfect structural conditions but low geomechanical characteristics, with a monoaxial compressive strength and an extremely low modulus of deformation. The classifications, not being calibrated for a cluster with these characteristics, lead to unrepresentative and overestimating results.

The calculation of the elastic modulus of the rock mass with the geomechanical classifications leads to a final value more significant than an order of magnitude compared to that evaluated in the laboratory: the overestimation is linked to the fact that the Bieniawski method does not assign massive importance, a fundamental aspect for plaster. For these reasons, it would be appropriate to reduce the RMR of about 20 pt, to be able to apply the geomechanical classifications correctly.

An elastic modulus of the rock mass was therefore assumed within the range 4000 -5000 MPa by making a precautionary choice for the fine-grained gypsum of the case in question.

The compression tests carried out in the laboratory, on the other hand, led to the definition of resistance lower than that previously assumed, with an inversion of behavior between the forms of crystallization: the coarse grain rather than the refined grain proved to be more resistant. In reality, the samples examined were not many; therefore, there was a substantial dispersion of data to the detriment of

representativeness. However, the assumption of a monoaxial compressive strength equal to 7.65 MPa is certainly a precautionary for the study in question.

## 5.5 Cultivation operations:

### 5.5.1 Cultivation method: (chambers and pillars)

The low geomechanical properties of gypsum do not allow the creation of large underground voids. Still, they require a proper balance between the excavated volumes and those kept in place to ensure the long-term stability of the supporting structure.

The cultivation method adopted is therefore for chambers and pillars, consisting in the creation of voids called "chambers" through the controlled removal of the plaster, delimiting in the stone in place suitable support pillars that will guarantee the stability of the chambers over time; in-depth study, material slabs will be placed to protect the rooms.

The pillars have a height equal to the thickness of the reservoir, a cross-section calculated with the formulas of the resistance of the materials, and the distance required by the self-supporting requirements of the site vault, usually less than 6 m.

The project aims to extract the maximum amount of mineral compatible with safe working conditions.

The method is inexpensive, easily mechanized, and very flexible as according to the geological configuration, it is possible to change the volume of the chambers and pillars and allows them to work on several fronts. It works starting from the cap, proceeding by successive declines, up to the thickness of the useful mineral bank.

The construction of the pillars takes place by opening short fronts which, after an advance equal to the size of the pillar, forks to the right and left, giving rise to two other quick galleries which will delimit, on a new side, the pillars to the right and left of the initial advancement.

The following figures illustrate the work progress procedure:

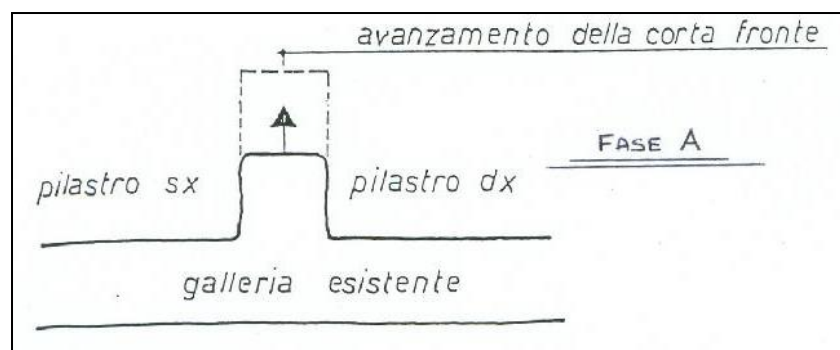


Figure 5.6: Phase A of progress.

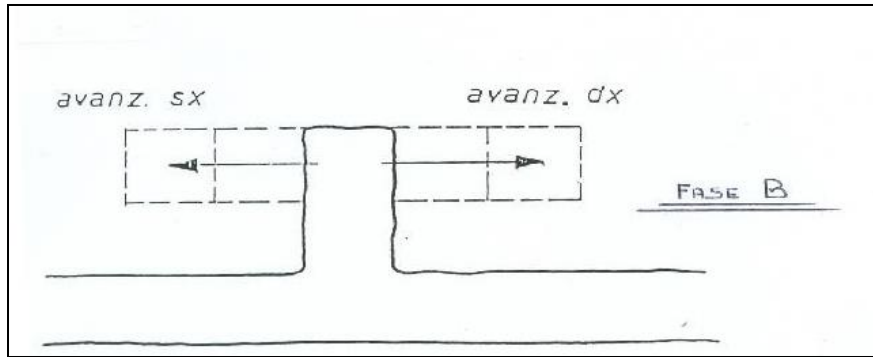


Figure 5.7: Phase B of progress.

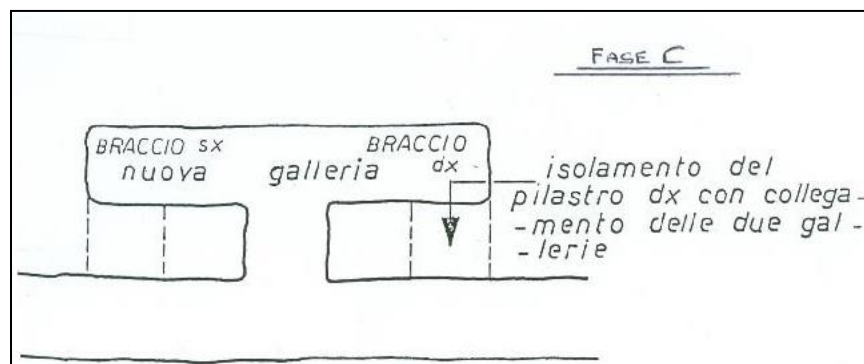


Figure 5.8: Phase C of progress.

Depending on the type of reservoir and the peculiarities of the cultivated area of the reservoir itself, the types of problems can occur, such as detachment, fall of blocks, and the pillars' collapse with the subsequent limited self-supporting time of the chambers, must be identified.

This method applies to sub-horizontal reservoirs with a thickness ranging from 2 to 30 m and maximum inclinations of 8-10 ° and has the following advantages:

- operational simplicity;
- possibility of using highly productive machines;
- low production costs.

and as disadvantages:

- substantial losses of useful mineral;
- variable dilutions up to 20%, generally contained at 6-7%.

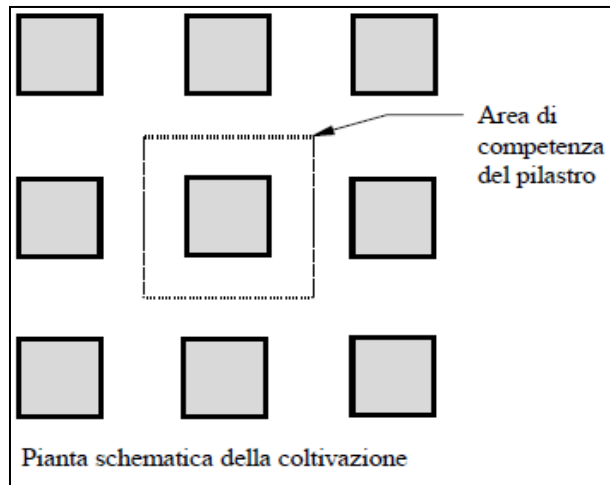


Figure 5.9: Scheme of the “chambers and pillars” cultivation method, plan.

In our case, the pillars have the three dimensions more or less equal; this gives more excellent stability to the structure, although it penalizes the extraction efficiency and even if more slender pillars are typical of the cultivation of less soft materials than gypsum.

### 5.5.2 Explosive abatement:

As an excavation technique, drilling and blasting are used, which consists of the drilling of mine holes, subsequently charged with explosives and suitably primed. The main stages are:

- drilling of blast holes;
- loading;
- blasting;
- smoke;
- Scaling;

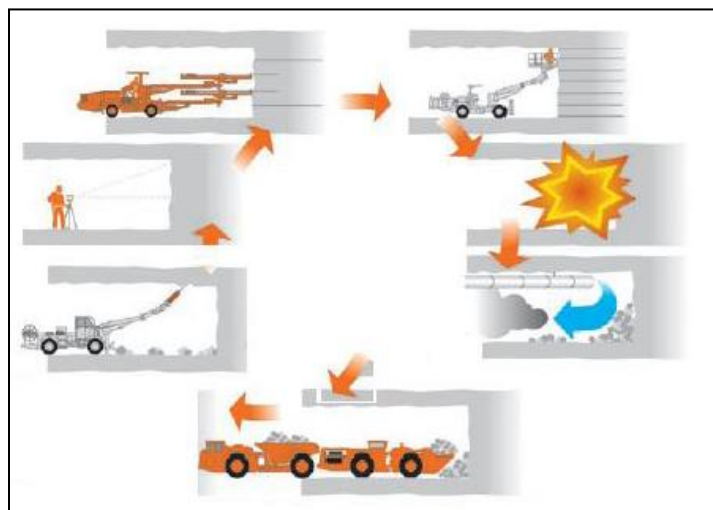


Figure 5.10: Drill & blast cultivation technique.

This technique has been successful for its simplicity and versatility: once the work has begun, it is much easier to change the firing mesh, the drilling diameter, or the type of explosive, rather than replacing an excavation machine that has proved unsuitable.

### 5.5.3 Analysis of the muzzle:

Drilling is carried out using electric rotary drilling machines and self-purging tools (verrine). Gypsum is a relatively "deaf" rock to the action of explosives, so we use explosives that are not excessively powerful and, therefore, cheaper.

The quarry uses an explosive called NITRAM TX1 consisting of:

- 90% of a concentrated solution of ammonium nitrate (aqueous oxidizing phase);
- 10% of oils, waxes, and paraffin (oily combustible phase).

Emulsions today represent an explosive of excellent quality in terms of impact sensitivity.

Nitram with low production of NO, CO, and CO<sub>2</sub> guarantees excellent environmental working conditions.

The linear charge is triggered at the bottom of the hole with a micro-delayed electric detonator. Given the high "deafness" of gypsum, the use of emulsions alone has often generated in the past a "cannon effect" with the firing of the cartridges from the hole without crushing the mass. To avoid this problem, it was decided to insert two gelatin cartridges in each mine in order to help the effect of the emulsion alone with greater disruption. The hole sequence of the cartridges is, therefore, the following:

- Downhole charge: 1 gelatin (32 mm x 200 mm of 0.25 kg) + electric det.;
- Central charge: 2 Nitram (35 mm x 350 mm of 0.50 kg each);
- Head charge: 1 jelly (32 mm x 200 mm of 0.25 kg).

The advancement patterns are called "fan", with a lower variable resistance from point to point, resulting in the subsequent opening of new free surfaces on which to work the explosive.

The following figures illustrate the muzzle scheme adopted. It should be remembered that the type of muzzle may undergo, during the works, some substantial adaptation changes to the conditions assumed by the individual yard.

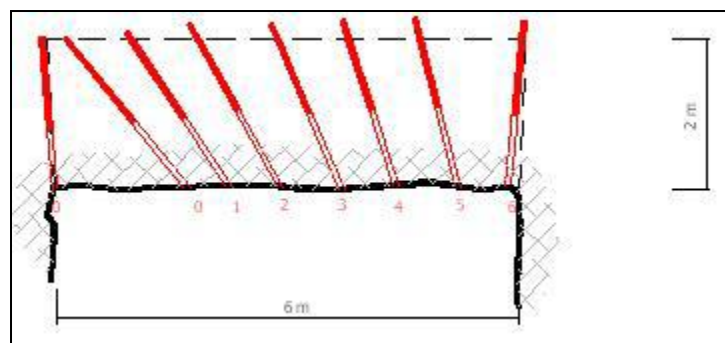


Figure 5.11: View of the muzzle diagram.

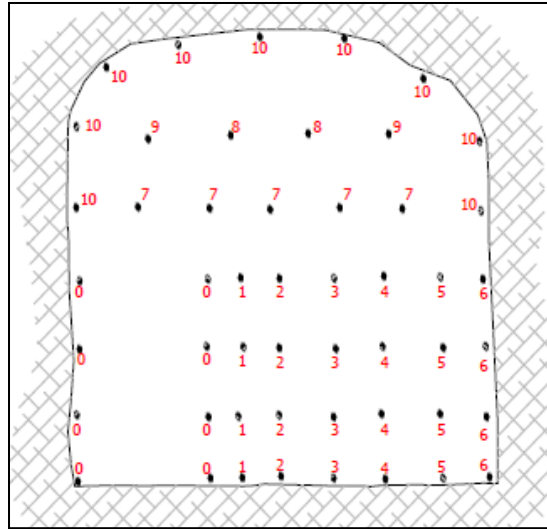


Figure 5.12: Section of the muzzle diagram.

The fans 1, 2,....., 6 are composed of 4 parallel mines superimposed in vertical planes (the sequence is that indicated by the ordinary numbers). That is, fan two must be exploded when fan one has already done its work, to unload part of the covering rock, and so on. To facilitate the task of the fans, the opening is operated for shorter "wedge" mines that start with a delay of 0. The completion of the section is done with contour mines: roof profiling and detection; these always shine last. However, given the intrinsic variability of configuration and rock structure, the miner adopts from time to time simple, already tested schemes of a few mines each, until the desired result is obtained.

The standard muzzle generally consists of the following characteristics:

- Excavation section: 39 m<sup>2</sup>;
- Drilling diameter: mines 40 mm;
- Mine depth: about 2 m;
- Number of mines: 50;
- Pattern of perforation with fan-shaped rhinestone;
- Explosive used: Nitram TX1 + gelatin;
- Maximum load of mines: 1.5 kg;
- Total flow rate: 75 kg;
- B.I. with the modular delay of 0.25 s and times from 0 to 8 - 10;
- Maximum charge for the delay: 12 kg;

With the adopted advancement scheme, it is possible to operate simultaneously on two fronts (right and left opening), allowing two daily sprints.

The size of the blast is ordinarily good and does not require secondary killing.

To secure the excavation sites at the end of each flight, an accurate check of the new wall is carried out, followed by the scaling operation, which allows the detachment of unstable blocks or slabs.

The felled material is cleared with tracked loaders and loaded onto dumpers to be transported to the crushing plant located near the offices. Such a plant is consisting of a HAZEMAG bar crusher and a reinforced concrete silo with a capacity of 350 m<sup>3</sup>. The product, once ground, is tapped from the loading nozzles of the silos and loaded onto the vehicles of the purchasing companies. On the square in front of the offices, there is an area used for stock storage where the mineral extracted is set aside to cope with any downtime of the mining activity. The crushing takes place through a mobile crusher mounted on the arm of a backhoe that allows simultaneous loading on the vehicles of the purchasing companies.

## 5.6 Bolting:

The bolting is used to support rock masses. For the design of the support system, the characteristics of the rock are important concerning its deformation mechanisms. It is also necessary to consider how the anchor itself reacts.

When a rock excavation is carried out, the redistribution of forces within the rock mass generates deformation states that the excavation surface can cause the release of blocks isolated from fractures or stratifications. Such blocks, if not held, can later trigger a collapse of the whole vault.

The primary function of an anchoring system is, therefore, to provide control of deformation phenomena and to support the disjointed rock prisms in order to maintain the interconnection forces of the rock mass and its geomechanical quality.

In choosing the most appropriate anchor for the specific project, particular attention should be paid to how the anchor manages to maintain the interconnections within the rock mass or, in other words, to how it generates its bearing capacity. The anchors resist the load through two mechanisms: adhesion and friction.



Figure 5.13: Principle of the adhesion mechanism on the left and the friction mechanism on the right.

### 5.6.1 Case of the Murisengo quarry:

In the quarry in question, to preserve the shape of the cable in situations where, through the inspection aimed at scaling the walls, the isolation potential of a unitary volume of considerable size (indicatively > one cubic meter) is highlighted through a consolidation system, with the aim of "sewing" the potentially unstable volume with the rocky portion behind it instead stable. This system, in addition to containing the single volume, represents a reinforcement element around the rock utilizing a containment action of the movements of distinct blocks of rock.

Among the various types of consolidation, the technique of anchoring with Swellex bolts and / or nails was chosen, which are well suited to the type of intervention to be carried out.



Figure 5.14: Swellex type bolts.

These fall within the so-called frictional anchors as they are integrally connected to the rock and operate in a traction and shear domain. The connection of the Swellex nails occurs through the mechanical expansion of the resistant element. Inside the hole, a hollow profile (tube) folded into an omega shape is inserted, which, subsequently, is expanded by pressurized water until a close contact is obtained along the walls of the hole itself. Once the expansion pressure is released, the surrounding rock tightens around the nail.

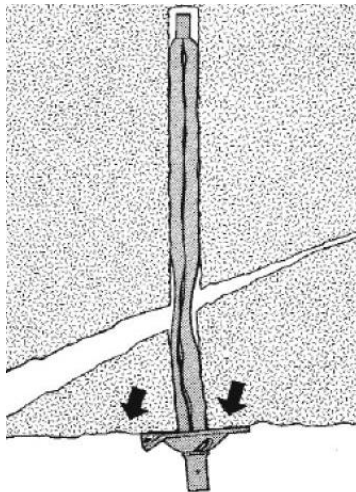


Figure 5.15: Pipe expansion.

The length of the nail must be to adequately deepen the portion of the stable mass, anchoring the potentially unstable amount of the mass to it. The resistance capacity of the nail, defined as the maximum load at which the system "slips off", is parameterized to the length of the nail itself, or the specific nail-rock friction.

To define the specific friction resistance, it was decided not to rely only on the table data provided by the manufacturer (which often coincide with the yield stress of the nail head) but to conduct pull-out tests in the field, calibrating the system according to the different types of gypsum (macro and microcrystalline, gypsum, etc.) and according to the length of the anchor. In this way, it was possible to define a specific resistance to extraction, then to size the

nailing with a standard mesh related to the length of the nails themselves. Therefore, once the weight of the volume of rock to be supported and its geometry is known, it will be possible to intervene with the insertion of n Swellex nails to guarantee the support of the rock volume to the healthy and stable rear mass.

The type of nails was also chosen based on the standard drilling diameters that can be adopted at the site and the relative capacity of the nail and rock coupling.

The characteristics of the nails used are summarized in the following table:

Table 5.3: Characteristics of the nails.

ERB 160	
Tube thickness	2 mm
Bolt diameter	38 mm
Original tube diameter	54 mm
Profile diameter	36 mm
Bushing head diameter	41/48 mm
Upper bushing diameter	38 mm
Hole diameter	43-52 mm
Optimal hole diameter	45-51 mm
Breaking load	160 kN
Minimum elongation	10 %
Typical elongation	20 %

It should be noted that the breaking load, equal to 160 kN, is related to a factory datum connected to the yielding of the head. The dimensioning of the plaster extraction capacity was the subject of specific in situ tests, carried out in collaboration with one particular company specialized in the sector.

### 5.6.2 Pull-out resistance tests:

To scientifically test the representative resistance of a Swellex type nail in plaster, a test campaign was carried out to subject the nails, through a controlled hydraulic system, to an incremental tensile force applied to the head until it reaches the extraction of the same.

The test was carried out by simulating representative applications in the different types of gypsum mass (micro / macrocrystalline and interference with geomechanical defects such as marly intercalations) and various types of nails (two other suppliers A and B).

The goal is to parameterize the pull-out resistance of the system concerning the unit length to identify an operating standard based on a model.

The tests were conducted on 12 nails installed on some sound pillars of Level E with lengths ranging from 80 to 300 cm. Each nail was previously prepared in a hole  $\Phi = 51$  mm at a pressure of 300 bar, using the supplied RX510E pump.

All tests were carried out by applying the sample nails on surfaces deriving from excavation operations with the traditional method; therefore, due to the effect of the seismic shock induced by the detonations, only the deep portion of the hole provides the maximum resistance capacity of the nail-hole-rock system. Even without knowing in a particular and defined way the least active portion towards the mouth of the hole, the tests conducted are also representative of this condition. From the first examination of the results, it is possible to make the following considerations:

- the pull-out resistance increases proportionally with the length of the nail itself, without showing substantial differences between the crystalline types of rock in which the preparations took place;
- the nails from supplier B provided a lower resistance than the factory data: these nails were purchased in 2012 but were kept in storage in the basement. The reasons for the behavior detected are being investigated.

Analyzing the data and referring to the variable "specific pull-out resistance [KN / m]", a trend that is hardly comparable with a normal distribution is highlighted. This condition is also maintained by eliminating any distribution outliers. However, the number of total components of the test is minimized and, therefore, also the representativeness of the statistical analysis itself.

By forcing a normal distribution on the available data, without identifying any anomalous data, the following distribution is obtained:

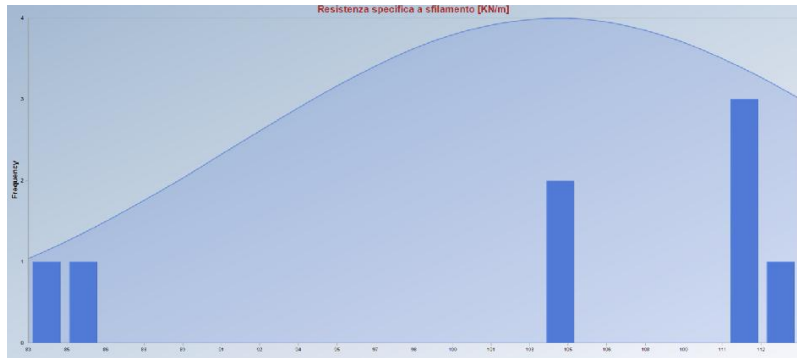


Figure 5.16: Normal distribution of available data.

By analyzing the distribution as a function of the percentile values, it is possible to make general and precautionary considerations:

- within the interval (there are 95.45% of the distribution values);
- over the value equivalent to the 5th percentile there are 95% of the distribution values.

Based on the above, it is clear that:

- in the interval (83.74; 135.06) KN / m there are 95.45% of the distribution values;
- over the 83.70 KN / m value, there are 95% of the distribution values.

Therefore, it is considered prudently to assume the following as the minimum representative value of the specific pull-out resistance in plaster of the Swellex type nails (having an internal resistance of 160 KN):

$$R \text{ unit sfilamento} = 83,70 \text{ KN/m}$$

Multiplying this value by the overall length of the nail, the widespread resistance to extraction will be obtained until the internal resistance dictated by the supplier's data is reached.

Therefore, in order to parameterize the pull-out resistance according to the technological characteristics of the nails to be used at the site in question, the following overall strengths are identified, meaning by nail length the only active length anchored in the compact rock that for the laying of protection net coincides with the size of the nail itself.

Table 5.4: Nail pull-out resistances.

<b>CHIODI TIPO SWELLEX (160 KN)</b>	
<b>Resistenze a sfilamento</b>	
Lunghezza attiva chiodo 80 cm	67 KN
Lunghezza attiva chiodo 100 cm	84 kN
Lunghezza attiva chiodo 120 cm	100 KN
Lunghezza attiva chiodo 150 cm	125 KN

## **5.7 Applications in the quarry:**

### **5.7.1 Museum area security:**

In the quarry in question, a museum project of part of the mining voids is underway which proposes a tourist and recreational-educational path based on gypsum, promoting visits to the heart of an underground deposit and attesting to its multidisciplinary culture: training, geology, process extraction, processing, the transformation of the raw material into a finished product, uses, comparison of gypsum in daily life.

The musicalization of a mining void passes through a series of functional requirements connected to the nature of the places. It is necessary to define the criteria to identify the instabilities and the related intervention schemes and principles of nailing sizing—arriving at a parameterization of the security level: a number that can be defined on an objective scale, the tranquility of the stay of visitors underground.

### **5.7.2 Stabilization of a rock block:**

I) Unstable unitary rock volume on the roof: this situation can be governed by a system of falling due to collapse or sliding; however, considering the attractive and cohesive actions along the fractures to be null and void, it allows us to return to the condition of instability due to collapse, certainly precautionary. The safety factor that is usually imposed for this type of potential failure is 2.0.

II) Unstable unitary rock volume on the wall: this situation is governed by a system of falling due to sliding along a fracture; therefore, to avoid excessive oversizing of the support system, it will be necessary to consider the attractive and cohesive actions along with the same fractures that isolate the block. If excessive dilations of the fractures are evident, it will, in any case, be precautionary to model the study in a condition of fall due to collapse. The safety factor that is usually imposed for this type of potential failure is 1.5.

### **5.7.3 Stabilization with a safety net:**

The geomechanical defects that intersperse the chalky rock mass can originate from fractures in the compact gypsum, interlayer sedimentary processes, or post-sedimentary marly injection processes. Often there is the case where the marly filling material, due to the geotechnical impoverishment, fragments falling by gravity towards the floor of the tunnels. On the other hand, the gypsum flaps are healthy on contact, i.e., they do not have further fractures and therefore do not require the interventions referred to in the previous paragraph. In this case, it is necessary to carry out interventions to support the marly fillings through the installation of special nets capable of absorbing static loads dictated by the volume of marl that is released over time from the original site, after appropriate sewing beyond the healthy rocky edges. The goal is to provide targeted support on the potentially unstable band, intercepting the flakes that may fall, and at the same time, offering passive support for subsequent detachments. This type of intervention is not systematic; therefore, we proceed with identifying a representative intervention criterion.

## **5.8 Conclusions:**

Following the aforementioned tests, assuming that the support nails of the protection nets must be set up in healthy rock volumes in contact with the edges of the intercalations to be protected (i.e. a correct rock-nail coupling is guaranteed), it is possible to assume the following representative levels of resistance:

SWELLEX TYPE NAILS (160 KN)

Pull-out resistors

Active nail length 80 cm 67 KN

Active nail length 100 cm 84 kN

Active nail length 120 cm 100 KN

Active nail length 150 cm 125 KN

SWELLEX TYPE NAILS

Tensile strength 160 KN

Breaking load for shear 70 kN

Specific pull-out resistance (in plaster) 83.7 KN / m

Based on the above, it is possible to proceed with the stability check for the support nails. Assuming to set up the nails, parallel to the development of the edges of the discontinuities to be protected, at a maximum pitch of 1.0 m and having a maximum traction tension of the network equal to 55 KN / m, it is possible to estimate the inclined force to which it is subject. each nail equal to 55 KN / m x 1.0 m = 55.0 KN.

This force can be broken down into the normal and orthogonal components to the head of the nail itself, obtaining, based on the inclination assumed for the deformation of the mesh, the following forces:

$$N = R \times \sin 5^\circ = 4,80 \text{ kN} < \text{pull-out resistance}$$

(always checked for active length > 80 cm)

$$T = R \times \cos 5^\circ = 54,80 \text{ kN} < 70 \text{ kN}$$

In conclusion, by using nails with the characteristics listed above to secure some areas of the quarry, it can be assumed that sufficient precautions have been taken for the environment in which the museum will be built and for the safety of underground visitors.

## 5.9 Introduction to Previous Solution for The Ventilation System of The Mine:

This Ventilation Plan quantifies and describes the techniques adopted at the San Pietro - PratoNuovo underground quarry, aimed at guaranteeing the ventilation of construction sites, or rather at maintaining a suitable working atmosphere over time. This document integrates and completes the documentation relating to S.I.A. to specifically adapt to the practical construction site of the attachment points, optimizing the

knowledge of the ventilation system and identifying appropriate implementation criteria according to the progressive progress of the works.



Figure 5.17: A view of the inside of the Murisengo mine.

#### 5.10 Ventilation System of the Murisengo Mine:

The ventilation of the San Pietro \_ PratoNuovo quarry is managed to utilize an inverted flow system between the hot and cold seasons, thanks to the presence of two vertical chimneys communicating with the third and fourth level of cultivation, exploiting the natural flows and accelerating them in the cultivation points. The closure of unproductive branches of tunnels employing mobile plastic sheets allows fresh air flows in the work areas, without dispersion. Cultivation, which takes place in descending levels, also allows vertical connections between the different levels and, therefore, a continuous link of the prominent chimneys with the construction site areas where a suitable working atmosphere must be guaranteed.

### 5.10.1 Minimum Capacity for Correct Sizing of the Ventilation System:

there is a need to quantify the quantity of healthy air guaranteed on-site preliminarily. To calculate the minimum flow rate, the available technical literature must be taken into account. In this case, the D.P.R. 128/59 and establishing that the ventilation must guarantee the suitable dilution of any harmful gases and dust, specifies that the air currents must have a speed between 0.1 and 6.0 m / s (see art. 262 of the decree mentioned above). This maximum value can be exceeded along with the opening wells, pipes, and the air tunnels not used by the personnel and/or transport of ore. Furthermore, the D.P.R. 320/56 art. 30 c.2, although not referring specifically to the mining sector but undoubtedly useful for further design indications, requires an air quantity of  $4 \text{ m}^3/\text{min}$  ( $0.066 \text{ m}^3/\text{sec}$ ) for HP Diesel and  $3 \text{ m}^3/\text{min}$  ( $0.05 \text{ m}^3/\text{sec}$ ) for each worker. These criteria were also taken from Technical Recommendations (see SIA 196) according to which the value of  $0.066 \text{ m}^3/\text{sec}$  KW diesel is recommended with the introduction of low-emission diesel engines and low-sulfur fuels; this parameter can be reduced up to 50% for vehicles not used at the front ( $K_u = 0.50$ ). A variable reduction between 75% and 50% considers the actual level of pollutants present in the tunnel concerning the TLV limit exposure values. A final safety factor  $k_s$  equal to 1.1 - 1.2 is also suggested to be applied to the final theoretical volume. Based on the operation of the Cava San Pietro - PratoNuovo, the following operational simulations can be considered representative:

Construction site using the Drilling & Blasting excavation method:

Drilling Wagon Tamrock HS 105 (diesel engine 55 kW used only for the translation of the vehicle; the hydraulic services of drilling and lighting are served by an ee generator placed at a distance of about 30 meters from the drilling point thanks to a power cable reel).

GEH 220 Electric Energy Generator (160 kW diesel engine): installed on a truck that allows it to be translated and moved at any time.

Mercedes Truck (97 kW diesel engine): used to transfer the electric generator.

Descerter(108 kW diesel engine): used as a preliminary to drilling operations.

The management of the construction site provides for the single presence as a function of the disgagger only, or only the single presence as a function of the Mercedes truck alone for the transfer of the electro generator positioned about 30 meters from the drilling point. The operator then proceeds with the transfer of the drilling rig with the diesel engine drive; once the placement has been completed, the generator is activated, which allows the service movements for drilling. During the drilling of the blast holes, the air purging of the same holes produces air-dispersible dust, which is picked up by an aspirator installed on the machine with a suction bell integrated into the arm with the whole mouth. The collected dust is discharged to the ground in cycles after passing through a bag filter fully timed with the drilling operations.

This construction site can therefore be simulated with an operating power of:

- disgagger in operation: 108 kW or
- generator transfer truck: 97 kW or

- electricity generator: 160 kW (positioned 30 meters from the construction site in a secluded position) or
- drill rig: 55 kW (during transfer only)
- presence of 1 employee (driller)

The worsening situation is that dictated by the presence of the generator with an installed power of 160 kW placed at a distance of 30 meters from the construction site where the operator remains.

Mine loading yard:

Company Pick-up (90 kW diesel engine used only for the transport of explosive material to the front).

ICARUS 36.16 Lifting Platform (75 kW diesel engine used for lifting the fire (s) for loading the upper part of the muzzle).

The management of the site involves the supply of explosive material with unloading at the front. The company vehicles arrive at the front, are turned off to proceed with the unloading of the explosives. There is a maximum of 2 front staff present (fires or help fires). Subsequently, the site is freed to make room for the ICARUS lifting platform, which is operated by the same two operators on the ground or with basket control for the movement of the arm only. During the muzzle loading (about 1.5 hours), the boom and the vehicle are moved about ten times, with actions that require the diesel engine to be switched on for less than a minute.

This construction site can therefore be simulated with the operating power of:

- liftable platform in ICARUS function: 75 kW (the brevity of the use of the diesel engine must, in any case, be considered);
- presence of 3 firefighters/help firemen

Mud yard:

963 D Track Loader (141 kW diesel engine): used for loading the felled ore on the excavation truck;

DAF CF85 Truck (340 kW diesel engine): used for the excavation of the crushing plant of the felled ore;

The management of the construction site foresees the presence in the action of the shovel or the truck. The phase can be carried out by a single operator who, after positioning the truck, loads it utilizing the shovel, or by two operators (a driver and a palista). For obvious reasons of space, the truck does not access the front but remains at a distance of about 15 -20 meters, while the shovel accesses the front to collect the ore and then move to the location of the truck for unloading. This construction site can therefore be simulated with an operating power of:

- Crawler Loader: 141 KW or
- DAF CF 85 Truck: 340 KW (positioned at a minimum of 30 m from the site but kept off during loading operations).

- the presence of a maximum of 2 employees (driver and palista).

The pejorative situation is that dictated by the presence of the shovel at the front (without the presence of workers on the ground) and the arrival of the truck at a minimum distance of 30 m from the front (without the presence of workers on the ground) with the presence of the two workers driving of vehicles. It is assumed that the vehicles do not work with the engine running at the same time.

Felling/Profiling site with a hammer:

CAT 325C Tracked Excavator (130 KW diesel engine) used for the felling of Patari or profiling of fronts/tunnels.

The management of the construction site foresees the presence in the action of the excavator equipped with the hydraulic tool consisting of a hydraulic breaker. The operator driving the excavator proceeds to cause breakages in the muzzle flaps after they have been hooked up at a unique isolated site. The operation does not require the presence of personnel on the ground.

This construction site can therefore be simulated with an operating power of:

- Crawler Excavator: 130 KW.
- Presence of 1 employee (excavator).

Construction site profiling with cutter:

LIEBHERR 944 Tracked Excavator (180 KW diesel engine): used for tunnel profiling and selective advancements.

GEP 55-2 Generator (40 KW diesel engine).

The management of the construction site foresees the presence in the action of the excavator equipped with the hydraulic tool consisting of a cutter with peaks. The operator driving the excavator proceeds to cause the tearing of flaps of rock by successive passes. The operation in correspondence with strongly cohesive benches and the operational phase in the upper part can produce air-dispersible powders. These powders are picked up by an electric aspirator (powered by the generator located about 50 meters from the front and in a secluded position) and fed with an aero tube into a blind tunnel for decantation. The operation does not require the presence of personnel on the ground.

This construction site can therefore be simulated with an operating power of:

- Crawler Excavator: 180 KW.
- Generator: 40 KW (installed about 50 meters from the front in a secluded position).
- Presence of 1 employee (excavator/miller).

Based on the considerations above of standardized organization of construction sites, the minimum flow rates to be guaranteed on construction sites to obtain optimal working conditions for operators and to allow sufficient dilution of exhaust gases of diesel vehicles operating in tunnels are deduced.

Table 5.5: Minimum air quantities in different sites.

Site/operation	Minimum capacity (m <sup>3</sup> /s)
DRILLING AND BLASTING	2.98
CARICAMENTO MINE	2.90
SMARINO	5.60
MARTELLONE	4.81
FRESA	7.38

The minimum flow rates expressed above derive from considerations of effective building site capability. Depending on the work organization, it is possible to have the following combinations between the different operations in contiguous construction sites:

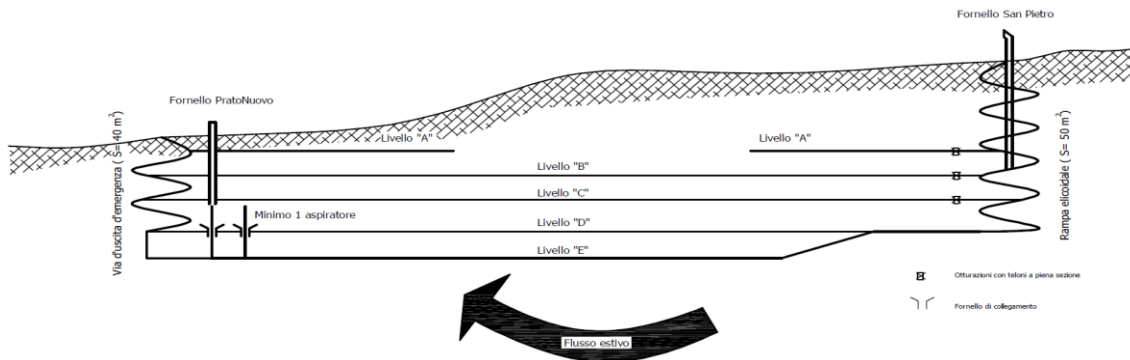
- drilling and blasting + excavation with an air requirement of 8.58  $m^3/sec$ .
- cutter with air requirement equal to 7.38  $m^3/sec$  (the spoil of the milled material must, for technical reasons, take place when the cutter is stationary).
- Muck with an air requirement of 5.60  $m^3/sec$ .
- loading of mines + spoil with air requirement equal to 8.50  $m^3/sec$
- hammer + spoil with air requirement equal to 10.41  $m^3/sec$

The heavier working conditions, therefore, require an inflow of healthy air equal to about 11  $m^3/sec$ .

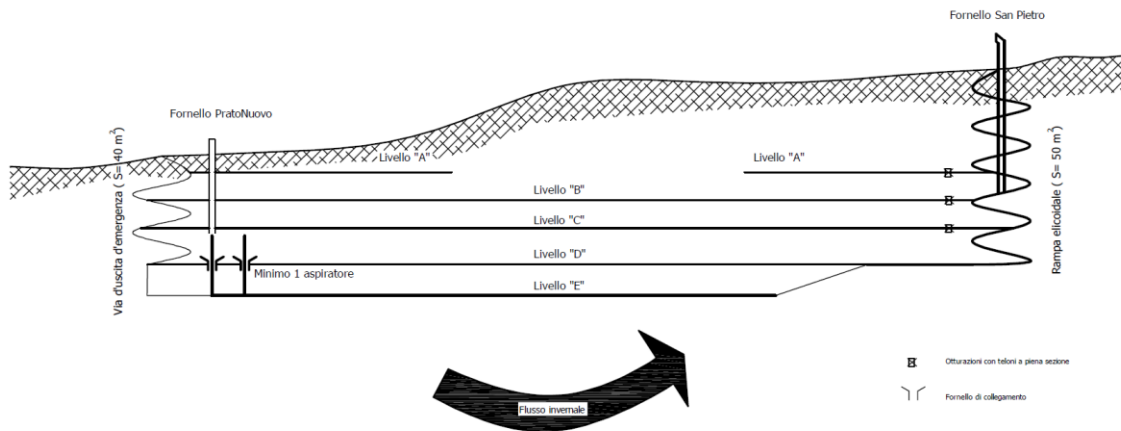
#### 5.10.2 Ventilation System:

The ventilation system adopted envisages the following general arrangement:

## Summer Period



## Winter Period



As shown in the diagrams above, ventilation occurs in the summer by inflows of healthy air through the Rampa San Pietro. Through the descent ramp to the fifth level (where two flow accelerators are also located), the healthy air reaches the construction sites of Level E, where the presence of vertical connecting stoves with Level D, creates a recall effect for the same healthy air.

In this case, the suction through the vertical cookers takes place via a primary fan installed in the mouth of the cooker for vertical connection with level E-D.

The vertical stoves are made in advance of the extraction sites. The barycentric stove on the construction site is set up with the primary fan; the secondary stoves (formerly barycentric but close to the site) are set up with secondary fans, which are not taken into account in the calculations, as a precaution. Where such secondary burners risk creating a short circuit, the flows are suitably occluded.

The unhealthy air flows are conveyed to the PratoNuovo area of level D, where the depression induced by the PratoNuovo stove and ramp facilitates its evacuation from the basement.

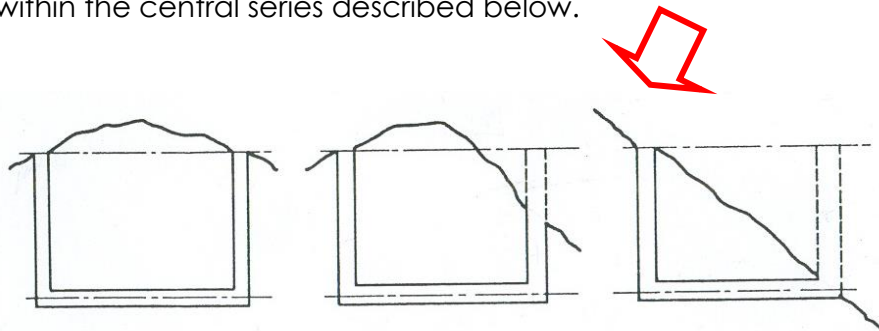
In the winter period, the flow described is reversed. Healthy air enters from the PratoNuovo stove and reaches Level D, from where it will get Level D through the barycentric stove at the construction site.

The unhealthy air then proceeds towards the San Pietro ramp with the aid of accelerators that facilitate its flow at critical points.

Any construction sites located in a non-barycentric position concerning the inter-floor stove system are managed by pumping air from the inflow tunnel with aero tubes.

### 5.11 Performance Verification:

Periodic anemometric measurements (already validated by the Politecnico di Torino) have shown over the years that, due to the geometry of the main burners and the differences in height between their mouths, the San Pietro - PratoNuovo quarry falls within the central series described below.



	Left	Center	Right
Need to induce .....	Yes	No	NO
Direction, winter .....	Either	Right to left	Right to left
Direction, summer .....	None	Left to right	Left to right

At the inlets and in the subsequent air tunnels (flow and outflow) the airflow is periodically checked, which assumes a minimum representative value of  $10 \text{ m}^3/\text{sec}$ .

Through plastic separating curtains, accelerators, and fans, it is necessary to continually ensure that the minimum flow rate is estimated in par. C is sucked/pumped to the construction site area.

### 5.12 Computation Theory:

For the air to move, inside a circuit, from a point A to a point B, the pressure  $P_A$  in A must be greater than the pressure  $P_B$  in B. This pressure difference can be induced by the topography of the inlets (differences in level as in the figure above), by the difference in temperature between the inside and outside of the tunnels, but above all with the

help of fans that produce a pressure/depression according to their pressing or suction action.

If the laws that regulate the movements of gases in the ducts are strictly applied to the air circuits in quarries/mines, calculation difficulties are encountered that are not easily overcome, with purely theoretical results, because underground pressures and temperatures vary from point to point.

To obtain practical results, the following hypotheses are formulated:

- it is assumed that the movement of air is comparable to the movement of incompressible fluids, i.e., it is assumed that the volume  $V$  of the moving air is constant;
- the law of continuity of motion is applied, and precisely, it is assumed that in a given point, the flow rate does not vary with time, nor does it vary from one point to another in the quarry/mine. That is, it is assumed that the equation is satisfied at every point and every moment

$$Q = S \cdot v = k$$

Where,

$Q$  represents the range,

$S$  represents the section of the circuit,

$v$  represents the air velocity,

Once all these hypotheses have been accepted, it is possible to apply Bernoulli's theorem to underground air circuits.

In reality, due to the resisting effect that the same air undergoes during its travel, braking action is generated on the flow itself, which is identified with the pressure drops " $h$ ".

The resistances that the air currents encounter in the underground circulation are due to friction, swirling motions, collisions against the walls due to section changes, etc., phenomena that result in a loss of live force of the flow. The pressure drops are the component to be calculated in advance in order to know how much energy must be transferred, by means of the fans or the topographic provisions of the inlets, to the air itself so that it can complete the entire path of the circuit, guaranteeing constant washing of the construction sites from gaseous polluting substances. To calculate the frictions or the head losses it is necessary to break down the basement into many homogeneous sections by flow section, condition of the walls, etc.

#### 5.12.1 Straight Sections:

In straight sections of tunnels, shafts, and stoves, the pressure drop  $h'$  is proportional to the length  $L$ , to the perimeter  $P$ , to the square of the speed, and inversely proportional to the area  $S$  of the free section, that is  $h' = \alpha L P V^2 / S$  where  $\alpha$  is a proportionality coefficient that depends on the nature of the duct and which, according to the technical literature, can be assumed according to the following criteria:

according to Murgue's experiments, the coefficient  $\alpha$  for straight tunnels normally would assume the following values:

in galleries with wooden armor:  $\alpha = 0.00156 - 0.00240$

in tunnels without armor:  $\alpha = 0.00094 - 0.00120$

in galleries lined with masonry:  $\alpha = 0.00033 - 0.00055$

According to petit's experiences, in the ventilation of sheet metal with circular diameter of diameter D, the coefficient  $\alpha$  would assume the following values:

for D = 0.26 m  $\alpha = 0.0004635$

for D = 0.45 m  $\alpha = 0.0003100$

for D = 0.60 m  $\alpha = 0.0002267$

for D = 1.00 m  $\alpha = 0.0002020$

### 5.12.2 Wellsa

The above formula can also be validated for wells, with the foresight to consider the total perimeter given by the real perimeter  $P_r$ , plus the fictitious perimeter  $P_f$ , which considers the obstacles to air currents that exist in the wells. In the case in question, the wells (stoves) are made by boring vertical holes or with concrete profiles without guides or crosspieces or stairs; therefore, there is no need to consider reductive factors. For wells, the coefficient  $\alpha$  assumes the following characteristic values.

**Nei pozzi il coefficiente  $\alpha$  assumerebbe i seguenti valori:**

<b>in roccia nuda e guide di legno frontali:</b>	<b><math>\alpha = 0,00238</math></b>
<b>in roccia nuda e guide di legno laterali:</b>	<b><math>\alpha = 0,00295</math></b>
<b>con rivestimento in muratura e guide frontali:</b>	<b><math>\alpha = 0,00117</math></b>
<b>con rivestimento in muratura e guide Briart:</b>	<b><math>\alpha = 0,00132</math></b>

### 5.12.3 Elbows:

The elbows are the cause of substantial load losses because the vortex motions that produce them are equivalent to a throttling of the section. Experience has shown that the pressure drop in an elbow is proportional to the square of the speed. Precisely if  $\beta$  is a coefficient of proportionality that depends on the angle of the elbow, the pressure drop  $h''$  due to an elbow is represented by the formula:

$$h'' = \beta V^2 / 2g$$

The coefficient  $\beta$  is difficult to determine as it varies with the angle of the elbow. To obviate this complexity, the virtual length of the elbow is considered, i.e., the length of the rectilinear tunnel with section and lining equal to those of the elbow, which has equal resistance to the passage of air. For non-joined elbows, which form angles of 45°, 90°, and 135°, the following equivalences are obtained:

$$45^\circ \text{ angle } L = 162 \text{ m}$$

$$90^\circ \text{ angle } L = 82 \text{ m}$$

$$135^\circ \text{ angle } L = 23 \text{ m}$$

#### 5.12.4 Changes of Section:

There are head losses due to section variations, which may come from roof irregularities or actual or proper narrowing of the tunnel section. If  $\delta$  is the specific weight of the fluid (air) and  $v$  and  $v_1$  are the speeds corresponding to sections of the tunnel where the section is respectively equal to  $s$  and  $S$ , the pressure drops  $h'''$  is given by:

$$h''' = \delta (v - v_1)^2 / 2g$$

#### 5.12.5 Chokes:

The effect of a restriction in the flow section of fluid is to induce a contraction of the flow lines; beyond the restriction, the fluid expands to resume the normal pre-existing movement. The pressure drops thus produced by the contraction and by the swirling movements that occur in the vicinity of the bottleneck derives from the following formulation:

$$h'''' = \left( \frac{\delta v^2}{2g} \right) [(S / \mu s) - 1]^2$$

The experimentally calculated  $\mu$  value can be considered equal to 0.65.

By parameterizing the shrinkage to an equivalent length, Petit elaborated the following equivalences:

$S/s$	10	22.5	40
$L_{eq}$	4177 m	22787 m	73875 m

#### 5.12.6 Total Pressure Losses and Power:

The total resistance  $h_t$  of the ventilation circuit is therefore given by:

$$h_t = h' + h'' + h''' + h''''$$

At steady state, i.e. with constant speed and flow rate, the useful work of the ventilation expressed in HP is given by:

$$P_u = Q \cdot h / 75$$

The motor coupled to the fan must therefore have a power given by:

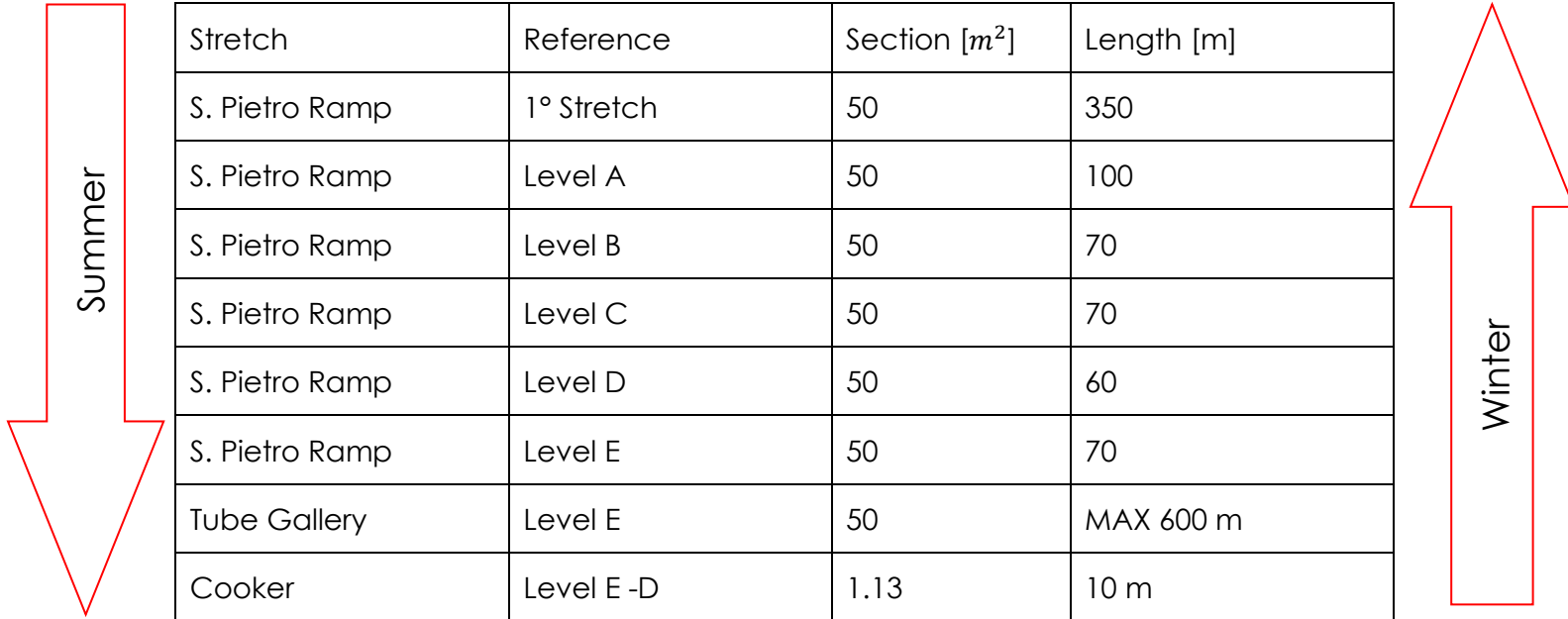
$$N_{HP} = Q \cdot h / (\gamma \cdot 75)$$

Where,

$\gamma$  represents the assumable mechanical efficiency of the motor equal to 0.65 -0.85.

### 5.13 Circuit Analysis:

The ventilation circuit of the San Pietro - PratoNuovo quarry has a natural capacity for air exchange between the two inlets. When the artificial ventilation is off, it is around  $10 \text{ m}^3/\text{sec}$ . Artificial ventilation, therefore, allows creating depression/overpressure useful for reaching fresh air flows even in construction sites further away from the inflow tunnel. Seasonally, the ventilation is reversed to have artificial ventilation of a sense concordant with natural ventilation. The annual time in which to carry out this operation is defined according to the monitoring conducted on the ventilation itself and the climatic conditions of the area. By analyzing the circuit, the following geometric flow structure is obtained:



Stretch	Reference	Section [ $\text{m}^2$ ]	Length [m]
S. Pietro Ramp	1° Stretch	50	350
S. Pietro Ramp	Level A	50	100
S. Pietro Ramp	Level B	50	70
S. Pietro Ramp	Level C	50	70
S. Pietro Ramp	Level D	50	60
S. Pietro Ramp	Level E	50	70
Tube Gallery	Level E	50	MAX 600 m
Cooker	Level E -D	1.13	10 m
Elbows	Ramp and Tapping Gallery	n. 25 da $90^\circ$	Equivalent to $82 \times 25 = 2050 \text{ m}$
Choking	Cooker Level E-D	S/s = 50	Equivalent to 80000 m
Well with Primary Fan	Cooker Level E-D	1.13	10 m
GALLERIA COLLEGAMENTO	Level D-D	50	50
Stove PratoNuovo	Covered Section	1.76	15

During the summer, natural ventilation is adopted combined with artificial suction

ventilation with inflow along the San Pietro ramp and outflow along with the PratoNuovo stove. In this setting, it is necessary to ensure that the ventilation system is sized in such a way as to create a depression that facilitates the arrival of healthy air to the construction sites and evacuates the unhealthy air. In the winter period when natural ventilation is adopted combined with artificial ventilation following the inflow along with the PratoNuovo stove and outflow along the San Pietro ramp. In this setting, it is necessary to ensure that the ventilation system is sized in such a way as to create an overpressure that facilitates the arrival of healthy air to the construction sites and evacuates the unhealthy air.

### 5.13.1 Calculation of Head Losses:

The pressure drops due to the resistances that the healthy air encounters in the path along the inflow tunnels considering the ramp sections and the elbows, the total lengths and the equivalent lengths are equal to about 40 Pa, as illustrated in the following table (as a precaution, the equivalent calculation length was rounded up to 100,000 m).

Portata di progetto		12	m <sup>3</sup> /s	
GALLERIA	PARAMETRI			
	α =	0,0012		
	L =	100000 m		
	S =	50 m		
	P =	30 m		
	Q =	12 m <sup>3</sup> /s		
	A =	50 m <sup>2</sup>		
	h =	4,1472 kg/m <sup>2</sup>		
		40,684 Pa		
		$h = \frac{\alpha L P Q^2}{A^3}$		

Along the E-D connection shaft, there is a localized leak of 100 Pa, as illustrated in the following table.

Portata di progetto		12	m <sup>3</sup> /s	
POZZO E-D	PARAMETRI			
	α =	0,00295		
	L =	10 m		
	Φ =	1,2 m		
	P =	3,768 m		
	Q =	12 m <sup>3</sup> /s		
	A =	1,1304 m <sup>2</sup>		
	h =	11,0815 kg/m <sup>2</sup>		
		108,71 Pa		
		$h = \frac{\alpha L P Q^2}{A^3}$		

Along with the PratoNuovo stove, there is a localized leak of 50 Pa, as illustrated in the following table.

Portata di progetto		12	m <sup>3</sup> /s
FORNELLO PRATONUOVO	PARAMETRI		
	α =	0,00295	
	L =	15	m
	Φ =	1,5	m
	P =	4,71	m
	Q =	12	m <sup>3</sup> /s
	A =	1,76625	m <sup>2</sup>
	h =	5,44678	kg/m <sup>2</sup>
		53,433	Pa
		$h = \frac{\alpha L P Q^2}{A^3}$	

As a result of the widening of the section between the PratoNuovo stove and the tunnel connecting with the E-D stove, with a flow velocity variation from 6.81 to 0.24 m / s, there is a pressure drop of 30 Pa.

By adding up the individual losses found, the following total pressure loss of the circuit is therefore deduced:

$$h_t = h' + h'' + h''' + h'''' = 230 \text{ pa}$$

The loss due to the dynamic pressure of approximately 100 Pa must be added, thus obtaining the total design head loss of 330 Pa, which can be rounded up to 350 Pa.

#### 5.13.2 Calculation of the Power:

to Install Using a standard fan with mechanical efficiency equal to 0.80, the need arises for a minimum installed power equal to:

$$N_{HP} = Q h / \gamma 75 = 10 \text{ KW}$$

Based on the calculations of the pressure drops, it is possible to proceed with the choice of the primary fan to be installed at the mouth of the suction cooker ED, which must be able to overcome the total losses of the circuit of 350 Pa and guarantee a flow rate of 12 m<sup>3</sup>/sec.

The supplied fan has a Δh = 1200 Pa, an airflow rate of 43,200 m<sup>3</sup>/sec = 12 m<sup>3</sup>/sec and installed power of 30 kW; therefore, it is suitable.

In this setting, it will be necessary to provide suction cookers in progress to the workings to satisfy the centrality of the sites with the suction point. Indicatively, based on the experience gained, it was found that every 50 meters of progressive progress of the site, it is functional to proceed with a new barycentric stove.

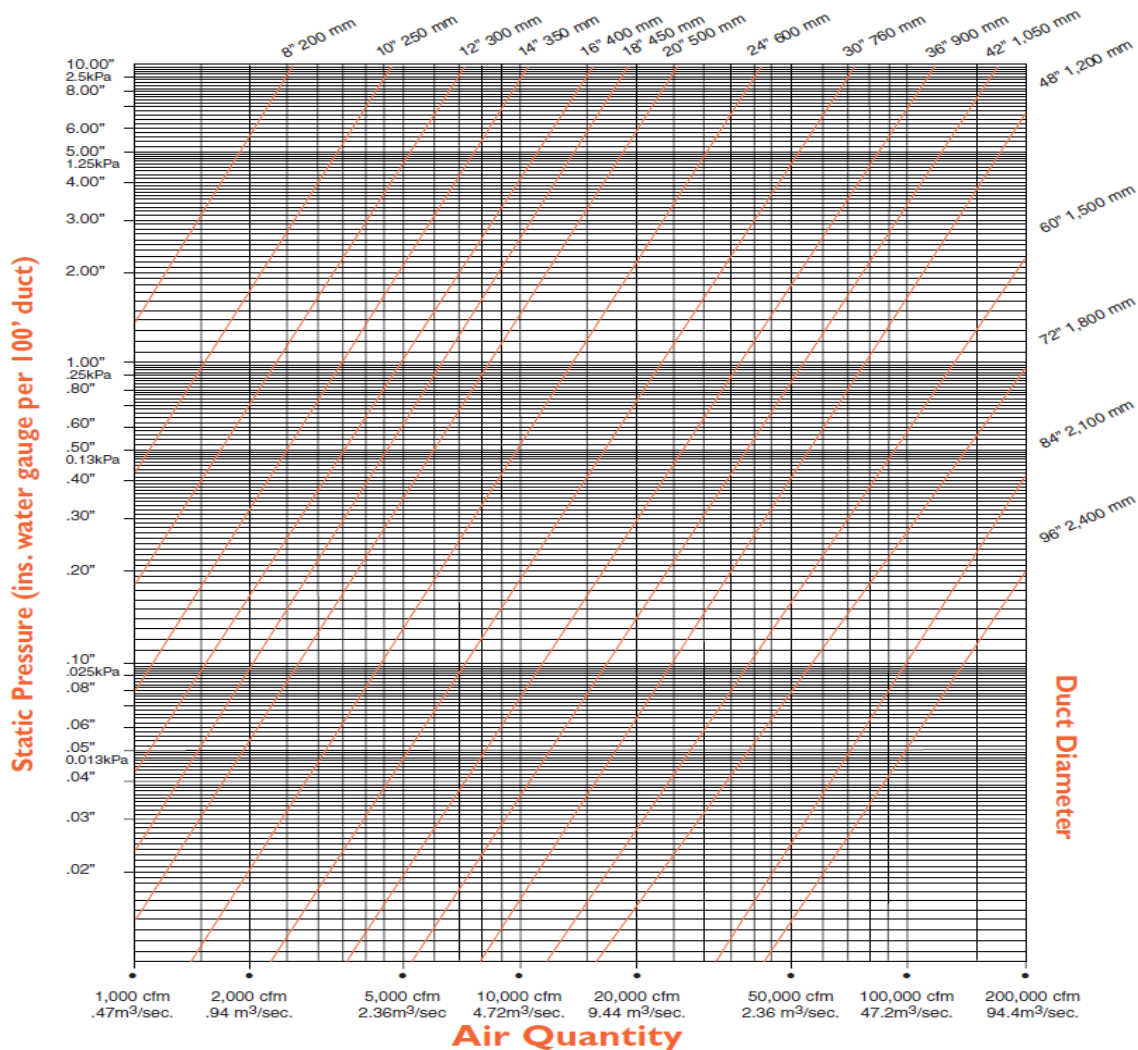
#### 5.13.3 Calculation of the Power to be Installed in Ventilation Arrangement Using an Air Pipe:

If there are difficulties in guaranteeing the connection employing inter-story ED stoves, it will be possible to manage the construction sites by pumping fresh air from the inflow or suction ducts of unhealthy air and its transfer to the outflow points utilizing a floppy aero

tube  $\Phi$  1000. It is conservatively estimated a maximum length of aero tube equal to 200 m. In this case, in addition to the head losses of the primary ventilation circuit calculated above, the head losses induced by the pipe itself must also be added. In this case, it is necessary to refer to specific schedules provided by the manufacturing companies.

Assuming a maximum length of the floppy pipeline of 200 m and a flow rate of 12  $m^3/sec$ , a pressure drop of 0.104 kPa every 100 feet is obtained, i.e., 104 Pa every 30 m or 690 Pa over the entire length of the pipeline (200 m).

### Flexible forced duct friction loss chart (Layflat duct)



Based on the calculations of the pressure drops, it is possible to proceed with the choice of the primary fan to be installed at the mouth of the pumping area, which must

be able to overcome the total losses of the circuit of  $350 + 690 = 1040$  Pa and guarantee a flow rate of  $12 \text{ m}^3/\text{sec}$ .

The supplied fan has a  $\Delta h = 1200$  Pa, an airflow rate of  $43,200 \text{ m}^3/\text{sec} = 12 \text{ m}^3/\text{sec}$ , and installed power of 30 kW; therefore, it is suitable.

#### 5.14 Secondary Ventilation:

In correspondence with processes characterized by producing powders (see milling), it is necessary to intervene with a dry collection system capable of sucking up the airborne particles and moving them away from the site.

The system adopted envisages suction at the front (dust production point) with a slightly higher flow rate than the inflow ( $> 12 \text{ m}^3/\text{sec}$ ) to always guarantee a slight depression at the front, which in any case favors correct healthy air exchange.

The system provides for the positioning of a silenced fan/aspirator about 20 meters from the front: on the suction side, installing a spiral pipe, while on the pumping side, the installation of the first section of spiral pipe and a subsequent one. Limp pipe section. Through the delivery duct, the flow of dusty air captured at the front is sent to the mouth of the E-D suction stove (and sent to the upper level for decanting) or to a blind tunnel for decanting.

The suction circuit, therefore, has a total head loss, which can be calculated as a function of the length of the ducts and the relative characteristic schedules.

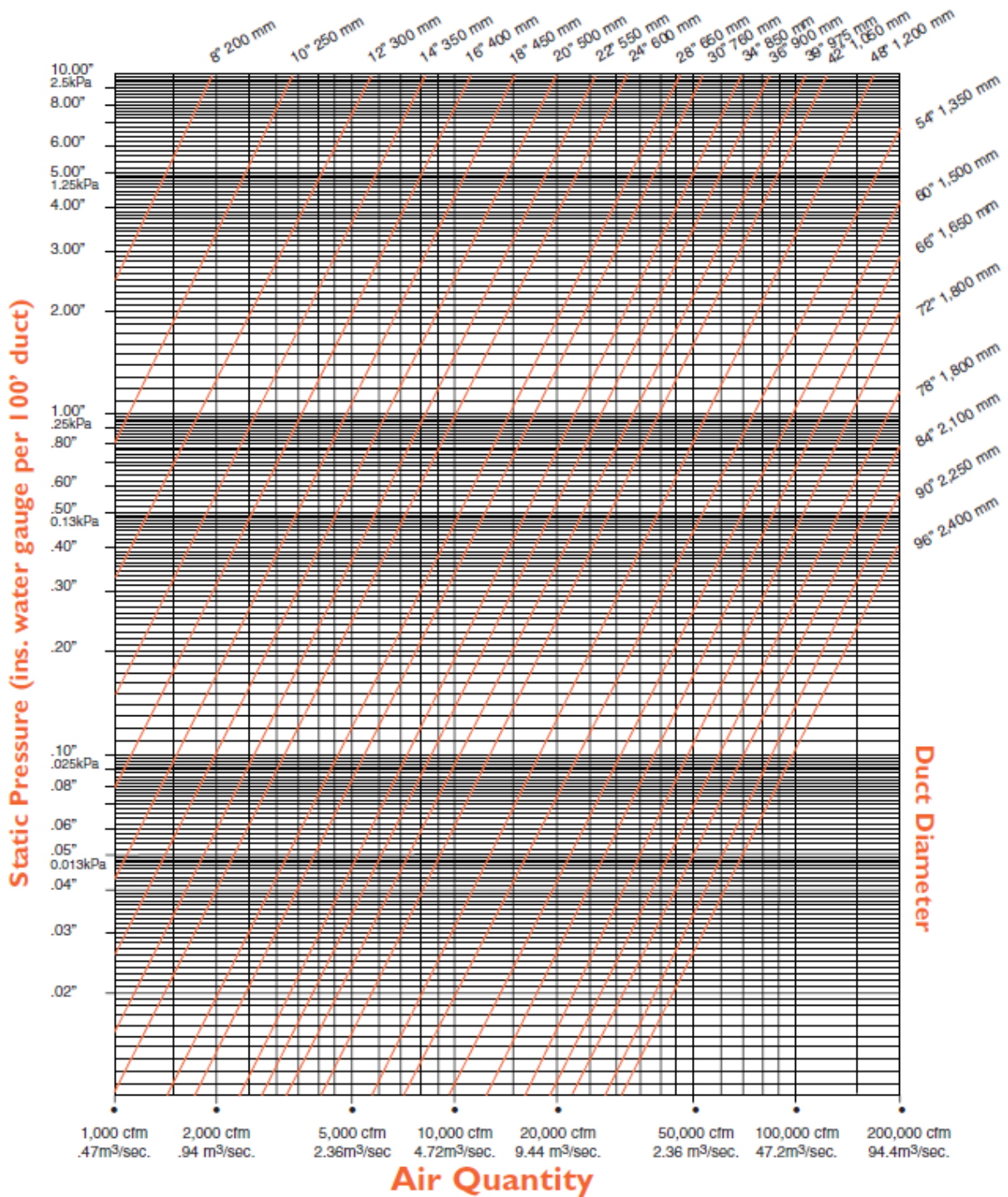
The stretch of the spiral duct is 30 m. The length of the limp pipeline is 20 m. The diameter of the pipes is 700 mm to minimize interference with the works.

Based on the previous (Layflat duct) and following (Spiral duct) abacus, a pressure drop equal to:

FLOSCIO:  $0.57 \text{ kPa} / 100 \text{ feet}$  or  $570 \text{ Pa} / 30 \text{ m}$  or  $380 \text{ Pa}$  every 20 meters.

SPIRAL:  $0.702 \text{ kPa} / 100 \text{ feet}$  or  $702 \text{ Pa}$  every 30 meters.

## Flexible suction duct friction loss chart (Spiral duct)



The total loss of the duct (suction/delivery without bottlenecks and bends) is, therefore, equal to 1100 Pa.

The supplied fan has a  $\Delta h = 1430$  Pa, an airflow rate of  $13 \text{ m}^3/\text{sec}$  ( $> 12 \text{ m}^3/\text{sec}$ ), and installed power of 30 kW; therefore, it is suitable.

This was the previous measure for the ventilation system of the Estrazione Gesso and the new solution for this ventilation system will come in the following chapters.

#### 5.15 Measurement Ratio of Airborne Pollutants:

UNDERGROUND GAS ( $\text{CO}_2, \text{CO}, \text{NO}, \text{NO}_2, \text{SO}_2$  and  $\text{O}_2$ ), (ex D.Lgs.81/08, DPR 128/59, D.Lgs.624/96), Reliefs of 12 February 2020:

This measurement report refers to a monitoring of airborne pollutants carried out, on February 12, 2020, at the gypsum quarry "San Pietro - Pratonuovo", Strada San Pietro n.14, Murisengo (AL), of the company ESTRAZIONE GESSO S.A.S.

The monitoring was aimed at determining the airborne concentration of the following underground gases:

- Carbon dioxide ( $\text{CO}_2$ );
- Carbon monoxide ( $\text{CO}$ );
- Nitrogen monoxide ( $\text{NO}$ );
- Nitrogen dioxide ( $\text{NO}_2$ );
- Sulphur dioxide ( $\text{SO}_2$ );
- Oxygen ( $\text{O}_2$ ).

This contains the results of the surveys carried out and the evaluations in this regard. The measurements were carried out in accordance with DPR 128/59, DLgs 624/96 and DLgs 81/08.

#### 5.16 General Farm Data:

Gypsum mining operates, in the field of industrial production of ore Gypsum; in the San Pietro area in the municipality of Murisengo (Prov. Alexandria) The company itself manages the underground excavation of the quarry called "San Pietro Pratonuovo" for the collection of gypsum stone intended, mainly, for the cement industry.

The cultivation work carried out on the date of the surveys consists of underground excavation at Level F (altitude c.ca 158m above sea level). Outside the quarry (altitude about 280m) there are storage areas, crushing and selection plant and storage, not far away are the technical offices.

#### 5.17 Job description

The palisade operator shall, by means of the Liebherr 576 wheeling machine, handle the felled ore and load the tout venant on the trucks, press or storage areas located at Level F; the operator operates from a closed cab with air.

The truck operator transports the ore outwards via the ASTRA 8450 HD 9 truck to the treatment plant (crushing); the operator operates from a closed cab with air conditioning.

The drill operator drills the tamrock HS105 drilling machine to drill the excavation front; this vehicle is not equipped with a closed cabin, the operator therefore operates from the ground near the excavation front.

The supervisor prepares the loading of the flywheel (loading and firing mine), occasionally using the D.DIECI Icarus platform and coordinates the construction sites and activities; the operator works mainly underground in the excavation area.

#### SAMPLING AND ANALYSIS METHODOLOGIES

The following is the sampling and analysis methodology used for the quantitative re-research and determination of the pollutants concerned.

Combustion gas (CO <sub>2</sub> , CO, NO, NO <sub>2</sub> , SO <sub>2</sub> and O <sub>2</sub> )	
Beginning:	determination of instantaneous concentration (every minute), by means of an electrochemical sensor and infrared sensor analyzer: for each gas examined, continuous acquisition was performed; the instantaneous concentration values acquired have, therefore, been mediated.
Sampling per instrumentation:	<ul style="list-style-type: none"> <li>➤ Dräger Xam-7000 Portable Analyzer with: <ul style="list-style-type: none"> <li>• infrared sensor for carbon dioxide (CO<sub>2</sub>);</li> <li>• electrochemical sensors for carbon monoxide (CO), nitrogen monoxide (NO) and sulphur dioxide (SO<sub>2</sub>).</li> </ul> </li>   <li>➤ Dräger Xam-5000 Portable Analyzer with: <ul style="list-style-type: none"> <li>• electrochemical sensor for nitrogen dioxide (NO<sub>2</sub>).</li> </ul> </li> </ul>

	<ul style="list-style-type: none"> <li>➤ Dräger Pac-5500 Portable Analyzer with: <ul style="list-style-type: none"> <li>• electrochemical oxygen sensor (O<sub>2</sub>).</li> </ul> </li> </ul>
--	---

### 5.18 Sampling mode:

Sampling of air in the working environment can be carried out in two ways:

- ❖ Staff
- ❖ (static, fixed point)

A personal sampling shall be carried out with a portable constant-flow pump worn by the worker and with the collection device (filter or vial), fixed to the bavero, so as to take the air close to his respiratory organs.

The respiratory area is defined, in the UNI EN 1540 standard, as "Atmosphere in the working environment – Terminology", as the space around the face of the operator, in which he breathes, that is, the hemisphere of the radius of 0.3 m that extends in front of the person's face, centered on the middle of the segment that joins the two ears, where the base of the hemisphere is the plane that passes through this segment (the top of the head and the larynx).

This sampling method makes it possible to take exactly the air which is breathed by the worker and to follow him on his movements, thus measuring the exposure to pollutants to which he is subject during the course of his task.

An environmental sampling, on the other hand, is carried out with a constant flow area sampler which, positioned at a given location, allows to measure the degree of pollution of the room or the circumscribed area.

The data can be used both to assess the effectiveness of the containments carried out (physical specifications, localized aspirations), to verify the efficiency of forced ventilation that may be present, and to identify the exposure to which those who are staying for a certain time in the room or at a specific area are subject.

UNI EN 482 specifies that fixed point measurement can also be used for comparison with occupational exposure limit values if the results are or represent exposure concentrations.

### 5.19 Sampling Plan:

In the present case, both personal sampling of workers and environmental sampling were carried out in accordance with the sampling plan described in the following tables:

Table 5.6: Personal sampling.

Measuring point no.	Attendant	Name	Certificate of analysis
1	Shovel attendant Liebherr 576	Mr. Canazza Graziano	C2396-01/20
2	Tamrock HS105 Drill Operator	Mr. Marforius Valerius	C2396-02/20
3	ASTRA 8450 HD9 truck operator	Mr. Caltran Roberto	C2396-03/20
4	Overseer	Mr. Caltran Sergio	C2396-04/20

#### ENVIRONMENTAL SAMPLING

Measuring point no.	Station	Certificate of analysis
5	CARREGGIO AREA at Pillar 1236 (transit tunnel between Level V and Level IV underground)	C2396-05/20

#### 5.20 Comparison Parameters:

For comparison with the limit values for agents investigated and detected by laboratory analyses, reference is commonly made to the "TLV-TWA" threshold values proposed by ACGIH® (American Conference of Governmental Industrial Hygienists - threshold limits under which most healthy workers can be exposed repeatedly day after day without adverse health effects. These values are also recognized by AIDII - Italian Association of

industrial Hygienists and carried in different National Employment Contracts) or, if existing, to the threshold values reported by Italian legislation (DLgs.81/08 All. XXXVIII), by EU Directives or recommended by the European body SCOEL (SCOEL Scientific Committee on Occupational Exposure and Limits, OEL Occupational Exposure Limit).

The occupational exposure limit value (VLE) is repeatedly invoked, in Title IX - Chapter I of Legislative Decree No. 81/08, as a time limit for comparing exposure levels measured in the risk assessment process; it is defined as "the time-weighted average concentration limit of a chemical agent in the air within a worker's breathing area in relation to a given reference period".

The TLV-TWA limits set out in the following tables are those proposed by ACGIH in issue 2019 (ACGIH TLVs and EIB, 2019; recognised by AIDII and reported in numerous national employment contracts), DLgs.81/08 All. XXXVIII, EU Directives and SCOEL recommendations.

The threshold limits for exposure to the gases considered, expressed in parts per million (ppm) per cubic meter of air, currently recognised as valid (ACGIH®, DLgs.81/08, SCOEL) are as follows:

Table 5.7: Exposure Threshold Values and DPR References 128/59

Gas		ACGIH TLV-TWA ppm	OEL-TWA ppm	notes and references
Dioxide	CO <sub>2</sub>	5000	5000	(1% DPR 128/59 art.411°)
Carbon monoxide	CO	25	20 (100 SET)**	(50 ppm DPR 128/59 art.411°)
Nitrogen oxides	NO <sub>x</sub>	--	--	(25 ppm DPR 128/59 art.411°)
Nitrogen monoxide	No	25	2 (25) **	--
Nitrogen dioxide	NO <sub>2</sub>	0,20	0.50 (1.0 SET)**	--

Sulphur dioxide	SO <sub>2</sub>	0.25 SET	0.50 (1.0 SET)**	(10 ppm DPR 128/59 art.411°)
-----------------	-----------------	----------	------------------	---------------------------------

Note:

Threshold Limit Value (TLV-TWA) means the 8-hour/day threshold limit for 40 hours per week of exposure to the agent considered to which "almost all workers can be repeatedly exposed without adverse health effects"

OEL-TWA (Occupational Exposure Limit - Time Weighted Average) means the recommended threshold limit calculated over 8 hours/day for 40 hours For week of exposure to the considered agent to which the majority of workers can be repeatedly exposed without adverse health effects.

Set (Short Time Exposure Level) is the limit concentration value for short exposure time, average concentration value over 15 minutes that must never be exceeded at any time of the working day

(\*) value reported by DLgs.81/08 All.XXXVIII

(\*\*) value reported by Had Directive No. 2017/164 (not yet transposed by All. XXXVIII 'update DLgs.81/08, it should be stressed that for underground mining activities this directive will have to be transposed into Italian law by 21/08/2023, in the light of the provisions of the English-language Directive and the Italian version seems to indicate that the indication of "mine in

## 5.21 Results:

### 5.21.1 Presentation of results:

The following tables show:

- sampling conditions;
- for each parameter analyzed:
  - concentration values measured by the method of analysis described;
  - the applicable exposure limit value.

The analysis certificates from which the results set out below have been drawn are set out in Annex 1.

Where the analysis carried out did not make it possible to determine the presence of the inquad, since its airborne concentration is below the detectability threshold of the

analytical method used, the substance is indicated as non-detectability (n.r.), in reference to the numerical value expressing this threshold.

When a pollutant is undetectable, the significance of such an outcome may be place:

- ❖ the pollutant is completely absent;
  
- ❖ the pollutant is present with such a low concentration (traces), that it is not measurable or quantifiable.

Personal sampling:

MEASURING POINT

No°1

Certificate of analysis: C2396-01/20

type: personnel Nominative: Mr. Canazza Graziano

Attendant Liebherr 576

Machining: Wheel loader conduction (air-conditioned vehicle), for material handling felled and load of the tout venant on the trucks (2 trucks in operation)

Position of the collection device: near the operator's respiratory tract

Pollutant	Average concentration measured [ppm]	VLE [ppm]
Carbon dioxide (CO <sub>2</sub> )	1900	5000
Carbon monoxide (CO)	3.62	20*
Nitrogen oxide (NO)	1.98	25*
Nitrogen dioxide (NO <sub>2</sub> )	0.07	0.5*
Sulphur dioxide (SO <sub>2</sub> )	n.r. < 0.1	0.5*

n.r. = undetectable

### MEASURING POINT

No°2

Certificate of analysis: C2396-02/20

Sampling date: 12/02/2020 Sampling

type: personnel Nominative: Mr. Marforius Valerius

TAMROCK HS105 Drill Operator

Working: Drilling conduction (ground processing, no cabin)

Position of the collection device: near the operator's breathing routes in prossimità delle vie respirato

Pollutant	Average concentration measured [ppm]	VLE [ppm]
Carbon dioxide (CO <sub>2</sub> )	1300	5000
Carbon monoxide (CO)	5.26	20*
Nitrogen oxide (NO)	2.71	25*
Nitrogen dioxide (NO <sub>2</sub> )	0.14	0.5*
Sulphur dioxide (SO <sub>2</sub> )	n.r. < 0.1	0.5*

n.r. = undetectable

MEASURING POINT

No°3

Certificate of analysis: C2396-03/20

Sampling date: 12/02/2020 Sampling

type: personnel Nominative: Mr. Caltran Roberto

ASTRA 8450 HD9 truck operator

Machining: Operation of trucks (means with air conditioning), for transport of the mineral outwards with exhaust in the wee way.

Position of the collection device: near the operator's respiratory tract

Pollutant	Average concentration measured [ppm]	VLE [ppm]
Carbon dioxide (CO <sub>2</sub> )	1800	5000
Carbon monoxide (CO)	< 1	20*
Nitrogen oxide (NO)	0.66	25*
Nitrogen dioxide (NO <sub>2</sub> )	n.r. < 0,04	0.5*
Sulphur dioxide (SO <sub>2</sub> )	n.r. < 0.1	0.5*

n.r. = undetectable

MEASURING POINT

No°4

Certificate of analysis: C2396-04/20

Sampling date: 12/02/2020 Sampling

type: personnel Nominative: Mr. Caltran Sergio

Processing: Underground activity control: supervision of drilling activities and pump control. Pre-loading of the flywheel load (loading and firing mine), occasionally using the D.DIECI Icarus platform

Position of the device: near the operator's respiratory tract

Pollutant	Average concentration measured [ppm]	VLE [ppm]
Carbon dioxide (CO <sub>2</sub> )	1000	5000
Carbon monoxide (CO)	3.36	20*
Nitrogen oxide (NO)	2.10	25*
Nitrogen dioxide (NO <sub>2</sub> )	0.19	0.5*
Sulphur dioxide (SO <sub>2</sub> )	n.r. < 0.1	0.5*

n.r. = undetectable

In all personal locations the concentration value of O<sub>2</sub> was always between 20.0 and 20.9 % Vol.

\* = value reported by EU Directive no. 2017/164 (not yet transposed by All. XXXVIII DLgs.81/08, it should be emphasized that for underground mining, this directive must be transposed into Italian law by 21/08/2023, as far as Nitrogen Monoxide is involved, the limit value reported in Directive 91/322/EEC of 25ppm can continue to be applied during the transitional period.

Environmental sampling:

#### MEASURING POINT 5

Certificate of analysis: C2396-05/20, Data sampling: 12/02/2020 Sampling

type: environmental

Location: CARREGGIO AREA at pillar 1236 (transit tunnel between Level V and Level IV in subterranean)

Workmanship: Normal construction activities (in wheeling wheel function, 2 trucks and platform D.DIECI Icarus)

Location of the collection device: about 1.6 meters above the ground.

Pollutant	Average concentration measured [ppm]	VLE [ppm]
Carbon dioxide (CO <sub>2</sub> )	700	5000
Carbon monoxide (CO)	< 1	20*
Nitrogen oxide (NO)	1.01	25*
Nitrogen dioxide (NO <sub>2</sub> )	0.07	0.5*
Sulphur dioxide (SO <sub>2</sub> )	n.r. < 0.1	0.5*

n.r. = undetectable

At this location the concentration value of O<sub>2</sub> was always between 20,0 and 20,9 % Vol.

#### 5.22 Evaluation of results:

From the analysis of the results presented, the following considerations can be drawn with regard to each agent sought:

##### ❖ Carbon dioxide (CO<sub>2</sub>)

Among the personal workstations examined, the one with the highest carbon dioxide value is at station 1 - blade operator Liebherr 576, where the concentration of this pollutant is 1900 ppm.

At the environmental location examined, the concentration of this pollutant is 700 ppm.

The occupational exposure limit value prescribed in Annex XXXVIII to Legislative Decree No 81/08 for carbon dioxide shall be 5000 ppm.

##### ❖ Carbon monoxide (CO)

Among the personal workstations examined, the one with the highest carbon monoxide value is at station 2 - drill operator, where the concentration of this pollutant is 5.26 ppm.

At the environmental location examined, the concentration of this pollutant was found to be undetectable (n.r. < 1 ppm).

The occupational exposure limit value set in the OEL's (EU Directive No 2017/164) for carbon monoxide is 20 ppm.

❖ Nitrogen monoxide (NO)

di azoto Among the personal workstations examined, the one with the highest nitrogen monoxide value is at station no. 2 - drill operator, where the concentration of this pollutant is 2.71 ppm.

In the environmental post examined, the concentration of this pollutant is 1.01 ppm. one ambientale.

The occupational exposure limit value for nitrogen monoxide reported by EU Directive No 2017/164 is 2 ppm (not yet transposed by All. XXXVIII DLgs.81/ 08, it is emphasized that for underground mining, this directive must be transposed into Italian law by 21/08/2023, as far as nitrogen monoxide is involved, the limit value reported in Directive 91/322/EEC of 25 ppm can continue to apply during the transitional period).

❖ Nitrogen dioxide (NO<sub>2</sub>)

di azoto Among the personal workstations examined, the one with the highest nitrogen monoxide value is at station no. 4 - monitoring operator, where the concentration of this pollutant is 0.19 ppm.

At the environmental location examined, the concentration of this pollutant is 0.07 ppm.

The occupational exposure limit value set in the OEL's (EU Directive No 2017/164) for nitrogen dioxide is 0.5 ppm.

❖ Sulphur dioxide (SO<sub>2</sub>)

In all monitored locations the sulphur dioxide concentration was undetectable (n.r. < 0.1 ppm).

The occupational exposure limit value set in the OEL's (EU Directive 2017/164) for sulphur dioxide is 0.5 ppm.

This is the table in which the CO emission values are summarized to the exhaust pipe of the machines in operation at our quarry.

CO RETURN TABLE ppm		
Operating machine	Min	Max

JUMBO TAMROCK HS 105	100	200
LIEBHERR 576 wheeling wheel piece	150	150
Dumper ASTRA HD9S	50	150
FH 300	--	--
ICARUS lift	150	150
Gen. VOLVO GX273V	50	50
Gen. OLYMPIAN GEP 55-2	--	--
CAT excavator 325 C	200	200

Similar to what is reasoned for CO can therefore be done for NOx, or at least for NO2.  
 At this point I will tell you the type of engine that the various machines mount in order to have an indication of the emissive capacities.

CO RETURN TABLE ppm		
CO RETURN TABLE ppm		
Operating machine	Engine type	HP

JUMBO TAMROCK HS 105	Year 1987	60
LIEBHERR 576 wheeling wheel piece	(YEAR 2006) LIEBHER D936 L A 6	200
Dumper ASTRA HD9S	Euro 6 (year 2017)	460
FH 300	--	--
ICARUS lift	(year 2002) IVECO AIFO 8045 SE00 7.00	102
Gen. VOLVO GX273V	(year 2020) Volvo TAD754GE	250
Gen. OLYMPIAN GEP 55-2	--	--
CAT excavator 325 C	(year 2004) TYPE CAT 3126B ATAAC-HEUI (compliant with EU 97/68/EC stage II	150

Depending on the year/type of engine, it can be traced back to tier and therefore to the emissive capacity.

In addition:

- coming out of the primary fan I detected a speed of 27 m/s and a temperature of 15°C.
- room temperature at other points 13.5 °C.

## Chapter 6

### The calculation method used (characteristics and ability)

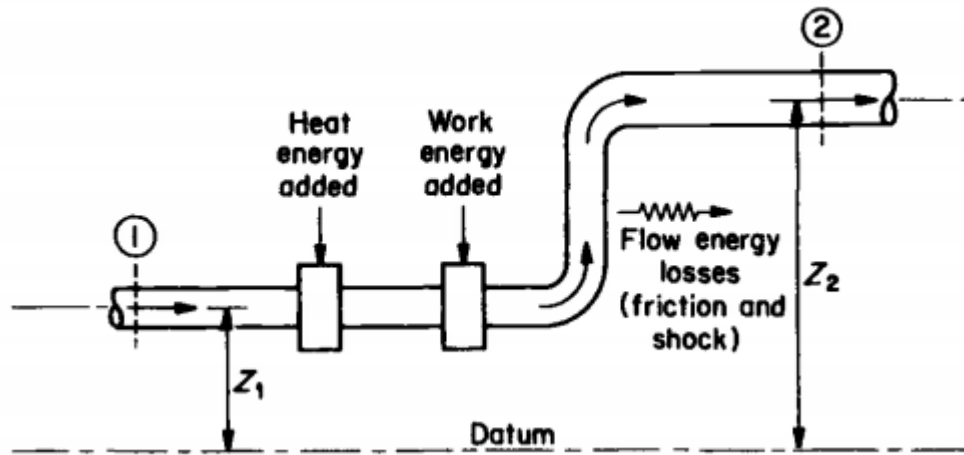


Figure 6.1: Fluid-flow system showing energy relations [22].

The total energy of the first section equals the total energy at second section, plus the flow energy losses occurring between 1 and 2, or

$$\text{Total energy}_1 = (\text{Total energy})_2 + (\text{Flow energy losses})_{1-2}$$

Substituting expressions for the various energy terms and disregarding the minor change in internal energy, the following general energy equation for fluid flow results [22]:

$$\frac{p_1}{w} + \frac{V_1^2}{2g} + Z_1 = \frac{p_2}{w} + \frac{V_2^2}{2g} + Z_2 + H_l \quad (6.1)$$

where  $p$  is the pressure,  $w$  is the specific weight,  $V$  is the velocity,  $p/w$  is the static energy,  $V^2/2g$  is the velocity energy,  $Z$  is the potential energy, and  $H_l$  is the flow energy loss. Equation 6.1 is recognized as the familiar Bernoulli equation, applicable to all fluid flow processes. In this form, it applies only to an incompressible fluid, which air is assumed to be in nearly all mine ventilation because of minor changes in air specific weight. Every term in the equation is a specific energy, in units of ft.lb/lb, or ft (m). Since ft (m) is a measure of the fluid head, these terms are referred to simply as heads. In dealing with air, it is customary to employ in. (mm) of water rather than ft (m) of air as the unit of the head, for two reasons: (1) the minuteness of the measurements and (2) the still-prevalent use of a manometer (or water gage) to measure heads. The specific energy and head are equivalent, hence the equation of general energy as written in

equation 6.1 can also be expressed [22]:

$$H_{t_1} = H_{t_2} + H_l \quad (6.2)$$

Where  $H_t$  is the total head; and equation 6.1 can be expressed:

$$H_{s_1} + H_{v_1} + H_{z_1} = H_{s_2} + H_{v_2} + H_{z_2} + H_l \quad (6.3)$$

Where  $H_s$  is the static head,  $H_v$  is velocity head, and  $H_z$  is the elevation or potential head. All heads have the unit of in. (mm) water.

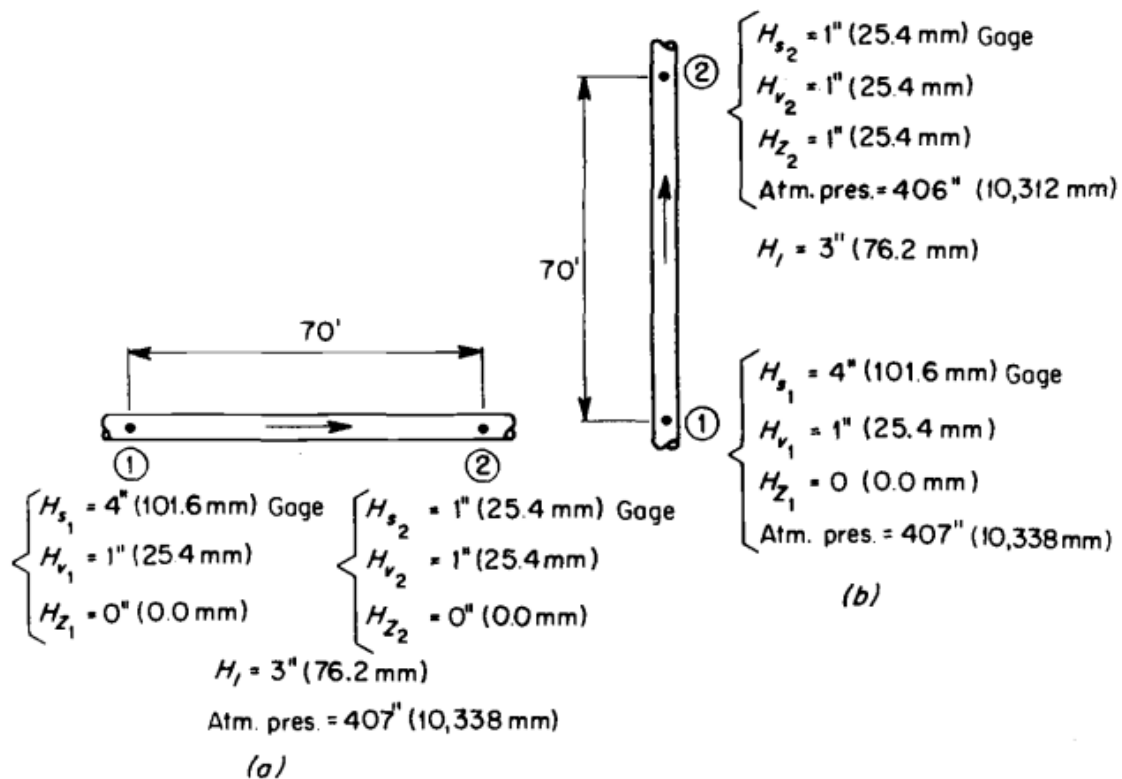


Figure 6.2: Arrangement of a duct (a) horizontally and (b) vertically to demonstrate the effect of elevation [22].

### 6.1 Head Losses in Fluid Flow:

In ventilation of the mine field, as in other fields applying fluid mechanics fundamentals, there is more interest in differences of pressure than in pressures. The energy that is provided to a steady-state process by either mechanical or natural means and this pressure difference is consumed in overcoming flow losses, represented by  $H_l$ . As with the general energy equation, the unit of the various pressure losses is fluid head, measured in in. (mm) of water [22].

The fluid flow head loss is made up of two components,  $H_f$  (friction loss) and  $H_x$  (shock loss):

$$H_l = H_f + H_x \quad (6.4)$$

all commonly expressed in in (mm) of water. Friction losses represent head losses in flow through ducts of constant area, whereas shock losses are losses resulting from changes in the direction of flow or area of the duct [22].

### 6.2 Overall or Mine Heads:

Mine static head (mine  $H_s$ ) represents the energy consumed in the ventilation system to overcome all flow head losses. It includes all the decreases in total head that occur between the entrance and discharge of the system and may be expressed simply:

$$\text{Mine } H_s = \sum H_l = \sum (H_f + H_x) \quad (6.5)$$

This applies to a series circuit or the equivalent series circuit in a network. Mine velocity head ( $H_v$ ) is taken as the velocity head at the discharge of the system. Mine total head (mine  $H_t$ ) is the sum of all energy losses in the ventilation system. Numerically, it is the total of the mine static and velocity heads [22]:

$$\text{Mine } H_t = \text{Mine } H_s + \text{Mine } H_v \quad (6.6)$$

The significance of these overall heads for the entire system will soon become apparent. Methods of calculating head losses and the mine heads will be discussed later. It is necessary to determine the head requirements of only a portion of the whole mine ventilation system.

These also might be found by equations 6.5 and 6.6, substituting the word airway or duct for mine.

### 6.3 Head gradients:

In representing the various head components of the general energy equation graphically, pressure or head gradients are obtained. Figure 6.3 depicts the gradients for a basic system involving any fluid in any conduit. This is simply a pictorial way of expressing the Bernoulli energy equation and depicts the head relations of equation 6.2, and 6.3. Three distinct gradients-elevation, static plus elevation (including atmospheric pressure), and total-appear in figure 6.3; the static and velocity heads are shown as the difference between the gradients and not as different gradients. Note that the cumulative head relations at any point in the system can be read from the graph. Usually, in mine ventilation, only two head gradients-static and total-need to be plotted by equation 6.4, the modified version of the general energy equation. The elevation effect is omitted, and the datum employed parallels the barometric pressure line for the system, which rises and falls inversely with elevation. Heads at any point are gage values, relative to the atmospheric pressure at that point [22].

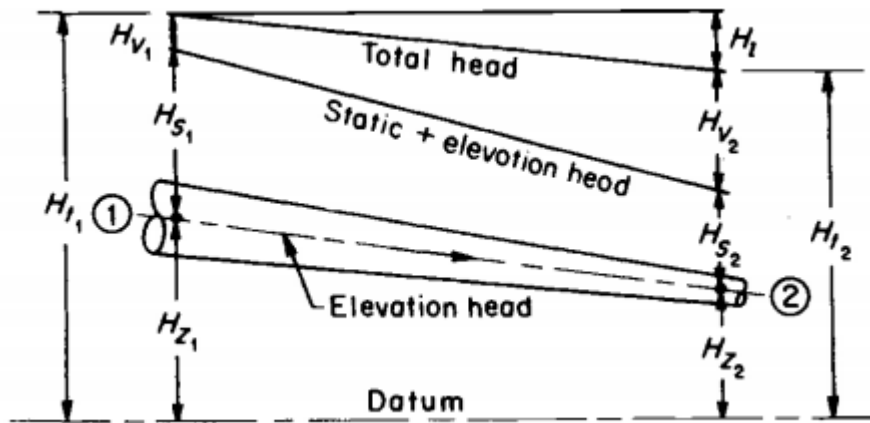


Figure 6.3: Head gradients for a basic fluid-flow system [22].

#### 6.4 Blower Systems:

A blower system is one in which the energy source (fan) is located at the inlet and raises the head of the mine or duct air above atmospheric.

An assumed mine ventilation system, together with the corresponding head gradients, is illustrated; head losses and velocity heads for each section or point in the airway are indicated. For velocity head  $H_v$  and friction losses  $H_f$ , the subscript for the appropriate duct section (a, b, or c) appears, and for shock losses  $H_x$ , the subscripts denote inlet (i), expansion (e), contraction (c), or discharge (d) [22]. This can be accomplished by converting some of the velocity head to static head in a diffuser duct or evasé discharge.

By convention, gage readings of heads (static or total) are expressed as positive if above the atmospheric datum line and negative if below it. It would not be necessary to employ plus and minus signs if absolute pressures were used (a reference to absolute zero as the datum), but since gage pressures are customary, this convention of signs is necessary. Special consideration is required in exhaust systems. Note that in a blower system, all heads are generally positive (concerning atmospheric), except at the entrance, or an expansion near the discharge. With other types of systems, negative total and static heads will be encountered, but the velocity head will always remain positive [22].

It is well to employ the following rules in plotting a head gradient for any type of ventilation system:

1. The total head is always zero at the inlet to the system but positive and equal to the velocity head at the discharge.
2. The static head is still negative and equal to the velocity head at the inlet to the system but zero at the discharge.
3. The total head at any point is plotted firsthand; the static head is then they have plotted as the total head less the velocity head.

With a blower system, the plotting is facilitated by starting at the discharge and working toward the intake. This permits the  $H_s$  line to begin at zero (the datum line). When all

individual head losses have been determined previously, this can be done readily. Note that at any point in the system [22]:

$$H_t = H_s + H_v \quad (6.7)$$

Following equation 6.3. The mine heads can quickly be found by equations 6.5 and 6.6. The individual head losses are either measured or calculated. They have plotted along with the total headline, not the static line. There is no contradiction here, however, because head losses should be reflected in the change in total head, which is continually dropping in the direction of airflow (except at the fan). In contrast, the static gradient fluctuates with conversions in the velocity head. Inlet loss does not appear in a blower system, because the fan must absorb any shock here. No allowance or correction need be made for elevation, so long as gage pressures are employed [22].

#### **6.5 Exhaust Systems: (Figure 6.4)**

If the energy source in the mine ventilation system is relocated at the discharge without changing the direction of airflow, an exhaust system results. The gradients are plotted as before, except the intake serves as the starting point, and they present the same general appearance.

Since all losses are determined on a gage basis and are negative, almost the entire gradient falls below the atmospheric datum line. This, of course, is because an energy source, when located in the exhaust position, receives air below atmospheric and discharges it at atmospheric pressure. Note, however, that the  $H_s$  and  $H_t$  lines begin and end at the same points as in the blower system.

In keeping with the sign convention regarding atmospheric pressure, the gradients represent negative static and total heads. At any point in the system, however, the algebraic equation 6.3 still holds.

$$H_t = H_s + H_v \quad (6.8)$$

The static head is negative since the fan creates a suction in the system, resulting in pressures below atmospheric. The velocity head is positive, resulting in the total-head line being above the static head (but still negative in sign, except at discharge). This is the regular or expected position, which does not change because  $H_s$  is negative [22].

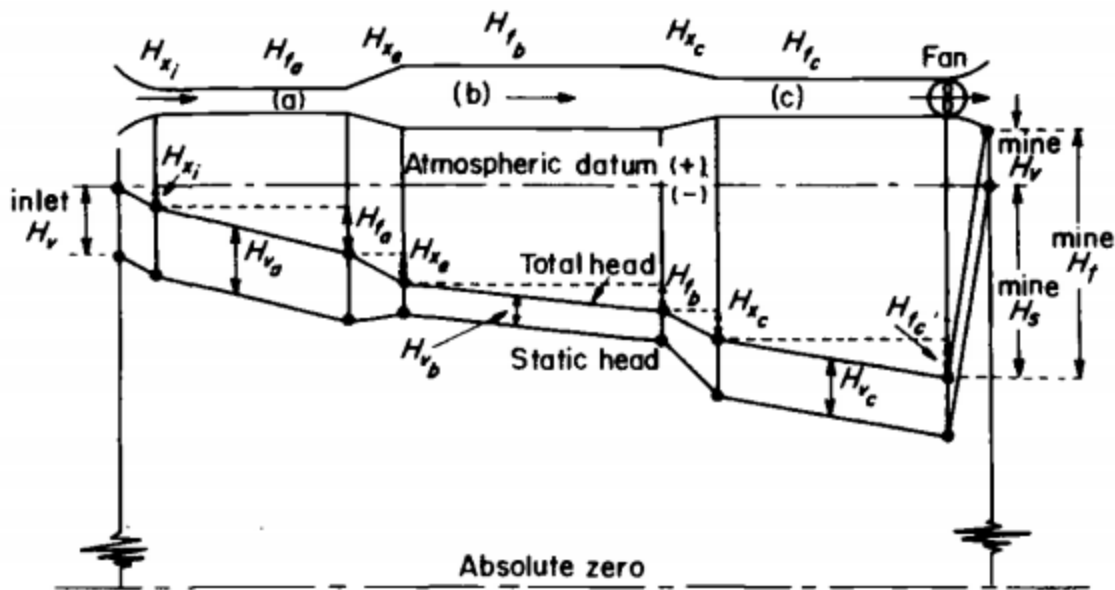


Figure 6.4: Head gradients for an exhaust system in mine ventilation [22].

### 6.6 Booster Systems:

Now let the same mine ventilation system be arranged as a booster system, with the energy source located at some point between the inlet and the discharge (figure 6.5). In a booster system, the fan receives air typically below atmospheric pressure and discharges it above atmospheric pressure. The mine static head is made up of two components:  $H_{s_i}$  on the intake side of the energy source and  $H_{s_d}$  on the discharge side. The sum of the two is the mine  $H_s$ , which for constant airflow, is nearly equal to that for the blower and exhaust systems discussed previously. Again, the mine velocity head is the  $H_v$  at discharge, and the mine total head is the sum of the mine  $H_s$  and the mine  $H_v$  [22].

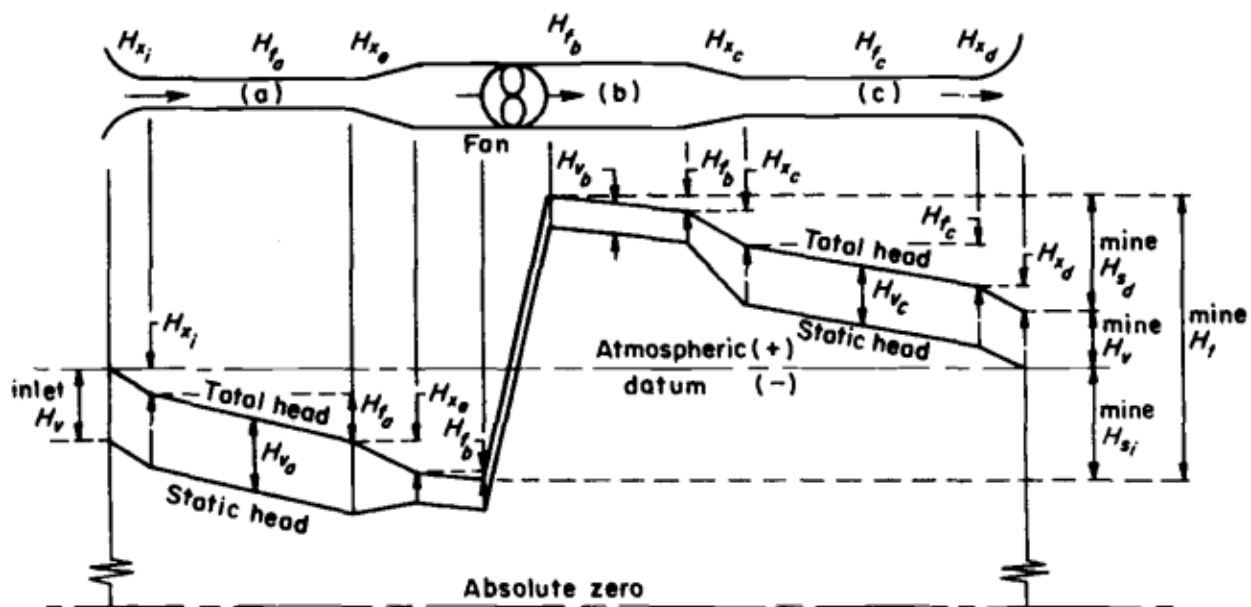


Figure 6.5: Head gradients for a booster system in mine ventilation [22].

### 6.7 State of airflow in mine openings:

The dimensionless criterion used in establishing boundaries for each state is called the Reynolds number  $N_{Re}$ . Laminar flow exists up to  $N_{Re} = 2000$  and turbulent flow above  $N_{Re} = 4000$ . These boundaries are only approximate, and the region between them is known as the intermediate range. The Reynolds number in fluid flow is a function of the fluid properties and can be determined as follows:

$$N_{Re} = \frac{\rho DV}{\mu} = \frac{DV}{\nu} \quad (6.9)$$

where  $\rho$  is fluid mass density (w/g) in  $lb. s^2/ft^4$  ( $kg/m^3$ ),  $\nu$  is kinematic viscosity in  $ft^2/s$  ( $m^2/s$ ),  $\mu$  is absolute viscosity ( $\rho\nu$ ) in  $lb. s/ft^2$  ( $pa. s$ ),  $D$  is diameter of conduit in ft (m), and  $V$  is velocity in fps (m/s). For air,  $\nu = 1.6 \times 10^{-4} ft^2/s$  ( $14.8 \times 10^{-6} m^2/s$ ) at normal temperatures, and Equation 6.9 reduces to:

$$N_{Re} = 6250DV \quad (6.10)$$

$$N_{Re} = 67.280DV \quad (6.10a)$$

The fluid velocity corresponding to  $N_{Re} = 4000$ , the lower boundary of the turbulent flow for a conduit of a given size, is called the critical velocity  $V_c$ . If the fluid velocity exceeds  $V_c$ , then the state of flow is always turbulent. The critical velocity can be found easily from the last relation above, solving for  $V_c$  in fpm (m/s) and setting  $N_{Re} = 4000$ :

$$V_c = \frac{60N_{Re}}{6250D} = \frac{(60)(4000)}{6250D} = \frac{38.4}{D} \quad (6.11)$$

or approximately

$$V_c \cong \frac{40}{D} \quad (6.12)$$

$$V_c \cong \frac{0.06}{D} \quad (6.13)$$

### 6.8 Effect of State of Flow on Velocity Distribution:

One way that the state of flow affects the dynamic characteristics of fluid is in the velocity distribution over the cross-section of the conduit. Different velocity distributions in a circular tube for the same average velocity of airflow over varying Reynolds numbers are shown in Figure 6.6 [22].

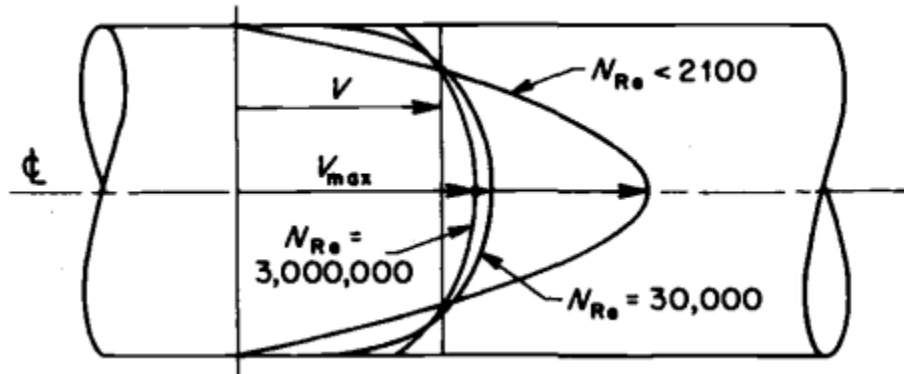


Figure 6.6: Velocity distributions in circular conduits, average velocity constant. (After Rouse, 1937. Reprinted from Trans. Amer. Soc. Civil Engl., Vol. 102, p. 163 with permission of the ASCE.)

The maximum velocity  $V_{max}$  occurs at the center of the conduit, but it varies in magnitude with the Reynolds number. The usual aim in ventilation is the measurement of average velocity  $V$ , not maximum velocity; and therefore, centerline measurements of velocity alone are not sufficient. The variation of  $V$  with  $V_{max}$  is determinable as a function of the Reynolds number, however, as shown in Figure 6.7. This graph enables one to estimate the average velocity when only one measurement along the centerline has been made. Discretion should be exercised in its use in mine ventilation, however, since mine openings are rarely circular, and the many irregularities of the walls tend to produce a nonsymmetrical flow pattern. Because the Reynolds number in mine ventilation generally exceeds 10,000, it is customary to assume for approximate work that:

$$V \cong 0.8V_{max} \quad (6.14)$$

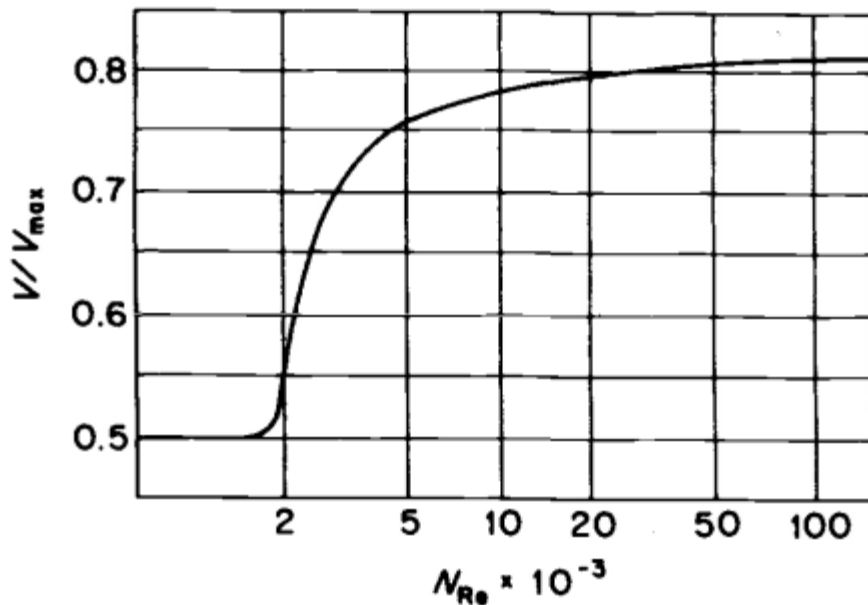


Figure 6.7: Relation of velocity ratio  $V/V_{max}$  and Reynolds number. (After Vennard, 1940. Reprinted by permission of John Wiley & Sons, Inc.)

## 6.9 Calculations of head losses:

### 6.9.1 Velocity Head:

Although not a conventional head loss within the ventilation circuit, the velocity head nevertheless represents kinetic energy that must be supplied to maintain flow and is lost to the system at discharge. The velocity head at discharge must be known to determine the mine heads. On other occasions, the measurement of the velocity head permits the velocity of airflow to be calculated. An equation for velocity head involving conventional units is desirable [22].

Starting with the fundamental relation appearing as equation 6.1:

$$H_v = \frac{V^2}{2g} \quad (6.15)$$

with  $V$  in fps (m/s) and  $H_v$  in ft (m) of fluid, and **applying Eq. 2.18**, the following might be obtained:

$$H_v = \frac{wV^2}{(5.2)(64.4)(60)^2} = w\left(\frac{V}{1098}\right)^2 \quad (6.16)$$

with  $V$  in fpm and  $H_v$  in in. water. For standard air at sea level ( $w = 0.0750 \text{ lb/ft}^3$ ), this becomes:

$$H_v = \left(\frac{V}{4009}\right)^2 \quad (6.17)$$

Using SI units, equation 6.16 takes the form:

$$H_v = \frac{\rho V^2}{2} = \frac{wV^2}{2g} \quad (6.18)$$

with  $H_v$  in Pa,  $V$  in m/s, and  $\rho$  and  $w$  in  $\text{kg/m}^3$ . Equation 6.17 states that velocity of about 4000 fpm (20.3 m/s) is equivalent to a velocity head of 1 in. Water (249 Pa). These equations might also be used to calculate the velocity when the head is known.

## 6.9.2 Friction Loss:

The friction losses in airflow through mine openings constitute 70-90 % of the sum of the head losses in a mine ventilation system.

### 6.9.2.1 Atkinson Equation for Friction Loss:

As a loss in static pressure that occurs in flow as a result of the drag or resistance of the walls of the opening or duct and the internal friction of the fluid itself, the friction loss in a mine airway is a function of the velocity of flow, the interior-surface characteristics of the conduit, and the dimensions of the conduit. (In addition, it would be expected from fluid mechanics that the friction loss would be dependent on the state of flow of the fluid. It has already been demonstrated, however, that in mine ventilation systems, airflow can nearly always be considered turbulent.) The fluid mechanics (Darcy-Weisbach) equation for calculating friction loss in any circular conduit is (Munson et al., 1994) [22].

$$H_l = f \frac{L V^2}{D 2g} \quad (6.19)$$

where  $H_l$  is the head loss in ft (m) of fluid,  $L$  is the length in ft (m),  $D$  is the diameter in ft (m),  $V$  is the velocity in fps (m/s), and  $f$  is coefficient of friction. A more versatile equation, one applicable to any shape of conduit, may be obtained by expressing the head loss in terms of the hydraulic radius  $R_h$  the ratio of the area  $A$  to the perimeter  $O$  of the duct. For a circular conduit:

$$R_h = \frac{A}{O} = \frac{(\pi/4)D^2}{\pi D} = \frac{D}{4} \quad (6.20)$$

Substituting equation 6.20 in equation 6.19, that results:

$$H_l = f \frac{L}{4R_h} \frac{V^2}{2g} \quad (6.21)$$

From this version of the Darcy-Weisbach equation for general fluid mechanics, the Atkinson equation for friction loss in mine ventilation can be derived as follows (Weeks, 1926):

$$H_f = \frac{f}{5.2} \frac{L}{4R_h} \frac{0.0750V^2}{2g(60)^2} = \frac{k}{5.2} \frac{L}{R_h} V^2 = \frac{KOLV^2}{5.2A} \quad (6.22)$$

$$H_f = \frac{KOLV^2}{A} \quad (6.23)$$

Where  $H_f$  is friction loss in in, Water (Pa),  $V$  is the velocity in fpm (m/s), and  $K$  is an empirical friction factor in  $lb \cdot min^2 / ft^4$  ( $kg/m^3$ ). The equation is frequently seen in the following form, although it is seldom so used directly:

$$H_f = \frac{KSV^2}{5.2A} \quad (6.24)$$

$$H_f = \frac{KSV^2}{A} \quad (6.25)$$

Where  $S$  is rubbing surface area in  $ft^2$  ( $m^2$ ) =  $O \times L$ . Often the air velocity is not known, but the quantity  $Q$  is given. Since  $V = Q/A$ , and rather than compute  $V$  separately, a convenient form of the friction loss equation to employ is:

$$H_f = \frac{KOLQ^2}{5.2A^3} \quad (6.26)$$

$$H_f = \frac{KOLQ^2}{A^3} \quad (6.27)$$

Equation 6.26 is the most useful form of the Atkinson formula and most used in this text. It should be noted that  $K$  takes units of  $lb \cdot min^2 / ft^4$  ( $kg/m^3$ ) in equations 6.22-6.27 as a result of the units assigned to the other variables. It has often been American practice to ignore the units of  $K$  because little in the way of physical meaning can be attached to the units. However, it is essential to specify the proper units, mainly when it is desirable to convert  $K$  values from one system of units to another. To emphasize the appropriate units and to overcome the improper practice of expressing  $K$  without units, the units  $lb \cdot min^2 / ft^4$  ( $kg/m^3$ ) are attached to  $K$  throughout this thesis. Engineers interested in converting  $K$  and other parameters to other unit conventions (e.g., SI units) **should consult** the references by Hunt (1960), McPherson (1971), and Rahim et al. (1976). It should also be pointed out that  $K$  is not a constant but varies directly with air specific weight; values of  $K$  are commonly expressed in tables at standard air specific weight [22]. The friction factor  $K$  in mine ventilation corresponds to the coefficient of friction in general fluid flow. Mathematically, from equation 6.22, the two are related approximately (for standard air specific weight):

$$K \cong (800)(10)^{-10} f \quad (6.28)$$

$$K \cong 0.148 f \quad (6.29)$$

Actually, in turbulent flow,  $f$  is not a constant for a given conduit but varies with the Reynolds number. In mine ventilation,  $K$  is assumed constant for a given airway, regardless of the Reynolds number. This is only an approximation, and on occasion, the error can be sizable (Falkie, 1958). However, for the usual range of Reynolds number (50,000 to 2 million) encountered in mine workings, the error is probably not excessive given the variability of the other factors involved. Hence it is ignored in all but precision measurements or research-type investigations [22].

#### 6.9.2.2 Determination of Airway Friction Factor:

The only accurate way to determine the friction factor for a given airway is to compute it (by Equation 6.22) from the pressure drop measured underground. For estimation or projection purposes, friction factors may have to be selected from experience. The most widely used are the values of friction factor listed in Table 6.1, based on exhaustive tests in a classic study by the U.S. Bureau of Mines (McElroy, 1935). Although these factors were designed principally for metal mine openings, they have had some use and acceptance for airways in coal mines as well. In recent years, other investigators have conducted empirical tests using models or actual mine openings to extend the range of McElroy's friction factors to other conditions, especially in coal mines (Pursall, 1960; Skochinsky and Komarov, 1969; Rahim et al., 1976). Perhaps more important than these others, because it was conducted in coal mines in the United States, was the study of Kharkar et al. (1974). Results are displayed in Table 6.2 in a format similar to McElroy's. Smooth lined corresponds to openings driven by boring-type continuous miners and tunneling machines and unlined to openings produced by conventional methods. Openings not specified timbered are assumed to be rock-bolted. Kharkar's

values for conditions comparable to McElroy's tend to be lower by 5-20%. Wala (1991) has also measured friction factors in coal mines. His values are in general agreement with those of Kharkar.

Two recent publications provide friction factors for mine situations that are not covered in Tables 6.1 and 6.2. McPherson (1987) outlines friction factors for longwall faces under different conditions. His measurements show friction factors from  $200 \times 10^{-10}$  to  $350 \times 10^{-10} \text{ lbmin}^2/\text{ft}^4$  ( $0.0370 - 0.0750 \text{ kg/m}^3$ ). An additional publication by McPherson (1985) provides friction factors for shafts with different wall constructions, structural obstructions, and conveyances. These references may be of use when these types of openings are encountered in mine ventilation circuits. Observe the following precautions in selecting a value of friction factor from the tables (6.1 and 6.2) for use in calculations [22]:

1. To provide correct values of K, multiply the numerical values obtained from the table by  $10^{-10}$ , and attach units of  $\text{lbmin}^2/\text{ft}^4$ . (For K in SI units of  $\text{kg/m}^3$ , multiply table values by  $1.855 \times 10^{-6}$ .)
2. Employ a value of K determined or checked experimentally, if at all possible. This should be based on the results of actual tests conducted underground in the mine opening or ventilation duct involved. Careful measurement of  $H_f$  over a known length of the airpath of a constant cross-section will allow a reliable experimental value of K to be calculated.
3. Tables 6.1 and 6.2 list values of K based on standard air specific weight. Since K is proportional to  $w$ , correct K for actual  $w$  by the formula:

$$\text{Corrected K} = (\text{table K}) \left( \frac{w}{0.0750} \right) \quad (6.30)$$

$$\text{Corrected K} = (\text{table K}) \left( \frac{w}{1.201} \right) \quad (6.31)$$

Before using equations 6.22 to 6.27.

4. Select K carefully for the conditions (rock type, straightness, cleanliness, irregularity, etc.) prevalent in the airway. When in doubt, use average values. Italicized values commonly occur and are safe to use in calculations. For noncoal mines, select K from Table 6.1; for coal mines, use Table 6.2 [22].
5. If the airpath is timbered and the sets are spaced on other than 5 ft (1.5 m) centers, modify K according to Figure 6.8. If roof bolting is used in place of timbering, assume an unlined airpath.

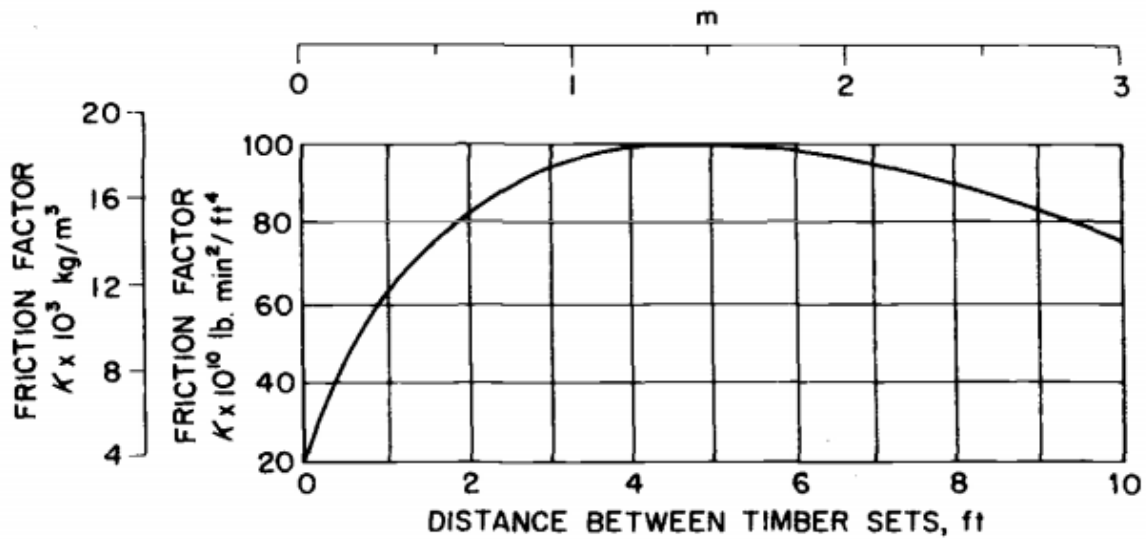


Figure 6.8: Effect of spacing of timber sets on friction factor K. (After McElroy, 1935)

Table 6.1: Friction factor K for noncoal mine airways and openings:

		Values of $K \times 10^{10}$ <sup>a</sup>											
		Straight			Sinuous or Curved								
		Clean (Basic Values)	Slightly Obstructed	Moderately Obstructed	Slightly		Moderately			High Degree			
Type of Airway	Irregularities of Surfaces, Areas, and Alignment				Clean	Obstructed	Obstructed	Obstructed	Obstructed	Clean	Obstructed	Obstructed	Clean
Smooth lined	Minimum	10	15	25	20	25	35	25	30	40	35	40	50
	Average	15	20	30	25	30	40	30	35	45	40	45	55
	Maximum	20	25	35	30	35	45	35	40	50	45	50	60
Sedimen- tary rock	Minimum	30	35	45	40	45	55	45	50	60	55	60	70
	Average	55	60	70	65	70	80	70	75	85	80	85	95
	Maximum	70	75	85	80	85	95	85	95	100	95	100	110
Timbered (5-ft centers)	Minimum	80	85	95	90	95	105	95	100	110	105	110	120
	Average	95	100	110	105	110	120	110	115	125	120	125	135
	Maximum	105	110	120	115	120	130	120	125	135	130	135	145
Igneous rock	Minimum	90	95	105	100	105	115	105	110	120	115	120	130
	Average	145	150	160	155	160	165	160	165	175	170	175	195
	Maximum	195	200	210	205	210	220	210	215	225	220	225	235

<sup>a</sup> To provide correct values of K, the numerical values obtained from the table are multiplied by  $10^{-10}$  and units of  $lb\min^2/ft^4$  attached. K is based on standard air specific weight (if =  $0.0750\ lb/ft^3$ ). Recommended values are in italics. To convert K to SI units ( $kg/m^3\ kg/m^3$ ), multiply table values by  $1.855 \times 10^6$  McElroy (1935) [22].

Table 6.2: Friction factor K for coal mine airways and openings:

Type of Airway	Value of $K \times 10^{10}$ <sup>a</sup>					
	Straight			Curved		
	Clean	Slightly Obstructed	Moderately Obstructed	Clean	Slightly Obstructed	Moderately Obstructed
Smooth lined	25	28	34	31	39	43
Unlined (rock-bolted)	43	49	61	62	68	74
Timbered	67	75	82	85	87	90

<sup>a</sup> To provide correct values of K, the numerical values obtained from the table are multiplied by  $10^{-10}$  and units of  $lb \cdot min^2 / ft^4$  attached. K is based on standard air specific weight ( $w = 0.0750 \text{ lb}/ft^3$ ). To convert K to SI units ( $kg/m^3$ ), multiply table values by  $1.855 \times 10^6$  Kharkar et al. (1974) [22].

#### 6.9.2.3 Determination of Friction Factor for Vent Pipe:

Friction factors to use with different types of ventilation pipe or tubing varying with the material and its condition. The following are satisfactory for routine calculations (based on  $w = 0.0750 \text{ lb}/ft^3$ ):

Pipe or Tubing	Friction Factor, $K \times 10^{10} \text{ lb} \cdot \text{min}^2 / \text{ft}^4 \text{ (kg/m}^3\text{)}$	
	Good, New	Average, Used
Steel, wood, fiberglass (rigid)	15 (0.0028)	20 (0.0037)
Jute, canvas, plastic (flexible)	20 (0.0037)	25 (0.0046)
Spiral-type canvas	22.5 (0.0042)	27.5 (0.0051)

#### 6.9.2.4 Estimation of Friction Loss by Graph:

The approximate determination of friction losses in mine ventilation is simplified using graphs. Knowledge of the velocity, friction factor, and hydraulic radius permits the friction loss per 100 ft (30 m) of the airway to be read directly. The friction factor should be corrected for air specific weight by equation 6.30 beforehand. Charts that require less manipulation have also been devised for various airway shapes and friction factors (Lee and Ember, 1946; Anon., 1955). For ventilation pipe or tubing, use Appendix Fig. A.3. Values of friction loss are read per 100 ft (30 m) of length and standard air specific weight (corrected  $H_f = \text{graph } H_f \times W/0.0750$ , or  $w/1.201$  in SI units). This graph is based on a circular sheet metal duct in good condition and is used without correction for a new steel vent pipe. Correct as follows for other tubing or condition [22]:

Pipe or Tubing	Correction Factor for Pipe Condition	
	Good, New	Average, Used
Steel, wood, fiberglass (rigid)	1.00	1.33
Jute, canvas, plastic (flexible)	1.33	1.67
Spiral-type canvas	1.50	1.83

The values of friction loss read from the graph are often more accurate than those calculated by the formula (Equation 6.22 or 6.27). The graph was constructed to compensate for the drop in friction factor with increasing Reynolds numbers, and values are correct within a few percent (Anon., 1993).

#### 6.9.2.5 Calculation of Friction Loss by Formula:

Friction loss in a mine duct or airpath can be calculated by Equation 6.22 or 6.27. A separate calculation is necessary for each airway of different characteristics ( $K$ ) or cross-sectional dimensions ( $A$ ,  $O$ ) and each additional airflow ( $V$  or  $Q$ ). For different airflows in a given airway, solve  $KOL/5.2A^3$  separately and multiply by  $Q^2$ . For different airway lengths or friction factors, multiply  $H_f$  by the ratio of sizes or friction factors, respectively.

#### 6.9.3 Shock Loss:

Shock losses occur in mine ventilation in addition to friction losses and are caused by changes in the direction of airflow or the shape or size of the duct. Obstructions cause shock loss by reducing the duct area.

##### 6.9.3.1 Calculation of Shock Loss by Increase in Friction Factor:

Either a calculated or estimated increment in the friction factor  $K$  may be applied to allow for shock losses in each airway in a mine ventilation system. Although an inexact procedure, it dramatically simplifies calculations and can yield acceptable results when used properly, especially in an extensive network where the sources of shock are numerous and repetitious. Note that Table 6.1 includes several allowances for shock loss: sinuosity (curvature), obstructions, and timber sets. Judgment in selecting the appropriate value of  $K$  for calculations is critical, if shock losses of these types are to be evaluated accurately. McElroy (1935) also discusses a method of calculating an increment in  $K$  to various kinds of shock losses [22].

##### 6.9.3.2 Calculation of Shock Loss by Equivalent Length Method:

The recommended method of determining shock loss considered most useful in mine ventilation calculations is that expressing each significant loss in terms of the equivalent length of the straight airpath (McElroy, 1935). In other words, an increment in the size of the airway is determined, similar to the increment in  $K$  discussed above. A shock-loss expression for the equivalent distance of straight airpath can be found by equating the formulas for friction loss and shock loss (equations 6.22 to 6.31):

$$H_x = H_f \quad (6.32)$$

$$XH_v = \frac{KLV^2}{5.2R_h} \quad (6.33)$$

$$X \frac{wV^2}{(1098)^2} = \frac{KLV^2}{5.2R_h} \quad (6.34)$$

Table 6.3: Equivalent Lengths for Various Sources of Shock Loss [22].

Source	ft	(m)	Source	ft	(m)
Bend, acute, round	3	(1)	Contraction, gradual	1	(1)
Bend, acute, sharp	150	(45)	Contraction, abrupt	10	(3)
Bend, right, round	1	(1)	Expansion, gradual	1	(1)
Bend, right, sharp	70	(20)	Expansion, abrupt	20	(6)
Bend, obtuse, round	1	(1)	Splitting, straight branch	30	(10)
Bend, obtuse, sharp	15	(5)	Splitting, deflected branch (90°)	200	(60)
Doorway	70	(20)	Junction, straight branch	60	(20)
Overcast	65	(20)	Junction, deflected branch (90°)	30	(10)
Inlet	20	(6)	Mine car or skip (20% of airway area)	100	(30)
Discharge	65	(20)	Mine car or skip (40% of airway area)	500	(150)

Simplifying and solving for L but using the special symbol  $L_e$  to represent equivalent length:

$$L_e = \frac{5.2wR_hX}{K(1098)^2} = \frac{3235R_hX}{10^{10}K} ft \quad (6.35)$$

$$L_e = \frac{wR_hX}{2gK} m \quad (6.36)$$

Calculation of, first, the shock loss factor X and then the corresponding equivalent length  $L_e$  for a given shock loss by the formula is time-consuming. Enough accuracy for routine calculations is obtained by selecting the appropriate value of  $L_e$  for a shock loss from Table 6.3, then using it (in equation 6.37) when computing overall head losses in airways. The table lists approximate average values of  $L_e$  calculated by a formula and

based on an airway with values of  $K = 100 \times 10^{-10} \text{ lbmin}^2/\text{ft}^4$  ( $0.0186 \text{ kg}/\text{m}^3$ ), and  $R_h = 2 \text{ ft}$  ( $0.61 \text{ m}$ ) and on standard air specific weight.

Certain precautions are necessary for calculating shock losses by this method:

1. Values of  $L_e$  from Table 6.3 need not be corrected for  $K$ ,  $R_h$ , or other conditions in most problems (the accuracy of the data and the shock loss formulas generally do not warrant it) [22].
2. With a change in the area (splitting not involved) or an inlet, include the shock loss in the airway section following the change. This also applies to a bend in conjunction with area change. Discharge is an exception; include it in the section preceding the change.
3. At splits and junctions in airways, use only the portion of the total flow involved in a change of direction or area. Values from Table 6.3 assume an even division of flow and allow for bend and area change. Include loss at split or junction within the pressure drop for the particular branch.
4. Judgment must be exercised in making proper allowance for unusual sources of shock loss (e.g., obstructions).
5. Exclude shock loss due to inlet or discharge if a fan is located there.

#### 6.10 Combined Head Losses and Mine Heads:

The equivalent length method of handling shock loss permits a single calculation (from equations 6.3 and 6.27) of the overall head loss for a given airway. Rewriting equation 6.27 to include equivalent length due to shock loss:

$$H_l = H_f + H_x = \frac{KO(L+L_e)Q^2}{5.2A^3} \quad (6.37)$$

$$H_l = H_f + H_x = \frac{KO(L+L_e)Q^2}{A^3} \quad (6.38)$$

The mine heads are then determined by cumulating the airway head losses, according to equations 6.5 and 6.6. This procedure is recommended for all routine ventilation calculations [22].

#### 6.11 Air power:

Since power is the time rate of doing work, the power required to overcome the energy losses in an airstream, called the air power  $P_a$  is in basic units:

$$P_a = pQ = 5.2HQ \text{ ft. lb}/\text{min} \quad (6.39)$$

And in more customary units:

$$P_a = \frac{5.2HQ}{33000} = \frac{HQ}{6346} \text{ hp} \quad (6.40)$$

$$P_a = \frac{HQ}{1000} \text{ KW} \quad (6.41)$$

With H expressed in in. Water (Pa), p in psf (Pa), and Q in cfm ( $m^3/s$ ). If the total airpower is desired, then the head H should be the mine total head  $H_t$ . If the mine static head  $H_s$  is used in equation 6.40, then only the static airpower is obtained. The power  $P_a$  varies directly as H but as the cube of Q (because  $H \propto Q^2$ ).

### 6.12 Thermodynamic approach to mine ventilation:

As discussed before, it is common to analyze airflow through mines as an incompressible flow problem on the assumption that changes in the air specific weight in mine ventilation are minor. However, this assumption is not reasonable where there is a significant exchange of heat and moisture between the air and the mine surroundings, particularly in deep and hot mines. Here, as it flows through the mine, air undergoes wide variations in heat content and temperature and pressure and density. Because the airflow processes in these cases are the same as the processes in a heat engine, a thermodynamic analysis of the mine ventilation system is possible. As mines or subsurface excavations for other purposes go more profound, and especially when natural ventilation is involved, the thermodynamic approach is not only desirable but may become essential. Hinsley (1950-1951) developed the thermodynamic approach to mine ventilation, comparing the ventilation system to a heat engine. An extensive treatment of the thermodynamic approach to mine ventilation analysis can be found in McPherson (1993). Other useful references include Williams (1960) and Hall (1967, 1981). Only a brief introduction is presented here.

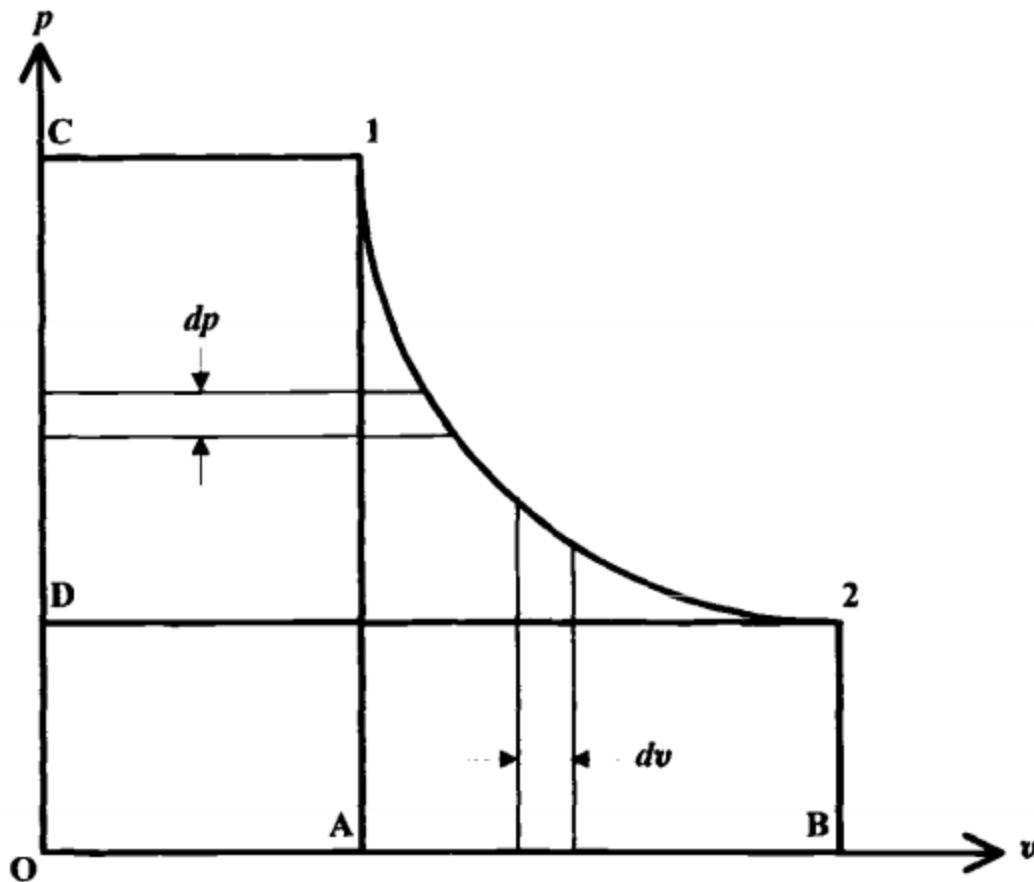


Figure 6.9: Indicator diagram for the system in Figure 6.1 [22].

Consider 1 lbm (kg) of air, whatever its volume, flowing between points 1 and 2 as shown in figure 6.9. Assume that no external mechanical work is done on the air (i.e., work energy added = 0), and no heat transfer takes place through the walls (i.e., external heat energy added, or heat lost to the outside = 0). As the air flows from point 1 to point 2, there is a drop in the absolute pressure from  $p_1$  to  $p_2$  and, in turn, an increase in specific volume from  $v_1$  to  $v_2$ . The indicator diagram ( $p$ - $v$  diagram) for the process is shown in Figure 6.9, the line from 1 to 2 representing the flow path. Now analyze the work done by and on the 1 lbm (kg) of air flowing from point 1 to point 2. In entering the system and overcoming pressure  $p_1$  the work done =  $p_1 v_1$  ftlb/lbm (J/kg). In expanding from  $v_1$  to  $v_2$  and overcoming changes in elevation, changes in velocity, and frictional resistance of flow, the work done =  $\int_{v_1}^{v_2} p dv$ . In discharging from the system against pressure  $p_2$ , the work done on the air =  $p_2 v_2$ . Therefore, the net work done by the air  $p_1 v_1 + \int_{v_1}^{v_2} p dv - p_2 v_2$ . From the indicator diagram, it may be seen that  $\int_{p_1}^{p_2} v dp = p_1 v_1 + \int_{v_1}^{v_2} p dv - p_2 v_2$ . The term  $\int_{p_1}^{p_2} v dp$  is known as the flow work, and  $\int_{v_1}^{v_2} p dv$  is called the non-flow work [22].

The Bernoulli equation for incompressible fluid flow (equation 6.1) follows, incorporating the external mechanical energy input between points 1 and 2. In this form, it is known as the mechanical energy equation for incompressible flow:

$$\frac{p_1}{w} + \frac{v_1^2}{2g} + Z_1 + \dot{W}_{12} = \frac{p_2}{w} + \frac{v_2^2}{2g} + Z_2 + H_{t_{12}} \quad (6.43)$$

Where  $\dot{W}_{12}$  is mechanical energy in  $ftlb/lb$  ( $J/kg$ ) of air added between points 1 and 2, and  $H_{t_{12}}$  is friction and shock energy (head) losses expended in  $ftlb/lb$  ( $J/kg$ ) of air between 1 and 2. In equation 6.43, any addition of heat energy between 1 and 2 does not appear explicitly, nor is it required. The added heat energy will, however, be reflected in the mechanical energy values at 2, preserving the energy balance. equation 6.43 can be rewritten as:

$$\left(\frac{v_1^2}{2g} - \frac{v_2^2}{2g}\right) + (Z_1 - Z_2) + \dot{W}_{12} = v(p_2 - p_1) + H_{t_{12}} \quad (6.44)$$

where the specific volume  $v = (l/w) lb/ft^3$  ( $kg/m^3$ ), assuming dry air. In compressible flow, the change in pressure from  $p_1$  to  $p_2$  takes place in infinitely small steps, changing the specific volume accordingly. Therefore, equation 6.44 for compressible flow can be written:

$$\left(\frac{v_1^2}{2g} - \frac{v_2^2}{2g}\right) + (Z_1 - Z_2) + \dot{W}_{12} = \int_{p_1}^{p_2} v dp + H_{t_{12}} \quad (6.45)$$

The mechanical energy relation, equation 6.43, can incorporate the heat energy added between points 1 and 2 and the internal energy of the air. Noting that friction and shock energy losses result in changes in the interior and mechanical energy terms, ensuring a balance between the mechanical energy and the internal energy in the system, the energy relation equivalent to equation 6.43 is:

$$v_1 p_1 + I_1 + \frac{v_1^2}{2g} + Z_1 + \dot{W}_{12} + \dot{q}_{12} = v_2 p_2 + I_2 + \frac{v_2^2}{2g} + Z_2 \quad (6.46)$$

Where  $I$  is internal energy and  $\dot{q}_{12}$  is amount of heat energy added per unit weight of air between points 1 and 2. The traditional unit for internal and heat energies is the Btu (J). With appropriate conversion factors ( $1 \text{ Btu} = 778 \text{ ftlb}$ ),  $I$  and  $\dot{q}$  can be expressed in specific energy (head) units ( $ftlb/lb$  or  $J/kg$ ).

Since the term ( $vp + I$ ) is the enthalpy  $h$  of the air, a state property, equation 6.46 can be restated as:

$$\left(\frac{v_1^2}{2g} - \frac{v_2^2}{2g}\right) + (Z_1 - Z_2) + \dot{W}_{12} = (h_2 - h_1) - \dot{q}_{12} \quad (6.47)$$

Where  $h_1$  and  $h_2$  are enthalpies at points 1 and 2, respectively. From equations 6.45 and 6.47, it is evident that:

$$\left(\frac{V_1^2}{2g} - \frac{V_2^2}{2g}\right) + (Z_1 - Z_2) + \dot{W}_{12} = \int_{p_1}^{p_2} v dp + H_{t_{12}} = (h_2 - h_1) - \dot{q}_{12} \quad (6.48)$$

Equation 6.48 explicitly states the balance that must exist among the mechanical, thermal, and internal energies of the mine ventilation system. Using equation 6.45, an expression for the head losses can be written [22]:

$$H_{t_{12}} = \left(\frac{V_1^2}{2g} - \frac{V_2^2}{2g}\right) + (Z_1 - Z_2) - \int_{p_1}^{p_2} v dp + \dot{W}_{12} \quad (6.49)$$

The integral  $\int_1^2 v dp$  can be evaluated in terms of measurable parameters from the relationships between  $p$  and  $v$  (the polytropic equation  $pv^n = C$  and the general gas law  $pv = RT$ ):

$$N = \frac{1}{1 - \frac{\ln(T_2/T_1)}{\ln(p_2/p_1)}} \quad (6.50)$$

$$\int_{p_1}^{p_2} v dp = R(T_2 - T_1) \left(\frac{\ln(p_2/p_1)}{\ln(T_2/T_1)}\right) \quad (6.51)$$

$$\int_{p_1}^{p_2} v dp = \left(\frac{n}{n-1}\right)R(T_2 - T_1) \quad (6.52)$$

Thus, knowing the absolute pressures  $p$ , absolute temperatures  $T$ , air velocities  $V$ , and elevations  $Z$  at points 1 and 2, both the index of the process  $n$  and the friction and shock energy (head) losses  $H_l$  can be calculated for the flow between points 1 and 2, using the following relationship [22]:

$$H_{t_{12}} = \left(\frac{V_1^2}{2g} - \frac{V_2^2}{2g}\right) + (Z_1 - Z_2) - \left(\frac{n}{n-1}\right)R(T_2 - T_1) \quad (6.53)$$

If the mass flow in the airway and the airway dimensions are known, both the resistance of the airway and the coefficient of friction can also be calculated. The following example illustrates the calculations involved.

### 6.13 Air specific-weight determinations:

The specific weight  $w$  (density in SI units) of standard air is required in ventilation and air conditioning calculations, detailed ventilation surveys, and selection of mine ventilation equipment. It is not usually measured directly but instead is determined from other air properties. From the general gas laws, the following formula can be derived for air specific weight:

$$w = \frac{1.325}{T_d}(p_b - 0.378p'_v) \quad (6.54)$$

$$w = \frac{1.325}{0.287T_d}(p_b - 0.378p'_v) \quad (6.55)$$

Where  $w$  is air specific weight in  $lb/ft^3$  ( $kg/m^3$ ),  $T_d$  is the absolute dry-bulb temperature in °R (K),  $p_b$  is atmospheric pressure in in. mercury (kPa), and  $p'_v$  is the vapor pressure at dew point in in. Hg (kPa). Other formulas can also be derived relating air specific weight with other psychometric properties of air.

#### **6.14 Humidity Calculations:**

Knowing the dry-bulb and wet-bulb temperatures and the barometric pressure, one can determine specific or relative humidities using psychometric charts or tables. Additionally, Table 6.1 can be used to estimate relative humidities with negligible error for altitudes up to 3000 ft above sea level. The table also provides the value for  $0.378 p'_v$  in equation 6.54 [22].

## Chapter 7

### The developed model and obtained results

#### 7.1 Automatic 3D underground mine mapping:

For several years, one research group has been developing methods for automated modeling of 3D environments. In 2002, the opportunity was given to them to demonstrate our mapping capability with a high-resolution 3D laser scanner mounted on a cart in an underground coal mine. Unfortunately, old maps may be incorrect, incomplete, or simply lost [28]. In the future, we can connect this kind of maps with Ventsim software in order to have more accurate simulations.

#### 7.2 Introduction to Ventsim:

For simulation of the underground mine tunnels, I used Ventsim Design 5.4 in order to know better what happens in each airway or each tunnel of the mine. Ventsim is working on the basis of formulas and equations were derived by different researchers and professors which explained in the previous chapters and are explained in details in the McPherson 1993 book and I've got the permission for rewrite some of the formulas in my thesis from the publisher [30]. An important thing would be rewrite and coding all of the calculations based on CFD models with MATLAB or other programming languages, however, it could be very expensive and each run of the software would take several hours; thus, CFD modeling for this kind of simulations could be very accurate but needs a lot of funds and time. In this simulation, I simulated the software for heat, contaminants, fumes, and airflows. I will discuss about them in the following paragraphs.

#### 7.3 Map of the levels of the mine:

In the following pictures we can see the different levels of the mine:

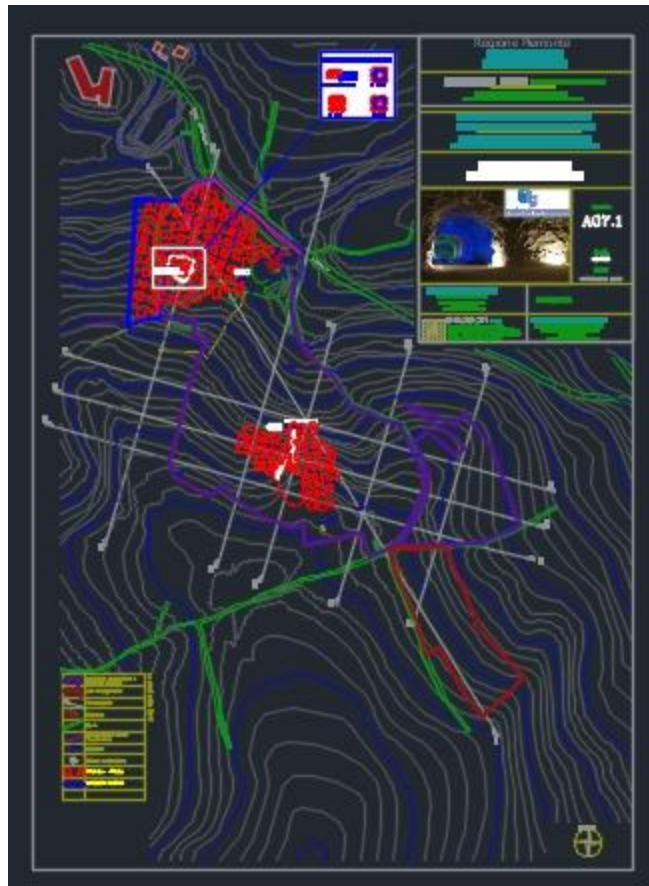


Fig 7.1: Level A of Murisengo Mine.

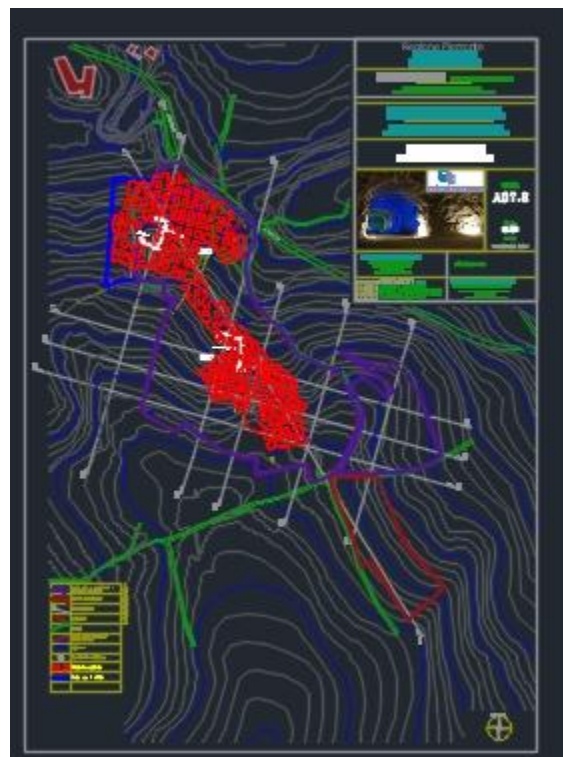


Fig 7.2: Level B of Murisengo Mine.

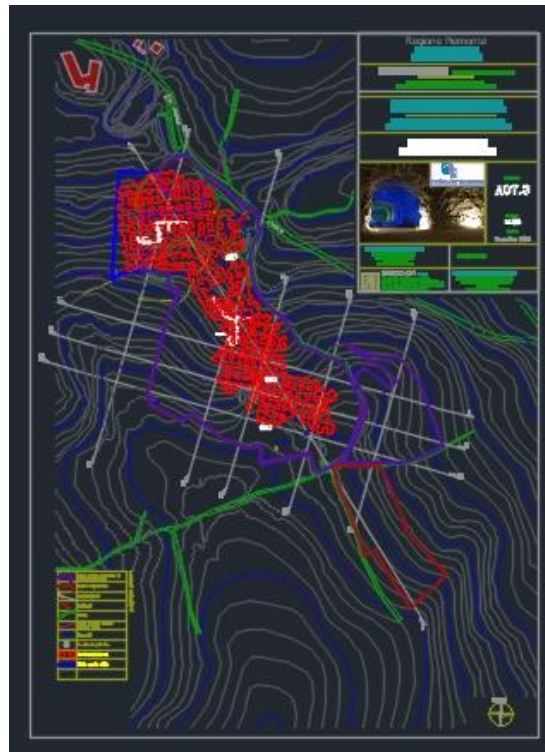


Fig 7.3: Level C of Murisengo Mine.



Fig 7.4: Level D of Murisengo Mine.

#### 7.4 First problem of the ventilation system in the Murisengo mine:

Currently only level F (fig 7.6) is under extraction; however, I simulated all 6 floors (A, B, C, D, E, F) with Ventsim software in order to know what are the airflows quantities in each airway and what are the directions and quantities of air when entering the mine until reaching level F then I have found out a very simple and interesting result. There was huge pressure loss due to many linked airways so there was very low ventilation in the levels C, D, E and F while only one fan exist in a shaft between levels E and F in order to move the unhealthy air from some airways to another airways in level E and F and it was like a recirculation of contaminated air between level E and level F (figure 7.27) and most of the healthy air enters the mine from level A then streams to level B and flows out through the other ramp (Prato Nuovo) of the level B. It's important to note that most of the healthy air does not even reach level C (figure 7.15) so a ventilation system would be necessary in order to direct the air from surface to level F and then force it out to the surface again [32].

The essence of controlled circulating ventilation technology is to purify the contaminated wind discharged from the work surface layer upon layer by using the existence of abandoned roadway engineering, and reuse the supply of underground operation when the air quality meets the health standards [31].

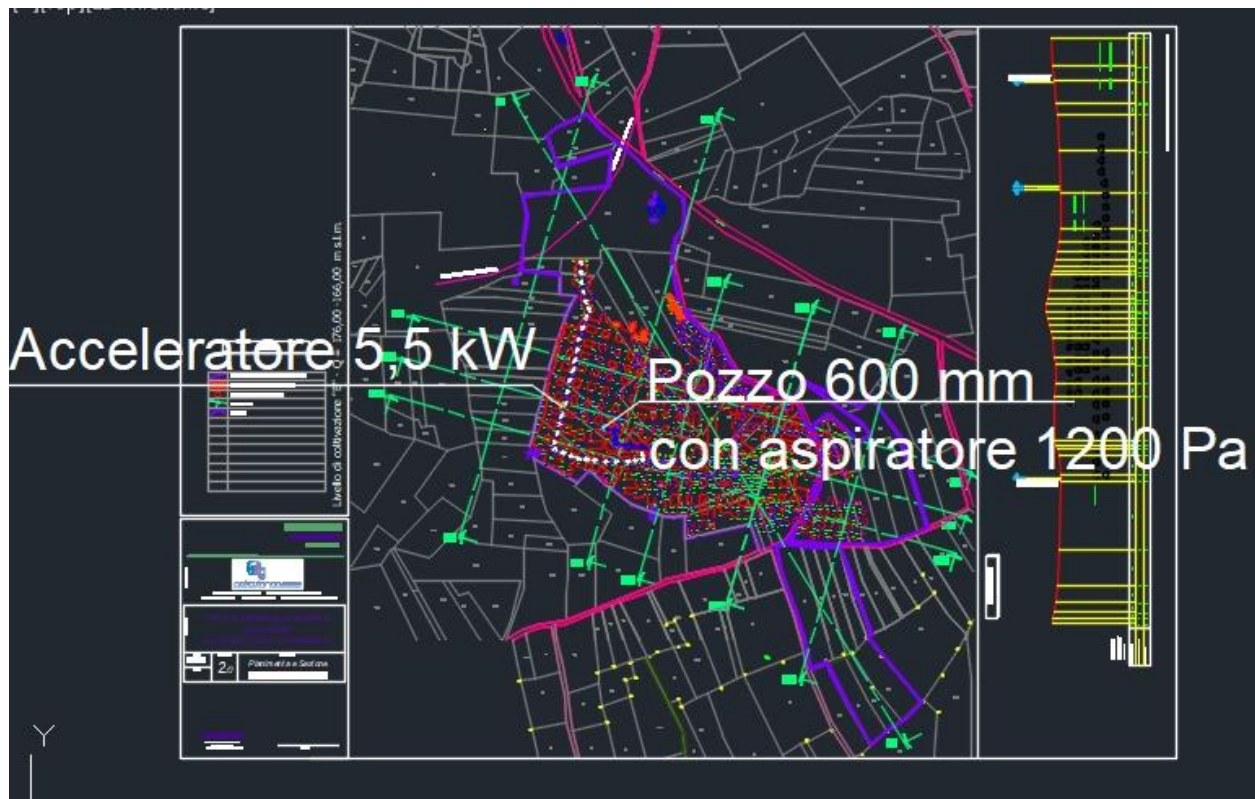


Fig 7.5: Level E of Murisengo Mine.

For too much pressure loss due to the large number of the airways we can design two kinds of solutions based on the mine's ventilation square Law in order to raise the amount of the air quantity:

$$P=RQ^2$$

We can reduce the pressure loss inside the airways with different tools such as concrete walls, orifice, regulators, ...

- 1

We can increase the the total pressure that force the air to flow with different tools such as fans, ...

- 2

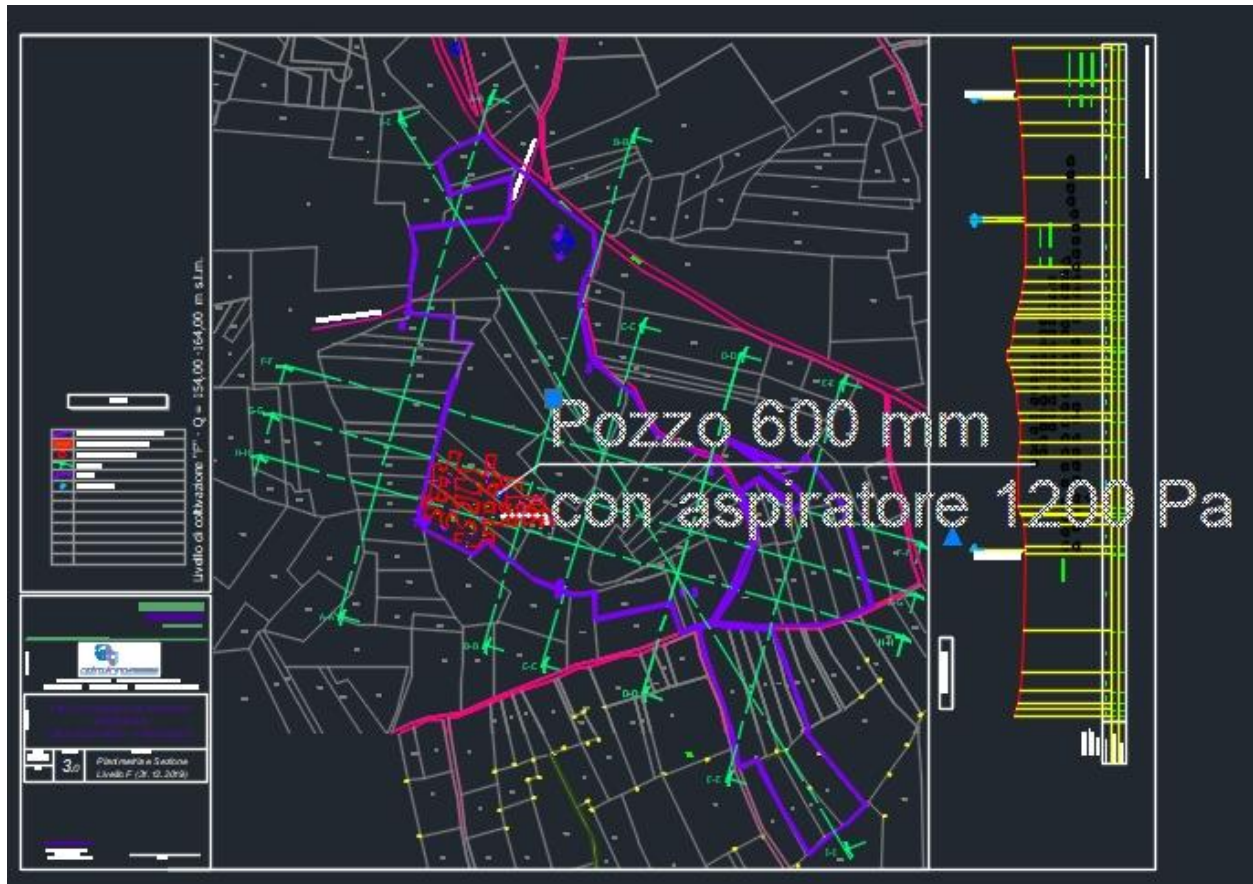


Fig 7.6: Level F of Murisengo Mine.

In the fig. 7.15, we can observe the 6 floors airflow simulation of the Murisengo mine in order to see where are the lowest velocities in the airways and simulate the existing situation of the ventilation system in the mine. With my calculations even a very big fan with 2 million € cost could not solve the problem so we have to reduce the huge pressure loss in the airways. I'll discuss about the solution in the next chapter.

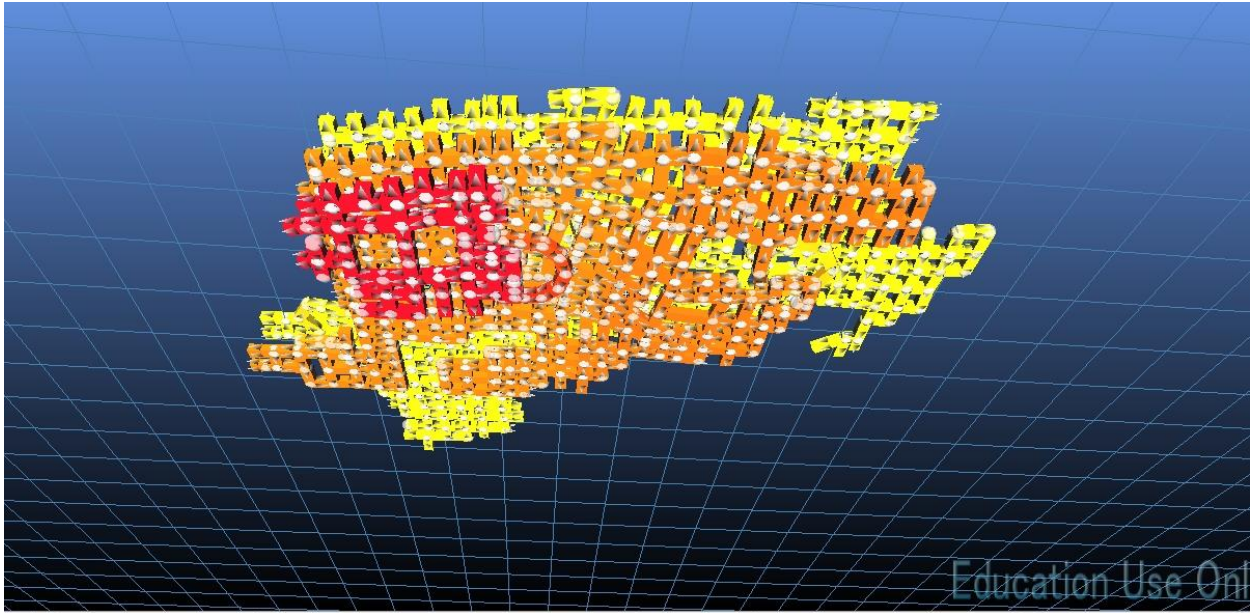


Figure 7.7: simulation of E, D, and F floors of the Murisengo Mine.

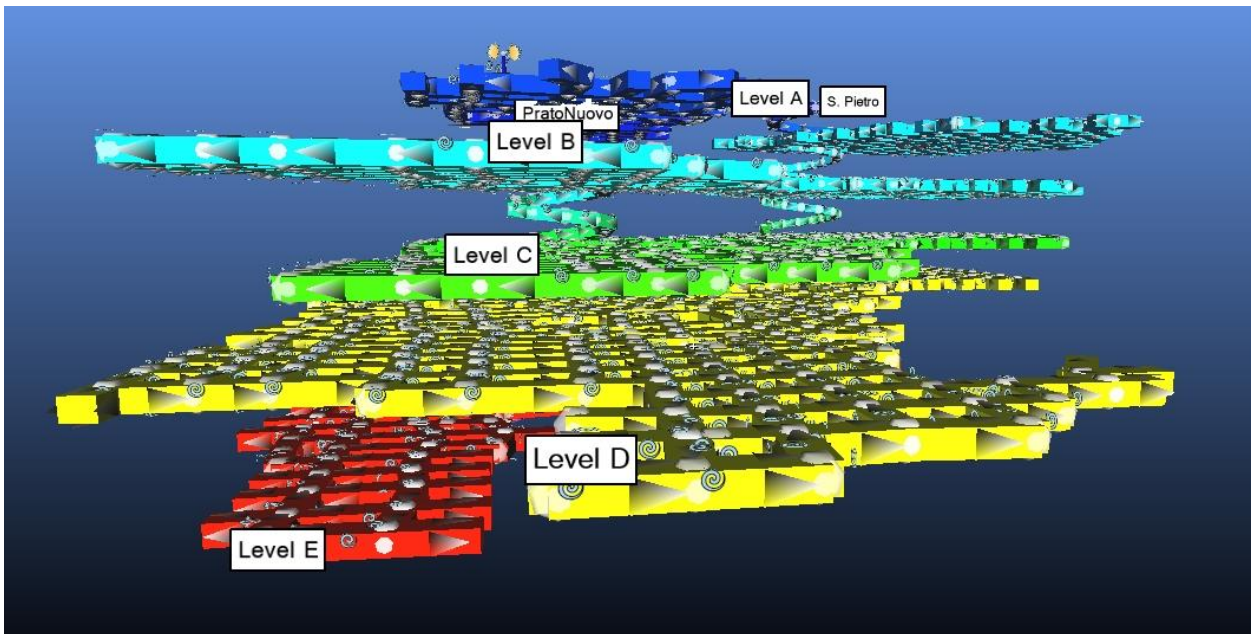


Figure 7.8: Front view 1st angle simulation of A, B, C, E, D, and F floors of the Murisengo Mine.

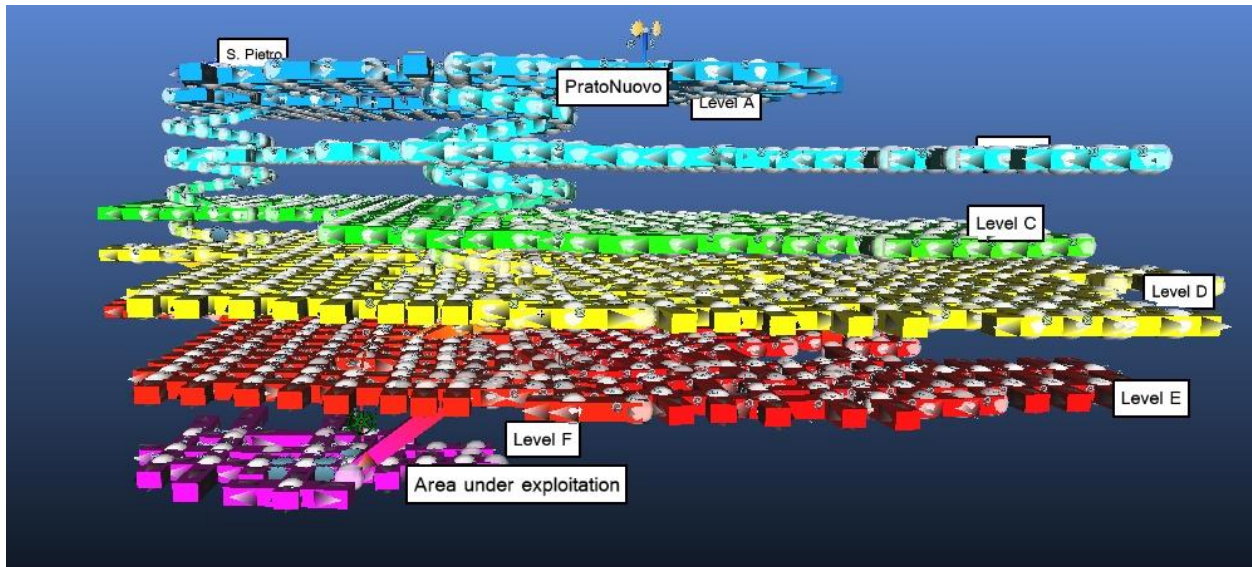


Figure 7.9: Front view 2nd angle simulation of A, B, C, E, D, and F floors of the Murisengo Mine.

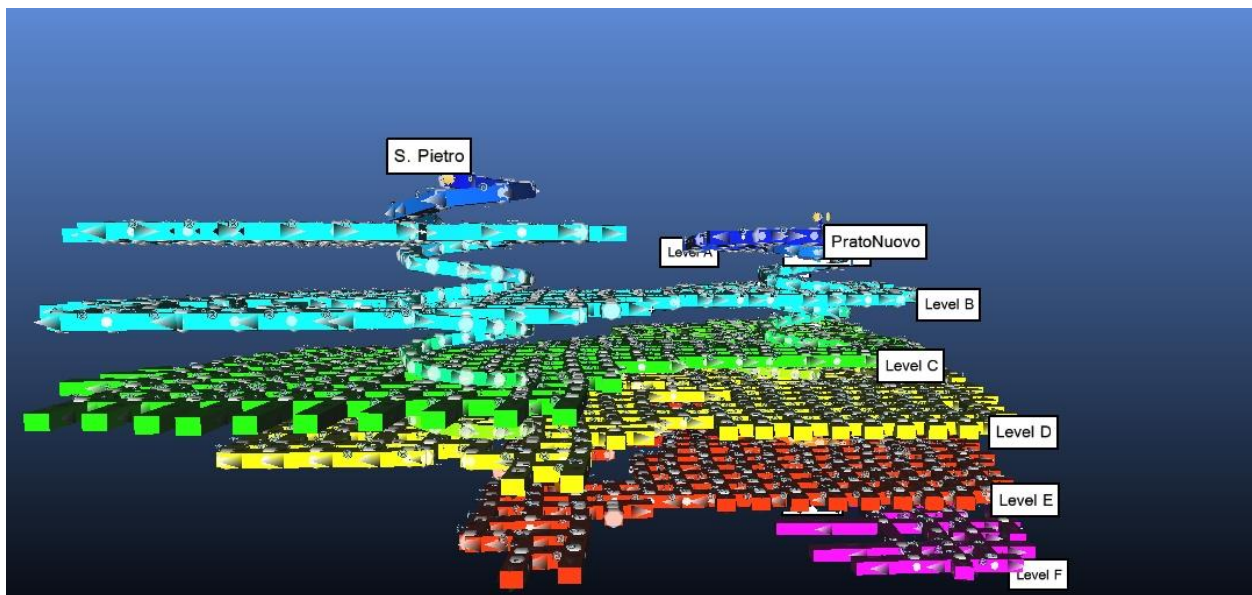


Figure 7.10: Front view 3rd angle simulation of A, B, C, E, D, and F floors of the Murisengo Mine.

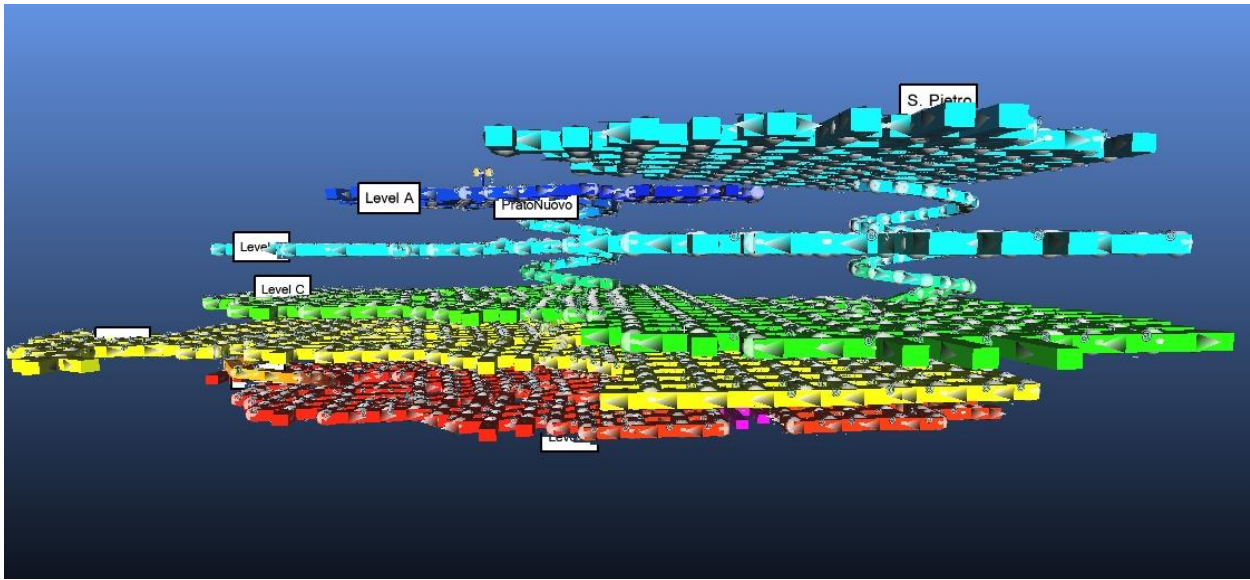


Figure 7.11: Front view 4th angle simulation of A, B, C, E, D, and F floors of the Murisengo Mine.

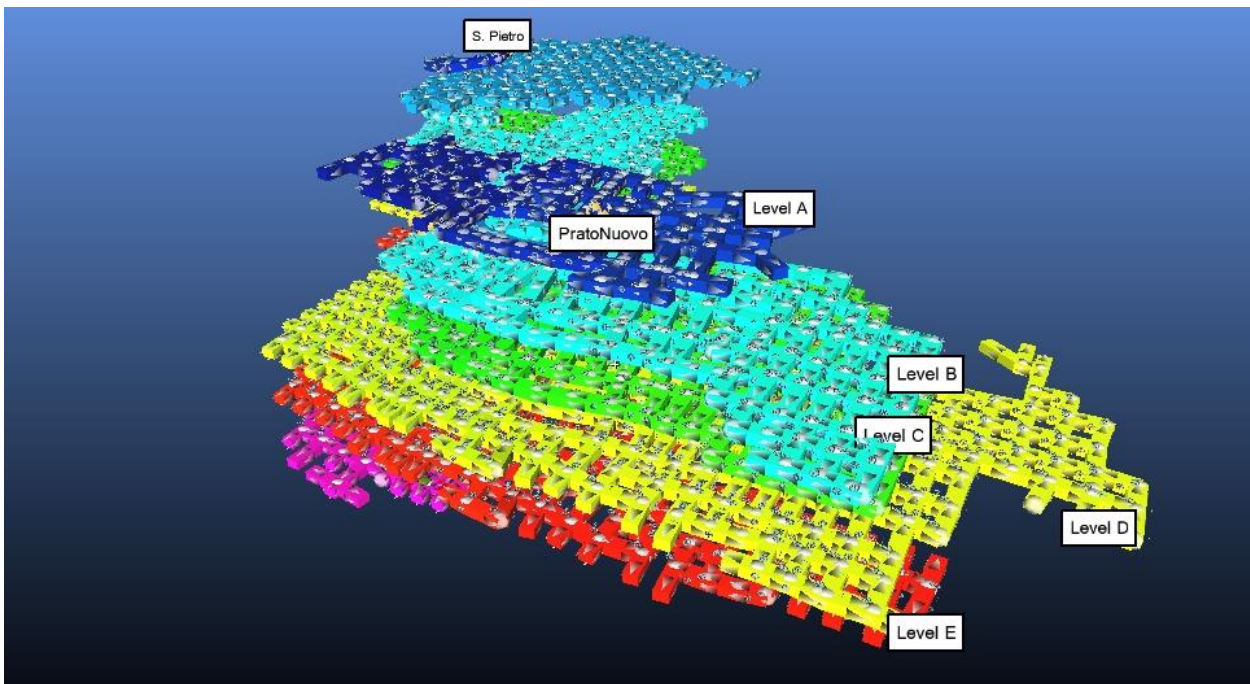


Figure 7.12: Top view simulation of levels A, B, C, E, D, and F of the Murisengo Mine.

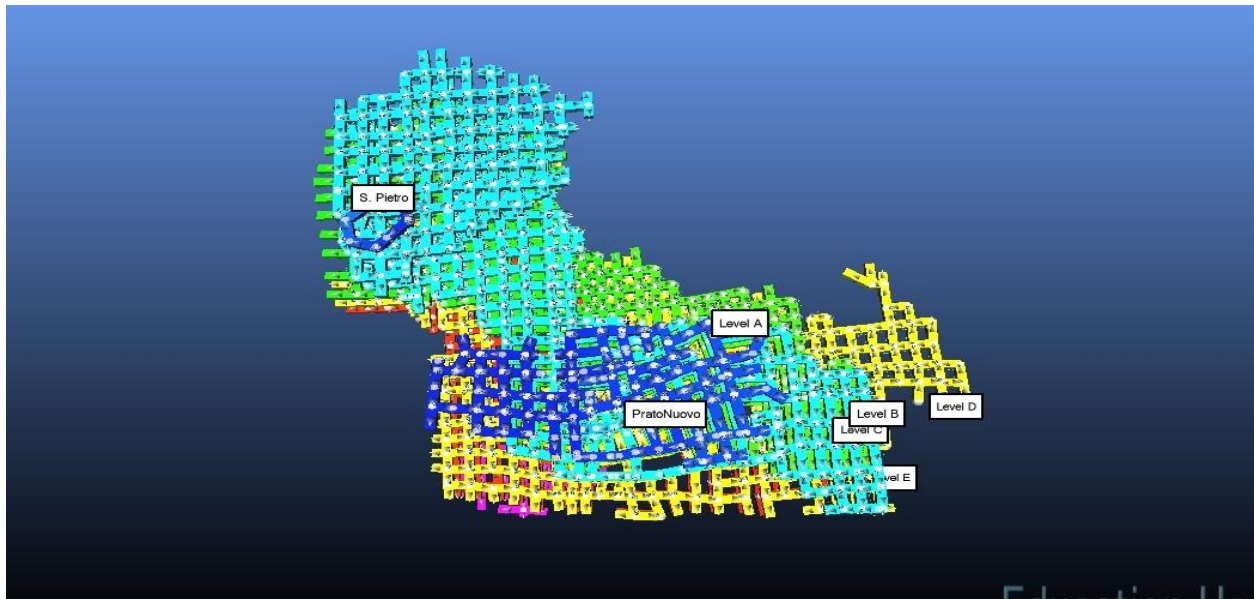


Figure 7.13: Top view simulation of A, B, C, E, D, and F floors of the Murisengo Mine.

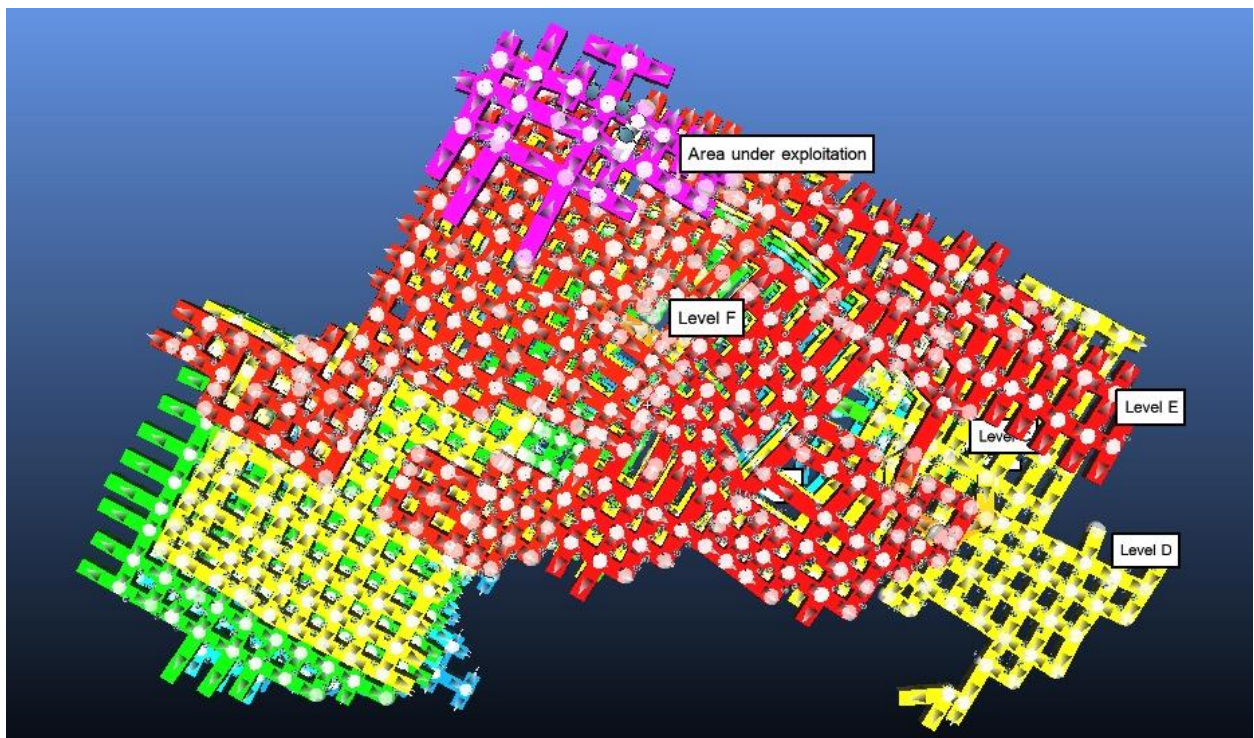


Figure 7.14: Bottom view simulation of A, B, C, D, E, and F floors of the Murisengo Mine

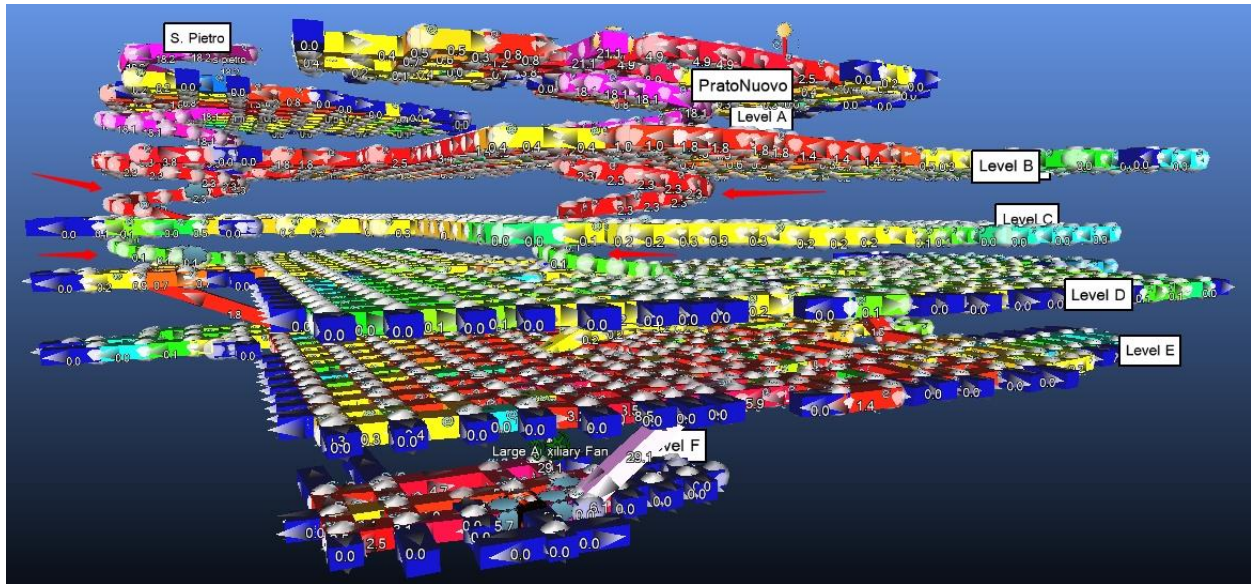


Figure 7.15: Airflow simulation of every airways of the Murisengo Mine. The highest airflow: pink color. The lowest airflow: blue color. The colors from highest airflow to lowest airflow: Pink, Red, Yellow, Green, Blue.

The red arrows in the figure 7.15 show that there are little flows of air in the ramps between levels B-C and levels C-D that mean very little amount of fresh air will reach level D, E, and F and there is huge recirculation of unhealthy air through level E and F that will be discussed later.

#### 7.5 Contaminations in Murisengo mine:

The following paragraphs show the amounts of contaminants in different locations of the mine based on direct on-site measurements and we can compare them with the contaminations inside the simulation. After comparing I found out these data are not similar to contaminations that are present in my simulation in the current situation of the mine figures 7.16, 7.17, 7.18, 7.19, 7.20, and 7.21.

#### MEASURING POINT

No°1

**Certificate of analysis:** C2396-01/20

**type:** personnel **Nominative:** Mr. Canazza Graziano

Attendant Liebherr 576

Machining: Wheel loader conduction (air-conditioned vehicle), for material handling felled and load of the tout venant on the trucks (2 trucks in operation)

**Position of the collection device:** near the operator's respiratory tract

<b>Pollutant</b>	<b>Average concentration measured [ppm]</b>	<b>VLE [ppm]</b>
Carbon dioxide (CO <sub>2</sub> )	<b>1900</b>	5000
Carbon monoxide (CO)	<b>3.62</b>	20*
Nitrogen oxide (NO)	<b>1.98</b>	25*
Nitrogen dioxide (NO <sub>2</sub> )	<b>0.07</b>	0.5*
Sulphur dioxide (SO <sub>2</sub> )	<b>n.r. &lt; 0.1</b>	0.5*

*n.r. = undetectable*

### **MEASURING POINT**

**No°2**

**Certificate of analysis:** C2396-02/20

**Sampling date:** 12/02/2020 Sampling

**type:** personnel **Nominative:** Mr. Marforius Valerius

TAMROCK HS105 Drill Operator

**Working:** Drilling conduction (ground processing, no cabin)

**Position of the collection device:** near the operator's breathing routes in prossimità delle vie respirato

<b>Pollutant</b>	<b>Average concentration measured [ppm]</b>	<b>VLE [ppm]</b>
Carbon dioxide (CO <sub>2</sub> )	<b>1300</b>	5000

Carbon monoxide (CO)	<b>5.26</b>	20*
Nitrogen oxide (NO)	<b>2.71</b>	25*
Nitrogen dioxide (NO <sub>2</sub> )	<b>0.14</b>	0.5*
Sulphur dioxide (SO <sub>2</sub> )	<b>n.r. &lt; 0.1</b>	0.5*

*n.r. = undetectable*

### MEASURING POINT

**No°3**

**Certificate of analysis:** C2396-03/20

**Sampling date:** 12/02/2020 Sampling

**type:** personnel **Nominative:** Mr. Caltran Roberto

ASTRA 8450 HD9 truck operator

Machining: Operation of trucks (means with air conditioning), for transport of the mineral outwards with exhaust in the wee way.

**Position of the collection device:** near the operator's respiratory tract

<b>Pollutant</b>	<b>Average concentration measured [ppm]</b>	<b>VLE [ppm]</b>
Carbon dioxide (CO <sub>2</sub> )	<b>1800</b>	5000
Carbon monoxide (CO)	<b>&lt; 1</b>	20*
Nitrogen oxide (NO)	<b>0.66</b>	25*

Nitrogen dioxide (NO <sub>2</sub> )	<b>n.r. &lt; 0,04</b>	0.5*
Sulphur dioxide (SO <sub>2</sub> )	<b>n.r. &lt; 0.1</b>	0.5*

*n.r. = undetectable*

### MEASURING POINT

#### No°4

**Certificate of analysis:** C2396-04/20

**Sampling date:** 12/02/2020 Sampling

**type:** personnel **Nominative:** Mr. Caltran Sergio

**Processing:** Underground activity control: supervision of drilling activities and pump control. Pre-loading of the flywheel load (loading and firing mine), occasionally using the D.DIECI Icarus platform

**Position of the device:** near the operator's respiratory tract

<b>Pollutant</b>	<b>Average concentration measured [ppm]</b>	<b>VLE [ppm]</b>
Carbon dioxide (CO <sub>2</sub> )	<b>1000</b>	5000
Carbon monoxide (CO)	<b>3.36</b>	20*
Nitrogen oxide (NO)	<b>2.10</b>	25*
Nitrogen dioxide (NO <sub>2</sub> )	<b>0.19</b>	0.5*
Sulphur dioxide (SO <sub>2</sub> )	<b>n.r. &lt; 0.1</b>	0.5*

n.r. = undetectable

In all personal locations the concentration value of O<sub>2</sub> was always between 20.0 and 20.9 % Vol.

\* = **value reported by EU Directive no. 2017/164 (not yet transposed by All. XXXVIII DLgs.81/08)**, it should be emphasized that for underground mining, this directive must be transposed into Italian law by 21/08/2023, as far as Nitrogen Monoxide is involved, the limit value reported in **Directive 91/322/EEC of 25ppm can** continue to be applied during the transitional period.

**Environmental sampling:**

**MEASURING POINT 5**

**Certificate of analysis:** C2396-05/20, **Data sampling:** 12/02/2020 Sampling

type: environmental

Location: CARREGGIO AREA at pillar 1236 (transit tunnel between Level V and Level IV in subterranean)

Workmanship: Normal construction activities (in wheeling wheel function, 2 trucks and platform D.DIECI Icarus)

**Location of the collection device:** about 1.6 meters above the ground.

<b>Pollutant</b>	<b>Average concentration measured [ppm]</b>	<b>VLE [ppm]</b>
Carbon dioxide (CO <sub>2</sub> )	<b>700</b>	5000
Carbon monoxide (CO)	<b>&lt; 1</b>	20*
Nitrogen oxide (NO)	<b>1.01</b>	25*
Nitrogen dioxide (NO <sub>2</sub> )	<b>0.07</b>	0.5*
Sulphur dioxide (SO <sub>2</sub> )	<b>n.r. &lt; 0.1</b>	0.5*

n.r. = undetectable

Then I put the contaminants of 3 sources of contaminations of 3 machines inside level F, a pick-up car inside the San Pietro ramp between levels C-D, and contaminations of a truck inside the San Pietro ramp between levels B-C then we can compare the results with the on-site measured data on the previous tables above. AN important thing would be the amount of contaminations produced by each machine are considered based on real contaminations produced by a diesel engine per KW and also the composition of the air of the exhaust of diesel engine as bellow:

Composition of the air in the exhaust of the diesel engine: O<sub>2</sub>: 11%, CO<sub>2</sub>: 15%, N<sub>2</sub>: 73%, CO: 10000 ppm. We assumed based on real data that will be 0.00005 l/sec injection of CO per KW of the diesel engines; hence, the total amount of injection of gas for each KW of the diesel engine would be 0.005 (0.00005\*1000000/10000) because there is 10000 ppm of CO in the composition of the gas which comes out of the diesel engine and at the end for a 100 KW diesel engine the total amount of gas injection would be 0.5 l/sec [(0.005 l/sec.KW)\*100KW] then I put 0.5 l/sec of injection of gas inside the simulation.

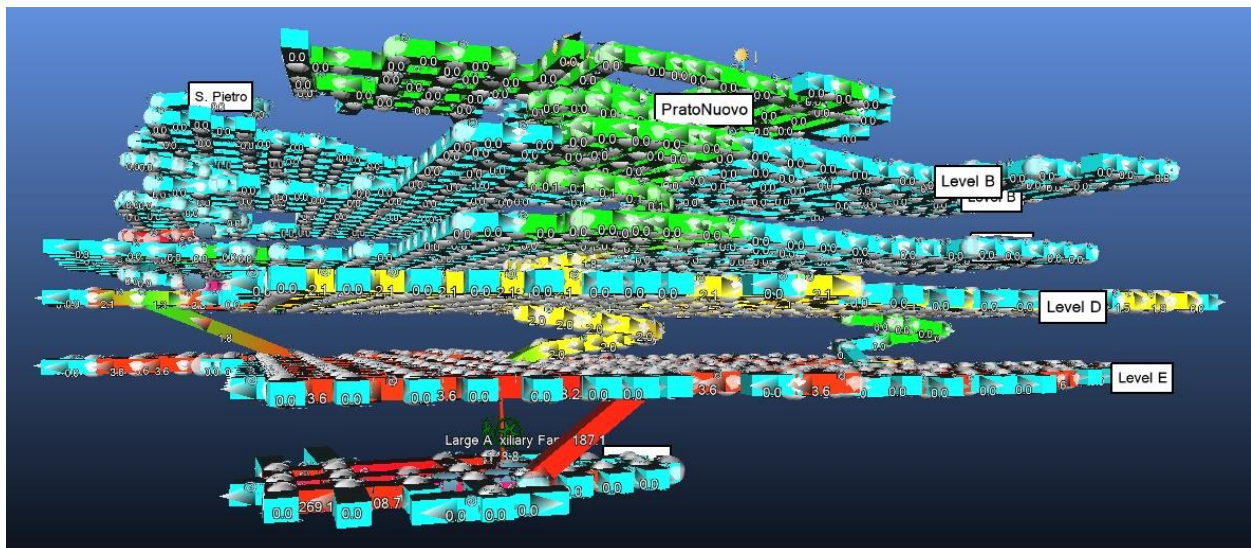


Figure 7.16: The distribution of CO (ppm) after 15 minutes of starting of machines.

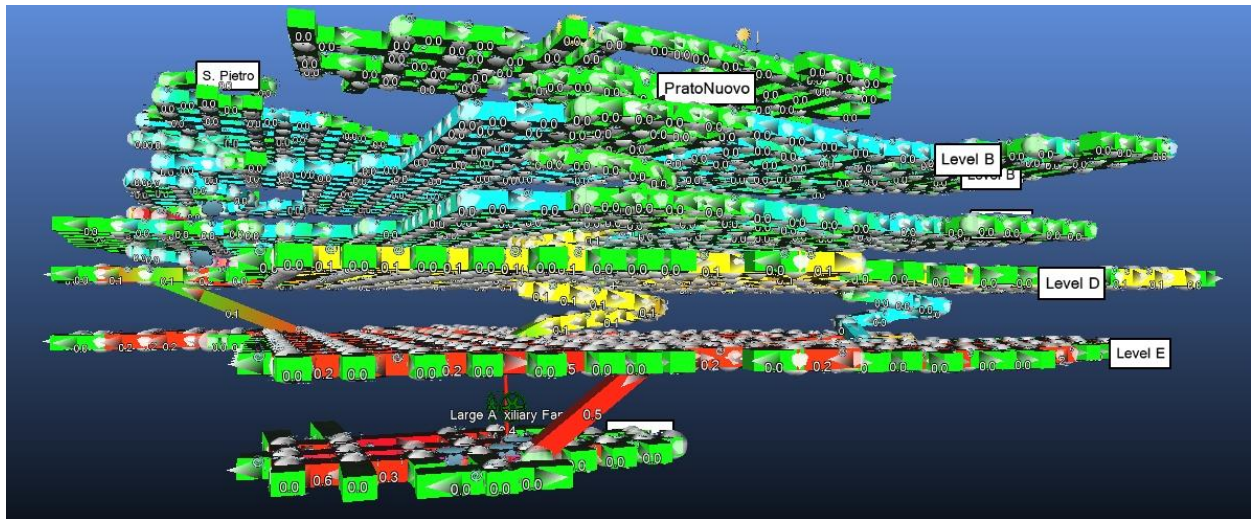


Figure 7.17: The distribution of CO<sub>2</sub> (%) after 15 minutes of starting of machines.

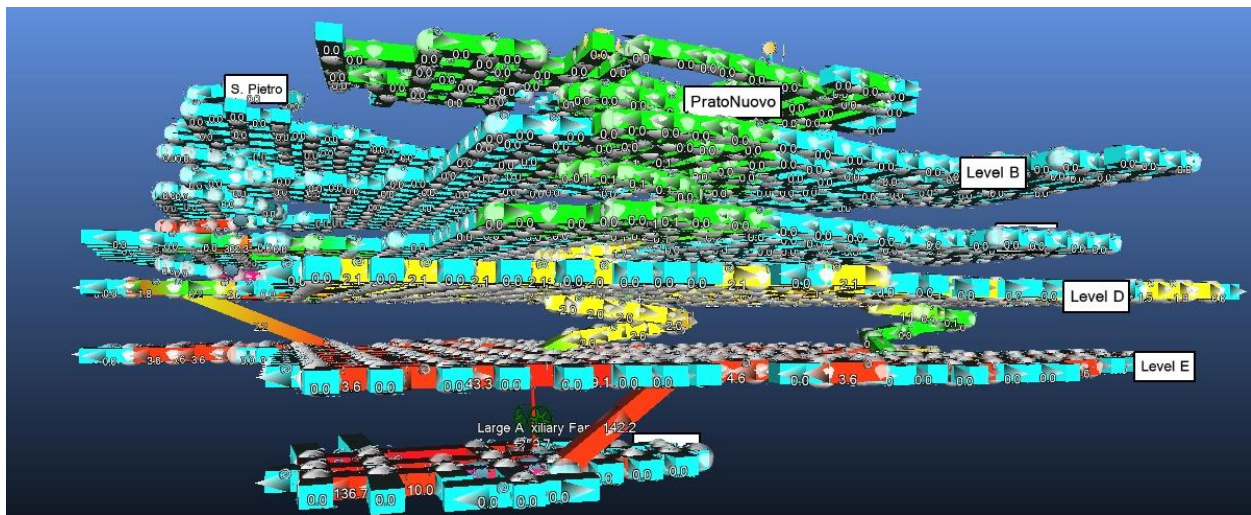


Figure 7.18: The distribution of CO (ppm) after 30 minutes of starting of machines.

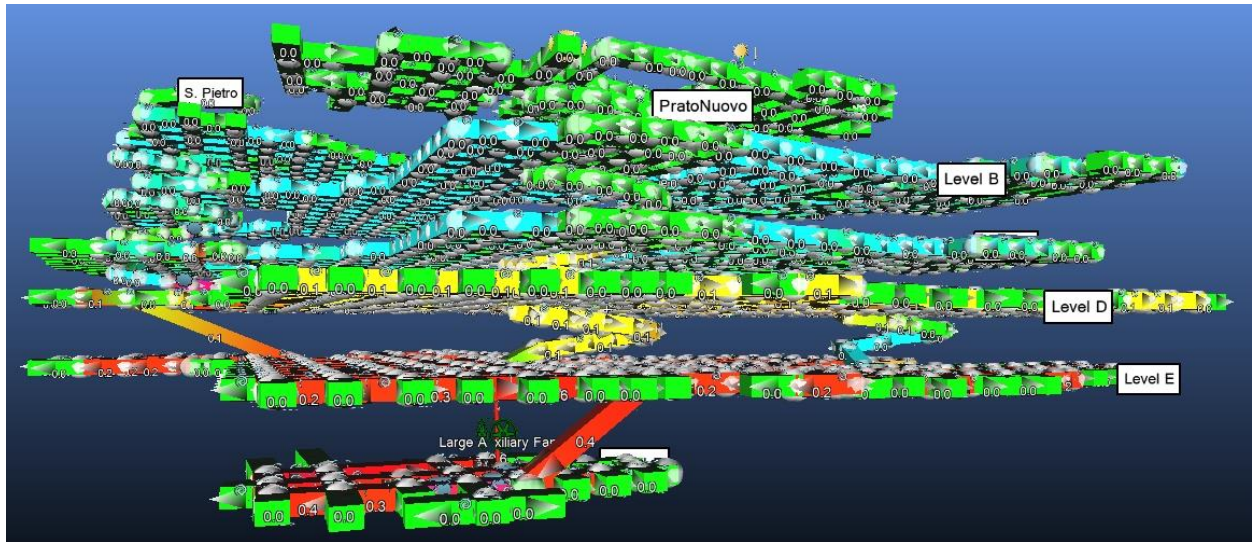


Figure 7.19: The distribution of  $CO_2$  (%) after 30 minutes of starting of machines.

There is a 30 KW fan inside the shaft between levels E and F and for that I simulated a large auxiliary fan with 86% of efficiency with efficiency of 68.7% and curve 1 of the Ventsim software in order to simulate the most similar fan to the fan existing in the shaft of the levels E and F. Another very important consideration is that I assumed that there are auto low shock loss due to the connections of the airways and irregularities of walls of the tunnels in every airway and tunnel to simulate as similar as possible the current characteristics of the mine.

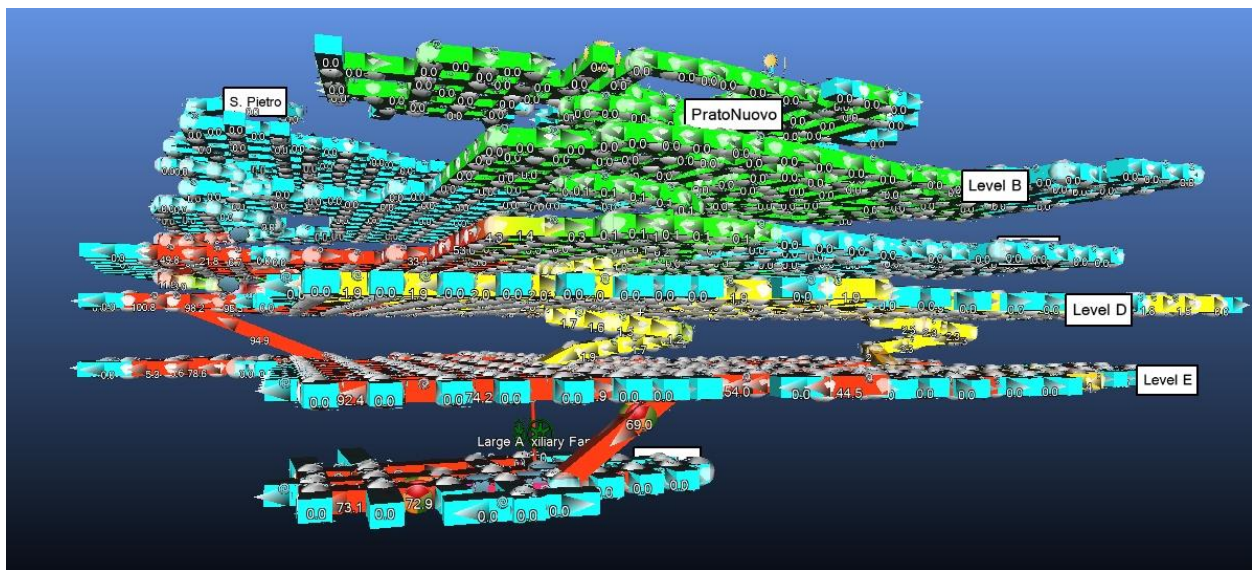


Figure 7.20: The distribution of CO (ppm) after 8 hours (1 shift) of starting of machines.

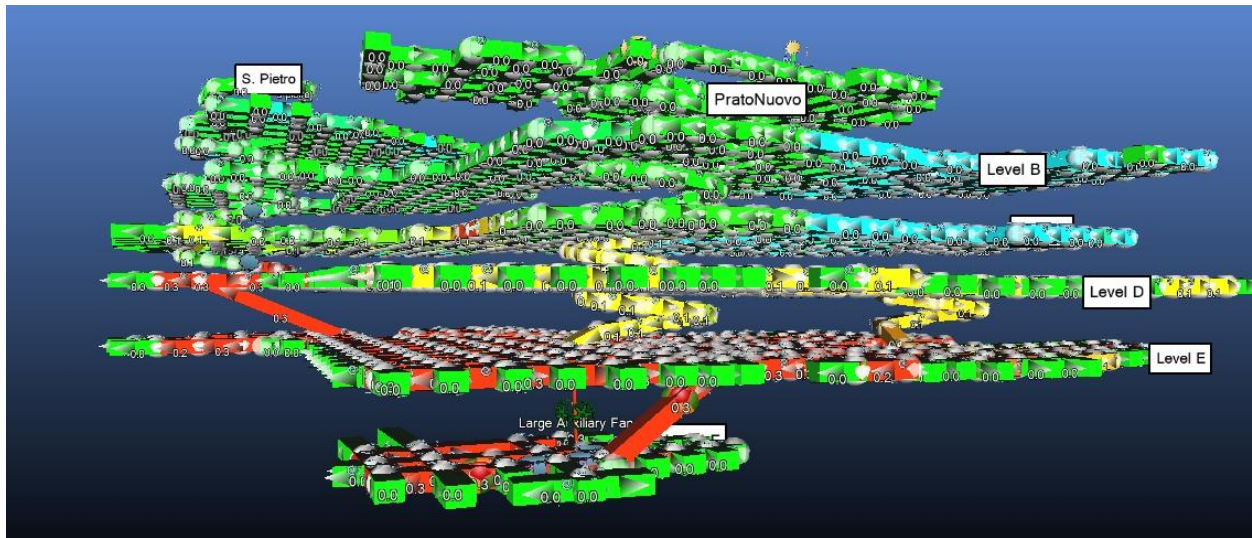


Figure 7.21: The distribution of  $CO_2$  (%) after 8 hours (1 shift) of starting of machines.

Also, we can simulate the spread of contaminations due to explosives, however, it is not necessary in our simulation because during explosion, there is no personnel present in the mine.

From figure 7.22 we can see better the recirculation of the unhealthy air in the Levels D, E, and F and it means that the large auxiliary fan inside the shaft is not able to direct the unhealthy air out of the mine in the current situation of the mine; thus, we need to plan a ventilation system to force contaminated air out of the mine which will be discussed in detail in the chapter 8.

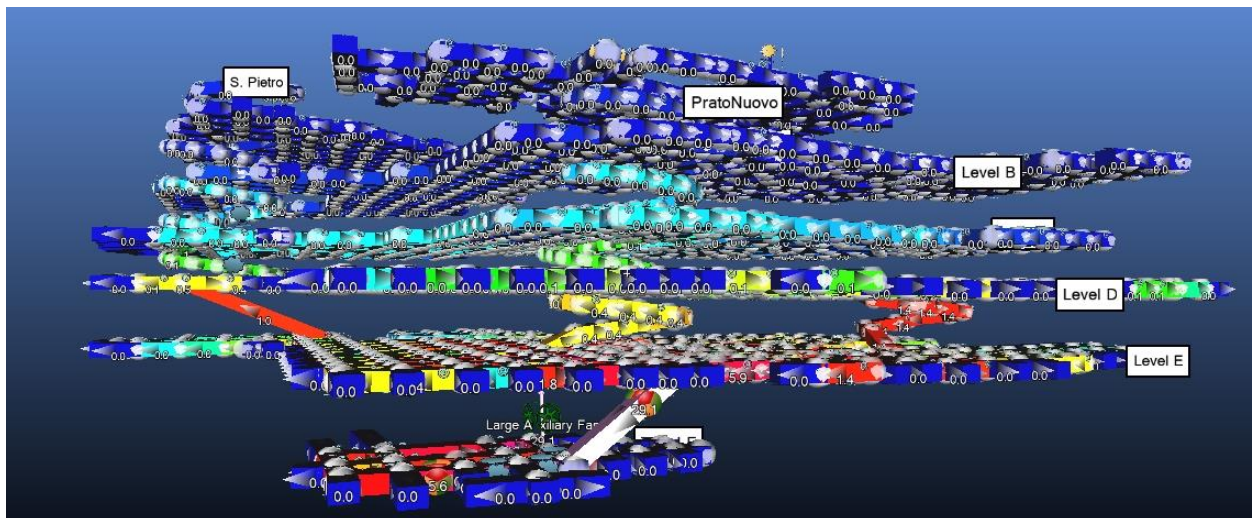
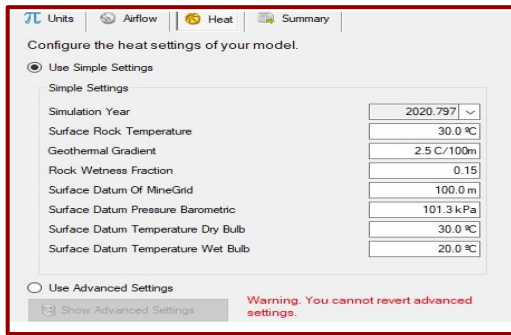
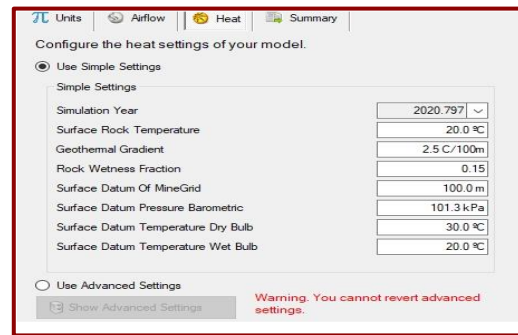


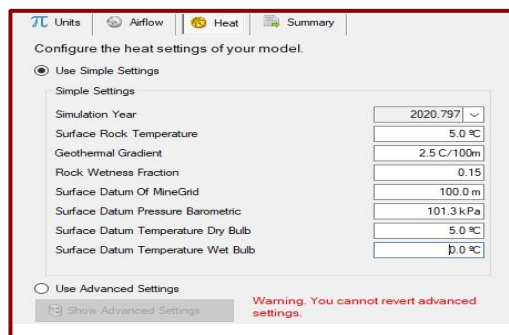
Figure 7.22: Airflow simulation of every airways of the Murisengo Mine without Natural ventilation. The highest airflow: pink color. The lowest airflow: blue color. The colors from highest airflow to lowest airflow: Pink, Red, Yellow, Green, Blue.



• Summer



• Spring



• Winter

Then by changing the temperature of the environments on the surface as the above 3 tables, I simulated the airflows inside the circuits of the mine in different seasons (Summer, Spring, winter) and I saw a very little change in the amounts of airflows, however, there was not any change of the direction in the ramps that is in contrast of what the miners thought before that was explained in the chapter 5. It would be interesting to put also the pictures of the airflows in different seasons but there are lots of pictures of different important features of the mine so I do not put the pictures of airflows in different seasons for this reason.

#### 7.6 Second problem of the ventilation system in the Murisengo mine:

It's obvious from figure 7.16 to figure 7.21 that in the current situation of the mine the distributions of the contaminants were very slow and mostly through airways of level F, E, and D. In figure 7.16, we can see that after 15 minutes from the working of the machines, most of the contaminants produced in level F reach only level E then the contaminants flew via ramp San Pietro to level D and after 30 minutes (figure 7.18) they disseminated in a small portion of airways of level D and after 8 hours (figure 7.20) they streamed the ramp PratoNuovo in order to reach level C. Finally, after 20 hours, a little amount of contaminants will reach level A and from there to the surface. It's important to note that during 20 hours lots of the contaminants such as dust, and some harmful gases will settle down on the ground and will disseminate through the air in the case of

moving of a truck, ... . Thus, an optimized ventilation system which could direct healthy air into the lowest levels of the mine and force the unhealthy air out of the mine to the surface would be necessary in order to guarantee the health of the miners in long term and also for safety reasons. It's observable in our simple solution (figures 8.9 and 8.11) in the chapter 8 that contaminants will reach more quickly to the surface and it's beneficial both reducing the concentrations of contaminants in the lower levels and no letting the contaminants settle down on the ground.

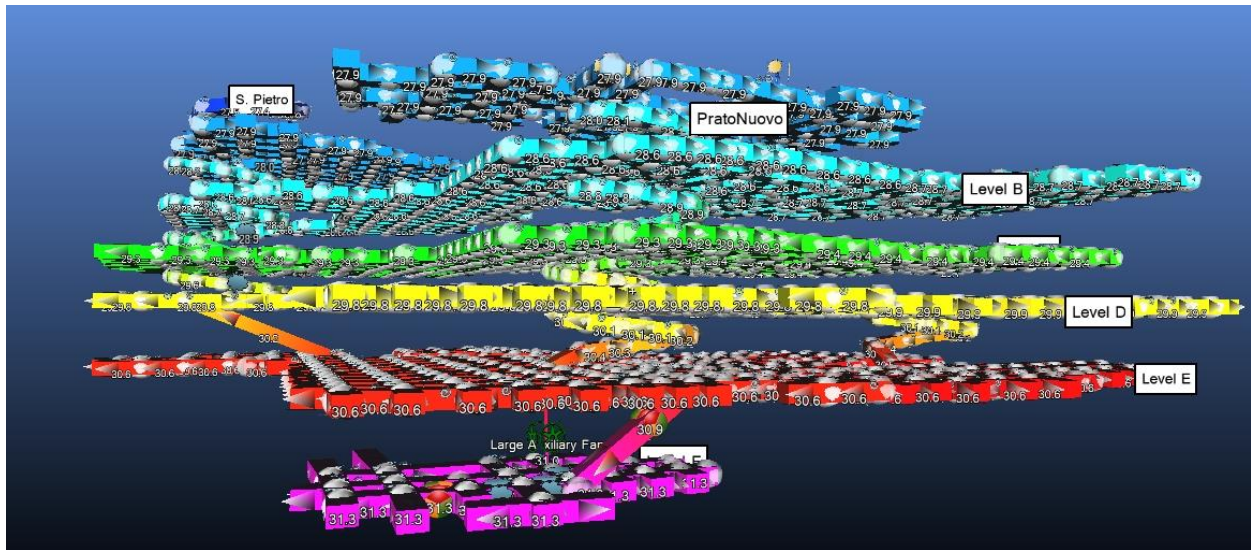


Figure 7.23: The amount of temperatures inside the rock for each level of the mine in the current condition.

There are five important recirculation of the air inside the mine as following pictures; hence, this is another reason that we need block some airways in order to force the air that come from smaller number of airways and going out.

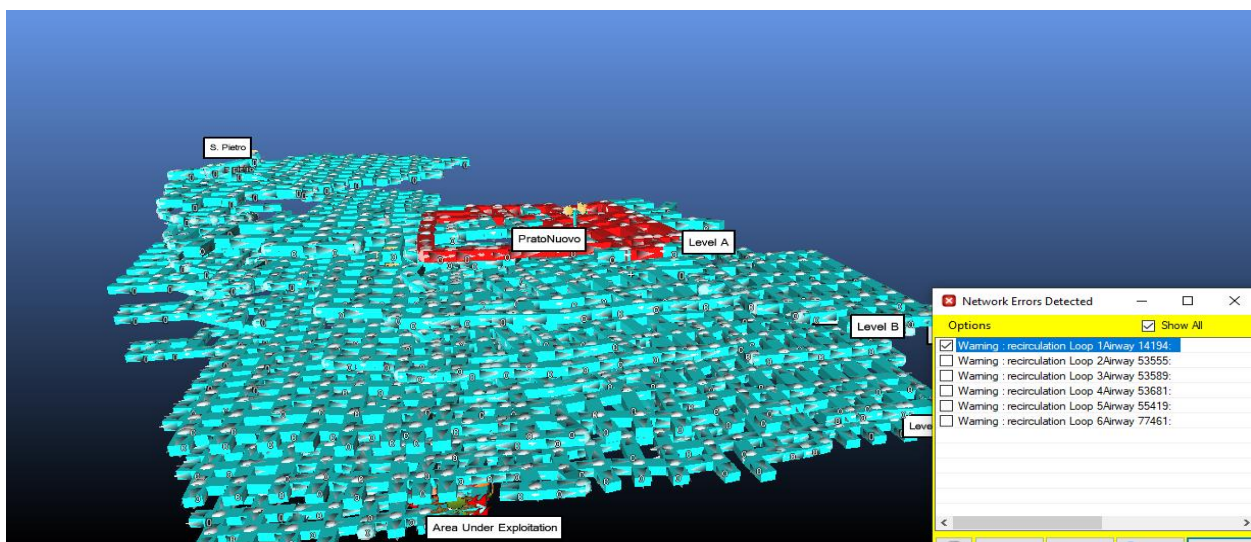


Figure 7.24: Recirculation of air inside some airways of the level A in the current situation of the mine.

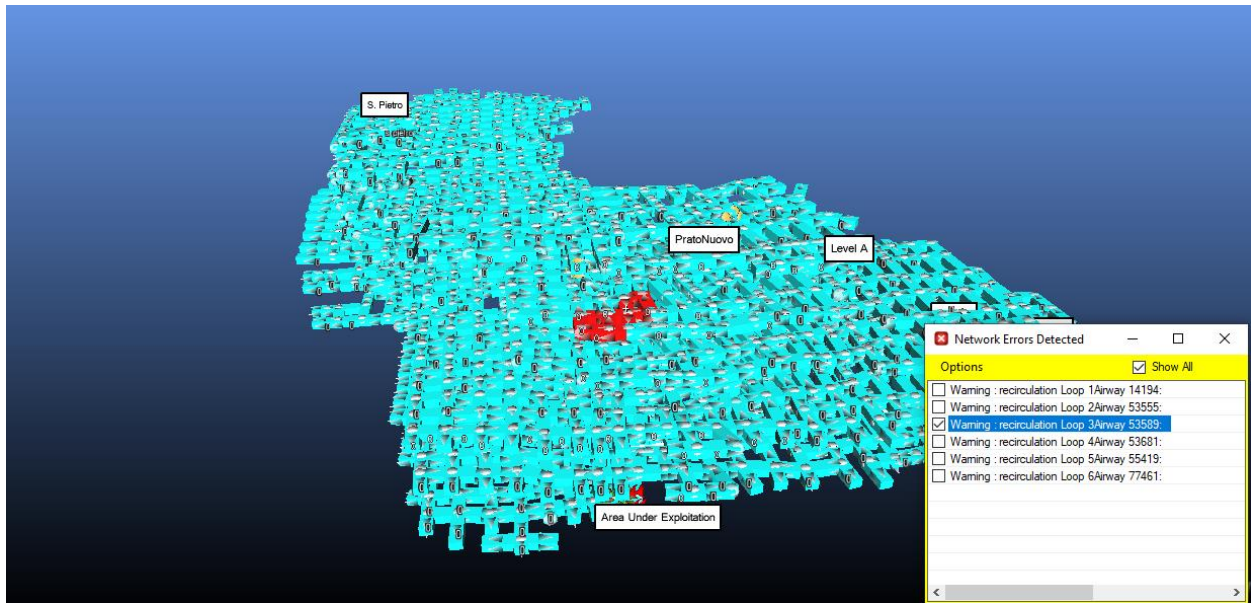


Figure 7.25: Recirculation of the air inside a small portion of the level B in the current situation of the mine.

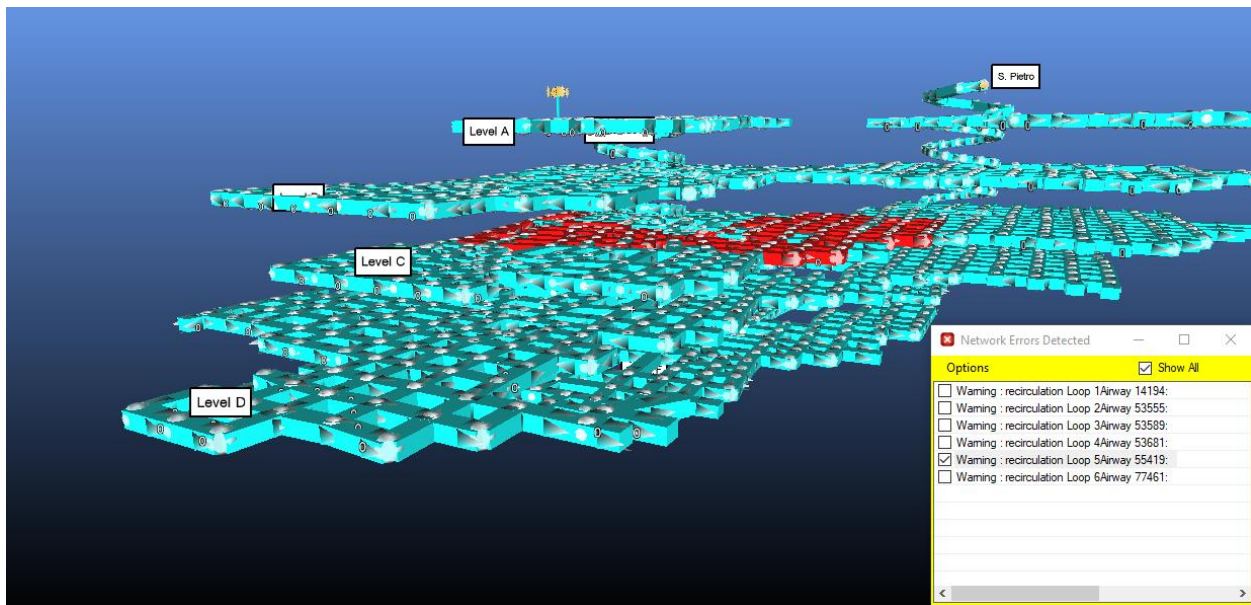


Figure 7.26: Recirculation of the air inside several airways of the level C in the current situation of the mine.

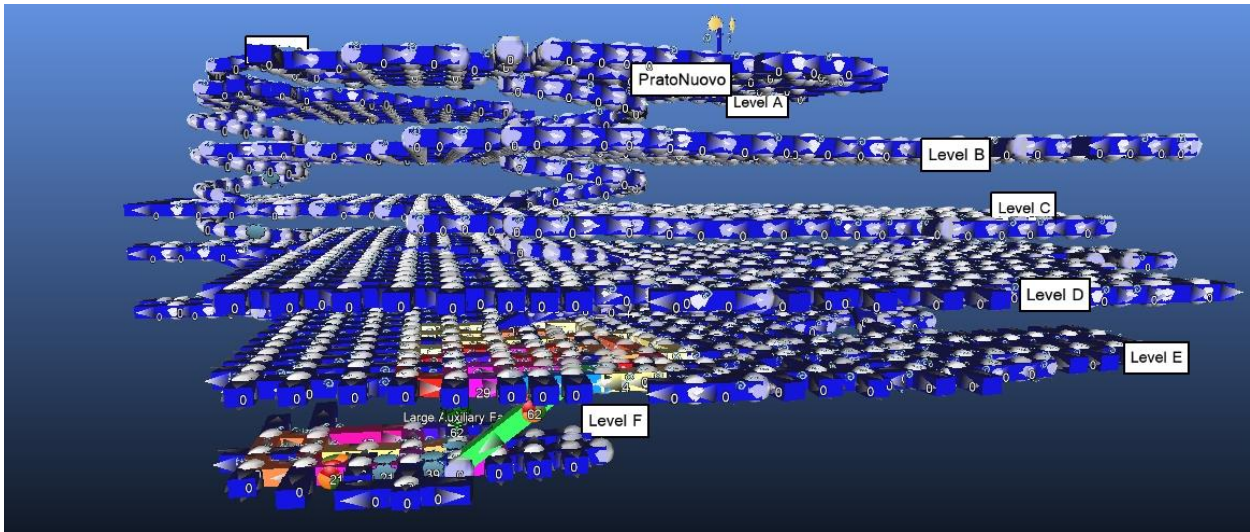
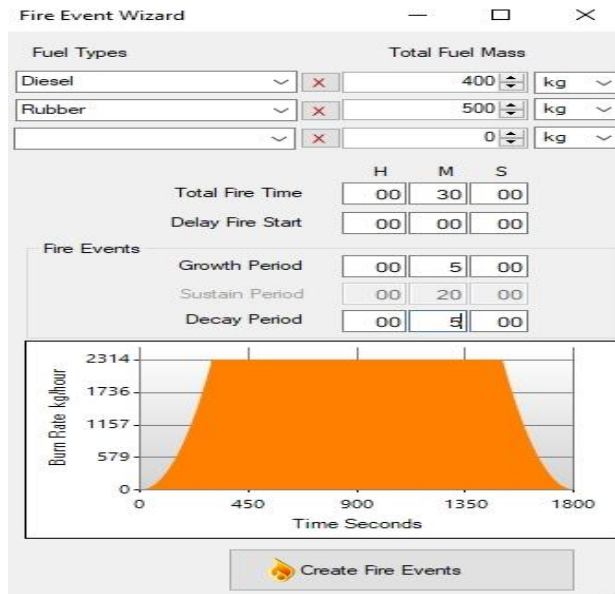


Figure 7.27: The most important recirculation of the air inside a large portion of the level D, E, and F in the current situation of the mine.

From figure 7.27, we can see that a large amount of recirculation of air through levels E and F. It is important for us because level F is the current working area and it means that the contaminants and dusts will circulate in this area of current situation of the mine and it needs an immediate measure.

For the fire we simulated the worst scenario that could happen in this mine. I assumed 500 liters of diesel and 500 kg of rubbers of the tires of the truck or loader. Then I assumed the density of diesel approximately  $8.0 \text{ Kg/m}^3$  so the amount of diesel would be 400 kg. It's also important to note that I assumed 30 minutes of fire with 5 minutes of growing of the fire, 20 minutes of the sustaining, and 5 minutes of decaying of the fire. The following data show these amounts were put in the Ventsim software:



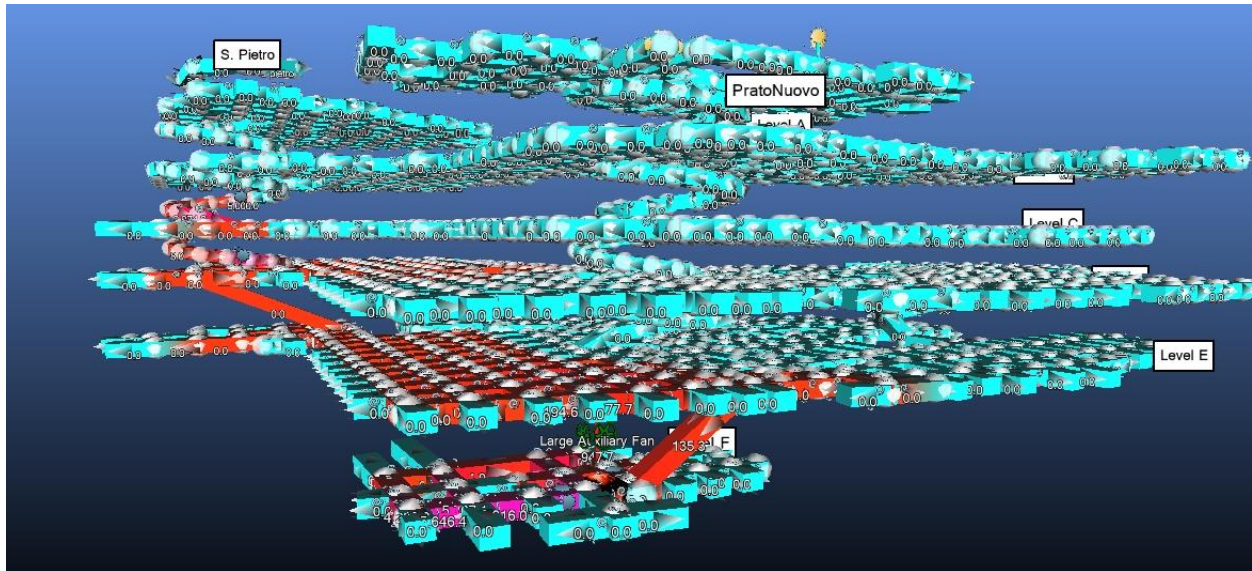


Figure 7.28: The dispersion of CO throughout the mine after 15 minutes of fire of a loader in level F and 5 machines produce contaminations are also present. It is also interesting to note that in this situation the direction of the flow in San Pietro ramp will change. It means that after we have a fire in the level F, most of the air will flow out of the mine through San Pietro.

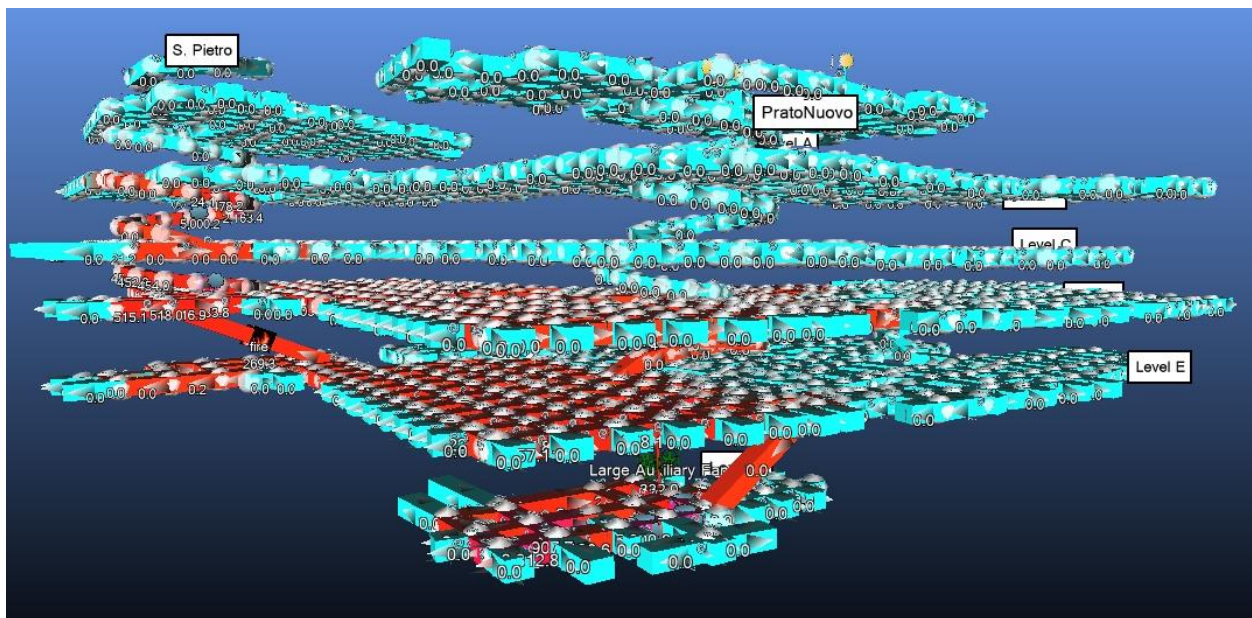


Figure 7.29: The dispersion of CO throughout the mine after 15 minutes of fire of a truck in the San Pietro ramp between levels D-E and 5 machines produce contaminations are also present. It is also interesting to note that in this situation the direction of the flow in San Pietro ramp and Prato Nuovo ramp will change.

It means that after we have a fire in the end of San Pietro ramp, the air will enter the mine from Prato Nuovo ramp and will flow out through San Pietro ramp.

After I found out why the unhealthy air cannot flow out of the mine with these interesting reasons, I tried to put more and larger fans in order to design a good ventilation system then the following fascinating results come out.

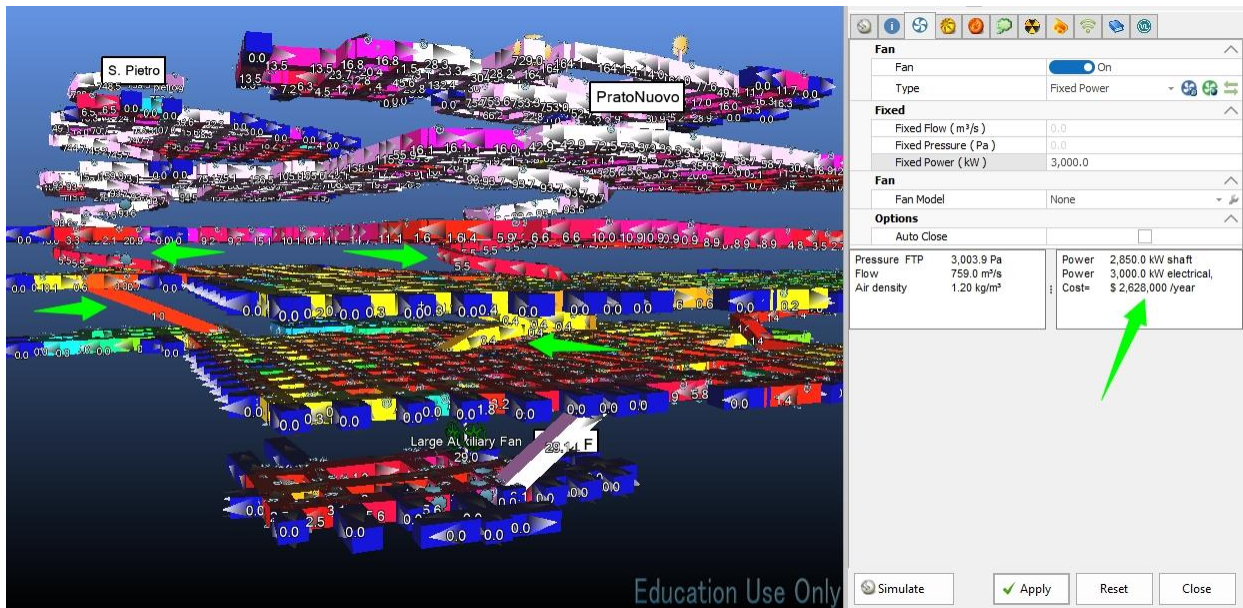


Figure 7.30: Putting a giant 3000 KW fan in the entrance of the San Pietro ramp. (Follow the green arrows)

In figure 7.30, it's shown that even with a giant 3000 KW fan with approximately 2 million Euros cost per year (which could not be available on the market at present but we can simulate it), we cannot solve the problem of the ventilation system of the Murisengo mine. The exact solution will be discussed in the next chapter.

## Chapter 8

### Proposals to improve the ventilation system in the mine

#### 8.1 First solution:

We blocked the airways around the ramps in Levels B, C, and D so the air cannot flow in other airways and pressure loss due to large number of airways will be reduced significantly. In the following pictures and paragraphs, we can see the results of this solution:

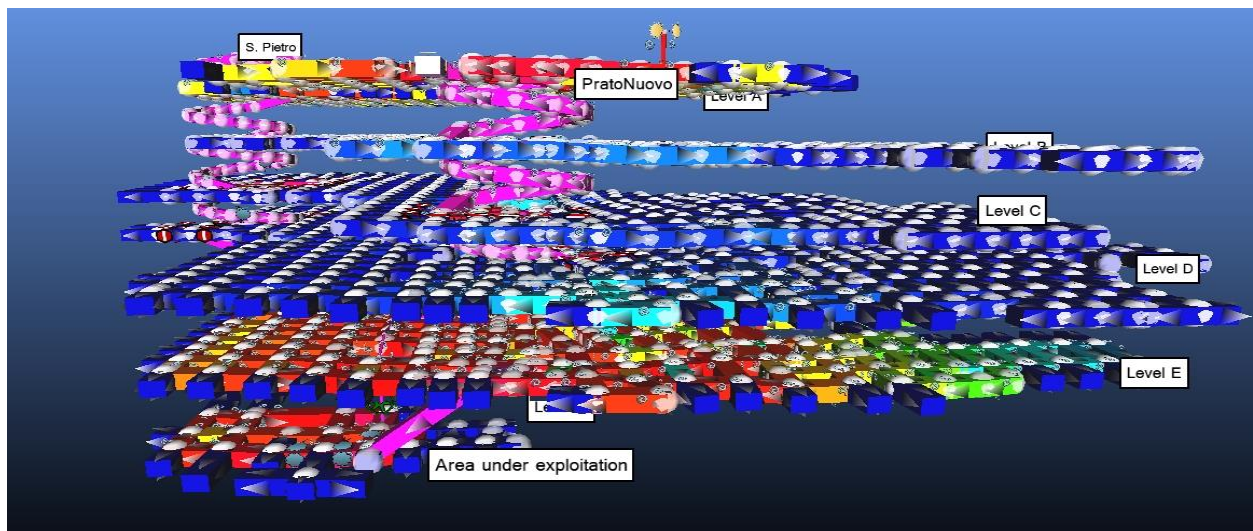


Figure 8.1: Front view 1st angle simulation of A, B, C, E, D, and F floors of the first solution for Murisengo Mine.

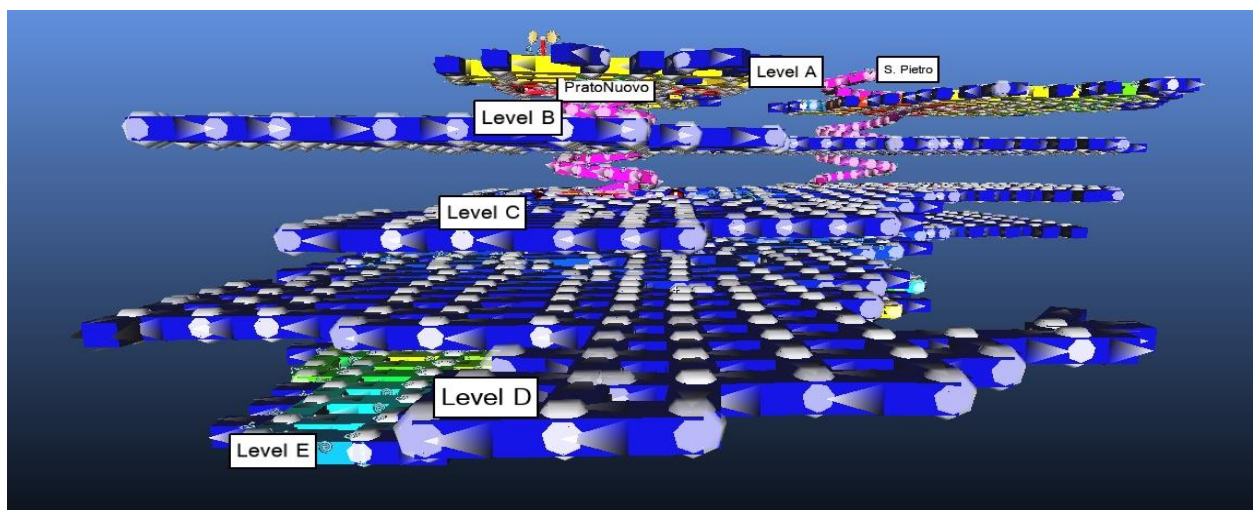


Figure 8.2: Front view 2nd angle simulation of A, B, C, E, D, and F floors of the first solution for Murisengo Mine.

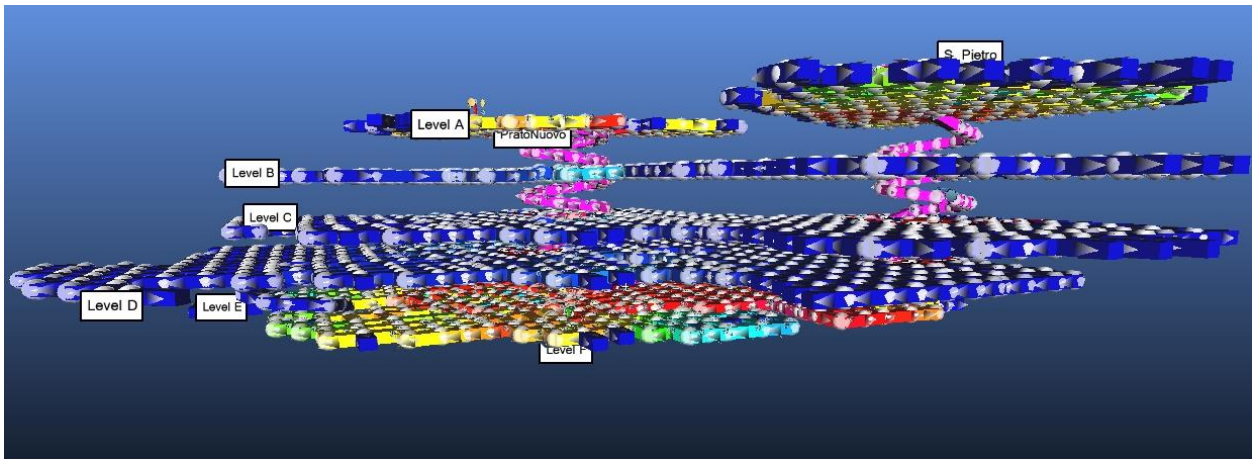


Figure 8.3: Front view 3rd angle simulation of A, B, C, E, D, and F floors of the first solution for Murisengo Mine.

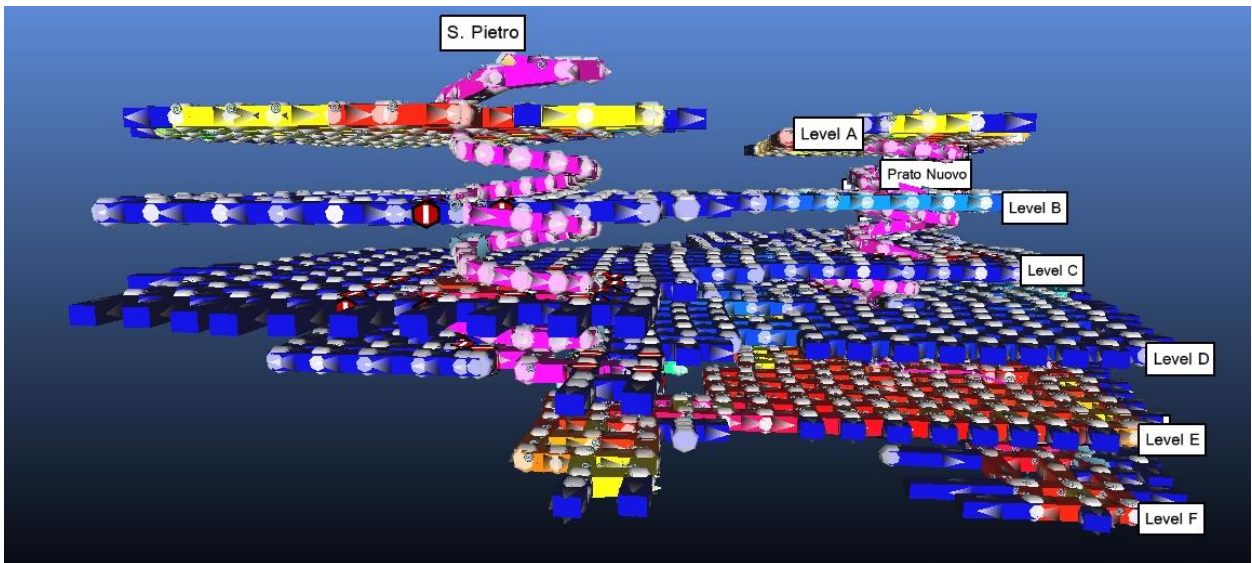


Figure 8.4: Front view 4th angle simulation of A, B, C, E, D, and F floors of the first solution for Murisengo Mine.

It's also important to note that I put exactly the same fan and other characteristics of the mine such as shock loss, ... of the current situation of the mine into the solution's simulation. Also, we used a duct that connects the exit of the shaft between levels E and F to the middle of the Prato Nuovo ramp between levels D and E.

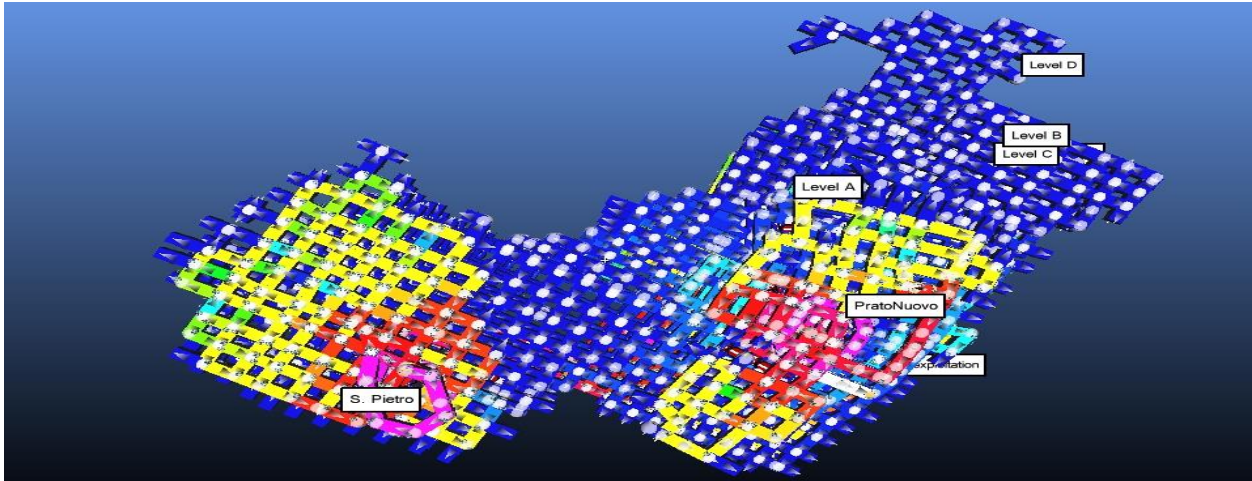


Figure 8.5: Top view simulation of A, B, C, E, D, and F floors of the first solution Murisengo Mine.

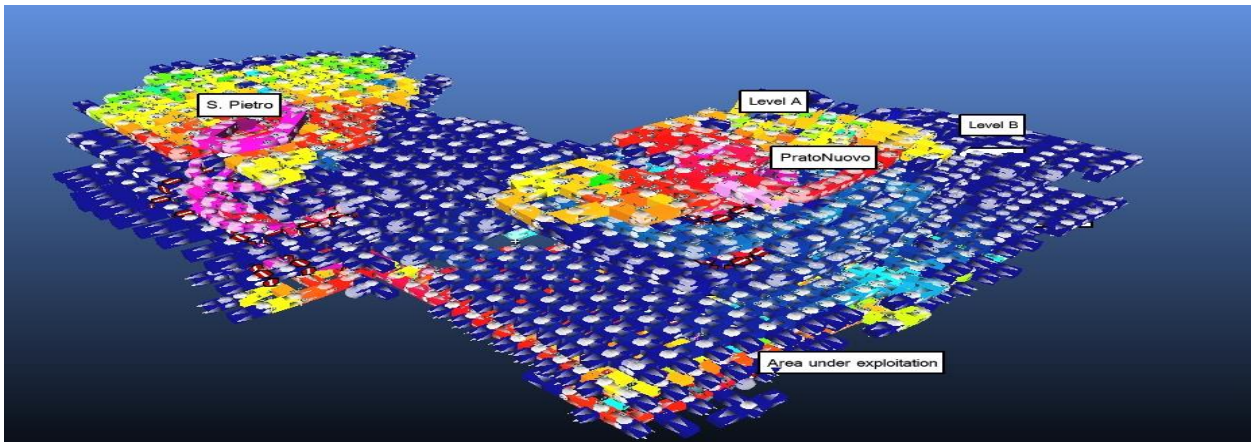


Figure 8.6: Top view simulation of A, B, C, E, D, and F floors of the first solution for Murisengo Mine.

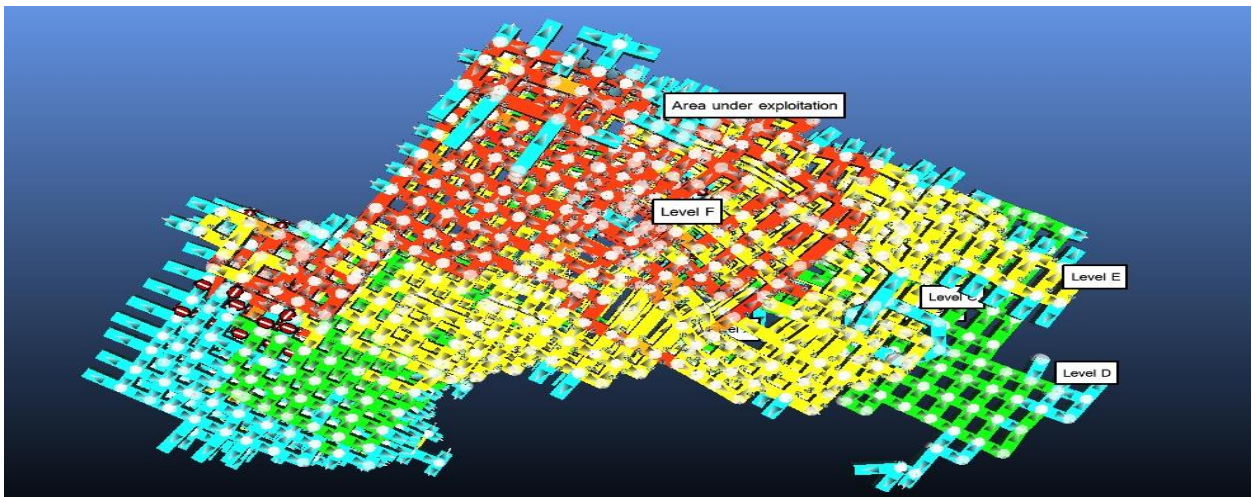


Figure 8.7: Bottom view simulation of A, B, C, D, E, and F floors of the first solution for Murisengo Mine.

Similarly, to the data of the contaminations of the 5 machines in the chapter 7, I put the contaminants inside the first and second solution simulations in order to see what will happen after dissemination of contaminants and after drill and blast.

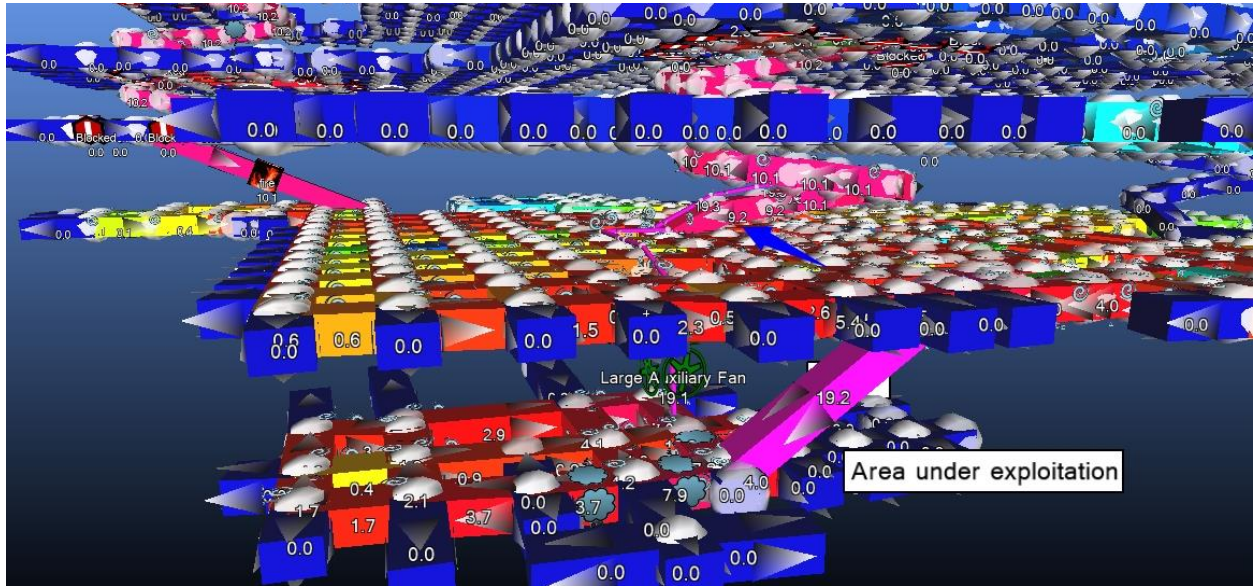


Figure 8.8: There is a recirculation of airflow in the entrance of Prato Nuovo ramp between levels D-E.

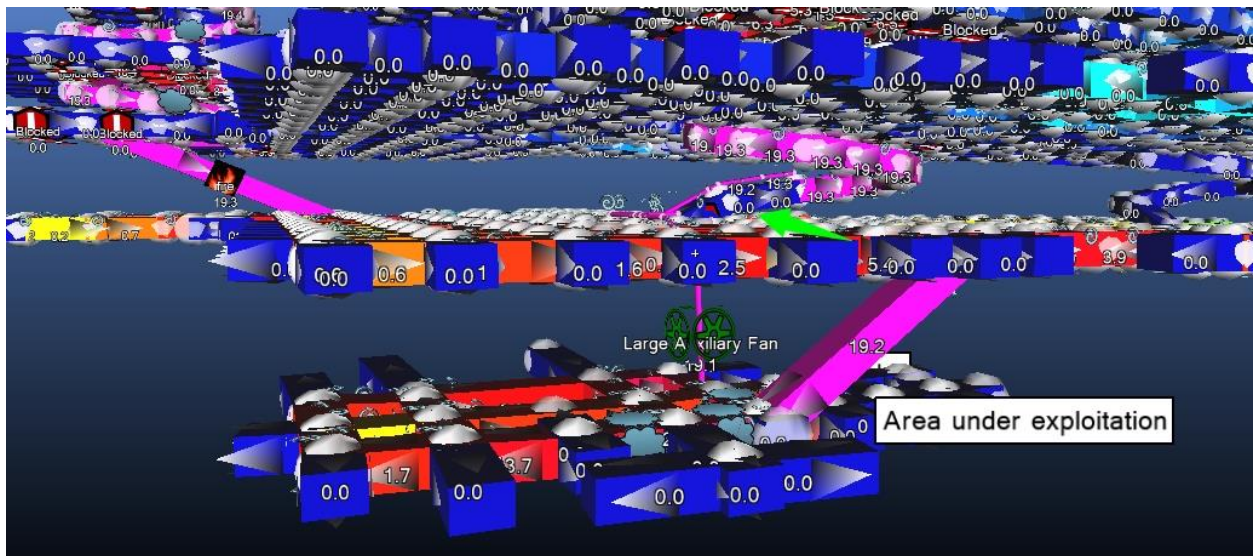


Figure 8.9: The block (door) at the entrance of Prato Nuovo ramp between levels D-E.



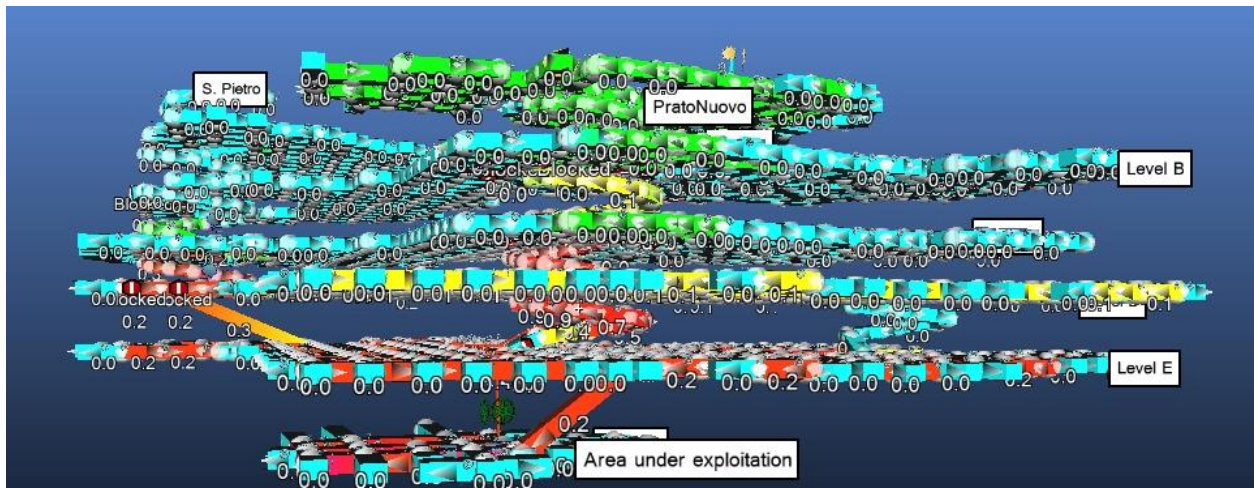


Figure 8.12: The distribution of  $CO_2$  (%) after 15 minutes of starting of machines.

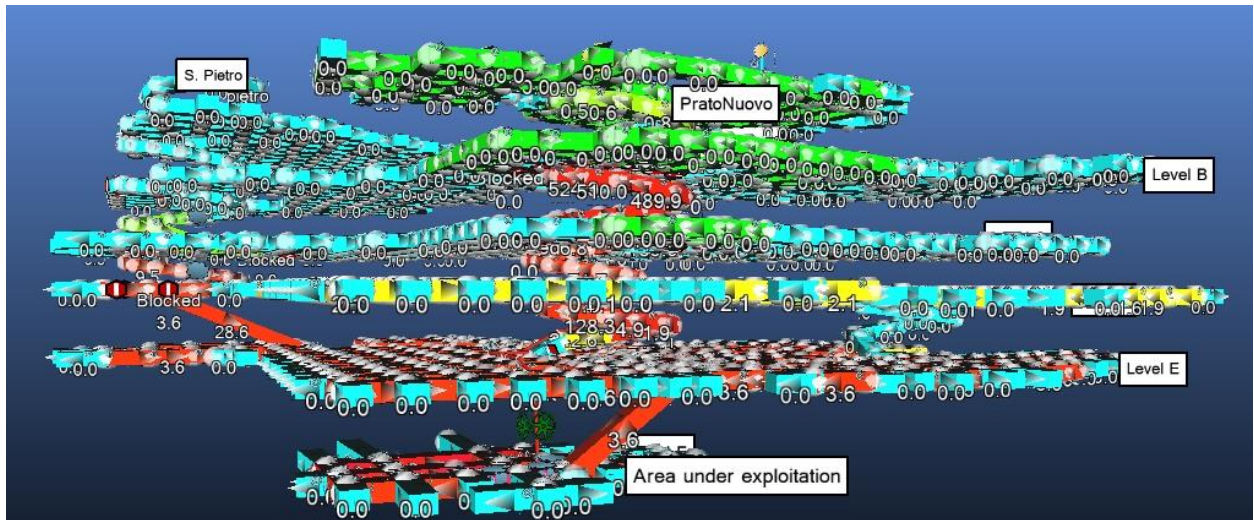


Figure 8.13: The distribution of CO (ppm) after 30 minutes of starting of machines.

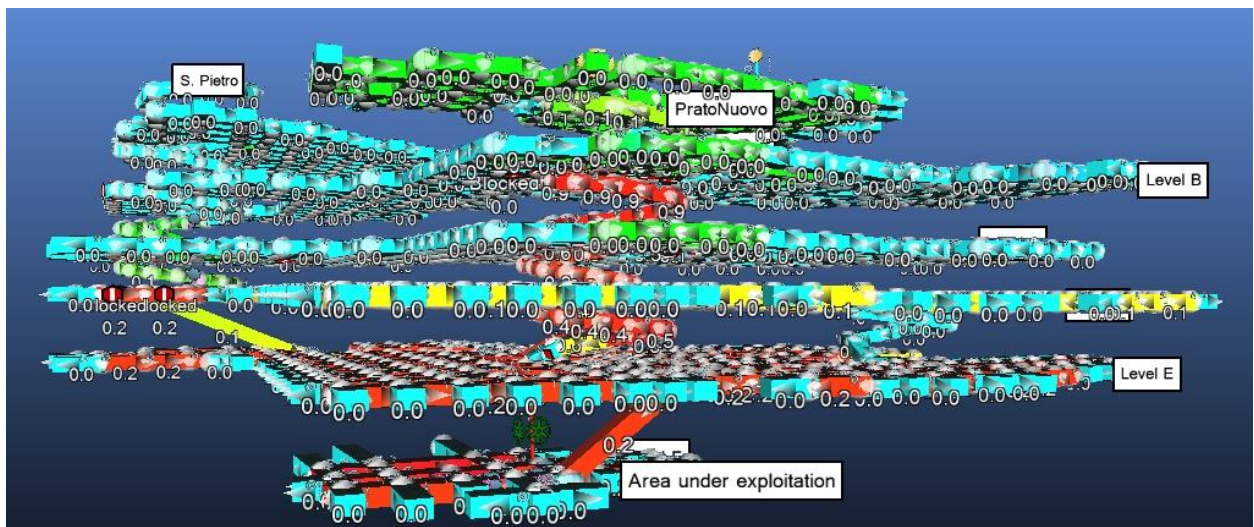
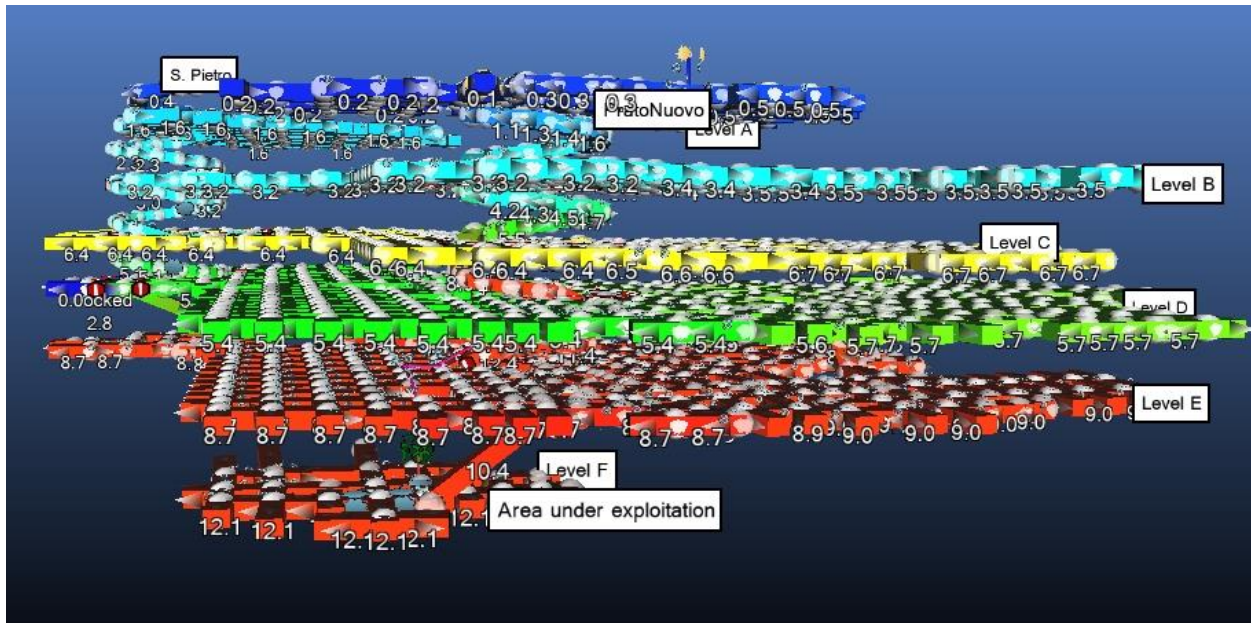
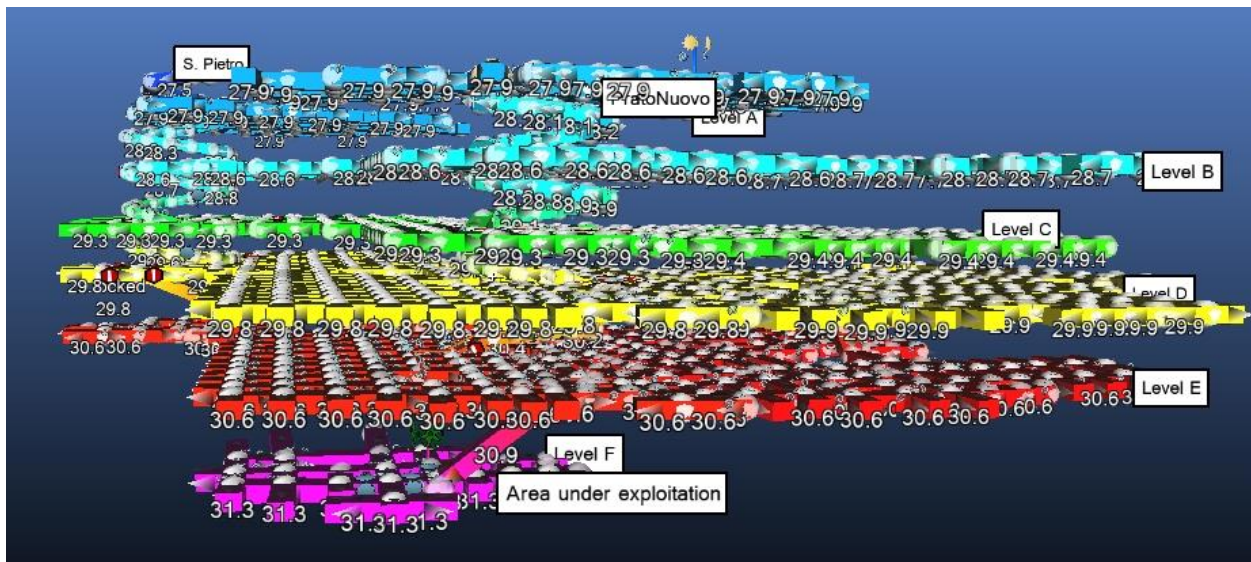


Figure 8.14: The distribution of  $CO_2$  (%) after 30 minutes of starting of machines.

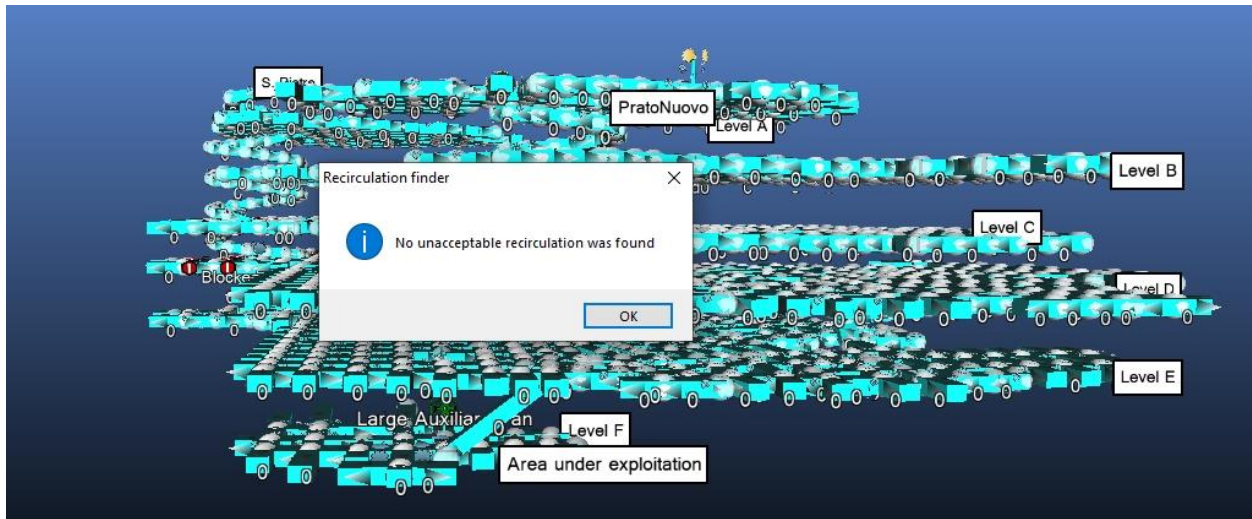


8.15: The amounts of pressures inside different levels of the mine in the simple solution.



8.16: The amounts of temperatures inside the rocks of each level of the Murisengo mine after putting blocks.

In figures 8.15 and 8.16, we can observe the quantities of pressures and temperatures inside different levels and circuits of the mine. Based on these figures we don't have any unacceptable pressure and temperature in any airway of the mine in this solution.



8.17: There is no recirculation of the air inside the airways in the simple solution of the ventilation system for Murisengo mine.

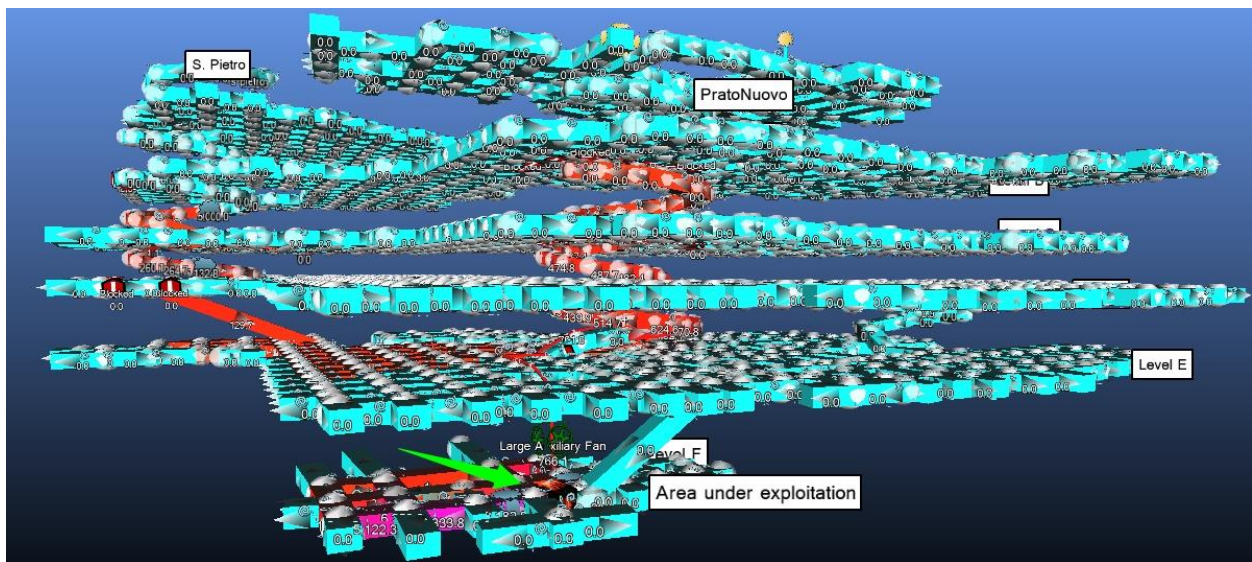


Figure 8.18: The dispersion of CO throughout the mine after 15 minutes of fire of a loader in level F and 5 machines produce contaminations are also present. It is also interesting to note that in this situation the direction of the flow in San Pietro ramp will change. It means that after we have a fire in the level F, most of the air will flow out of the mine through San Pietro.

It is obvious that in the figure 8.17 that there is not any recirculation of contaminated air in the mine after implementing this solution so this could be the final solution of the mine, however, I want to compare it with other solutions and improving it in order to reach the highest efficiency and best performance of the ventilation system.

It is also clear that the dispersion of the contaminants after fire in the mine is reasonable (figures 8.18 and 8.19), however, I want to write some instructions for the personnel after ignition of an event of fire and suggesting some ideas.

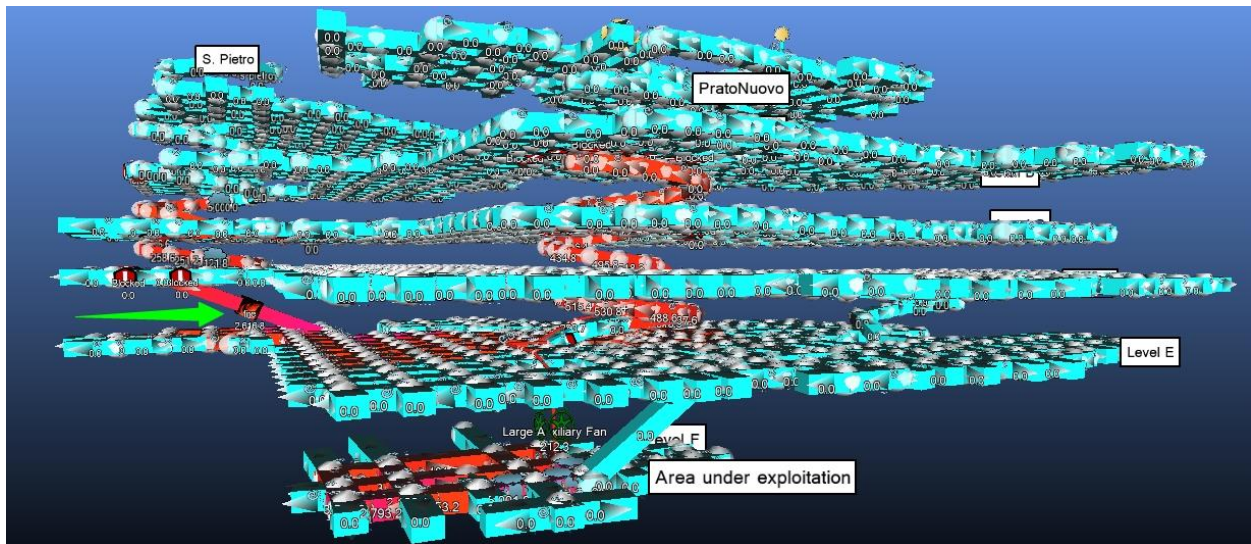


Figure 8.19: The dispersion of CO throughout the mine after 15 minutes of fire of a truck in the San Pietro ramp between levels D-E and 5 machines produce contaminations are also present. It is also interesting to note that in this situation the direction of the flow in San Pietro ramp and Prato Nuovo ramp will change. It means that after we have a fire in the end of San Pietro ramp, the air will enter the mine from Prato Nuovo ramp and will flow out through San Pietro ramp.

## 8.2 Second solution:

This solution has lower cost with lower efficiency but still it is reasonable and they can use it in the mine if they want to spend less and achieve less result.

In this solution we blocked the airways in the middle of the level B, C, and D, thus, the air could not flow to the Prato Nuovo ramp in the level B, C, and D.

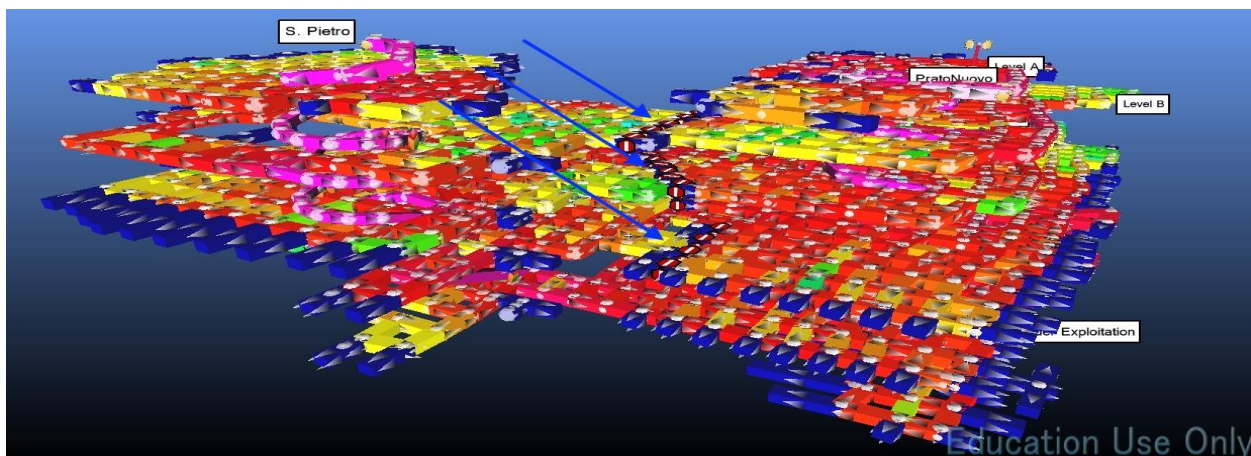


Figure 8.17: The blocks in the middle of level B, C, and D.

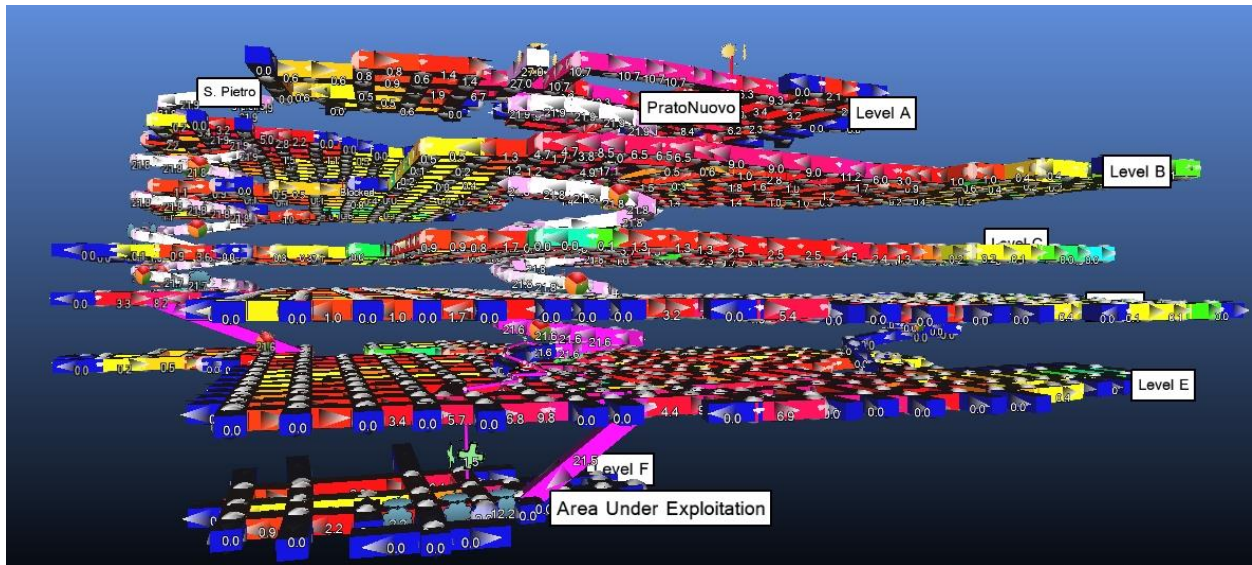


Figure 8.18: The amount of airflows inside different airways in the second solution.

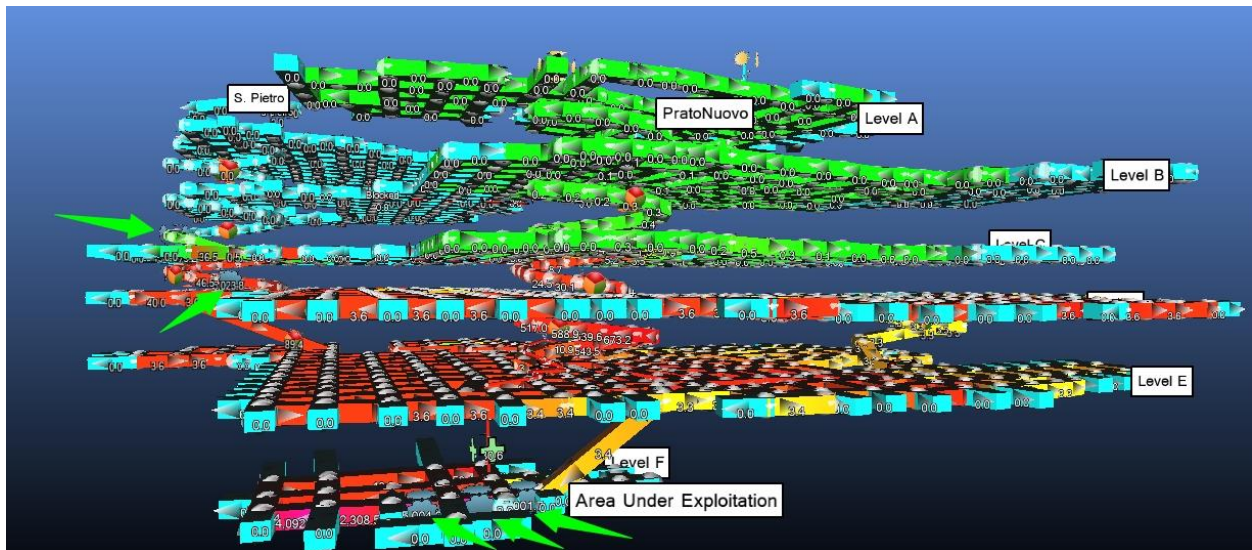


Figure 8.19: The dispersion of contaminations (co (ppm)) after 15 minutes from the start of 5 machines in the second solution. The red area is with highest contamination (CO), then the yellow area, and green and blue areas are with lowest amounts of contaminations.

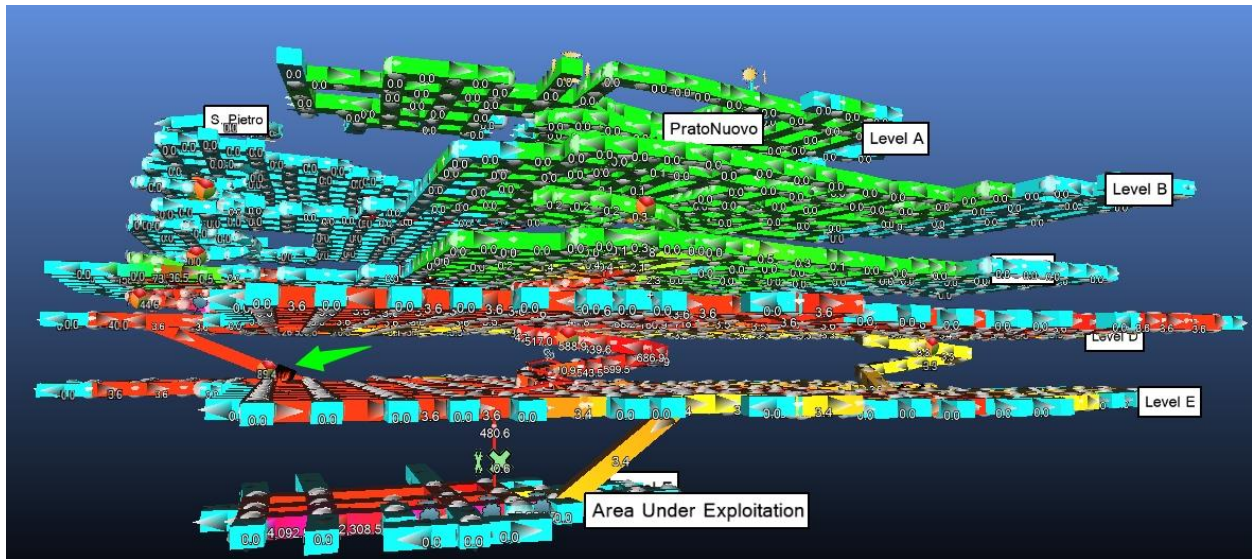


Figure 8.20: The dispersion of CO in the second solution of the mine after 15 minutes from the start of fire of a truck in the inclined ramp between level D-E. The red area is with highest contamination (CO), then the yellow area, and green and blue areas are with lowest amounts of contaminations.

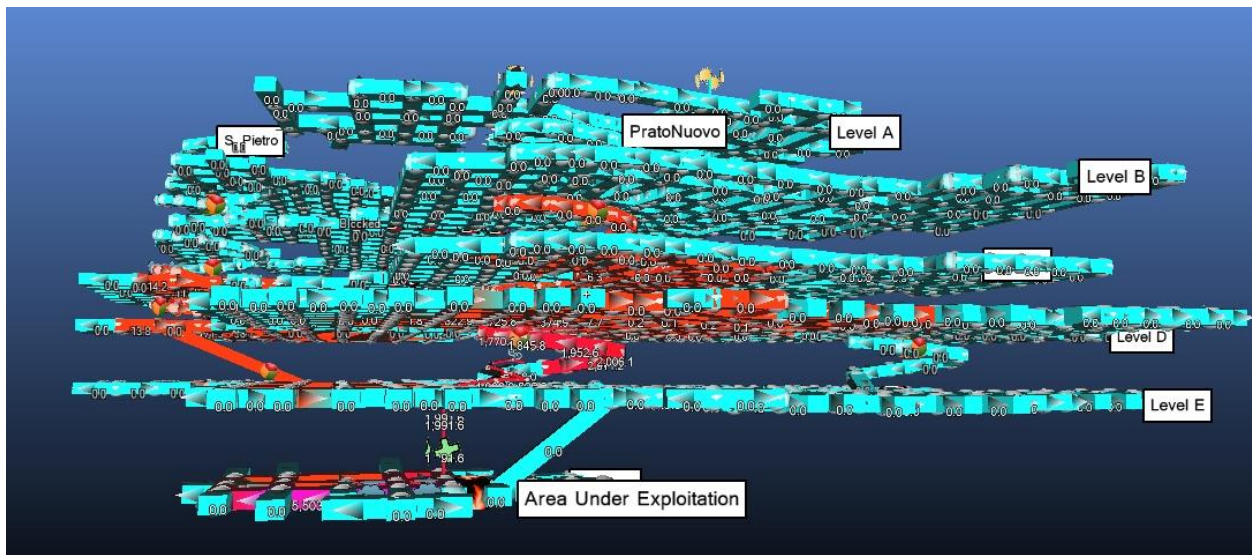


Figure 8.21: The dispersion of CO in the second solution of the mine after 15 minutes from the start of fire of a loader in level F. The red area is with highest contamination (CO), then the yellow area, and green and blue areas are with lowest amounts of contaminations.



According to the results of the figures 8.17 to 8.21, this new solution for ventilation system of the mine could work, but it's not as efficient as the first solution (comparing figures 8.17 to 8.21 with the figures 8.10 to 8.19) and the second solution would be less expensive. It's also important to notice that in this case we have 12 recirculations of contaminated air inside the mine so the first solution is the best scenario.

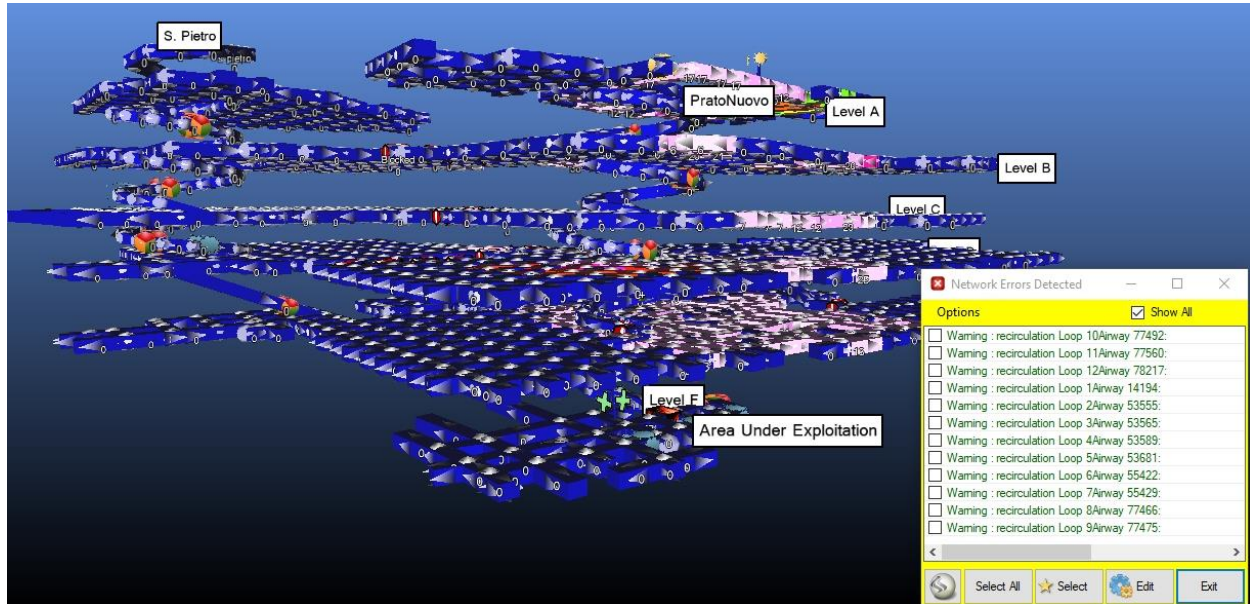


Figure 8.24: The recirculation inside second solution of the ventilation system.

### 8.3 Future works:

The company of Estrazione Gesso has decided to build a new inclined ramp between levels E and F and the construction will be finished in few months so I simulated this new ramp in order to see what will be the new conditions of the ventilation system as following figures and paragraphs:

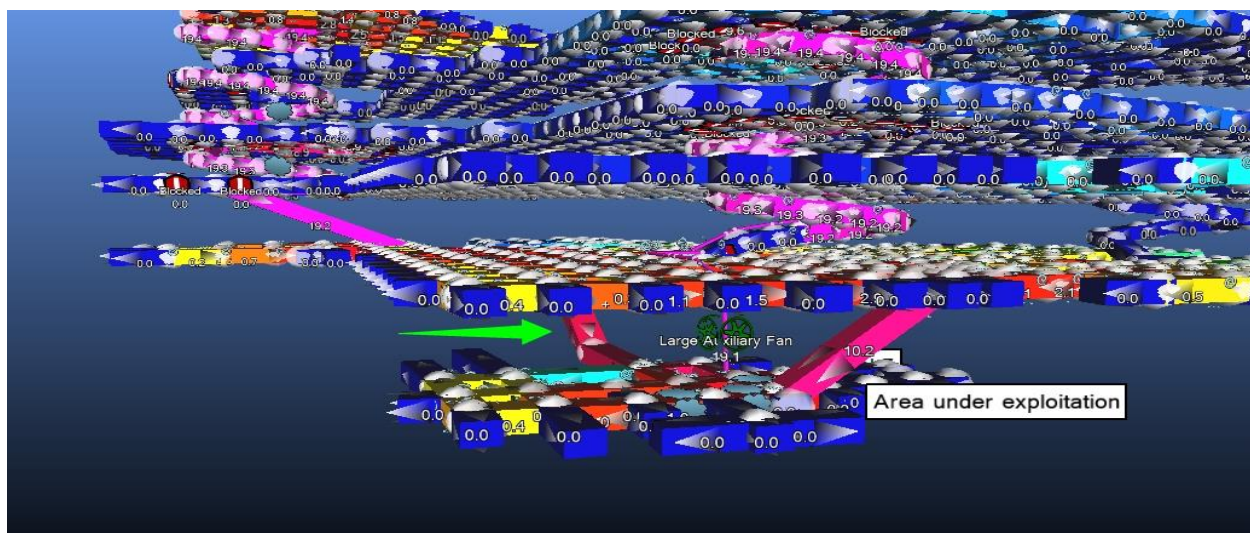


Figure 8.25: New ramp at the left side of Level F.

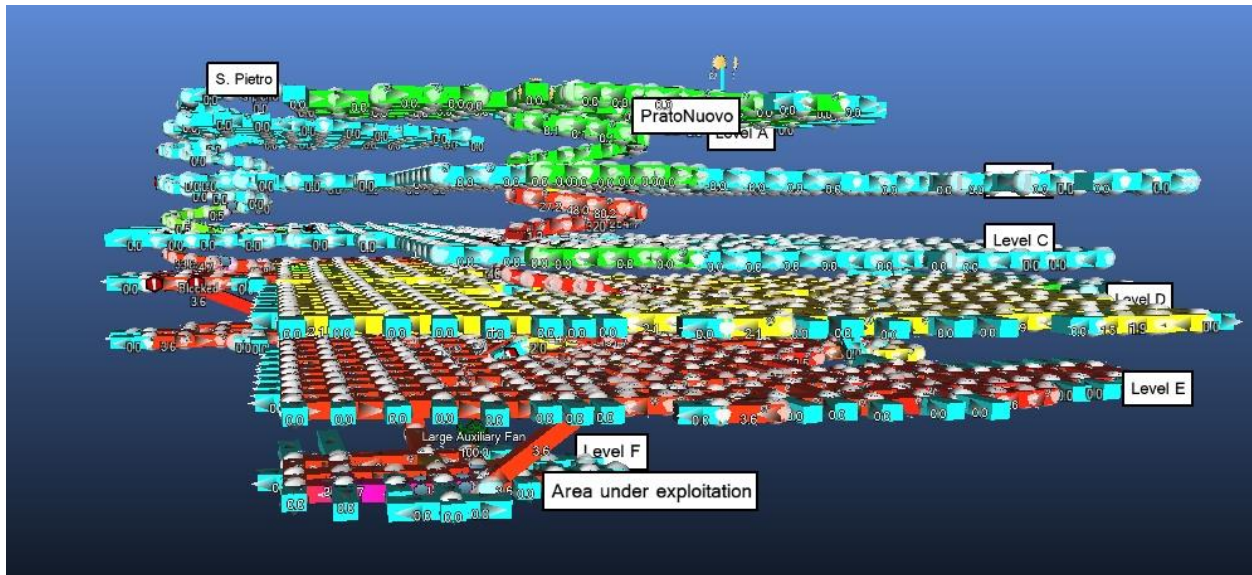


Figure 8.26: The spread of contaminations (CO (ppm)) after 15 minutes from the starting of the machines' working.

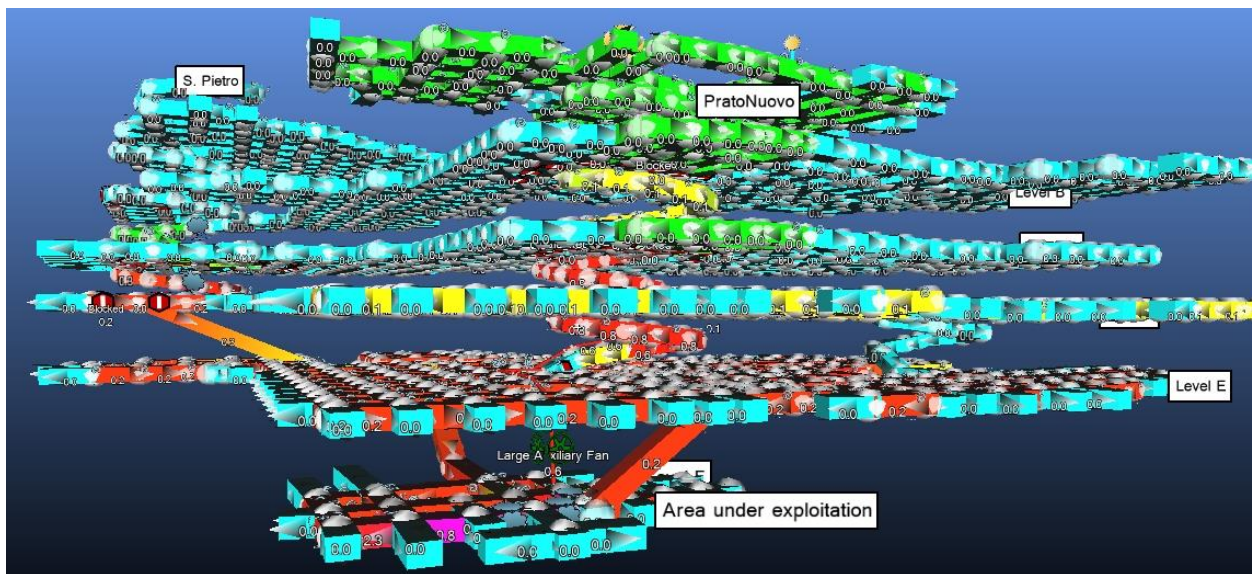


Figure 8.27: The spread of contaminations (CO<sub>2</sub> (%)) after 15 minutes from the starting of the machines' working.

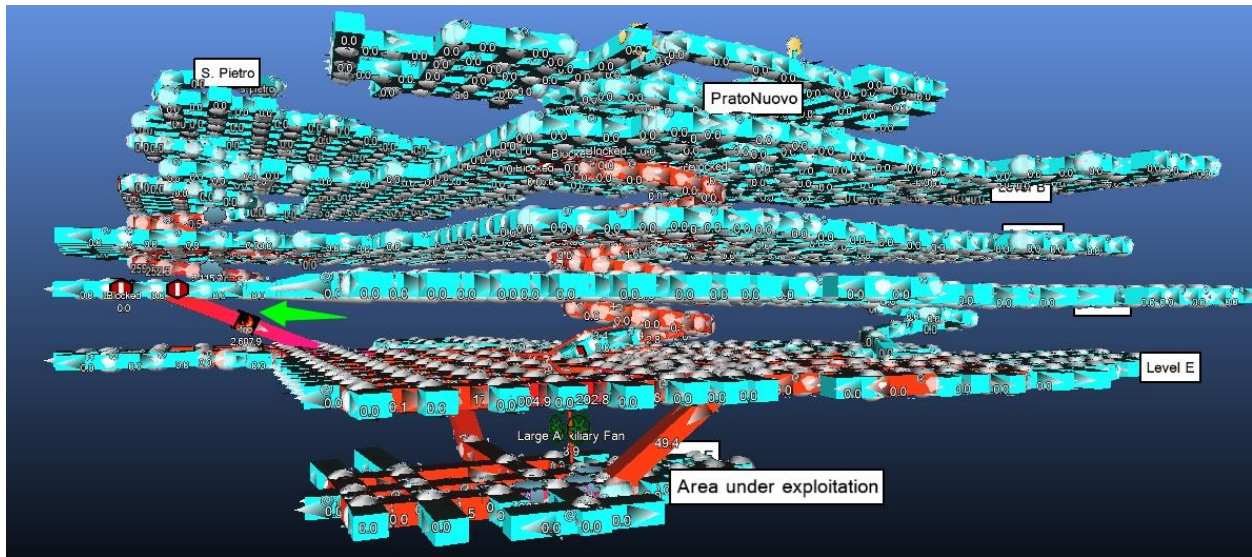


Figure 8.28: The dispersion of CO (ppm) in the second solution of the mine after 15 minutes from the start of fire of a truck in the inclined ramp between level D-E. The red area is with highest contamination (CO), then the yellow area, and green and blue areas are with lowest amounts of contaminations.

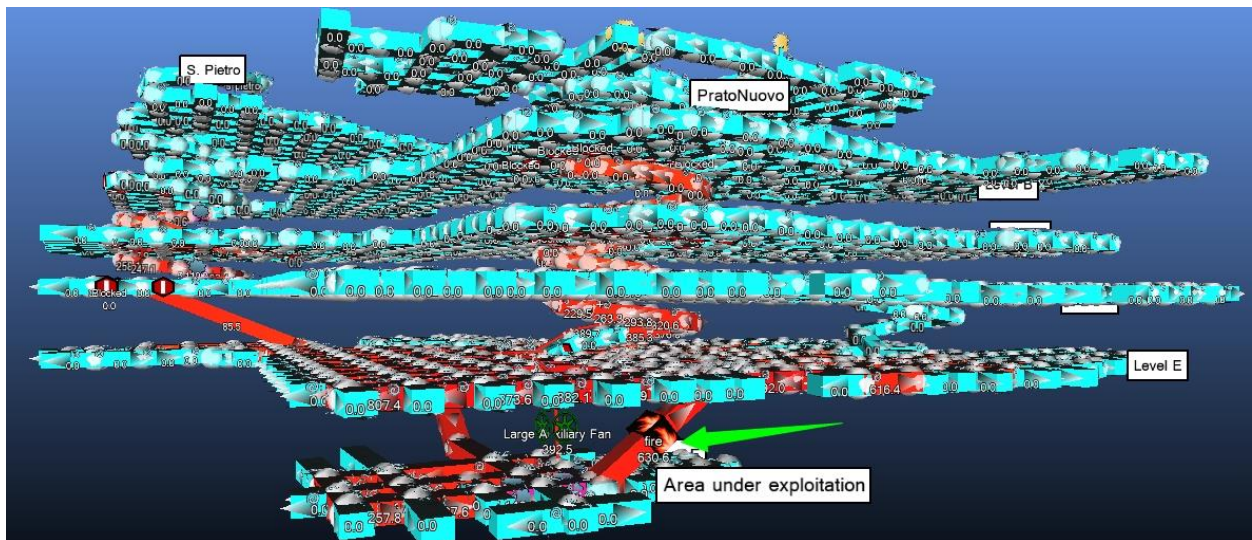


Figure 8.29: The dispersion of CO (ppm) in the second solution of the mine after 15 minutes from the start of fire of a loader in the entrance of the current ramp in level F. The red area is with highest contamination (CO), then the yellow area, and green and blue areas are with lowest amounts of contaminations.

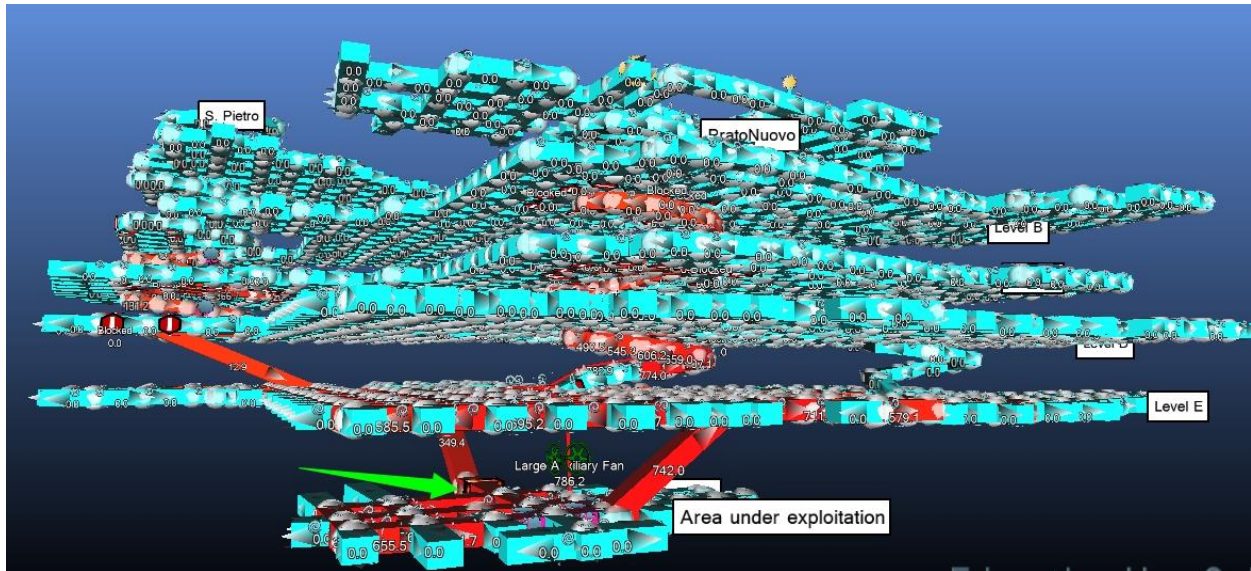


Figure 8.30: The dispersion of CO (ppm) in the second solution of the mine after 15 minutes from the start of fire of a loader in the entrance of the future ramp in level F. The red area is with highest contamination (CO), then the yellow area, and green and blue areas are with lowest amounts of contaminations.

It seems that the construction of the second ramp (Figure 8.26) is not a good idea because it helps the recirculation of the unhealthy air through the read area of level E and F and I suggest to put a door in the entrance of one of the ramps between levels E and F and use it just for emergency situations (fire, explosion, ...).

#### 8.4 Final improvement of the ventilation system:

We can add two booster fans in order to achieve the highest airflow through present circuits of the mine as the following figures:



Figure 8.31: The amount of airflows inside different airways in the final solution.

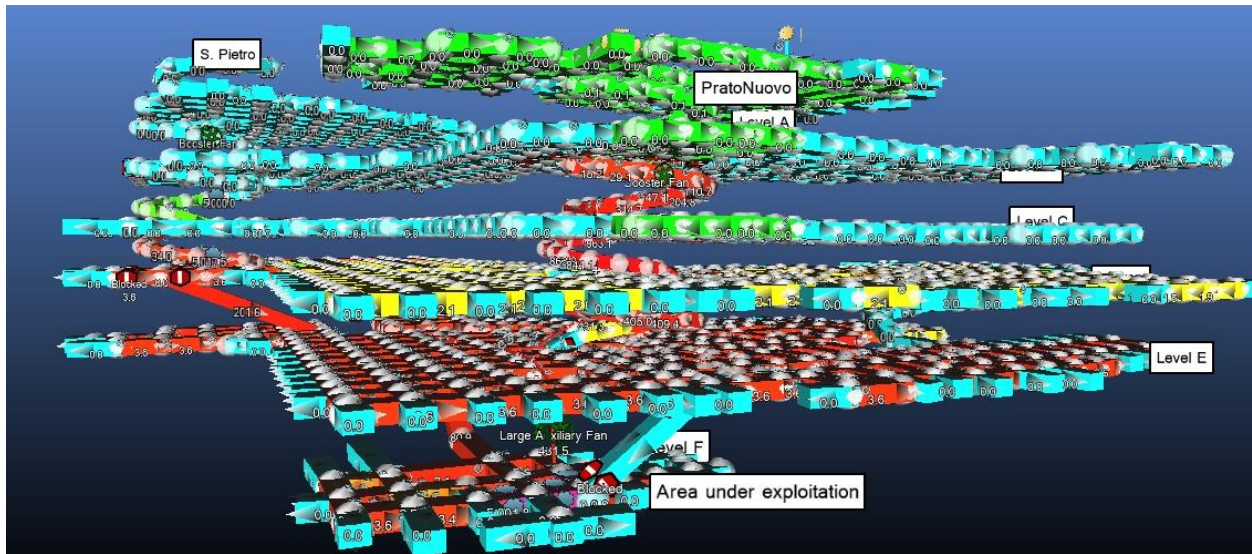


Figure 8.32: The spread of contaminations (CO (ppm)) after 15 minutes from the starting of the machines' working.

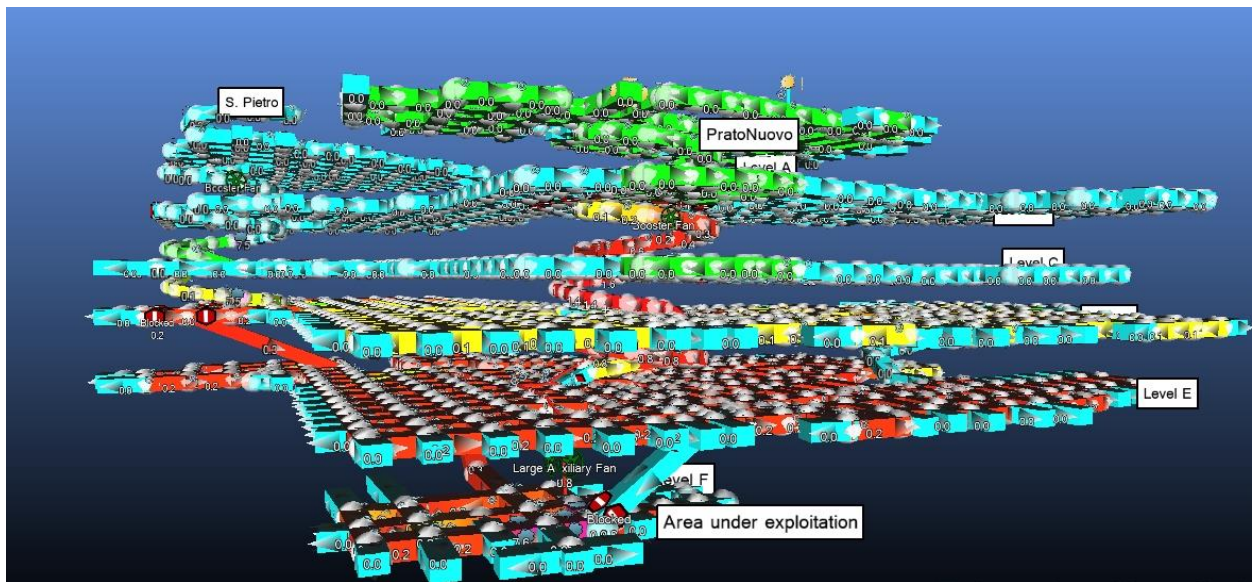


Figure 8.33: The spread of contaminations ( $CO_2$  (%)) after 15 minutes from the starting of the machines' working.

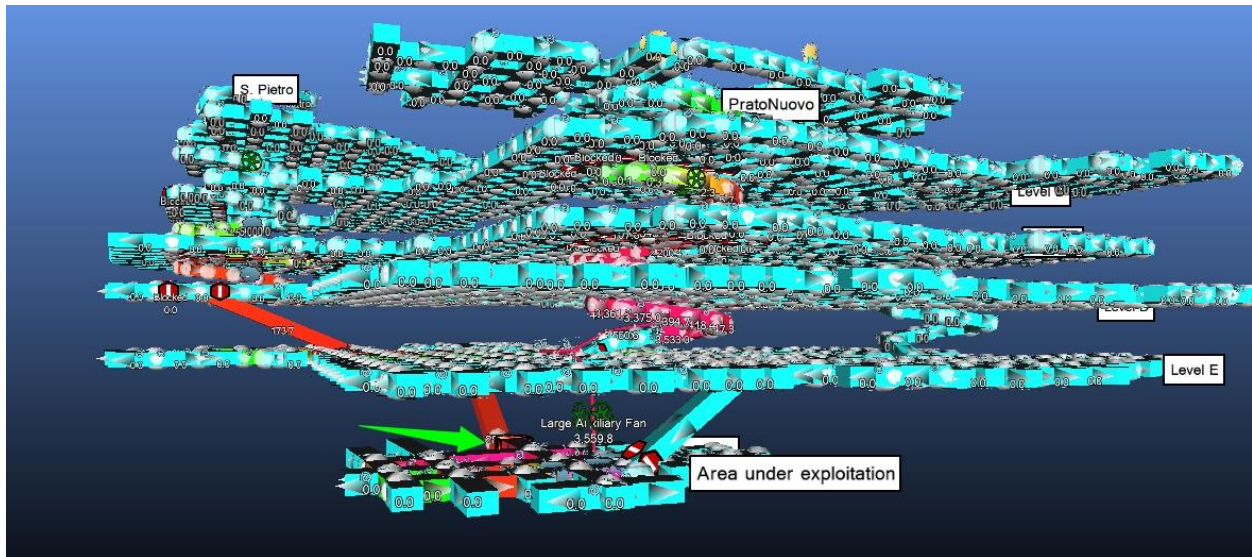


Figure 8.34: The dispersion of CO (ppm) in the final solution of the mine after 15 minutes from the start of fire of a loader in the entrance of the future ramp in level F. The red area is with highest contamination (CO), then the yellow area, and green and blue areas are with lowest amounts of contaminations.

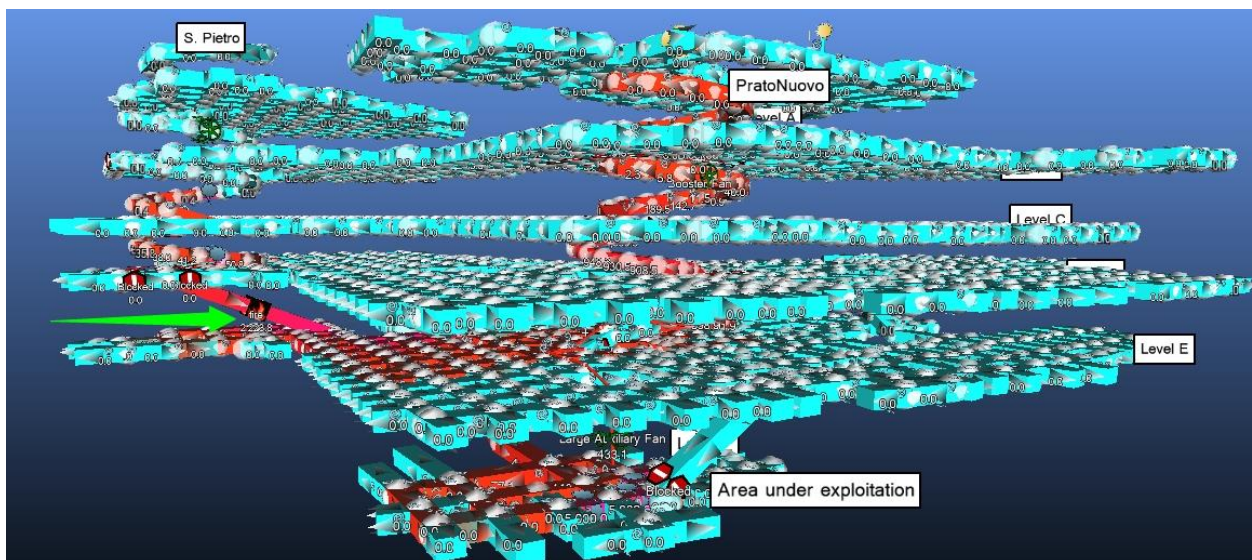


Figure 8.35: The dispersion of CO (ppm) in the final solution of the mine after 15 minutes from the start of fire of a truck in the inclined ramp between level D-E. The red area is with highest contamination (CO), then the yellow area, and green and blue areas are with lowest amounts of contaminations.

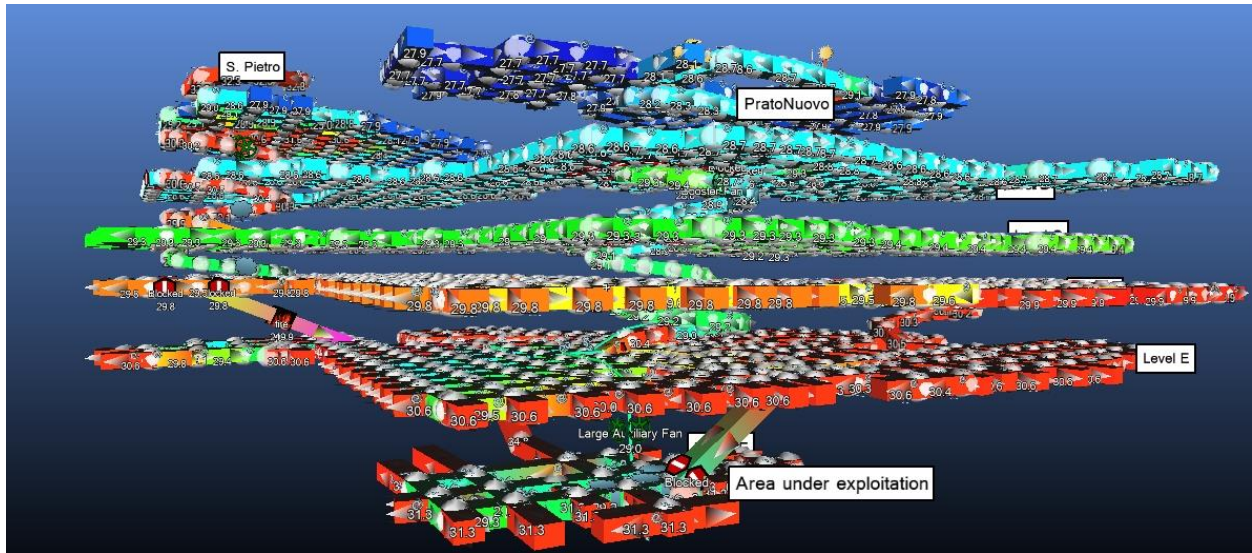


Figure 8.36: The dispersion of heat of temperature dry bulb ( $^{\circ}\text{C}$ ) in the final solution of the mine after 15 minutes from the start of fire of a truck in the inclined ramp between level D-E. The red area is with highest temperature ( $^{\circ}\text{C}$ ), then the yellow area, and green and blue areas are with lowest amounts of contaminations.

Finally, we can see from the results of figures 8.31 to 8.36 that adding two booster fans inside two ramps of the mine will work well and there is only the risk of not working of the fan in the shaft between levels E and F. If that will occur, then we need to change this fan because we do not want to reduce the efficiency of the whole ventilation system of the mine only because of a fan.

## Chapter 9

### Conclusions

For simulation of the underground mine tunnels, I used Ventsim Design 5.4 in order to know better what happens in each airway or tunnel of the mine. As I said before, currently only level F (fig 7.6) is under extraction, however, I simulated all 6 floors (A, B, C, D, E, F) with Ventsim software in order to know what happens to air when entering the mine until reaching level F then I have found out a very simple and interesting result. There was huge pressure loss due to many linked airways so there was very low ventilation in the lower levels (C, D, E, and F) and only one fan exists in the shaft between levels E and F in order to move the unhealthy air from some airways to another airways in level E and F and it was like a recirculation of contaminated air between level E and level F and most of the healthy air enters the mine from level A then streams to level B and flows out through the other ramp of the level B. It's important to note that most of the healthy air does not even reach level C so a ventilation system would be necessary in order to direct the air from surface to level F and then force it out to the surface again. first result would be the resistance due to number of airways are too much in room and pillars mining method.

Then I put the contaminants of 3 sources of contaminations of 3 machines inside level F, a pick-up car inside the San Pietro ramp between levels C-D, and contaminations of a truck inside the San Pietro ramp between levels B-C then we can compare the results with the on-site measured data on the previous tables above. An important thing would be the amount of contaminations produced by each machine are considered based on real contaminations produced by a diesel engine per KW and also the composition of the air of the exhaust of diesel engine as discussed previously in chapter 7.

There is a 30 KW fan inside the shaft between levels E and F and for that I simulated a large auxiliary fan with 86% of efficiency with efficiency of 68.7% and curve 1 of the Ventsim software in order to simulate the most similar fan to the fan existing in the shaft of the levels E and F. Another very important consideration is that I assumed that there is auto low shock loss due to the connections of the airways and irregularities of walls of the tunnels in every airway and tunnel to simulate as similar as possible the current characteristics of the mine.

There are two important problems in the ventilation system of the Murisengo mine. It's obvious from figure 7.16 to figure 7.21 that in the current situation of the mine the distributions of the contaminants were very slow and mostly through airways of level F, E, and D. In figure 7.16, we can see that after 15 minutes from the working of the machines, most of the contaminants produced in level F reach only level E then the contaminants flew via ramp San Pietro to level D and after 30 minutes (figure 7.18) they disseminated in a small portion of airways of level D and after 8 hours (figure 7.20) they streamed the ramp Prato Nuovo in order to reach level C. It's important to note that during long time of recirculation lots of the contaminants such as dust, and some harmful gases will settle down on the ground and will disseminate through the air in the case of moving of a truck, ... . Thus, an optimized ventilation system which could direct healthy air into the lowest levels of the mine and force the unhealthy air out of the mine to the surface would be necessary in order to guarantee the health of the miners in

long term and also for safety reasons. It's observable in our simple solution (figures 8.9 and 8.11) in the chapter 8 that contaminants will reach more quickly to the surface and it's beneficial both reducing the concentrations of contaminants in the lower levels and no letting the contaminants settle down on the ground.

There are five important recirculation of the air inside the mine as discussed in chapter 7 hence, this is another reason that we need block some airways in order to force the air that come from smaller number of airways and going out.

From figure 7.27, we can see that a large amount of recirculation of air through levels E and F. It is important for us because level F is the current working area and it means that the contaminants and dusts will circulate in this area of current situation of the mine and it needs an immediate measure.

For the fire we simulated the worst scenario that could happen in this mine. I assumed 500 liters of diesel and 500 kg of rubbers of the tires of the truck or loader. Then I assumed the density of diesel approximately  $8.0 \text{ Kg/m}^3$  so the amount of diesel would be 400 kg. It's also important to note that I assumed 30 minutes of fire with 5 minutes of growing of the fire, 20 minutes of the sustaining, and 5 minutes of decaying of the fire as discussed before in chapter 7.

It is also interesting to note that in this situation the direction of the flow in San Pietro ramp and Prato Nuovo ramp will change. It means that after we have a fire in the end of San Pietro ramp, the air will enter the mine from Prato Nuovo ramp and will flow out through San Pietro ramp.

In figure 7.30, it's shown that even with a giant 3000 KW fan with approximately 2 million Euros cost per year (which could not be available on the market at present but we can simulate it), we cannot solve the problem of the ventilation system of the Murisengo mine.

In the first solution I blocked the airways around the ramps in Levels B, C, and D so the air cannot flow in other airways and pressure loss due to large number of airways will be reduced significantly.

Similarly, to the data of the contaminations of the 5 machines in the chapter 7, I put the contaminants inside the first and second solution simulations in order to see what will happen after dissemination of contaminants and after drill and blast.

Then the results of spreading of the contaminations ( $\text{CO}$  (ppm),  $\text{CO}_2$  (%)) are illustrated in the figures 8.11, 8.12, 8.13, 8.14.

In figures 8.15 and 8.16, we can observe the quantities of pressures and temperatures inside different levels and circuits of the mine. Based on these figures we don't have any unacceptable pressure and temperature in any airway of the mine in this solution.

It is obvious in the figure 8.17 that there is not any recirculation of contaminated air in the mine after implementing this solution so this could be the final solution of the mine, however, I wanted to compare it with second solution and improving it in order to reach the highest efficiency and best performance of the ventilation system.

In the second solution that has lower cost with lower efficiency but still it is reasonable and they can use it in the mine if they want to spend less and achieve less result.

In the second solution we blocked the airways in the middle of the level B, C, and D, thus, the air could not flow to the Prato Nuovo ramp in the level B, C, and D.

According to the results of the figures 8.17 to 8.21, this new solution for ventilation system of the mine could work, but it's not as efficient as the first solution (comparing figures 8.17 to 8.21 with the figures 8.10 to 8.19) and the second solution would be less expensive.

In the future works, the company of Estrazione Gesso has decided to build a new inclined ramp between levels E and F and the construction will be finished in few months so I simulated this new ramp in order to see what will be the new conditions of the ventilation system.

It seems that the construction of the second ramp (Figure 8.25) is not a good idea because it helps the recirculation of the unhealthy air through the read area of level E and F and I suggest to put a door in the entrance of one of the ramps between levels E and F and use it just for emergency situations (fire, explosion, ...).

Finally, we can see from the results of figures 8.31 to 8.36 that adding two booster fans inside two ramps of the mine will work well and there is only the risk of not working of the fan in the shaft between levels E and F. If that will occur, then we need to change this fan because we do not want to reduce the efficiency of the whole ventilation system of the mine only because of a fan.

Moreover, it's very important to note that I can add more details of the data (heats after fire in each section, graphs of the changing of the airflow after each fire, changing in amounts of oxygen after the fire in each section, monitoring of different airways after the fire, designing scenarios of different fire events in other sections of the mine, designing different scenarios of locations of three fans in different positions to compare the result in order to find the best places for locating fans, changing density of air to see what will happen in different worst scenarios, ... ), however, because there are already lots of pictures, details, and data, I decided not to do. In that case, the document will be extended more than 300 pages and it might not be a good idea and will be boring for the readers.

## References:

1. Patton, S., Best Practices in Effective Ventilation of Underground Coal Mines, U.S. Practices and Regulations, Workshop on Best Practices in Coal Mine Methane Capture and Utilization, Bogotá, Colombia, July 2018.
2. SME Mining Engineering Handbook, Michael A. Tuck, Associate Professor of Mining Engineering, University of Ballarat, Victoria, Australia.
3. Mine Ventilation Systems Practical Mine Ventilation Engineering, Chapter 9.
4. 11th U.S./North American Mine Ventilation Symposium, Mutmansky & Ramani (eds), © 2006 Taylor & Francis Group, London, ISBN 0-415-40148-8.
5. Air Contaminants, Ventilation, and Industrial Hygiene Economics, The Practitioner's Toolbox and Desktop Handbook, ROGER LEE WABEKE, © 2013 by Taylor & Francis Group, LLC.
6. BUOYANCY EFFECTS ON NATURAL VENTILATION, Torwong Chenvidyakarn, Cambridge University Press, © Torwong Chenvidyakarn 2013.
7. COAL MINE SAFETY, TERRANCE V. NEWHOUSE EDITOR, © 2009 by Nova Science Publishers, Inc.
8. Eighth International Mine Ventilation Congress, July 2005, Brisbane, Australia, Published by THE AUSTRALASIAN INSTITUTE OF MINING AND METALLURGY, © The Australasian Institute of Mining and Metallurgy 2005.
9. Fans & Ventilation, A Practical Guide, W T W (Bill) Cory, published 2005, © Roles & Associates Ltd, ISBN 0-08044626-4.
10. Handbook of Domestic Ventilation, Rodger Edwards, © 2005, Elsevier Ltd.
11. Handbook of Heating, Ventilation and Air Conditioning for Design and Implementation, ALI VEDAVARZ, SUNIL KUMAR, MUHAMMED IQBAL HUSSAIN, © 2007 by Industrial Press Inc., New York, NY.
12. Heating and Ventilation Air Conditioning, Richard Nicholls, 2001, ISBN 0-9539409-1-8.
13. Air Quality and Ventilation, Controlling Dust Emissions, Ivan Nikolayevich Logachev Konstantin, Ivanovich Logachev, © 2014 by Taylor & Francis Group, LLC, ISBN: 978-1-4822-2217-3.
14. Mine Ventilation, Euler De Souza, © 2002 Swets & Zeitlinger B.V., Lisse, The Netherlands, ISBN: 90-5809-387-5.
15. Local Exhaust Ventilation, Aerodynamic Processes, and Calculations of Dust Emissions, Ivan Logachev, Konstantin Logachev, Olga Averkova, © 2016 by Taylor & Francis Group, LLC, ISBN: 978-1-4987-2064-9.
16. M.F. Bromley. Flow pattern in the effective area of suction inlets. Heating and Ventilation. 1934. No. 3 pp. 2-8.
17. V.V. Baturin. The Fundamentals of Industrial Ventilation. Moscow, Russia: Profizdat, 1990. 448pp.

18. G.A. Maksimov and V.V. Deryugin. Air Motion in Operation of Ventilation Systems. Leningrad, Russia: Construction Literature Publishing, 1972. 97pp.
19. E.M. Ivanus, S.S. Zhukovsky, and Yu.S. Yurkevich. The Study of Local Ventilation from Brazing Joints of Radio Equipment Units. Lvov, Ukraine: Lvov Polytechnic Institute, 1985. 5pp. Ukraine NIINTI Department, December 22, 1986. No. 2797.
20. Mine Planning and Equipment Selection, Hardygóra, Paszkowska & Sikora, Wrocław University of Technology, Poland, © 2004 Taylor & Francis Group, London, ISBN 04-1535-937-6, p.791.
21. Mine Health and Safety Management, Edited by Michael Karmis, © 2001 Society for Mining, Metallurgy, and Exploration, Inc. ISBN: 0-87335-200-9.
22. Mine ventilation and air conditioning, third edition, Howard L. Hartman, The University of Alabama, Jan M. Mutmanský, The Pennsylvania State University, Raja V. Ramani, The Pennsylvania State University, Y. J. Wang, West Virginia University, © 1997 by John Wiley & Sons, Inc. ISBN 0-471-11635-1. With permission from John Wiley & Sons, Inc.
23. McPherson 1993; with permission from Springer Science and Business Media.
24. <https://www.slideshare.net/AlekseyKashnikov/automatic-mine-ventilation-control-system>.
25. <https://www.abc-industries.net/products/brattice-curtains-flypads>.
26. <https://www.systemair.com/>.
27. <https://www.911metallurgist.com/dust-scrubbers/>
28. The 4th International Conference on Field and Service Robotics, Automatic 3D underground mine mapping, Daniel F. Huber, Nicolas Vandapel, The Robotics Institute, Carnegie Mellon University July 14–16, 2003.  
[https://www.researchgate.net/publication/2829845\\_Automatic\\_3D\\_underground\\_mine\\_mapping](https://www.researchgate.net/publication/2829845_Automatic_3D_underground_mine_mapping).
29. Analysis of the effect of ducted fan system variables on ventilation in an empty heading using CFD, by T. Feroze and B. Genc, The Journal of Southern African Institute of Mining and Metallurgy, February 2017, <http://dx.doi.org/10.17159/2411-9717/2017/v117n2a7>.
30. Ventsim manual.
31. Research and application of controlled circulating ventilation in deep mining, WANG Peng, ZHU Kunlei, ZHOU Yu, LIU Jingxian, SHI Changyan, Procedia Engineering 84 ( 2014 ) 758 – 763, doi: 10.1016/j.proeng.2014.10.493.
32. Clearing the Air Author(s): Christopher Tavener Source: APT Bulletin: The Journal of Preservation Technology , Vol. 50, No. 4, Special Issue: Preservation Engineering (2019), pp. 42-50 Published by: Association for Preservation Technology International (APT), <https://www.jstor.org/stable/10.2307/26893537>.
33. THE CONTROL OF ATMOSPHERIC CONDITIONS IN MINES Author(s): F. B. HINSLEY Source: Journal of the Royal Society of Arts, JANUARY 1967, Vol. 115, No. 5126 (JANUARY

1967), pp. 73-89 Published by: Royal Society for the Encouragement of Arts, Manufactures and Commerce, <http://www.jstor.com/stable/41369837>.

34. Process technology adoption in European coal, 1850-1900, Mechanical ventilation in coal mines, John E. Murray, and Javier Silvestre, August 2016, Yale University.

35. F. B. HINSLEY (1969) The Development of Coal mine Ventilation in Great Britain up to the End of the Nineteenth Century, *Transactions of the Newcomen Society*, 42:1, 25-39, DOI: 10.1179/tns.1969.002.

36. Tong, R.; Yang, Y.; Ma, X.; Zhang, Y.; Li, S.; Yang, H. Risk Assessment of Miners' Unsafe Behaviors: A Case Study of Gas Explosion Accidents in Coal Mine, China. *Int. J. Environ. Res. Public Health* 2019, 16, 1765.

37. Kayode M. Ajayi, Khosro Shahbazi, Purushotham Tukkaraja, Kurt Katzenstein, Prediction of airway resistance in panel cave mines using a discrete and continuum model, *International Journal of Mining Science and Technology*, Volume 29, Issue 5, 2019, Pages 781-784, ISSN 2095-2686, <https://doi.org/10.1016/j.ijmst.2019.02.004>.

38. Demirović, Safer & Marković, Jelena. (2020). A Real Application of Air Recirculation in Underground Coal Mine.

39. Souza, Euler. (2017). Application of ventilation management programs for improved mine safety. *International Journal of Mining Science and Technology*. 10.1016/j.ijmst.2017.05.018.

40. Wang, Qingdong & Shang, Deyong & Yang, Zhiyong & Zhu, Changjun. (2009). Design of coal mine main fan performance optimization. 58 - 60. 10.1109/PACIIA.2009.5406536.

41. Johnny Qin, Qu Qingdong, Hua Guo, CFD simulations for longwall gas drainage design optimisation, *International Journal of Mining Science and Technology*, Volume 27, Issue 5, 2017, Pages 777-782, ISSN 2095-2686, <https://doi.org/10.1016/j.ijmst.2017.07.012>.

42. Brake, Rick & Nixon, T. (2006). Design and operational aspects in the use of booster, circuit and auxiliary fan systems.

43. Acuña, Enrique & Alvarez, Roberto. (2017). Ventilation and fire door coverage solution at the Chuquicamata underground mine project. 10.36487/ACG\_rep/1710\_13\_Alvarez.

44. Feroze, T., & Genc, B.. (2016). Estimating the effects of line brattice ventilation system variables in an empty heading in room and pillar mining using CFD. *Journal of the Southern African Institute of Mining and Metallurgy*, 116(12), 1143-1152. <https://dx.doi.org/10.17159/2411-9717/2016/v116n12a8>.

45. Dean Millar, Michelle Levesque & Stephen Hardcastle (2017) Leakage and air flow resistance in mine auxiliary ventilation ducts: effects on system performance and cost, *Mining Technology*, 126:1, 10-21, DOI: 10.1080/14749009.2016.1199182.

46. Babu, V.R., Maity, T. & Prasad, H. Energy saving techniques for ventilation fans used in underground coal mines—A survey. *J Min Sci* 51, 1001–1008 (2015). <https://doi.org/10.1134/S1062739115050198>.

47. Ugwu, Gabriel. (2015). Journal of Geology and Mining Research An overview of pore pressure prediction using seismically–derived velocities. Journal of Geology and Mining Research. 7. 31-40. 10.5897/JGMR15.0218.
48. Nyaaba, Wedam & Frimpong, Samuel & Professor, K & Chair,. (2015). Optimization of Mine Ventilation Networks Using the Weighted Augmented Lagrange Method.
49. Lilic, Nikola & Cokorilo, Vojin & Cvjetic, Aleksandar & Milisavljevic, Vladimir. (2012). Ventilation planning and design of the Omerler B mine. Underground Mining Engineering. 33-42.
50. A. Herrán-González, J.M. De La Cruz, B. De Andrés-Toro, J.L. Risco-Martín, Modeling and simulation of a gas distribution pipeline network, Applied Mathematical Modelling, Volume 33, Issue 3, 2009, Pages 1584-1600, ISSN 0307-904X, <https://doi.org/10.1016/j.apm.2008.02.012>.